

# City Research Online

## City St George's, University of London

**Citation:** Antia, F. K. (1980). Metal oxides as flame retardants for organic polymers. (Unpublished Doctoral thesis, The City University, London)

This is the accepted version of the paper.

This version of the publication may differ from the final published version. To cite this item please consult the publisher's version.

**Permanent repository link:** https://openaccess.city.ac.uk/id/eprint/37063/

**Copyright and Reuse:** Copyright and Moral Rights remain with the author(s) and/or copyright holders. Copies of full items can be used for personal research or study, educational, or not-for-profit purposes without prior permission or charge, unless otherwise indicated, provided that the authors, title and full bibliographic details are credited, a hyperlink and/or URL is given for the original metadata page and the content is not changed in any way. For full details of reuse please refer to City Research Online policy.

City Research Online: http://openaccess.city.ac.uk/ publications@citystgeorges.ac.uk

842

A THESIS

entitled

# Metal oxides as flame retardants for organic polymers

by

FEROZE K. ANTIA

Submitted for the Degree of

Doctor of Philosophy

The City University, London

July 1980

CONTENTS


| | | |
|---|---|---|
| 1. | INTRODUCTION | 14 |
| 1.1 | Fire Retardancy in Polymers | 15 |
| 1.2 | The burning of thermoplastics | 18 |
| | 1.2.1 Combustion and organic polymers | 18 |
| | 1.2.2 Mechanism of thermal decomposition | 19 |
| | 1. General | 19 |
| | 2. Polyethylene | 30 |
| | 3. Acrylonitrile-butadiene-styrene | 38 |
| | 1.2.3 Tests for polymer flammability | 58 |
| | 1. Screening tests | 61 |
| | 2. Use-evaluation tests | 78 |
| | 3. Miscellaneous tests | 89 |
| | 4. Oxygen Index Test: its development into a standard test method in the study of flammability | 97 |
| | 5. Oxygen Index Test: its use in the determination of the mechanism of flame-retardance | 106 |
| | 1.2.4 Fundamental Studies | 108 |
| | 1.2.5 Flame Retardancy: Methods and mechanisms | 123 |
| | 1. Generalised Mechanism of flame-retardant action | 123 |
| | 2. Some chemical flame-retardant systems | 128 |
| | 3. Some physical methods of flame-retardance | 158 |
| 1.3 | Analysis of Experiments with mixtures | 163 |
| 2. | EXPERIMENTAL | 172 |
| 2.1 | Materials | 173 |
| | 2.1.1 Polymers | 173 |
| | 2.1.2 Additives | 173 |
| | 1. Halogen compounds | 173 |
| | 2. Metal oxides | 173 |
| | 3. Other metal compounds | 177 |
| | 4. Stabilisers, anti-oxidants and lubricants | 177 |

2.1.3 Gases 177
2.2 Apparatus 179
2.2.1 The thermobalance 179
2.2.2 Oxygen-index apparatus 190
2.2.3 Mass spectrometer 192
2.3 Procedure 194
2.3.1 Preparation of polymer samples 194
2.3.2 Procedure of thermal analysis 196
2.3.3 Measurement of Oxygen Index 198
3. RESULTS 199
3.1 Thermogravimetric experiments 200
3.1.1 General 200
3.1.2 Metal Oxides 202
3.1.3 Halogen compounds 207
3.1.4 Metal Oxides + Halogen compounds 212
1. Mixtures of halogen compounds and single metal oxides 212
2. Mixtures of chlorinated wax S70 and two metal oxides 231
3.1.5 Polymers 253
3.1.6 Polymer + Halogen 256
3.1.7 Polymer + Halogen + Single metal oxide 256
1. General 256
2. In polyethylene (HDPE) 258
3. In acrylonitrile-butadiene-styrene (ABS) 263
3.1.8 Polymer + Mixed Metal Oxides + Halogen Compound 267
1. General 267
2. Polyethylene/Halogen/mixed metal oxide systems 267
3. ABS/Halogen/mixed metal oxide systems 272
3.2 Flammability measurements 276
3.2.1 The Experimental Designs 276
3.2.2 Polymers 284
1. HDPE 284
2. ABS 284

3.2.3 Polymer/Halogen compound 285
3.2.4 Polymer/Halogen compound/Single metal Oxide 290
1. General 290
2. Polymer/Halogen compound/$Sb_2O_3$ 290
3. Polymer/Halogen compound/Oxides of Alumina 305
3.2.5 Polymer/Halogen compound/Two metal oxides 311
1. $Sb_2O_3/SnO_2$/Halogen compound 311
2. $Sb_2O_3$/ZnO/Halogen compound 315
3. $Sb_2O_3/Fe_2O_3$/Halogen compound 320
4. $Sb_2O_3$/AlOOH/Halogen compound 324
5. $Sb_2O_3/Al_2O_3.3H_2O$/Halogen compound 327
6. $Sb_2O_3/Al_2O_3$/Halogen compound 331
7. $Sb_2O_3$/Talc/Halogen compound 334
8. $Sb_2O_3$/Ammonium molybdate/Halogen compound 334
9. $SnO_2/Fe_2O_3$/Halogen compound 337
10. SnO/ZnO/Halogen compound 339
11. SnO/AlOOH/Halogen compound 343
3.2.6 Polymer/Inert fillers 348
4. DISCUSSION 351
4.1 Synergism and Pseudo-synergism 352
4.2 The Antimony-Halogen System 353
4.3 The screening of other metal oxides as possible synergists 356
4.3.1 Metal oxides 356
4.3.2 Metal "oxy-salts" 359
4.4 Mixed metal oxide/Halogen systems 361
4.5 Flammability and triangular diagrams 363
4.6 Synergism : The aluminium oxides/Halogen systems 368
5. CONCLUSION 371
6. APPENDIX : The computer programme used to calculate the statistics and plot the triangular diagrams 374
7. REFERENCES 393

LIST OF TABLES


1. Mechanism of thermal decomposition of polymers
2. Thermal degradation reactions of vinyl polymers
3. The yield of monomer formed from some vinyl polymers during thermal degradation
4. Postulated mechanism of char formation
5. Thermal degradation of polyethylene
6. Mass-spectrometric analysis of $V_{-80}$ fraction from pyrolysis of polyethylene and polymethylene
7. Pyrolysis of high-density polyethylene at 530°C in helium
8. Mechanism for the decomposition of polyethylene
9. The products of thermal degradation of polybutadiene
10. Mechanism of the thermal cyclisation of polybutadiene
11. UL94 test flammability classification for polymeric materials
12. BS 476: part 7 test classification
13. Major products formed during the burning of polymers containing chlorine compounds
14. Some halogen flame retardant compounds
15. Flammability of flexible urethane foam containing ~6.3%Cl, $Sb_2O_3$, and other metal oxides
16. The physical and chemical properties of the polymers
17. The physical and chemical properties of the halogen compounds
18. Stabilisers, antioxidants and lubricants used during milling of polymer samples
19. Thermal analysis of: hydrated metal oxides
20. : chlorinated wax
21. : decabromobiphenyl
22. : Electrofine S70 and Adine 0102
23. : $Sb_2O_3$ and S70
24. : SnO and S70
25. : $SnO_2$ and S70
26. : AlOOH and S70
27. : Metal oxides and S70
28. : Aluminium oxychloride and S70
29. : $Sb_2O_3$/ZnO and S70
30. : $Sb_2O_3$/AlOOH and S70

31. Thermal analysis of: $Sb_2O_3/Fe_2O_3$ and S70
32. : $Sb_2O_3$/metal oxides and S70
33. : $SnO_2$/ZnO and S70
34. : $SnO_2$/AlOOH and S70
35. : SnO/metal oxides and S70
36. : $SnO_2$/SnO and S70
37. : SnO/ZnO and S70
38. : SnO/AlOOH and S70
39. : SnO/metal oxides and S70
40. : ZnO/$(NH_4)_6Mo_7O_{24}.4H_2O$ and S70
41. : Polymers in nitrogen
42. : Polymers in air
43. : Polymer/halogen systems
44. : HDPE/S70/metal oxide systems
45. : ABS/Adine/metal oxide systems
46. : HDPE/S70/two metal oxide systems
47. : ABS/Adine/two metal oxide systems
48. The percentage composition at various points in the triangular diagrams
49. The oxygen index of samples of: HDPE/S70
50. : ABS/Adine
51. : ABS/metal oxides/Adine
52. : ABS/Adine/$Sb_2O_3$
53. : ABS/Adine/$Sb_2O_3$
54. : HDPE/S70/$Sb_2O_3$
55. : ABS/Adine/$Sb_2O_3$
56. : HDPE/S70/$Sb_2O_3$
57. : HDPE/S70/oxides of alumina
58. : ABS/Adine/oxides of alumina
59. : PE/S70/metal oxides for use in triangular diagrams
60. : PE/S70/metal oxides for use in triangular diagrams
61. : ABS/S70/metal oxides for use in triangular diagrams
62. : ABS/S70/metal oxides for use in triangular diagrams

63. The oxygen index samples of: HDPE/oxides of alumina

64. : ABS/oxides of alumina

65. : ABS/Adine/$Sb_2O_3$ for use in synergistic calculations

LIST OF FIGURES


1. Reaction regions in polymer combustion
2. Mechanism of the thermal degradation of polyacrylonitrile
3. DTA and TGA curves for polyacrylonitrile
4. Mole percent of volatile material produced by heating polyacrylonitrile for 30 min. at the indicated temperatures
5. Rate of gas evolution from polyacrylonitrile fibres
6. ASTM D2863: Oxygen Index test apparatus
7. Rate and time of burning of self-supporting plastics in a horizontal position
8. Rate and time of burning of flexible plastics in a vertical position
9. ASTM D 757
10. ASTM D 3014 test apparatus
11. ASTM E 162-67 test apparatus
12. ASTM E 84-70 test apparatus
13. BS 476 part 7 test apparatus
14. BS 476 part 6 test apparatus
15. BS 476 part 6 calibration curves
16. Cross section of Hot-air Ignition Furnace Assembly
17. N.B.S. smoke chamber assembly
18. Burning of a polymeric candle
19. Temperature profiles above burning polymers
20. Composition profiles of flames burning above polyethylene
21. Schematic diagram of polymer burning as defined by Martin
22. Oxygen concentration in flame on various polymers
23. Special cubic : k = 3, m = 2
24. Special cubic : k = 4, m = 2
25. Bifilar quartz spiral furnace
26. Crucible holder for DTA
27. The thermogravimetric analysis of Electrofine S70
28. Block schematic diagram of the balance mechanism
29. Block schematic diagram of the balance mechanism and the recording and electric systems
30. Schematic layout of the oxygen-index apparatus

31. Oxygen index apparatus sample holder unit

32. The interaction of Electrofine S70 with $SnO_2$

33. The differential thermal analysis of aluminium oxide trihydrate

34. The interaction of Electrofine S70 and Echantillon 3947

35. The interaction of Electrofine S70 and Echantillon 3948

36. The interaction of Electrofine S70 and Echantillon 3949

37. The interaction of Electrofine S70 and ammonium molybdate

38. The thermogravimetric analysis of Electrofine S70

39. The interaction of $Sb_2O_3$ with ZnO during the decomposition of S70

40/41. The weight loss/rate of weight change traces for:HDPE/S70 metal oxide systems

42/43. :ABS/Adine/ metal oxide systems

44/45. :HDPE/S70/ mixed metal oxide systems

46/47. :ABS/Adine/ mixed metal oxide systems

48. The ternary system

49. Triangular diagrams : Component ratios

50. The oxygen index of samples of:HDPE/S70

51. :ABS/Adine

52. :ABS/Adine/$Sb_2O_3$

53/56. :HDPE and ABS composite designs with halogen and $Sb_2O_3$

57. :HDPE/oxides of alumina/S70

58. :ABS/oxides of alumina/Adine

59/60. The oxygen index of three-component systems: $Sb_2O_3/SnO_2$

61/62. : $Sb_2O_3/ZnO$

63/64. : $Sb_2O_3/Fe_2O_3$

65/66. : $Sb_2O_3/AlOOH$

67/68. : $Sb_2O_3/Al_2O_3.3H_2O$

69/70. : $Sb_2O_3/Al_2O_3$

71. The oxygen index of three-component systems: $Sb_2O_3$/talc

72/ : $Sb_2O_3/(NH_4)_6$

73. $Mo_7O_{24}.4H_2O$

74/ : $SnO_2/Fe_2O_3$

75

76/ : SnO/ZnO

77.

78/ : SnO/AlOOH

79

ACKNOWLEDGEMENTS

I wish to sincerely thank Professor C.F. Cullis for the help, encouragement and guidance given to me throughout this work and in many other ways.

I am grateful to Produits Chimiques Ugine Kuhlmann for their generous support and gift of chemicals used.

I also wish to thank [redacted] for advice and discussions, and my colleagues in the Combustion Research Group who provided a convivial atmosphere in which to work. My thanks also to [redacted] for their encouragement throughout and to [redacted] for her patience.

Finally I would like to thank my family for their support and [redacted] for her understanding and encouragement throughout this work.

May 1980

Feroze

"In many areas of the fire problem, proposed solutions rest on limited experience, shaky assumptions, and guess work".

"America Burning: The Report of the National Commission on fire prevention and control" 1973.

## ABSTRACT

Studies have been made of the effects of a number of anhydrous metal oxides, hydrated metal oxides, mixed metal oxides and metal oxy-salts on the thermal decomposition of chlorinated wax in an attempt to predict those compounds which are most likely to be effective, synergistic flame retardants. It was hoped that the results, when coupled with mass spectrometric data, would throw light on their possible mode of action. The flammability of high-density polyethylene and acrylonitrile-butadiene-styrene, flame retarded by metal oxide-halogen systems, was then studied on the basis of an experimental design.

In the Introduction, the mechanisms of the thermal decomposition of polyethylene and acrylonitrile-butadiene-styrene are discussed. The different tests available for the evaluation of the flammability of various polymers have been described and the need for more stringent rules for the measurement of flammability is emphasised. The different modes of flame-retardant action are also reviewed and the use of and need for a simplexlattice experimental design are discussed.

In the Experimental Section the materials and procedures used are described and accounts are given of the construction and operation of the thermobalance, the polymer mill, the hydraulic press used for preparing polymer "candles", and the oxygen index apparatus.

The Results Section describes the experimental measurements made on the decomposition of a variety of metal oxides when heated alone, with polymers and with appropriate halogen compounds. The results show that thermogravimetric behaviour is at best only a qualitative indicator of any possible flame retardant activity. The results of the flammability measurements show that in general the oxygen index for samples containing polyethylene was easier to measure for samples containing acrylonitrile-butadiene-styrene, as the flames on top of polyethylene samples were generally clean and ablation of the candles did not occur. The samples containing acrylonitrile-butadiene-styrene generally burned with sooty flames, produced large amounts of char and had a tendency either to undergo ablation or periodically to shed char, thereby causing the flame to flare up.

In the Discussion Section, various possible modes of flame retardance for the systems studied are suggested. It can be seen that the introduction of other metal oxides as partial substitutes for antimony oxide does not, in general, improve the flame retardance. The decrease in flame retardance is smallest with iron(III)oxide, talc and aluminium oxide monohydrate. Iron(III)oxide acts predominantly by promoting char formation and by catalysing the decomposition of the halogen compound. Talc undergoes endothermic dehydration in the flame zone near the temperature of combustion of the polymer and hence smothers the flame. Aluminium oxide monohydrate appears to undergo dehydration as well as to inhibit combustion by acting as a filler. Evidence has also been obtained (for what is believed to be the first time) for some chemical interaction between anhydrous alumina and the halogen (particularly bromine) compounds in the polymers studied.

# 1 INTRODUCTION

## 1.1 Fire Retardancy in Polymers

The rapid increase in the production of synthetic polymers in the 1960s has recently continued at an ever-increasing rate so that today these low-cost and increasingly useful materials are produced at a yearly rate in excess of 20 million metric tons. Depite the fact that the flammability of these newer materials is higher and in many cases less well characterized than that of many older, more conventional materials, the great versatility of these man-made products has extended their markets in our technological society to include furniture, construction and transportation materials and packaging. Additionally they have become the preferred materials in such markets as toys and electrical appliances.

The combination of rapidly expanding markets and production coupled in many cases with ill defined flammability characteristics have recently led to the definition of areas of fire hazard, where the flammability of specific synthetic polymers has resulted in apparent threats to public safety.

Each year in the United Kingdom, fire brigades attend about 120,000 fires in buildings and just under a half of these occur in domestic dwellings. Details of these fires are published annually in statistical form[1]. In these statistics, casualties are subdivided into categories involving "smoke and toxic gases", "burns and scalds" and

"other and undefined injuries". The first two of these categories account for some 90% of the total and hence are of special concern to the polymer industry. Furthermore many commonly used methods of reducing the flammability of synthetic polymers are reported to increase the production of smoke and toxic gases associated with their combustion[2-5].

The increasing concern with regard to the safety and flammability of polymeric materials and the likely introduction of additional government fire standards covering these materials have led increasing numbers of polymer manufacturers and fabricators to investigate methods for reducing the flammability of their products. To accomplish these objectives, manufacturers make use of available flame/fire-retardant monomers and chemicals. The ability of these materials to satisfy the demand for safer products and the related technology have varied widely. Nevertheless, this demand has resulted in a rapid increase in the development and sales of fire-retardant materials despite their relatively high cost.

There is a voluminous literature concerning fire retardancy of commercial polymers and a list of commercially available fire-retardants has recently been published[5].

Since 1970, the total consumption of all additive and reactive materials for imparting flame-retardancy to plastics has been growing at about 13% per year[7]. Inorganic flame retardants, at present representing only some 50% of the total[8], are

expected to grow at about the same annual rate for several years.

One of the keys to this growth is the availability and price status of antimony(III) oxide. In mid-1969, antimony oxide cost only £0.45 per kilo, but after fluctuating, its present price is £1.90 per kilo. In spite of the uncertainty over its future availability, antimony (III) oxide is expected to find even greater usage as a flame retardant in the 1980s but the commercial risks involved are forcing many of its users to look for replacements.

In this work, an attempt has been made partially to replace antimony (III) oxide as a "synergistic" flame-retardant for use in combination with halogens in polymers. The flame-retardant activities of a number of mixtures of metal oxides, hydrated metal oxides, ammonium tetraborate and ammonium molybdate have been studied in conjunction with the antimony/halogen system; and the degree of flame-retardance introduced into a polymer by the incorporation of different ratios of these flame-retardant additives has been studied using the oxygen-index test method[9].

## 1.2 The burning of thermoplastics.

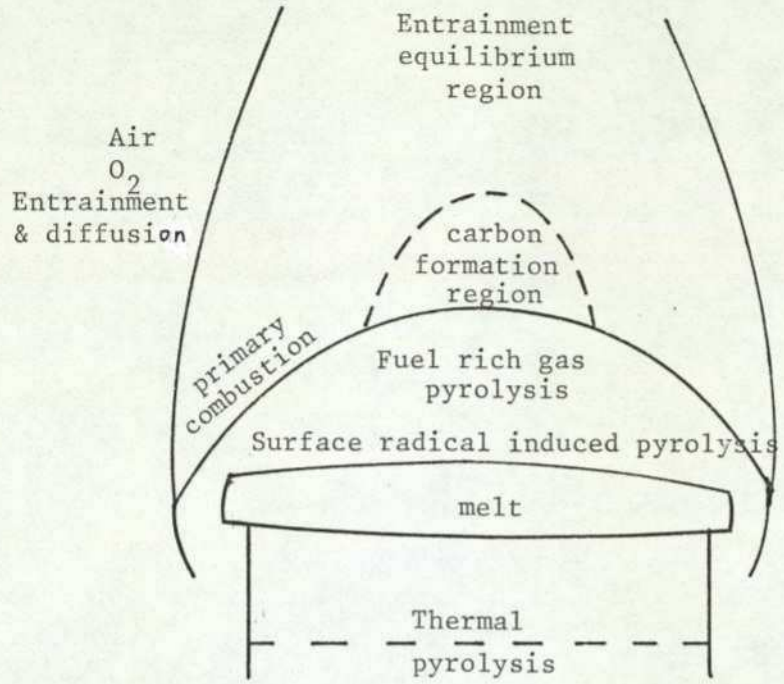
### 1.2.1 Combustion and organic polymers

The term 'combustion' is used to describe a wide class of chemical reactions. It can be defined as an autocatalyzed, exothermic reaction with the ability to propagate through the phase concerned. Fire is a common term for combustion, particularly when it is uncontrolled. Combustion usually involves two reactants, a fuel and an oxidizer. In the case of fires, the reactants are usually a condensed-phase fuel and a gaseous oxidizing agent. Flames are gas-phase combustion processes. The temperatures of most combustion processes are high, and the products are generally gaseous. Most of the heat release occurs in the gas phase. Flames are usually associated with non-equilibrium phenomena such as high concentrations of radicals, atoms, ions and light emission.

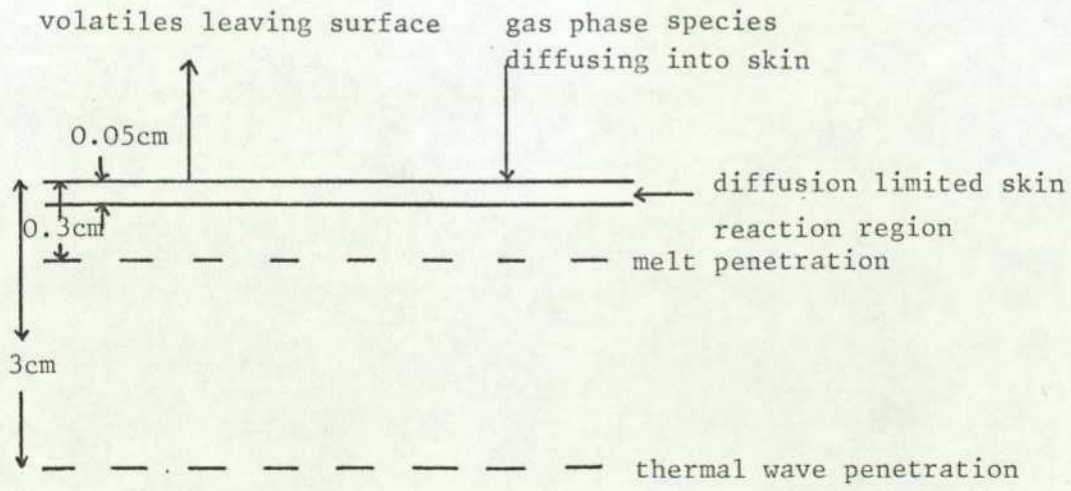
A burning polymer is a very complex combustion system and can be separated conceptually into several discrete stages. In particular, combustion involves three interacting regions, viz. the gas phase, the condensed phase surface and the condensed phase (Fig.1). Reactions in the gas phase and the condensed phase pyrolysis have been extensively studied, whereas surface reactions have received less attention.

FIGURE 1

Reaction regions in polymer combustion(a) Schematic of combustion regions in a polymer candle burning flame




b) Detail of condensed phase region

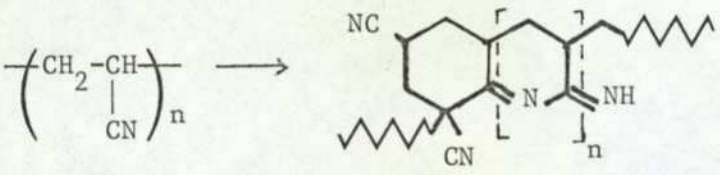


When a thermal wave induced by combustion travels into the polymer, initially the temperature simply increases due to thermal conduction. Polymers being high in molecular weight, decompose before vaporization[10-11]. If the polymer is pure, thermal initiation would need to rupture a C-C or C-X bond (where X is usually H, O, N, S or halogen) and the process would have a high activation energy(200-400 kJ $mol^{-1}$). Once initiated however, the process would proceed rapidly because a free radical chain reaction would take over. Each ruptured bond produces two radicals each of which can react readily with other polymer chains. This can result in both depolymerisation producing gaseous products and crosslinking which produces an involatile char. A brief summary of the mechanisms of thermal degradation can be found in the following section. Studies of the thermal decomposition of polymers have been useful in elucidating the action of flame retardants.

## 1.2.2 Mechanisms of thermal decomposition.

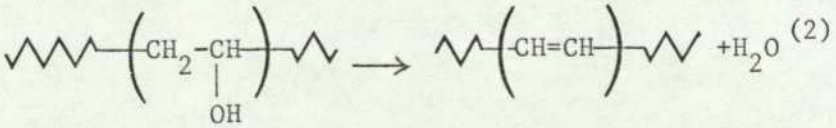
### 1.2.2.1 General

Vinyl polymers, of general formula $-(CH_2-CXY)-_n$ vary considerably in their thermal stability, and can undergo degradation via various routes when heated under vacuum or in an inert atmosphere; these polymers decompose by one of the mechanisms shown in Table 1[11]. With some polymers, thermal rearrangement is the first reaction to occur when these materials are heated in the absence of oxygen. This behaviour is found with polyacrylonitrile (PAN), which cyclises to produce short conjugated sequences in the polymer chain[12,13].




(1)

"Chain stripping" is another route that leads to degradation in some groups of vinyl polymers. On pyrolysis, large quantities of one volatile product (other than the monomer) are formed. In the degradation of poly (vinyl alcohol), water is the principal product[14]:




(2)

Table 1

Mechanism of thermal decomposition of polymers.

| | Example Polymer | Product |
|---|---|---|
| a) Random Chain Scission: | | |
| | General | Species with Mn<2000 |
| | polystyrene $(CH_2-\underset{Ph}{CH})_n$ | styrene, dimers, trimers |
| | polyethylene $(CH_2-CH_2)_n$ | etc. alkanes and alkenes |
| b) End Chain Scission: | General | |
| (depolymerisation or unzipping) | poly α-methyl $(CH_2-\underset{Ph}{\overset{Me}{C}})_n$ | 99% monomer |
| | polymethyl-mathacrylate $(CH_2-\underset{CO_2Me}{\overset{Me}{C}})$ | 98% monomer |
| | polytetrafluorethylene $(CF_2-CF_2)_n$ | 100% monomer |
| c) Chain Stripping: | General | volatiles and char |
| | poly(vinylchloride) $(CH_2-\underset{Cl}{CH})_n$ | HCl, aromatics and char |
| | poly(vinylalcohol) $(CH_2-\underset{OH}{CH})_n$ | water and char |
| d) Cross-Linking: | General | |
| | polyacrylonitrile $(CH_2-\underset{CN}{CH})_n$ | little volatile material much char |

A large amount of hydrogen chloride and a residual material containing long conjugated sequences of unsaturation are the main pyrolysis products of poly(vinylchloride)[15].

$$\sim\!\!\left(\mathrm{CH_2\text{-}CH}\right)\!\!\sim \longrightarrow \sim\!\!\left(\mathrm{CH{=}CH}\right)_n\!\!\sim \quad + \mathrm{nHCl} \qquad (3)$$

Cl

In this "chain stripping" reaction, Ouchi[16] has detected unpaired electron spin, thus providing evidence for a radical chain reaction, instead of a unimolecular elimination process. Additional support for a radical chain mechanism is seen from the work of Geddes[17], who has reported that the addition of compounds which breakdown to yield free radicals increases the rate of decomposition of poly(vinylchloride).

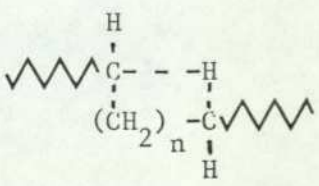
The most common mechanism of degradation of vinyl polymers is "chain scission" to form two chain-end radicals, which subsequently undergo further reaction. The rate of production of free radicals, which can propagate chains, depends on the rate of chain scission, the rate of recombination of radicals inside the polymer "cage" and the rate of diffusion of radicals out of the "cage".

$$\mathrm{R - R} \rightleftharpoons \underbrace{\mathrm{R^{\cdot} + R^{\cdot}}}_{\text{cage}} \longrightarrow 2\mathrm{R^{\cdot}} \qquad (4)$$

The chain-end radicals formed by chain scission propagate either by depolymerisation or by chain transfer depending on the ease of hydrogen abstraction. These reactions are shown in Table 2. When hydrogen abstraction is difficult, as in

poly(α-methyl styrene) and polytetrafluoroethylene, the rate of the depolymerisation reaction is greater than the rate of the transfer reaction and an almost complete conversion into monomer is observed in the temperature range 200-500°C[10]. Hence, in vinyl polymers $\text{-}(CH_2\text{-}CXY)\text{-}_n$ when neither X or Y are hydrogen atoms, yields of monomer are always high. In polystyrene, replacement of the α-hydrogen atom, even by deuterium, increases the monomer yield. When X and Y are both hydrogen atoms, the rate of radical transfer reaction exceeds the rate of the depolymerisation reaction. The high rate of radical transfer is due to the presence of easily abstracted α-hydrogen atoms. In linear polyethylene, the effect of a relatively high rate of radical transfer causes scission to take place in random fashion along the chain[18]. The rapid decrease in molecular weight which accompanies the onset of degradation[19-22] conclusively demonstrates the random nature of the chain scission reaction in polyolefins. Table 3 shows the monomer yields formed from some vinyl polymers[23].

Hydrogen abstraction by alkyl radicals in radical transfer reactions can be intermolecular and intramolecular during thermal degradation. The intramolecular radical transfer reactions generally involve cyclic transition states:

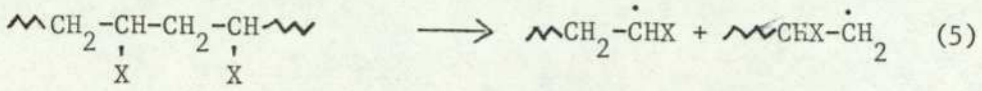


where n=0, 1, 2 . . etc.

Table 2

Thermal degradation reactions of vinyl polymers.

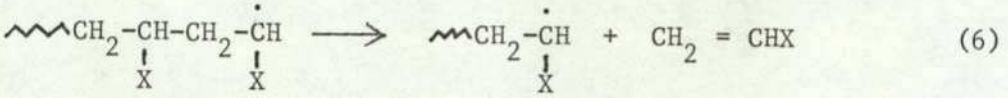
Initiation:



(5)

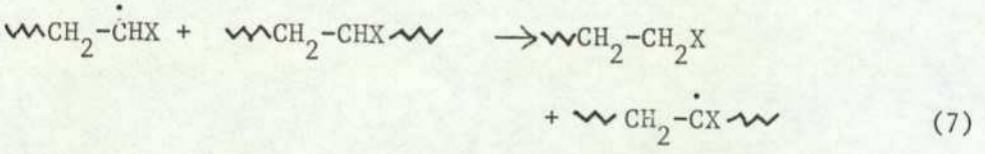
Propagation:

Depolymerisation (β-scission at chain-end)



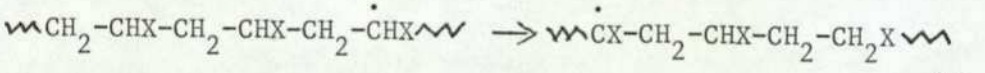
(6)

Intermolecular Transfer



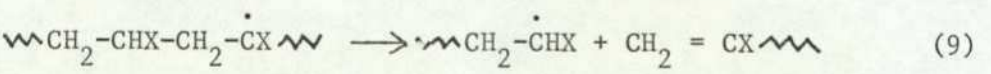
(7)

Intramolecular Transfer



(8)

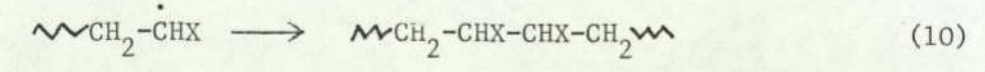
β-scission



(9)

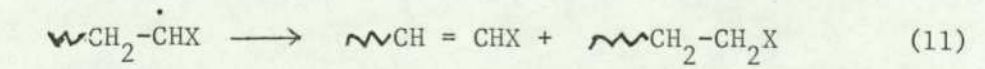
Termination

Recombination



(10)

Disproportionation



(11)

Five and six-membered ring transition states are energetically the most favourable. The "mid-chain" radicals formed as a result of radical transfer either undergo further transfer or breakdown, by β-scission, to form a new chain-end radical and an olefin.

$$R - CH_2 - \underset{\displaystyle R}{\overset{\displaystyle \cdot}{C}} - R^1 \quad \longrightarrow \quad R^{\cdot} + CH_2 = CRR^1 \qquad (9)$$

Alkyl radicals are generally stable and break down at appreciable rates only at high temperatures (>350°C)[24]. The stability of alkyl radicals and their rate of production account for the fact that volatile products are formed from thermally degrading polyolefins at temperatures below 350°C.

The mechanism of char formation involves crosslinking and also formation of conjugate double bonds followed by cyclization and dehydrogenation(Table 4). These reactions are generally the result of the elimination of a stable molecule such as water, one of the halogen acids or carbon monoxide[25].

The concept of weak links has been used to explain the non-ideal behaviour of a number of polymers[19-22]. During studies of the degradation of polystyrene, Jellinek[26] noticed that certain bonds were especially susceptible to scission for no apparent reason. The presence of weak links has been ascribed to various causes, such as the incorporation of oxygen into the polymer molecule producing

Table 3

The yield of monomer formed from some vinyl polymers during thermal degradation.

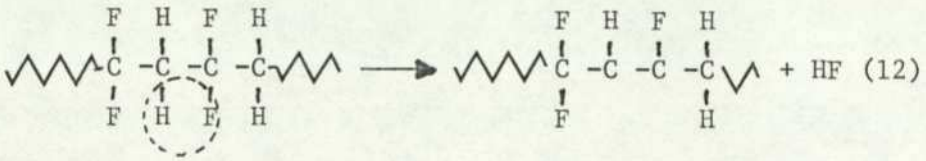
| Polymer | Formula | Monomer Yield(%) |
|---|---|---|
| Poly(α-methyl styrene) | $-(CH_2-CMePh)_n-$ | 100 |
| Poly(methyl methacrylate) | $-(CH_2-\underset{\displaystyle CO_2Me}{\underset{\vert}{C}}Me)_n-$ | 98 |
| Poly tetrafluoroethylene | $-(CF_2-CF_2)_n-$ | 96 |
| Poly(α-deuterostyrene) | $-(CH_2-CDPh)_n-$ | 70 |
| Polystyrene | $-(CH_2-CHPh)_n-$ | 41 |
| Polybutadiene | $-(CH_2-CH=CH-CH_2)_n-$ | 20 |
| Polyacrylonitrile | $-(CH_2-CHCN)_n-$ | 5 |
| Poly(methyl acrylate) | $-(CH_2-\underset{\displaystyle CO_2Me}{\underset{\vert}{C}}H)_n-$ | 1 |
| Polypropylene | $-(CH_2-CHMe)_n-$ | 0.17 |
| Poly(vinyl chloride) | $-(CH_2-CHCl)_n-$ | 0.10 |
| Polyethylene | $-(CH_2-CH_2)_n-$ | 0.03 |

a peroxide link in the chain, trace impurities in the monomer, branching of the polymer chain and the presence of"head-to-head" units. Generally these effects reduce the thermal stability of polymers. HoweverMacCallum[24] has reported results for the degradation of a number of vinyl polymers which do not involve "weak links".

Table 4

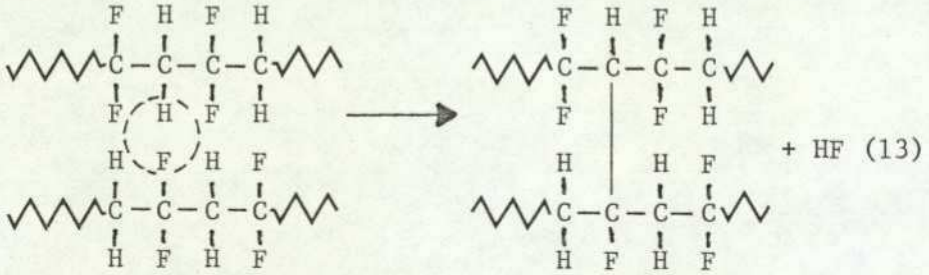
Postulated mechanism of char formation

1. Elimination (poly(vinylfluoride))



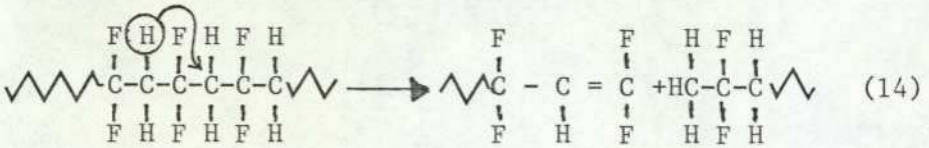
(12)

Cross linking



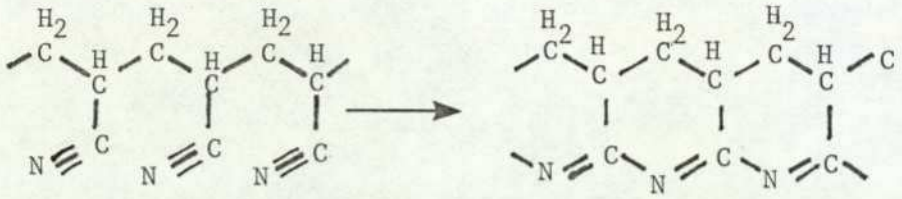
(13)

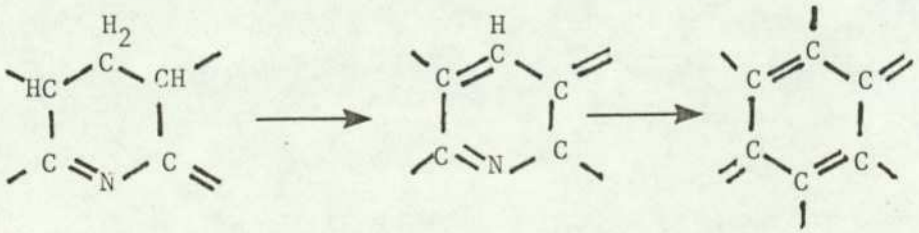
Double bond formation



(14)

2. Cyclization and Dehydrogenation (Acrylic Fibres)





graphite rings

1.2.2.2 Polyethylene

For the purpose of discussing the mechanism of decomposition and flammability, there are essentially two types of polyethylene, according to whether the polymer has linear or branched chains. The presence of branches reduces the ability of polymer chains to pack together closely and regularly, that is, to crystallize. As a result the various types of commercially available polyethylene have somewhat different properties. Thus the more highly branched polymers have lower density, crystalline melting point, stiffness, surface hardness, and softening temperatures and greater permeability to gases and vapours. To a first approximation, these properties are dependent only on the degree of branching. Other physical properties are more difficult to correlate since they are also affected by variations in average molecular weight and molecular weight distribution.

In the absence of oxygen, polyethylene is stable up to ca.290$^{o}$Cwhere the molecular weight first starts to fall. At about 360$^{o}$C, volatile products begin to appear, while at higher temperatures (above 450$^{o}$C) complete disintegration of the polymer occurs.

Wall and Straus[28] have proposed a free radical mechanism for the thermal degradation of polyethylene. Radicals are formed in the initiation step by the rupture of C-C bonds in the polymer chain. The initiation of the

decomposition process is usually assumed to take place either randomly or at chain ends. In certain cases, several competing initiating processes may occur at chemical or physical irregularities along the polymer chain. The initiation step is followed by a chain-propagation step, in which monomer fragments are split off stepwise along the chain. Hydrogen transfer reactions occur in competition with the propagation reaction. In highly branched, high-density polyethylene, an increase in intra-molecular hydrogen transfer seems to occur at the expense of intermolecular transfer. The fact that changes in high-density polyethylene occur at about 200°C in inert atmosphere[29,30], while hexadecane[31] is stable up to 390°C shows that initiation is not due to scission of $-CH_2-CH_2-$bonds but must be caused by a reaction taking place in some much more sensitive structures.

Bailey et al[32,33], van Schooten and Evenhuis[34], and Tsuchiya and Sumi[35], have pointed out that intramolecular hydrogen abstraction (backbiting) taking place simultaneously with the intermolecular mechanism will explain both the intermediate formation of volatile material and the composition of these products.

Measurements of the rate of decomposition, based on loss of weight were carried out by Madorsky et al.[36-38] on a wide range of polyethylenes. The influence of the extent of chain-branching on the decomposition was also investigated and it was found that the activation energy for polyethylene is higher

(301.3 k $J.mol^{-1}$) than that for a low molecular weight linear polyethylene (263.6 k $J.mol^{-1}$) or a branched polyethylene (267.8 k $J.mol^{-1}$). The breakdown of polyethylene was found to represent an almost ideal case of first-order dependence of rate on the weight of polymer residue throughout the reaction. The results for the highly branched polymer resembled very closely those for the less branched polyethylene, giving two distinct stages of reaction (Table 5).

Oakes and Richards[39], Madorsky et al.[40] and Iring et al.[41] have studied the decomposition products of polyethylene. Examination of the solid residue present after pyrolysis showed it to be a waxy substance, similar to the original starting material[39] with an empirical formula corresponding closely to $CH_2$. The degree of unsaturation of the residue increased as pyrolysis proceeded and decomposition produced one double bond in each product molecule. It was concluded therefore that the primary products of decomposition were monoalkenes. Three distinct types of alkenes were produced by pyrolysis viz. (1) $RCH = CH_2$ ii) $RCH = CHR^1$ and (iii) $RR^1C = CH_2$. Of these (ii) and (iii) increased to a constant value by the time the molecular weight of polyethylene had been reduced to 5-10% of its original value and only the concentration of (i) increased throughout the course of the reaction.

Madorsky et al.[40] studied the volatile products formed during the pyrolysis of a commercial grade polyethylene

Table 5

Thermal Degradation of Polyethylene: Values of Overall Activation Energy

| Polymer | Extent of reaction | Order with respect to residue | Activation Energy ($kcalmol^{-1}$) | Ref |
|---|---|---|---|---|
| Polyethylene Mol.wt. 11,000 16,000 23,000 | Bulk of reaction | Zero | 46.0 52.6 66.1 | 38 |
| Polyethylene Mol.wt. 11,000 23,000 | Initial rate only | - | 60-70 | 39 |
| Polymethylene | Bulk of reaction | First | 72.0 | 36 |
| Polyethylene Mol.wt. 20,000 | Initial rate<br>Later stages | First<br>First | 48.0<br>63.0 | 37 |
| Branched Polyethylene | Later stages | First | 64.0 | 38 |
| Polyethylene Mol.wt. 20,000 | 0- 3% wt. loss<br>3-15% wt. loss<br>35-95% wt. loss | Zero<br>Zero<br>First | 48.0<br>61.0<br>68.0 | 44 |
| Polymethylene Mol.wt. 9,000-13,000 | Bulk of reaction | - | 76-82 | 48 |

(mol.wt = 20,000). Samples of the polymer were pyrolysed in vacuo at temperatures between 335 and 450°C. The volatile products were condensed and separated into three fractions; Vpyr (volatile at the temperature of pyrolysis), $V_{25}$ (volatile at 25°C) and $V_{-80}$ (volatile at -80°C). The $V_{-80}$ fraction, which formed about 1% of the weight of the polymer volatilised, was analysed by mass spectrometry and was found to consist of a complex mixture of $C_1$- $C_7$ straight chain alkanes and alkenes with trace quantities of dienes (Table 6). The less volatile, $V_{25}$, fraction was presumed to consist of higher members of the alkane and alkene series. The monomer yield was 0.025% by weight of the volatilised polymer. Hence, the flammable nature of polyethylene is understandable inasmuch as the same long-chain saturated hydrocarbon structure responsible for the excellent physical and chemical properties of polyethylene readily breaks down at high temperatures, yielding highly volatile low-molecular weight saturated and unsaturated hydrocarbons that are very flammable (Table 7). The various mechanisms for the decomposition of polyethylene have been extensively reviewed[42-52] and the two main routes can be found in Section 1.2.1 and Table 8.

Table 6

Mass-spectrometric analysis of $V_{22-80}$ fraction from pyrolysis of polyethylene and polymethylene.

| Compound | Polyethylene | | Polymethylene | |
|---|---|---|---|---|
| | mole% of fraction | wt% of total volatiles | mole% of fraction | wt% of total volatiles |
| Ethylene | 4.3 | 0.025 | 12.3 | 0.03 |
| Ethane | 12.4 | 0.076 | 4.3 | 0.02 |
| Propadiene | 0.3 | 0.002 | 1.4 | 0.01 |
| Propene | 5.2 | 0.045 | 20.7 | 0.11 |
| Propane | 14.8 | 0.136 | 3.6 | 0.02 |
| Butadiene | - | - | 2.1 | 0.04 |
| Butene | 24.6 | 0.282 | 13.0 | 0.09 |
| Butane | 19.1 | 0.225 | 11.2 | 0.09 |
| Pentadiene | 0.4 | 0.005 | 2.8 | 0.03 |
| Pentene | 7.5 | 0.108 | 9.6 | 0.01 |
| Pentane | 6.2 | 0.091 | 6.1 | 0.05 |
| Hexadiene | 0.3 | 0.005 | 2.6 | 0.03 |
| Hexene | 3.2 | 0.056 | 8.7 | 0.09 |
| Hexane | 1.2 | 0.022 | 1.6 | 0.02 |
| Heptene | 0.2 | 0.004 | - | - |
| Heptane | 0.4 | 0.008 | - | - |
| | 100.0 | 1.092 | 100.0 | 0.64 |

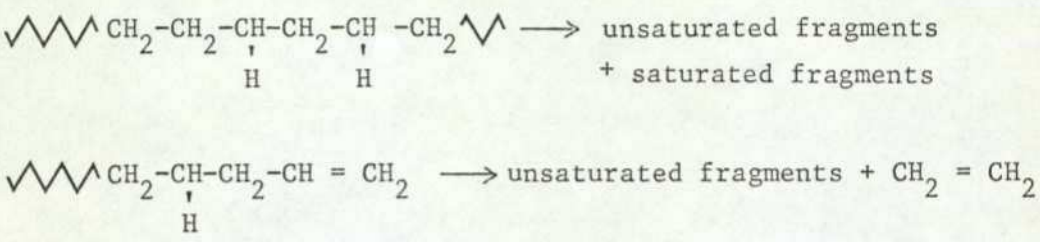
Table 7

Pyrolysis of High-Density Polyethylene at 530°C in Helium

| Product | Yield (Mole %) |
|---|---|
| Methane | 8.0 |
| Ethane | 8.9 |
| Ethylene | 20.9 |
| Propane | 7.3 |
| Propylene | 9.9 |
| Butane | 1.9 |
| Isobutene | 0.9 |
| 1-Butene | 2.3 |
| 1,3-Butadiene | 1.6 |
| Pentane | 1.0 |
| 1-Pentene | 2.7 |
| Hexane | 0.8 |
| 1-Hexene | 8.0 |
| Heptane | 1.4 |
| 1-Heptene | 8.2 |
| Isooctane | 0.3 |
| Octane | 1.9 |
| 1-Octene | 3.7 |
| Isononane | 0.6 |
| Nonane | 1.1 |
| 1-nonene | 3.5 |
| Isodecane | 0.3 |
| Decane | 0.9 |
| 1-Decene | 3.9 |

Table 8

Mechanism for the decomposition of polyethylene.



1.2.2.3 Acrylonitrile-Butadiene-Styrene

The extensive series of polymers based on combinations of acrylonitrile, butadiene and styrene are referred to as ABS copolymers. They comprise a continuous phase consisting of a copolymer of styrene (or α-methylstyrene) and acrylonitrile in which is dispersed an elastomer (butadiene rubber) exhibiting some compatibility with the copolymer employed. By varying certain parameters, such as monomer content, ratio of elastomer to styrene/acrylonitrile copolymer, and the method of polymerising the continuous and dispersed phases, a range of products of widely varying properties can be obtained. Hence one cannot discuss, in generalised terms, the thermal decomposition of ABS copolymers.

The chemical formula of ABS is generally written as:

$$-\left(CH_2 - \underset{\underset{CN}{|}}{CH} - CH_2 - \underset{\underset{-\left(CH - CH = CH - CH_2\right)_n-}{|}}{CH} - Ph\right)_m-$$

and hence the separate modes of thermal decomposition of styrene-acrylonitrile copolymer and of polybutadiene are of some relevance.

1.2.2.3.1 Polybutadiene

There are three different structures that can be incorporated in various proportions to form polybutadiene. They are cis or trans 1,4-polybutadiene: $-(CH_2-CH = CH-CH_2)_n-$ and 1,2-polybutadiene:

$$-(CH_2-\underset{\displaystyle CH = CH_2}{\underset{|}{CH}})_n-$$

The most important synthetic elastomer based on butadiene is a random copolymer of butadiene and styrene, known as SBR, which consists of approximately 75% butadiene (containing predominantly the trans 1, 4 structure) and is of relatively low vinyl content[53].

A number of workers have studied the products of the thermal decomposition of polybutadiene[54-59]; the analytical results are shown in Table 9.

The activation energy of the thermal degradation of polybutadiene has been reported to be between 234 and 259 k J.mole$^{-1}$ [60,61]. Nagao and Hikita[54] have calculated the bond dissociation energies of polybutadiene and have shown that the most favoured site for the occurrence of chain scission is the β-position to the C=C bond.

The dissociation energy of this bond is lowered by the resonance stabilisation of the two allylic radicals formed by scission:

TABLE 9

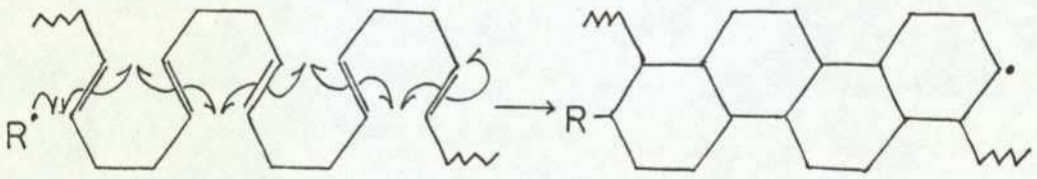
The products of thermal degradation of polybutadiene

| Polymer | Carboxy-terminated | Not described | Not described | cis 1,4 | Not described | cis 1,4 |
|---|---|---|---|---|---|---|
| Pyrolysis temp.(°C) | 450 - 1000 | 350 - 500 | 400 | 600 | 600 - 800 | 350° |
| Atmosphere | Nitrogen | Vacuum | Vacuum | Nitrogen | "inert" | Vacuum |
| Method of analysis | G.C. | Mass Spec. | Mass Spec. | G.C./M.S. | G.C. | Mass Spec. |
| Reference | 43 | 44 | 45 | 46 | 47 | 48 |
| Hydrogen | X | | X | | | |
| Methane | X | | | X | X | |
| Acetylene | X | | | X | X | |
| Ethylene | X | X | | X | X | |
| Ethane | X | X | X | X | X | |
| Propyne | | | | | | |
| Propadiene | | X | | | | |
| Propylene | | X | X | X | X | |
| Propane | | X | X | X | X | |
| Butadiene | X | X | X | X | X | X |
| Butenes | | X | | X | X | X |
| Butanes | | X | | X | X | |
| Cyclopentadiene | | X | | | | |
| Pentadienes | | X | | X | X | X |
| Pentenes | | X | X | X | X | |
| Pentanes | | X | X | | | |
| Cyclohexadiene | | X | | | | X |
| Hexadienes | | X | X | X | | X |
| Cyclohexene | | | X | | | |
| Hexenes | | X | | X | X | |
| 4-vinyl cyclohexene | X | X | X | X | | X |
| Benzene | | | X | | | X |
| Toluene | | | | X | | |
| Styrene | | | | X | | |
| Ethyl Benzene | | | | X | | |

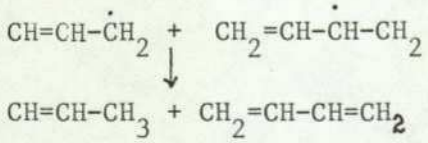


A number of other reactions are also known to occur when polybutadiene is heated. Hence the polymer structure is extensively modified before volatilisation temperatures are reached, except at high heating rates.

Loss of saturation at 300°C has been confirmed by a number of workers[62-65]. Golub[63] has postulated a mechanism for thermal cyclisation to explain this loss of unsaturation and the nature of the degradation products (Table 10). In addition to cyclisation taking place at chain-ends, by the mechanism of Golub[65], this process can occur when a radical adds to a C=C bond:



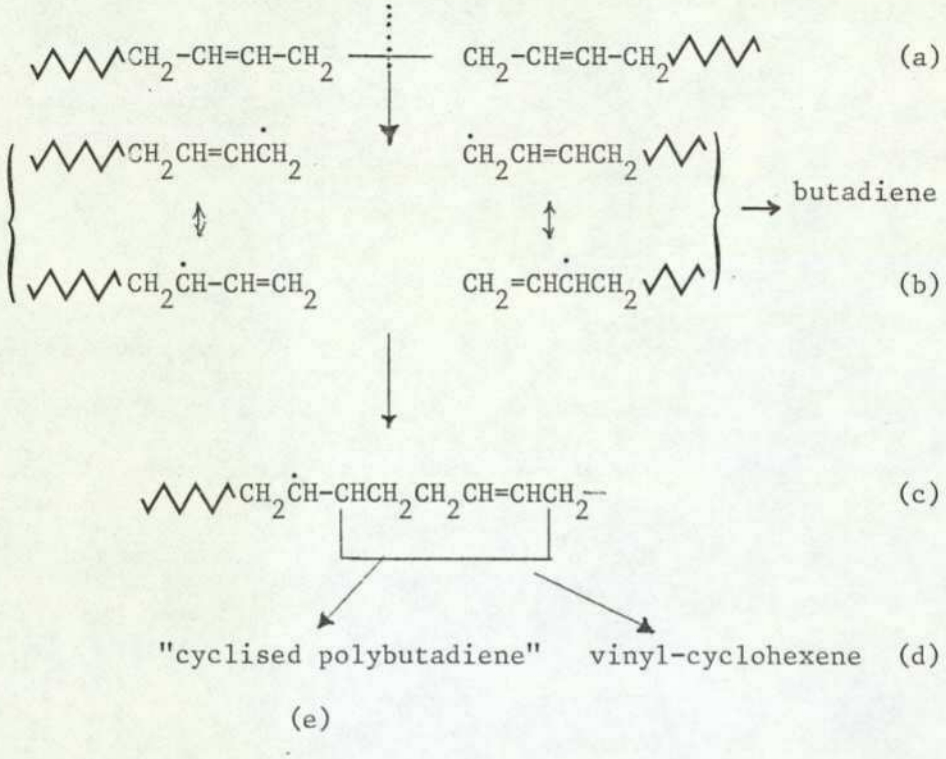

The presence of methyl groups and conjugated unsaturation in degraded polybutadiene has been reported by Golub and co-workers[64,65]. This can be explained by radical disproportionation:



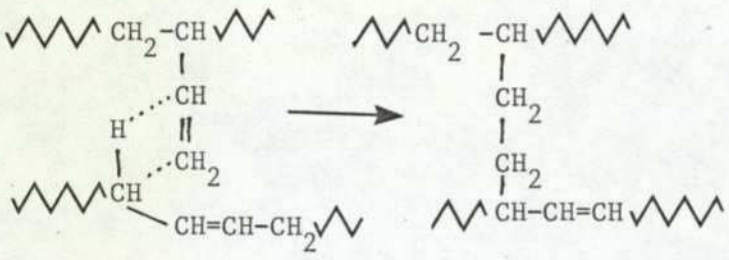
Grassie and Heaney[66] have shown that, when polybutadiene is heated at 230°C, there is an increase in the molecular

Table 10

Mechanism of the thermal cyclisation of polybutadiene of Golub and Gargiulo[12]



weight of the polymer due to crosslinking. Loss of vinyl groups, as followed by infrared spectrometry, were shown to be kinetically of the first order with respect of the vinyl groups. The energy of activation of this reaction is 63 k J.mole$^{-1}$. As the incorporation of free-radical inhibitors, such as diphenyl picryl hydrazyl and 1,4-diamino anthraquinone, produced no discernible effect on the rate of the vinyl loss curves, the reaction was assumed not to occur by a free radical mechanism. The following mechanism was proposed[66]:



1.2.2.3.2 Copolymers of Styrene and Acrylonitrile

It has become clear that the stability of copolymers can seldom be predicted accurately from the stabilities of the corresponding homopolymers[67-72]. Grassie and his co-workers[67-69] have demonstrated some of the ways in which comonomers may influence the stability of homopolymers either favourably or adversely. A series of papers[67-72] have demonstrated how traces of one monomer can influence the thermal decomposition of the other. However, in order to understand these effects, the decomposition of polystyrene and polyacrylonitrile is of some relevance.

(i) Polystyrene

Its high positive heat of formation indicates that polystyrene is an inherently unreactive material. The few routes by which polystyrene is decomposed are thermal degradation, thermal oxidative degradation, photodegradation and mechanical and shear degradation.

Pyrolysis of polystyrene[73-76] under high vacuum at temperatures within the range 330-380$^{o}$C results in the formation of 43% volatile materials (composed mainly of styrene) and 57% residue[77,78]. This residue contained a mixture of dimers, trimers, and tetramers with some remaining high polymers.

A rapid decrease in molecular weight of the

residue during the first 10% weight loss has been noted for samples having different values of initial molecular weight[79]. The "weak link" theory[80-83] has been proposed as an explanation for this rapid decrease. In later stages of the reaction, free-radical depolymerization causes the slower decrease in average chain lengths. Other workers contend however that there is no essential difference between the initial and final stages of the decomposition, and that the changes in molecular weight are mainly due to intermolecular chain transfer[79-84]. A third suggestion[85], based on a radiochemical study, is that both processes are simultaneously important. Experimental difficulties have clouded the development of an understanding in this area. Strong evidence against the weak link proposal has been provided by studies of the decomposition of poly(deuterostyrenes)[86] which show a much reduced initial decrease in molecular weight. On the other hand, arguments[87-89] that this observation is accounted for by intermolecular transfer have been shown to be ambiguous[90].

One limitation of some theoretical studies on the thermal decomposition of polystyrene stems from the inherent assumption of a constant molecular-weight distribution. More recently, the dependence of this distribution has been examined[91] for polystyrene prepared by free radical and anionic mechanisms.

Provided that the initial molecular weight is high, results showed that both the polymers rapidly approached a ratio of 1.5 (initial weight-to-number molecular-weight) as the volatilization proceeded. In addition to intermolecular transfer, this finding requires a radical-radical recombination process, probably by some sort of cage recombination.

Isothermal work[92] showed that the activation energy for the main decomposition step was about $250 \pm 20$ k J.mole$^{-1}$ and that this step was first order with respect to the polymer.

Pyrolysis at higher temperatures has been reported[91] but the results are even more difficult to interpret because secondary cracking reactions become important, especially if the primary degradation products are not removed very rapidly from the pyrolysis zone. At 800°C and 1200°C, the yield of styrene decreases rapidly, and ethylene and benzene appear in increasing amounts.

Pyrolysis of polystyrene under an inert atmosphere generally results in breakdown patterns basically similar to those occurring under high vacuum, although increased secondary fragmentation often takes place. In the presence of air, however, very much higher rates of degradation are observed. Oxidative degradation of polystyrene is a free-radical chain reaction, the rate of which is strongly influenced by light, heat, oxygen concentration, and impurities. The main propagation

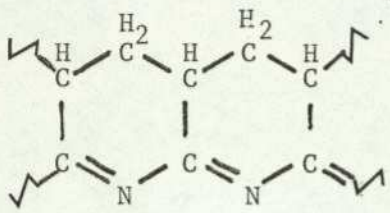
reaction occurs in two steps:

$$R^{\cdot} + O_2 \longrightarrow RO_2^{\cdot} \quad \text{and} \quad RO_2^{\cdot} + RH \longrightarrow RO_2H + R^{\cdot}$$

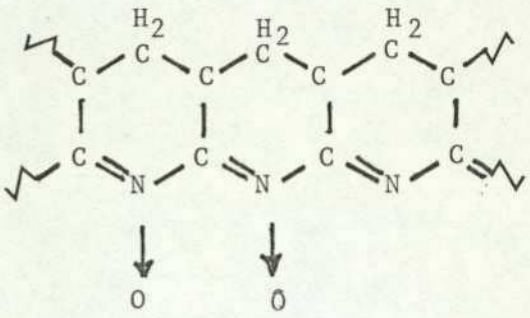
Decomposition of the hydroperoxide is catalysed by metal ion impurities and this; together with the chain reaction itself, is responsible for the autocatalytic nature of polymer oxidation processes. Infrared analysis of thermally oxidized polystyrene has shown the presence of ketones, esters or peroxides, and of ether or hydroxy groups[93]. A large number of volatile products are formed, including water, carbon dioxide, carbon monoxide, hydrogen, styrene, xylenes, and ethyl, propyl and butyl alcohols; the residue is highly crosslinked[94-95].

ii) Polyacrylonitrile

When polyacrylonitriles are heated to temperatures in the range of 150°C, intense colours slowly develop. The extent of colour formation will depend on the environment of the acrylic segment in the chain, the presence or absence of oxygen; the type of comonomers present; and the inevitable presence of impurities, polymerisation defects, and molecular chain ends. Various workers[96-105] have suggested a variety of routes and colour-producing species. Chemical tests have however established that the imine-nitrone structures are most probably responsible[104,105].



(imine)



(imine-nitrone)

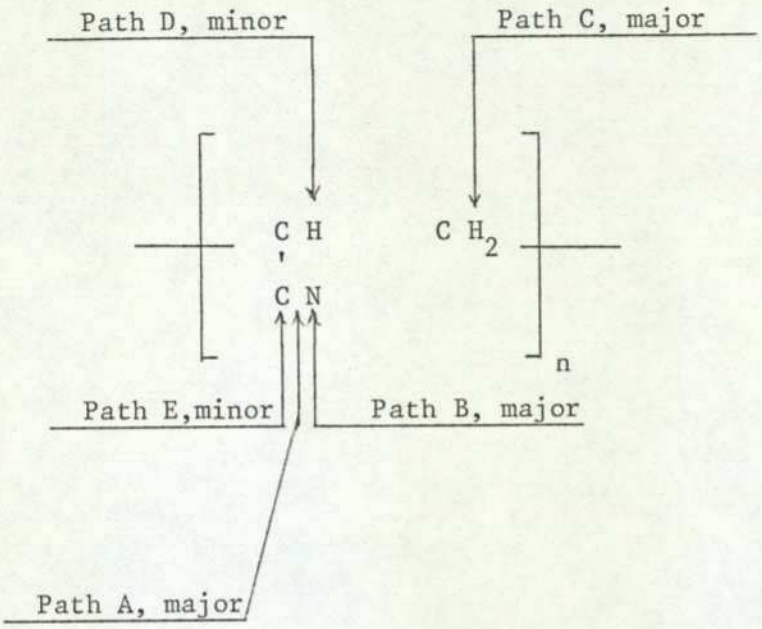
The polymerisation of the nitrile groups not only results in colour formation but also in the polymer becoming insoluble when it is degraded in the solid state.

The susceptibility of the acrylic repeat unit to decomposition is represented in Figure 2[105]. Paths A, B and E refer to attack on the nitrile group, whereas paths C and D indicated attack on the hydrogen atoms. The paths are labelled either as major or minor as a means of ranking their importance in thermo-oxidative degradation.

The rapid heating of polyacrylonitrile generally intiates an exothermic reaction followed by a loss in weight (Figure 3). The volatile products of this exothermic reaction have received extensive study. Figure 4 shows the mole percent of volatiles produced by heating a sample of polyacrylonitrile for 30 min. in a vacuum at various temperatures between 250 and 400°C. The products include volatile gases, such as hydrogen cyanide, and less volatile materials, such as monomers and dimers. The amount of heat

Figure 2

Mechanism of the thermal degradation of polyacrylonitrile




Path A: Nucleophilic agents either added as impurities, end groups, comonomers or as a result of Path B-E.

Path B: β-ketonitrile defect in the chain introduced during polymerisation.

Path C: Attack by oxygen.

Path D: Attack by oxygen.

Path E: Attack by oxygen.

Figure 3

DTA and TGA curves for Polyacrylonitrile heated at $10^{o}$/min : nitrogen (—), air (····), and vacuum(--)

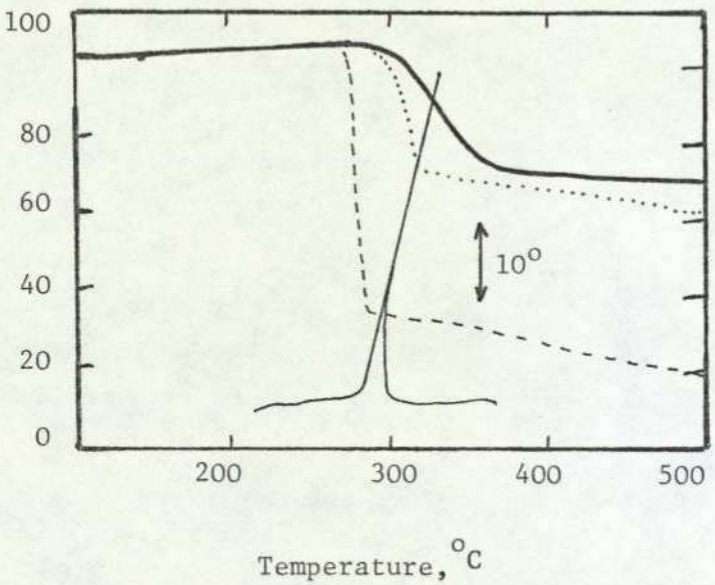
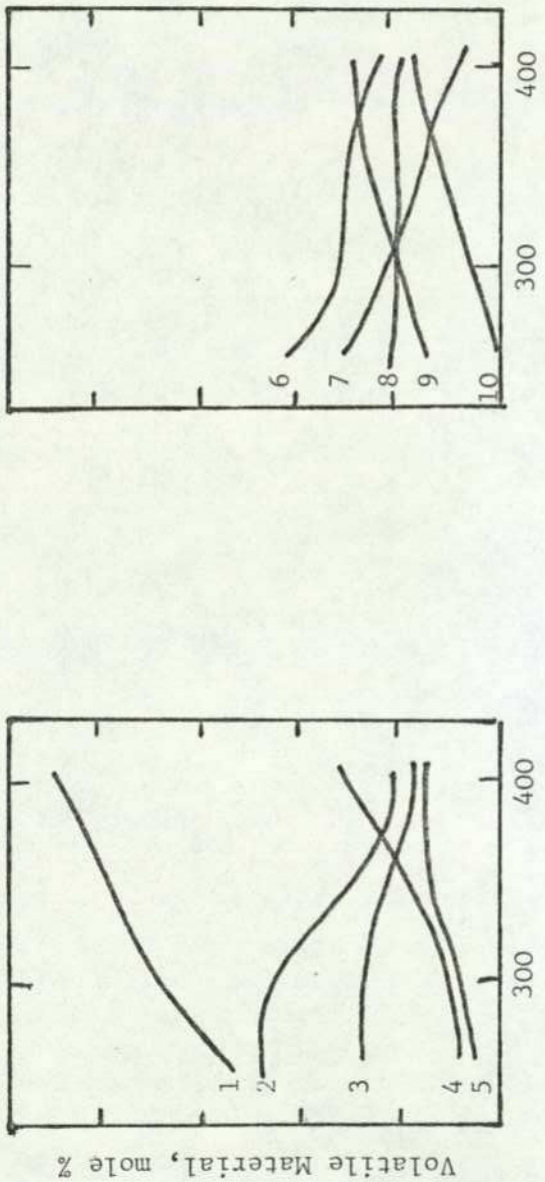


Figure 4

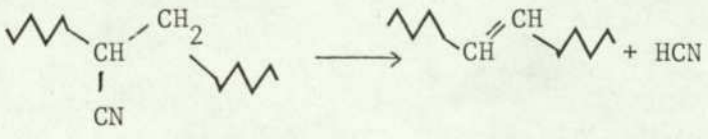
Mole percent of volatile material produced by heating polyacrylonitrile for 30 min. at the indicated temperatures.



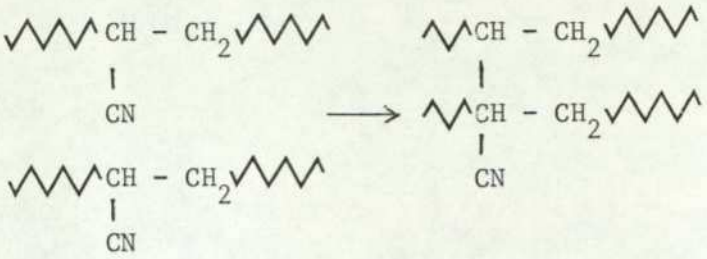

key: 1 hydrogen cyanide
2 acrylonitrile
3 methacrylonitrile
4 acetonitrile
5 propionitrile
6 2-methyleneglutaronitrile
7 2-methyl-4-methylene glutaronitrile
8 2-methylglutaronitrile
9 succinonitrile
10 glutaronitrile

released and the composition of the volatilized material are dependent on the conditions under which the exothermic reaction occurs[106]. Quantitative measurements of the heat liberated vary from 21.0 to 46.0 k J $mole^{-1}$. Part of the difference is due to the amount of heat required for volatilization. The reaction is caused by the uncontrolled polymerization of nitrile groups[106]; that is, the reaction reaches explosive speeds with an accompanying destruction of the polymer chain. The destructive reaction can occur at quite low ambient temperatures if the heat of polymerisation is not adequately removed and the interior of the polymer reaches the critical temperature[107]. Infrared spectra of polyacrylonitrile film after various heating times suggest that the α-hydrogen is involved in the reaction at high temperatures[106] and that the nitrile content decreases with exposure time.

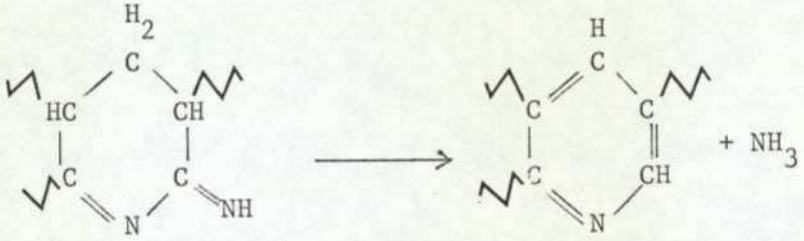
When polyacrylonitrile is heated in air under isothermal conditions, there is an increase in the oxygen uptake[108], and only small amounts of volatile materials are released, mainly ammonia and hydrogen cyanide, with some water and carbon dioxide. The structure of the oxidized polymer is the subject of much debate. The production of hydrogen cyanide at around 200°C can be a simple HCN elimination reaction occurring either - within a given polymer chain:[111]



or between different polymer chains[112,113].



Alternatively HCN can be produced during several steps involved in the thermal oxidation reaction[110]. Two mechanisms have been postulated for the production of ammonia : deamination of the polymerized nitrile chain end



or coupling of two chain ends

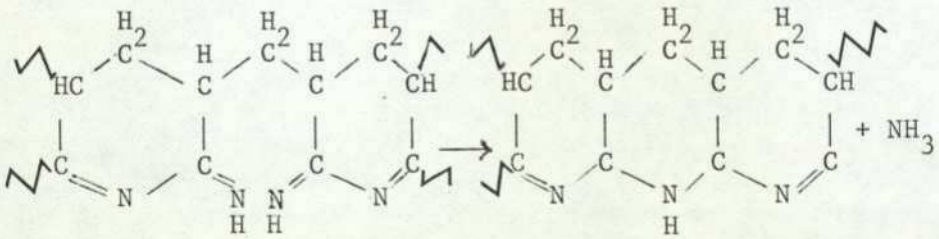
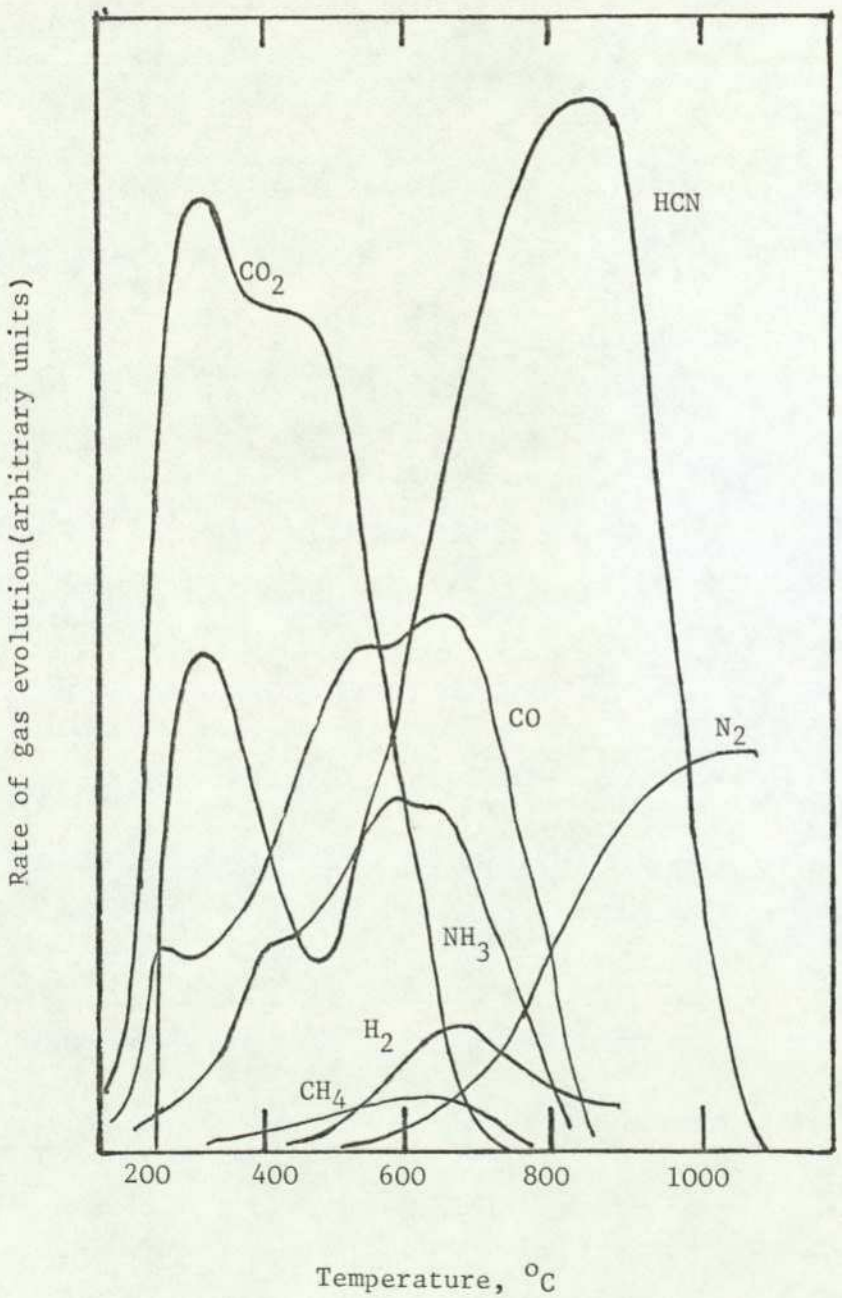


Figure 5 shows the rate of gas evolution, in arbitrary units, from a homopolymer previously heated in air for 5 hours at 250°C. The major part of the oxygen comes off as carbon monoxide, carbon dioxide and water. The

Figure 5

Rate of gas evolution for polyacrylonitrile fibres previously oxidized in air for 5 hours at 250°C, as a function of heat treatment temperature in helium.

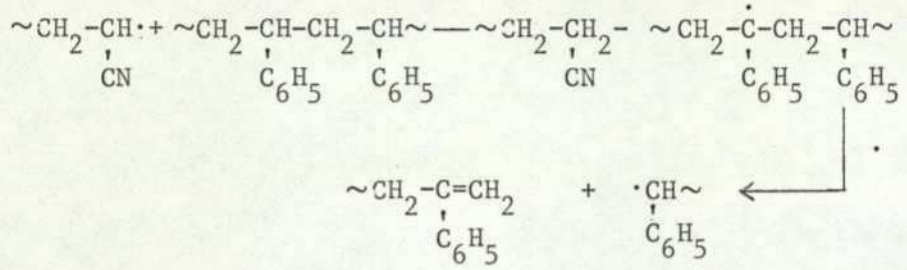


hydrogen is given off as water, hydrogen cyanide, ammonia and smaller amounts of methane and hydrogen, and the nitrogen is emitted as hydrogen cyanide, ammonia and nitrogen.

(iii) Styrene-acrylonitrile co-polymer (SAN)

A qualitative picture of the influence of copolymerised acrylonitrile on the thermal decomposition of polystyrene emerges from the work of Grassie and Bain[114]. The invariant position of the maximum and shape of the TGA curves suggest that the presence of acrylonitrile does not alter the reaction mechanism in any significant way. This is confirmed by the negligible influence of up to 4.7% acrylonitrile on both the rate of volatilisation and on changes in molecular weight. With higher acrylonitrile contents, there is an increase in rate of volatilisation which is closely proportional to the acrylonitrile content and which, in terms of the radical chain nature of the reaction, must be due either to an increased rate or to an increase in zip-length. It is found that the primary influence of the acrylonitrile is to increase the rate of chain scission to produce depropagating radicals. The zip-length is relatively little affected, showing that depolymerisation can occur relatively easily throughout acrylonitrile units in the polymer chain. An increasing ratio of chain fragments to monomer among the products, as the acrylonitrile content is increased, demonstrates however that acrylonitrile-terminated radicals show a greater tendency than styrene-terminated radicals to

liberate large chain fragments rather than monomer in intramolecular transfer processes. Since the amount of intramolecular transfer thus clearly increases with acrylonitrile content; the acrylonitrile-terminated decomposition radicals may also show a greater tendency than the styrene-terminated radicals to take part in intermolecular transfer processes:



The prinicipal products of the decomposition of styrene-acrylonitrile co-polymers containing up to 33% acrylonitrile can be explained in terms of the same kind of depolymerisation mechanism as occurs in polystyrene. This involves depropagation to produce monomer and intramoleculer transfer to give chain fragments, principally dimer and trimer. Inspite of the fact that acrylonitrile is not a significant decomposition product of polyacrylonitrile, depropagation can readily pass through isolated acrylonitrile units into polystyrene rich copolymers, liberating monomer. The appearance of hydrogen cyanide as a minor product is associated with the development of ethylenic unsaturation in the residual polymer. Although the amounts of hydrogen cyanide have not been accurately measured, they are clearly proportionately greater than those obtained from pure polyacrylonitrile. This may be associated with the fact that separation of acrylonitrile units by styrene

in the copolymers inhibits the nitrile condensation reaction which occurs so readily in polyacrylonitrile[115] at much lower temperatures. The intact acrylonitrile units are thus still free to decompose to acid and olefin at high temperatures.

The minor products, toluene and benzene, are produced in about the same proportions, relative to styrene, as from polystyrene but, as in previous studies of the decomposition of polystyrene, their precise mode of formation is not fully understood.

### 1.2.3 Tests for polymer flammability

"An incombustible material means to the user of the word a material which will not burn under the conditions of exposure which he has in mind. It will not necessarily have the same meaning to others unless those conditions are defined"[116].

Over the years, the field of fire-retardant polymers has been plagued by terms without clearly defined meanings. Such terms as fire proof, fire retardant, fire resistant, flame resistant and noncombustible have been used indiscriminately and often interchangeably. These can be misleading even when qualified by a description of the fire conditions of a recognised test. Polymers in general, will burn, pyrolyze, or char at elevated temperatures, although their individual burning characteristics may vary widely. Any meaningful comparison can be made only on the basis of standardized testing procedure. The development of suitable test methods have been a major objective of many governmental bodies, industry and recognised standards organisations as the American Society for Testing and Materials, the British Standards Institute, the Underwriters' Laboratories and various other bodies.

Until 1976, most fire-retardancy test methods logically classified the polymer tested into one of the following three general categories:

1) Those samples that were virtually consumed under the test conditions were classified as burning.

2) Samples that burned for a limited period of time after removal of the test flame, but became extinguished before the test specimen was completely consumed, were generally classified as self-extinguishing.

3) Test specimens that did not ignite under the conditions or became extinguished so rapidly after the removal of the test flame that the self-extinguishing time could be conveniently measured were usually classed as non-burning or, in some cases, immediately self-extinguishing.

The ambiguous classifications such as nonburning and self-extinguishing have now been eliminated from test results and replaced with new test designations.

The general lack of correlation of most of the small-scale laboratory test methods with real fire conditions, where large quantities of materials are involved, has led to an uncertainty concerning the interpretation and meaning of the test results. A recent analysis of test resultsobtained from a spectrum of nationally approved test methods and standards presently in force in Europe shows an array of inconsistent results[117]. Hence there is a need to develop more large-scale tests and models that would give a more realistic evaluation of real fire hazards[118]. Methods for the evaluation of polymer flammability are presently in a high

state of flux owing to these uncertainities. However, many of the ASTM test methods remain as the only standards currently available. In addition, some others are still useful as comparative measures of polymer flammability on a laboratory scale. As such, they remain a significant force in fire-retardancy technology at the present time.

1.2.3.1 Screening tests (small-scale)

The importance of such tests has drastically decreased recently, with the advent of government regulations limiting the reference of screening test results as a measure of polymer fire retardancy in technical literature and product advertising. It is doubtful whether they will be of appreciable future importance as a measure of polymer flammability except as a comparative assessment of relative flammability in experimental research or for quality control assessment in industry which was the primary purpose of their development. The many variables affecting polymer burning characteristics cause the problem to behave differently depending upon the test method used. Thus, it is important to understand the various test characteristics and conditions in order to relate the results to polymer behaviour in specific commercial applications. Some of the more common test methods are discussed below.

ASTM D2867-77 Oxygen Index Test.

The oxygen index test method was originally developed by Fenimore and Martin[119] and determines the relative flammability of plastics by measuring the minimum oxygen concentration in a slowly rising mixture of oxygen and nitrogen that will just support combustion of a candle-like sample of the material to be evaluated. A schematic diagram of the test

apparatus is indicated in Figure 6. The minimum concentration of oxygen in a mixture of oxygen and nitrogen flowing upwards in a test column that will support combustion is measured under equilibrium conditions of candle-like burning. The equilibrium is established by the reation between the heat generated from the combustion of the specimen and the heat lost to the surroundings as measured by one or other of two arbitrary criteria, namely, a time of burning (3 min.) or a length of specimen burned (50mm.).

The test column consisted of a heat-resistant glass tube of 75 mm. minimum inside diameter and 450 mm. minimum height. The bottom of the column or base to which the tube is attached contained a noncombustible material to mix and distribute evenly the gas mixture entering at the base. The sample holder consisted of a small holding device that could support the specimen at its base and hold it vertically in the centre of the column.

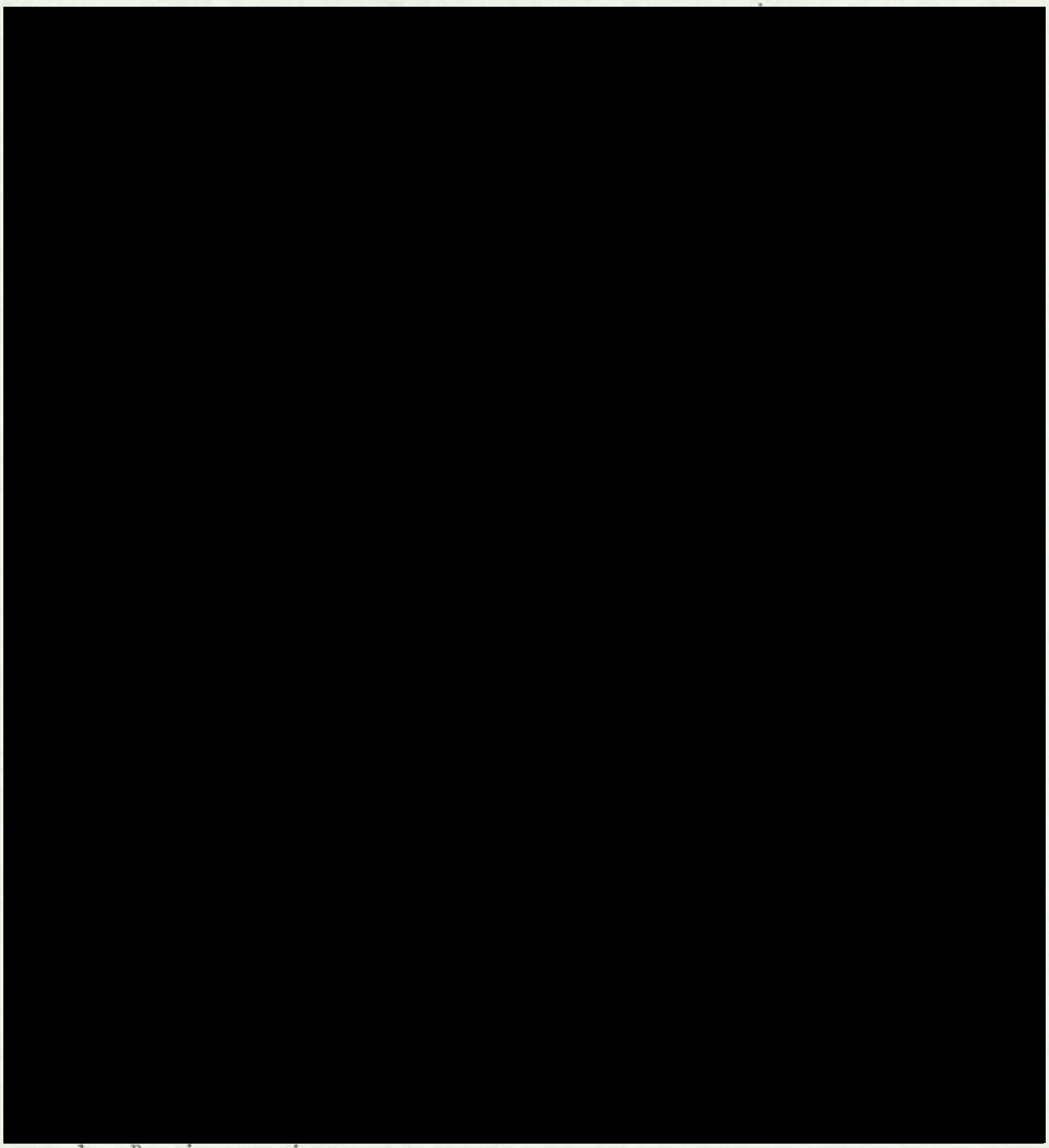
Commercial grade (or better) oxygen and nitrogen are used. Suitable flow measurement and control devices are employed which allow the volumetric flow of each gas into the column within 1% in the range being used.

To ensure the removal of toxic fumes, soot, heat and other possible noxious products, the column was installed in a hood providing adequate exhaust.

The oxygen index test method is perhaps the most commonly

FIGURE 6

Oxygen Index Test Apparatus



| | | | |
|---|---|---|---|
| 1 | Burning specimen | | |
| 2 | Clampwith rod support | 9 | Cut-off valve |
| 3 | Igniter | 10 | Orifice in holder |
| 4 | Wire screen | 11 | Pressure gauge |
| 5 | Ring stand | 12 | Precision pressure regulator |
| 6 | Glass beads in a bed | 13 | Filter |
| 7 | Brass base | 14 | Needle valve |
| 8 | T junction | 15 | Rotameter |

used flammability screening test for polymeric materials at the present time. Its major advantages are excellent reproducibility and the fact that the results can be arranged in a numerical scale of values upon which all presently available polymers can be ranked in an order of decreasing flammability. However, the results cannot necessarily be used to predict the flammability behaviour under end-use conditions and must not be used for the description or appraisal of the fire hazard of materials, products, or systems under actual fire conditions.

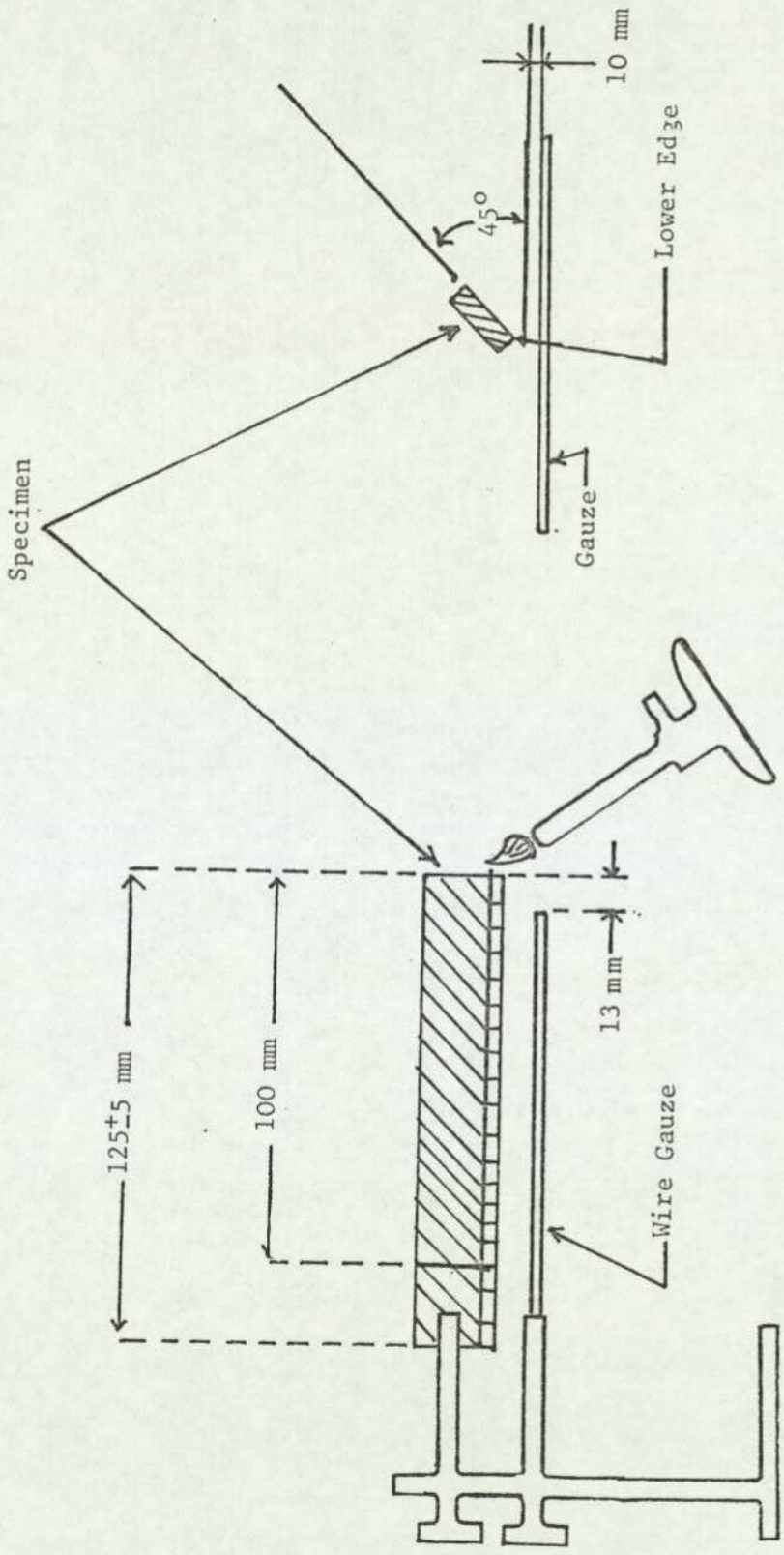
The tests and various parameters affecting the results will be described in Section 1.2.3.4 and 1.2.3.5.

ASTM D635-77. Rate of burning and/or extent and time of burning of self-supporting plastics in a horizontal position.

This test is a standard method for obtaining comparative data on moderately fire-retardant polymeric materials. The apparatus used is shown in Figure 7. A blue flame, 25mm high, is touched to a specimen of the polymer (125mm x 12.5mm x 12.5mm) for 30 sec. The procedure is repeated until three specimens have burned to the gauge mark previously inscribed 100mm from the ignition end of the specimen or until a total of ten specimens have been tested. The burning rate, average time of burning (ATB) and average extent of burning (AEB) are then calculated relative to the gauge mark. The burning rate is reported in cm per min. if two or more of the

FIGURE 7

Rate and time of burning of self-supporting plastics in a horizontal position



ten specimens burn to the gauge mark. ATB and AEB are given by:-

$$ATB = \Sigma\frac{(t - 30s)}{n} \; ; \quad AEB,mm = \Sigma\frac{(100mm - \text{unburned length})}{n}$$

where n = number of specimens.

The most serious deficiences of the test are that it fails to measure the actual fire hazard and to distinguish between polymers which do not drip and those which melt, as the flame progresses down the sample, with quantities of flaming molten polymer falling away from the test sample in the process. This can lead to erroneous results as the flame front may be carried away by the falling drips or the flame can be spread by this drip.

The Underwriters' Laboratories have suggested a modification of ASTM D635 on account of the deficiences discussed above. A distinction is made between those samples which ignite a wad of cotton placed beneath the burning end of the specimen and those in which the drip is nonexistent or insufficient to ignite the cotton. In spite of the additional information obtained by this modification, the results do not necessarily correlate with the larger fire hazard tests.

ASTM D568-77 Rate of burning and/or extent and time of burning of flexible plastics in a vertical position.

This test is similar to the ASTM D635-77 except that the plastic is flexible and is heated in a vertical position

so that the heat from the flames rises to heat the remaining polymer and helps to propagate the flame.

The test involves ten test specimens 25mm wide, 450 mm long and 3 mm thick. A gauge mark is drawn across the specimens 70 mm from one end, defining a 380 mm gauge length over which the burning rate is to be measured.

The apparatus is shown in Figure 8. The specimen is clamped vertically so that 430 mm is exposed below the clamp gauge mark at the top. A burner is placed directly under the specimen and provides a flame about 25 mm in total height. The time taken for the specimen to ignite (t's) is recorded. This should not exceed 15s. If the specimen melts and shrinks away from the flame as far as the gauge mark without igniting, the test is not applicable. If the specimen ignites, it is then enclosed by a chimney and the time is recorded in seconds (t) when the flame front reaches the gauge mark or when the flame is extinguished. If the flame is extinguished before reaching the gauge mark, the length (l cm) of unburned test length is recorded. The procedure is repeated until three samples have burned up to or beyond the gauge mark or ten samples have been tested. The rate of burning is calculated in cm $min^{-1}$ by dividing 38 cm by the time in minutes (t/60). The average time of burning (ATB) and average extent of burning (AEB) are given by:

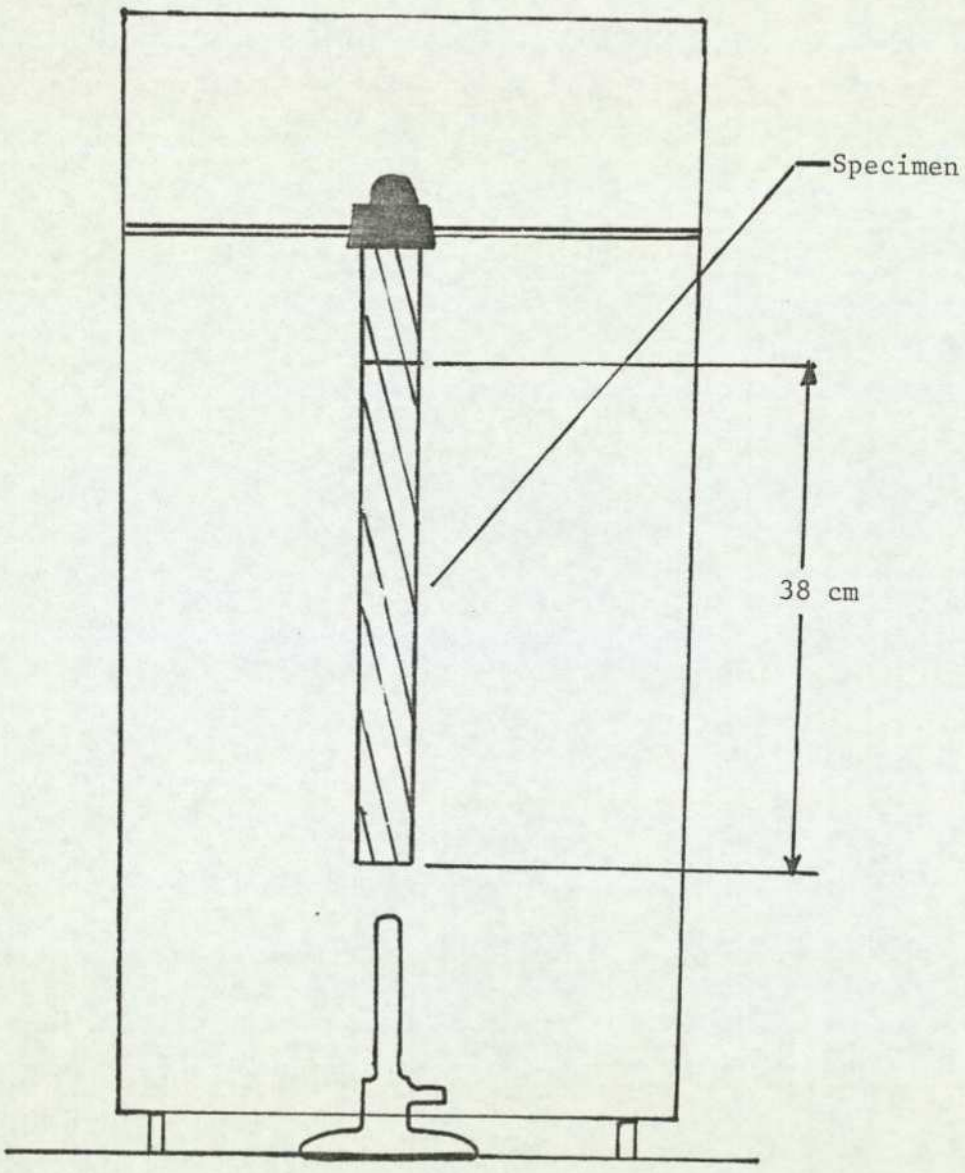
$$ATB = \Sigma(t-t')/\text{number of specimens}$$

$$AEB = \Sigma(38-1)/\text{number of specimens}$$

FIGURE 8

Rate and time of burning of

flexible plastics in a vertical position



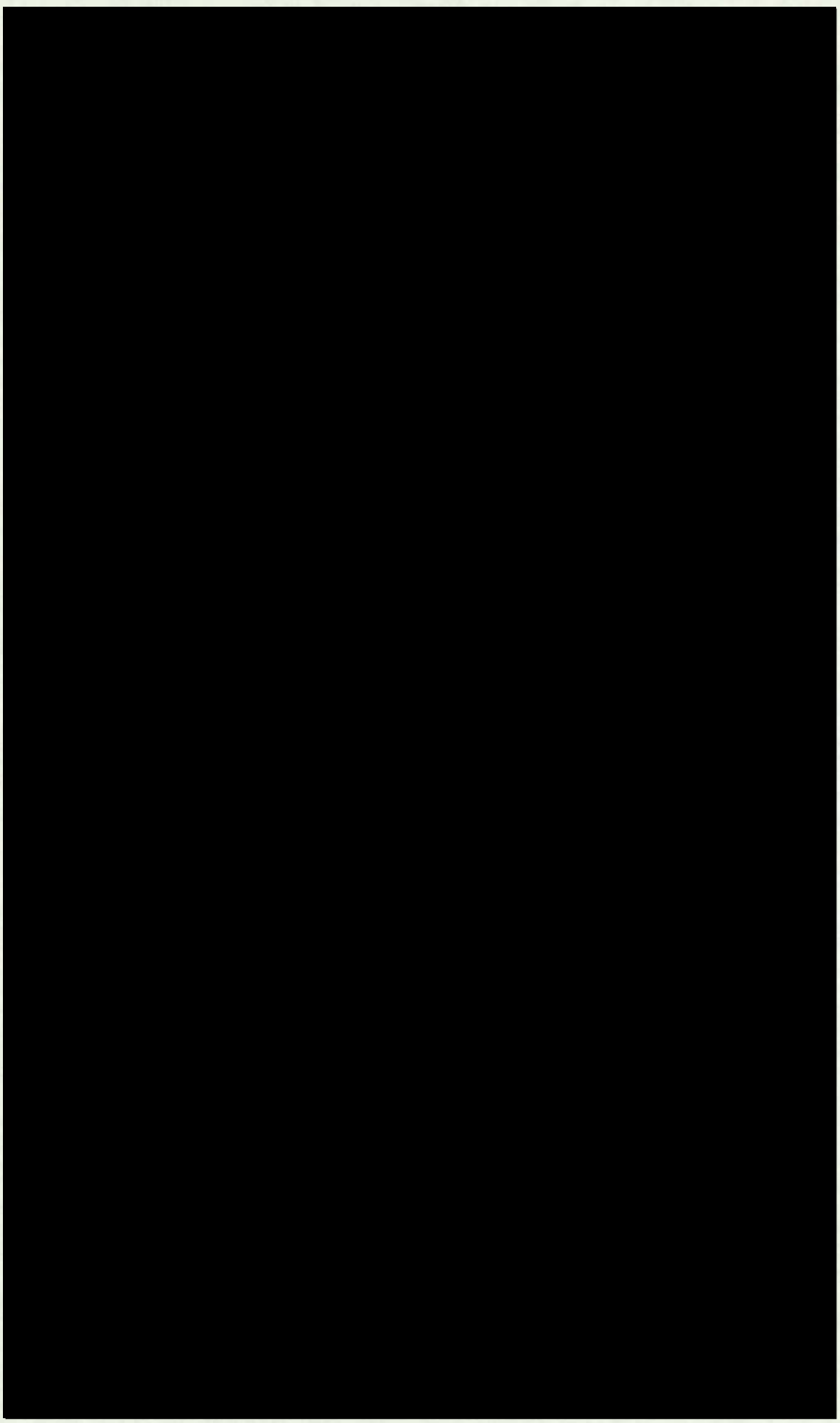
In recent variations of the test, a piece of cotton wool is placed vertically below the burning sample and any ignition of the wool caused by burning material dropping from the sample is taken into account when determining the degree of flammability of the sample. The test still gives only an indication of dripping or non-dripping burning and gives no quantitative data about the rate of dripping etc.

ASTM D757-77 In candescence resistance of rigid plastics in a horizontal position.

This test was developed specifically for the comparison of rigid plastic sheets or plates at least 1.3 mm thick. It may be used to supplement the results obtained from a flame source ignition test such as ASTM D635. This test follows ASTM D635 in increasing severity and was found to be necessary on account of the wide variety of plastics showing little or no burning by the latter test. The test specimen is brought into contact with an electrically heated ignition bar set at a specified temperature of 950$^{o}$C for a period of 3 min or until the specimen ceases to burn. (See Figure 9). At the end of this test period any flame remaining is extinguished and the burning rate in mm min$^{-1}$ is calculated from the length of the burned part of the specimen for those specimens which continue to burn for the 3-min. test time. The burning time in seconds and extent of burning in mm are reported for those compositions which do not burn for the full 3-min. period. Highly fire-retardant compositions will be extinguished before completion

FIGURE 9

ASTM D 757



of the ignition period. Although this test is useful in comparing the flammability characteristics of different materials, it also does not directly correlate with flammabilities to be expected under conditions of an actual fire.

HLT 15. Hooker Laboratory Intermittent Flame Test

This is a more severe laboratory test capable of distinguishing between materials rated as non-burning by all of the above tests[120]. It is principally intended for highly flame-retardant materials. In this test, a flame is applied to the bottom of a specimen, vertically suspended, intermittently and for increasingly longer periods. The time of burning is noted after each application of the flame. A rating from 0 to 100 can then be calculated from the time to extinguishment after each ignition period. On account of the relative severity of the conditions, this test is capable of differentiating between more heavily fire-retarded materials which exhibit low burning rates according to ASTM D757. It is unsuitable, however, for accurate measurement of materials with moderate or low fire retardancy. Highly fire-retardant materials produce numerical ratings of 80-100 under these test conditions.

UL Subject 94. Standards for tests for flammability of plastic materials for parts in devices and appliances.

This test is an important method for classifying polymeric materials to be used in electrical applications. Although the standards include a D635-type test for less fire-retardant requirements, the vertical test method has assumed overriding importance because of greater severity and the increasing requirement for more fire-retardant materials in these market-areas.[121] Only the vertical test is discussed here.

The test specimens are 125 mm. long and 12 mm. wide, in both 3 and 1.5 mm. thickness. Two sets of specimens of each thickness, with three specimens per set, are provided for each test. One set of each thickness is treated in the "as received" condition; the other set is treated after being aged in an oven at 70°C for a duration of 7 days. The burning test is conducted in an area free from draughts. The test specimen, supported vertically by its upper end, is ignited at the lower end for 10 sec by a Bunsen burner (tube placed 4.5 mm below the specimen with a 9 mm blue flame). If flaming or glowing combustion stops within 30 sec after the removal of the flame, the sample is reignited for 10 sec. The duration of flaming or glowing is again noted. If the specimen drips flaming particles, these are allowed to fall into a layer of surgical cotton wool placed 300 mm below the sample. The dripping particles are considered significant if the cotton ignites. Flammability ratings of V0, V1 and V2 are applied depending upon the specimen behaviour during

the test. Partial definitions of these ratings are given in Table 11.

ASTM D3014-76 Flame height, time of burning, and loss of weight of rigid cellular plastics in a vertical position.

This test is very similar to D 568 and is also conducted in a chimney as illustrated in Figure 10. The chimney is galvanized. In it is fastened an insert made of 0.025 mm aluminium foil. The insert is held in place by a stainless steel channel which supports the specimen. A scale, reading in mm, graduated at 10-mm intervals, is provided to determine flame height. The specimen 254 x 19 x 19 mm is ignited at the bottom by a burner with the blue inner cone of the flame (35 mm high). The maximum height of the flame, the time of burning, and the average weight per cent retained for six specimens are reported.

ASTM E162-67 Surface flammability of materials using a radiant heat energy source.

This test measures the surface flammability of materials and is to be used for research and development purposes only. The method employs a 305 x 457 mm radiant-panel heat source in front of which is placed a 152 x 457 mm specimen of the test material on a plane $30^{o}$ from the vertical plane of the panel (Figure 11). The specimen is oriented relative to the heat source in such a manner that it is closest to the source on the top, so that ignition

Table 11

Ul 94 Test flammability classification for Polymeric Materials.

| | |
|---|---|
| VO | no test specimens burn longer than 10 sec. after each removal of flame. No specimens exhibit flaming drip that ignites dry surgical cotton wool placed 500 mm. below the test specimen, nor does afterglow persist for longer than 30sec. |
| V1 | this classification is identical to VO above except that test specimens must extinguish within a 30 sec. interval after flame removal and no afterglow persisting for longer than 60 sec. |
| V2 | this classification is identical to V1 except that flaming drip from some specimens ignites the dry cotton wool placed below the specimen. |

FIGURE 10

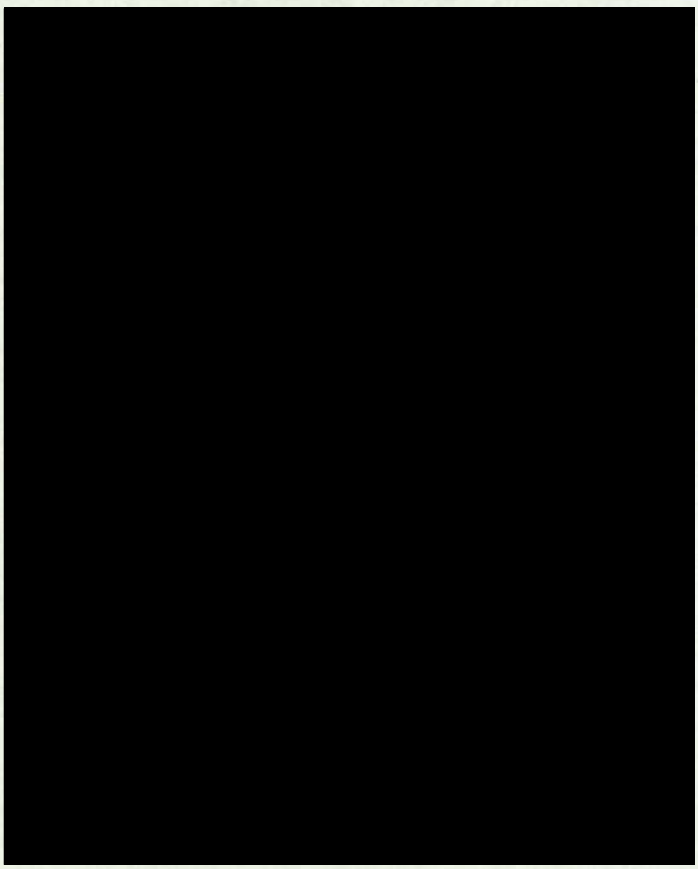
ASTM D 3014-76 : Flame height, time of burning and loss of weight of rigid cellular plastics in the vertical position





FIGURE 11

Radiant panel flame spread test equipment, ASTM E162-67



is forced at the upper end and the flame front progresses downwards. The radiant-panel heat source consists of a porous refractory material heated by gas at a temperature of 670°C(1238°F). The entire apparatus is placed below a vented stack containing thermocouples and a smoke-sampling device.

The test is conducted by placing the holder containing the specimen in the required position adjacent to the heat source until the flame front has progressed the full length of the sample or for an exposure time of 15 min. During this time the stack temperature is continually recorded while the progress of the flamefront down the specimen is noted by observing the time at which it arrives at a series of marks spaced 76 mm apart on the specimen holder. During this time a portion of the stack gases is passed through a sampling device containing a glass-fibre filter which is weighed before and after the test period. The flame-spread index is calculated as a product of a flame-spread factor and heat-evolution factor which are obtained from the test data. The smoke is reported as the total weight of the solid collected on the filter of the smoke-measuring device during the test period. Highly fire-retardant materials exhibit index values of 25 or less by this test method, while standard red oak yields an index of 100.

1.2.3.2 Use evaluation tests (large scale)

These tests usually give a better approximation to the flammability behaviour of large sized polymer samples under more realistic conditions, such as, good oxygen supply caused by controlled draught of air, flaming ignition and radiant heat. The basic apparatus is expensive and the tests become more wasteful as they increase in size and approach more nearly the conditions found in a large scale fire.

ASTM E84-77 Test for Surface Burning Characteristics of Building Materials - Tunnel Test.

This test was developed by the Underwriters' Laboratories,Inc., and is used to determine the surface burning characteristics of any building material that is capable of supporting itself in position on the roof section of the test furnace. The test correlates the burning characteristics of the material directly with its behaviour under conditions of use. The apparatus schematically illustrated in Figure 12, consists of a chamber 7.62 m. in length and 450 x 300 mm. in cross-section, one end of which contains two gas burners. A 7.62 x 6.00 m test sample is exposed to the gas flame for 10 min, while the maximum extent of the flame spread and the temperature down the tunnel

FIGURE 12

U L Tunnel test - ASTM E 84-70, cross section



are observed. In addition to flame spread, the test has been modified to yield a measure of smoke evolution from the material by the installation of a photo-electric cell in the exhaust stack downstream from the test specimen. The smoke density of the exhaust gases is measured continuously and assigned a value relative to the behaviour expected in a standard evaluation of red oak. The flame spread and smoke evolution are reported on an arbitrary scale upon which asbestos board and red oak have a value of 0 and 100, respectively. More highly fire-retardant materials obtain ratings of 0-25 by this method.

BS476: Part 7: 1971 Surface spread of flames.

This specification contains two tests which differ only in size. The test is intended for the classification of the exposed surfaces of walls and ceilings, according to the rate and distance of spread of flame across them. The larger test is described below.

Six specimens are used, which are of dimensions 230 x 900 mm each and of normal thickness where this does not exceed 50 mm. They are backed by the normal backing material used in industry. The edges of the samples, and also a strip 40 mm wide from the edges on the unexposed face, are painted with sodium silicate of a specified consistency.

The apparatus consists of a vertically mounted radiation panel, 900 mm square, provided with a refractory concrete surround projecting about 225 mm from the face of the panel. On each side of the panel, at midheight, are mounted sample holders, hinged to the side of the furnace. These consist of steel frames with asbestos insulation board horizontal guides to locate the sample. In each experiment, the sample is placed on one side of the furnace and the sample holder on the other side carries the thermocouples used for controlling the temperature of the furnace. The apparatus is shown in Figure 13.

When the sample is brought into position, the end nearest the panel is ignited with a standard flame for 60 sec. The time for the flame front to reach a series of marks at given distances from the panel are noted. Samples are classified as in Table 12.

BS 476: Part 6: 1970 Fire propagation test.

This test provides a means of comparing the contribution of combustible building materials with the growth of a fire. It must be carried out in conjunction with the ignitibility test specified in BS476, Part 5; which will be described in Section (C).

FIGURE 13

BS 476 : part 7 : 1971 : Surface spread of flames





Table 12

BS476: Part 7 Test : flame spread classification

| Classification | Flame spread at 90sec. | | Final flame spread | |
|---|---|---|---|---|
| | Limit | Tolerance for 1 specimen in sample batch | Limit | Tolerance for 1 specimen in sample batch |
| | mm | | mm | |
| Class 1 | 165 | 25 | 165 | 25 |
| Class 2 | 215 | 25 | 455 | 45 |
| Class 3 | 265 | 25 | 710 | 75 |
| Class 4 | exceeding class 3 limits | | | |

The apparatus for this test is shown in Fig. 14. It consists of a combustion chamber measuring internally 190 x 190 x 190 mm with one 190 mm square vertical face open and an air inlet slot 95 mm x 25 mm cut out at the centre of the lower edge of the opposite face which also has a mica window for observation purposes. On the top face of the chamber a 1.0 mm thick sheet steel chimney, 38 mm in internal diameter and 190 mm in length is fixed over a 38 mm diameter central hole, and provided with a removable steel cowl 152 mm high by 76 mm internal diameter having two diametrically opposite bushed holes to accommodate the thermocouples.

The specimen is initially placed in position, the chamber is closed and the gas jets are ignited. After 165 sec, the electrical elements are switched on to an input of 1800 watts. After a further 135 sec. the power is cut to 1500 watts and then held constant for the normal duration of the test (20 min.).

The apparatus is calibrated with asbestos board, immediately before each of three runs. A calibration curve of the type shown in Figure 15 is obtained. This must be reproducible within the defined limits.

Temperature readings are obtained either continuously, or at specified time intervals and the index of performance is defined as:

$$I = \sum_{1/2}^{3} \frac{Tm-Tc}{10t} + \sum_{4}^{10} \frac{Tm-Tc}{10t} + \sum_{12}^{20} \frac{Tm-Tc}{10t}$$

FIGURE 14

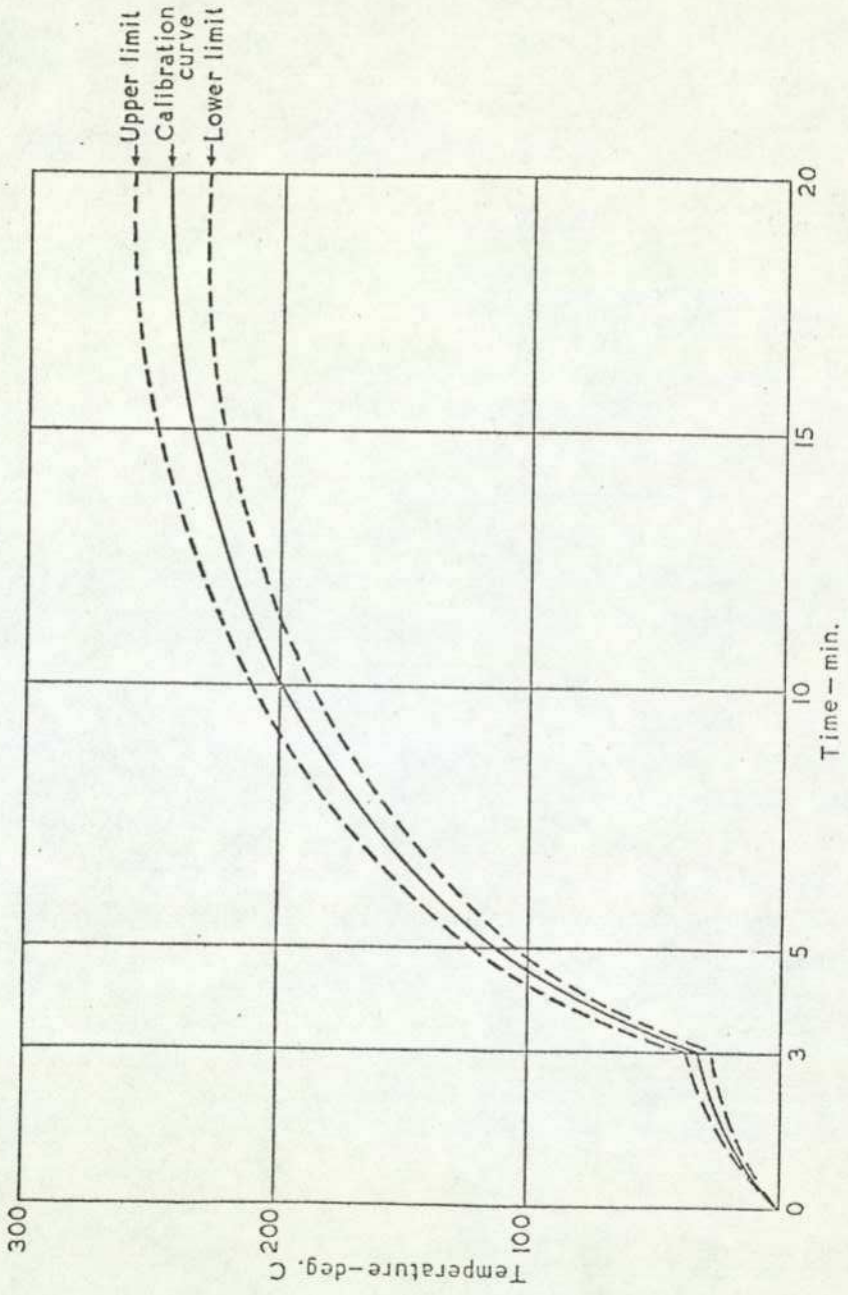
BS 476 : part 6 : 1970 : Fire Propagation Test





FIGURE 15

BS 476 : part 6 Calibration curves



where I = Index of performance

t = Time in min from the origin at which readings are taken.

Tm = Temperature in deg C of the mean curve for the material at time t.

To = Temperature in deg C of the calibration curve for the apparatus at time t.

In computations only the positive value of $\frac{Tm-Tc}{10t}$ is used.

The Corner Test

This test has recently been under intensive study as a candidate test method capable of yielding results more representative of the actual behaviour of real building fires[122]. This test requires the construction from materials to be tested of a full-scale mockup of one corner of a room complete with ceiling. The corner is considered to be more representative of an actual fire hazard because of the enhanced chimney effect and a concentration of radiation effects. Generally, an ignition source is set in the corner on the floor and the rate of propagation of the fire up the wall and across the ceiling can be used to evaluate the fire hazard expected in common building construction. Williamson and Baron[118] have investigated the severity of several ignition sources in such a corner configuration. Additionally, they have evaluated the behaviour of some commercial

polyurethane foam insulation products reported to have flame-spread ratings by ASTME-84 of 25 or less and found the materials to be extremely flammable by this test method.

1.2.3.3 Miscellaneous Tests

In addition to those tests already discussed, there are many that review special properties. Some of these will be discussed below.

ASTM D1929-77 Ignition properties of plastics.

This test determines the self-ignition and flash ignition temperatures for a polymer using a hot-air ignition furnace of the type shown in Figure 16.

Self-ignition temperature is defined as the lowest initial air temperature passing round a sample at which it will ignite in the absence of an ignition source.

The flash ignition temperature is the lowest initial temperature at which enough combustible fuel is evolved from the sample to be ignited by an external source.

The sample, in the form of pellets or sheets of polymer, is placed in a steel pan which can be raised and lowered to a given depth in the furnace by means of the support rod. Chromel-alumel thermocouples, T1, T2 and T3, are situated in the test chamber in such a way that T1 measures the temperature of the sample, T2 that of the air flowing past the specimen and T3 that of the coil.

1.2.3.3 Miscellaneous Tests

In addition to those tests already discussed, there are many that review special properties. Some of these will be discussed below.

ASTM D1929-77 Ignition properties of plastics.

This test determines the self-ignition and flash ignition temperatures for a polymer using a hot-air ignition furnace of the type shown in Figure 16.

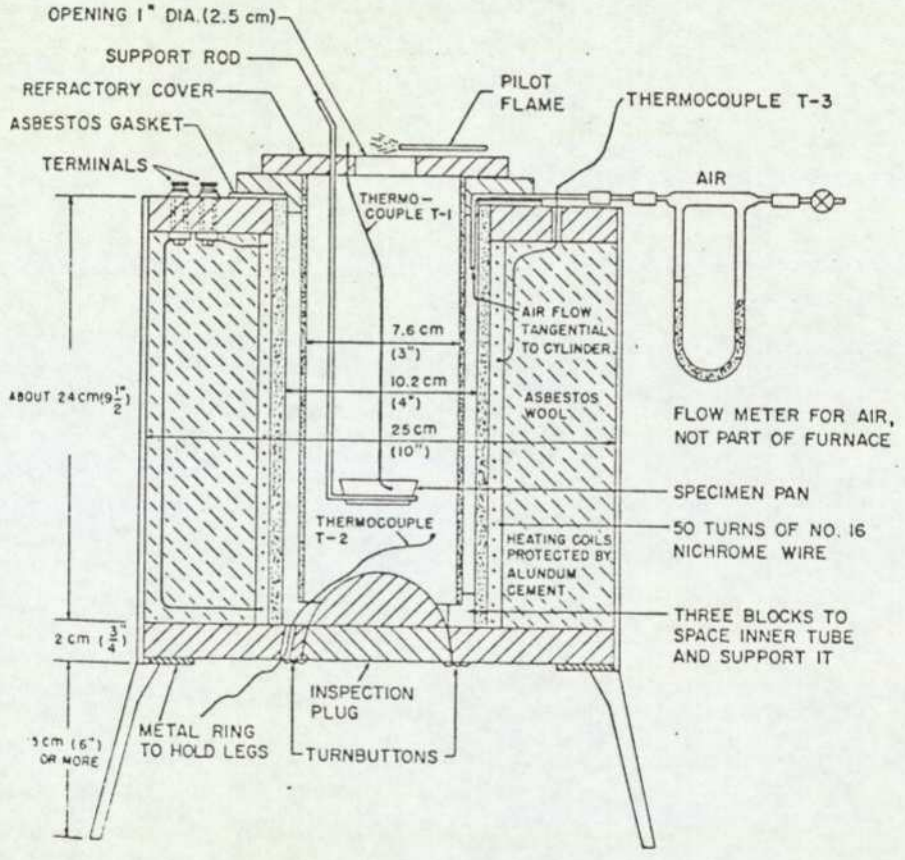
Self-ignition temperature is defined as the lowest initial air temperature passing round a sample at which it will ignite in the absence of an ignition source.

The flash ignition temperature is the lowest initial temperature at which enough combustible fuel is evolved from the sample to be ignited by an external source.

The sample, in the form of pellets or sheets of polymer, is placed in a steel pan which can be raised and lowered to a given depth in the furnace by means of the support rod. Chromel-alumel thermocouples, T1, T2 and T3, are situated in the test chamber in such a way that T1 measures the temperature of the sample, T2 that of the air flowing past the specimen and T3 that of the coil.

FIGURE 16

Cross Section of Hot-Air
Ignition Furnace Assembly



The test procedure is quite complicated, but gives accurate, reproducible results. Initial approximate tests are carried out at three different air flow rates. The sample is placed in the furnace and the temperature of the gas is slowly raised until the pilot light ignites the gases at the exit from the furnace and causes flash-back to the sample. The flash-back is shown by a sudden rise in T1. The value of T2 corresponding to this gas temperature is the approximate flash ignition temperature. To determine this more accurately, the air flow rate is chosen which gives the lowest value to the approximate flash temperature and the furnace is kept isothermally at such a temperature as to give a gas temperature ca. $5^{o}C$ below the approximate flash temperature. Observations are made of the length of time required for a sample, introduced into the furnace at such a temperature, to flash-ignite. The gas temperature is lowered in steps of $5^{o}$ until the sample does not flash for at least 30 min. The lowest temperature at which flash ignition is noted is then the accurate flash ignition temperature.

The self-ignition temperature is measured in a similar manner without the pilot flame at the exit to the furnace.

The "combustibility" test BS476 Part 4 is very similar to this test. The difference is that the furnace is kept at a constant temperature ($750^{o}C$) and if, during

the test period, any of the six samples (a) bursts into flames (b) produces sufficient combustible vapours to be ignited by a pilot flame or (c) causes a temperature rise of more than $50^{o}$ above $750^{o}C$, then that batch is considered "combustible".

BS476: Part 5: 1969 Ignitability test.

This test is of little use for studying the flammability characteristics of plastics. A sample 228 mm square and of thickness of the material it represents is held with its plane faces vertical. A standard gas flame is played on its centre for 10 sec. If after this time the flame is extinguished in less than 10 sec, the sample is rated Class P - not easily ignitable. If the burning continues for more than 10 sec, it is rated Class X - easily ignitable.

ASTM D2843-77 Density of smoke.

This is the first smoke-density test method for burning plastics. The method measures the loss of light transmission when a standard specimen (25x25x6mm) is burned in a test chamber under standardized conditions. The test specimen on a metal screen is exposed to a standard propane burner flame in a test chamber, which is instrumented with a light source, a photoelectric cell, and a meter to measure light adsorption horizontally across a 300 mm light beam path. The chamber is closed during the 4 min test

period except for small ventilation openings around the bottom of the chamber. During the test, the variation of light obscuration with time is recorded together with the ignition time of the sample, the time for flame extinction or specimen consumption, the obscuration of the exit sign by smoke together with any general or unusual burning characteristics, such as melting, dripping, charring etc. The light obscurations are then plotted as a function of time on linear graph paper and the total smoke produced is calculated as the total area under the curve, while the smoke-density rating, in percentage, is determined as the total amount of smoke present in the chamber during the test interval.

The three major deficiencies of this test method are that the test conditions are only those of flaming combustion, a portion of the smoke tends to be lost through the bottom vents, and the light obscuration data are inaccurate because the horizontal light path cannot compensate for vertical stratification of the smoke in the chamber. Hence an improved smoke test was subsequently developed by the National Bureau of Standards[123]. The major improvements introduced in this test method were a larger test chamber to ensure sufficient oxygen for combustion of the test specimen without the need for ventilation openings in the chamber,

a vertical light path to eliminate the uncertainty associated with the horizontal light path, and the introduction of a 2.5 $W/cm^2$ radiant heat flux equipped with a small pilot flame so that smoke measurements can be conducted under flaming or smouldering conditions. A schematic diagram of the test chamber is included in Figure 17. This method also makes it possible to study coatings, as only the surface of the specimen is exposed to the heat flux, in contrast to the complete envelopment by the flame source of the ASTM D2843 specimen, leading essentially to complete combustion of the specimen.

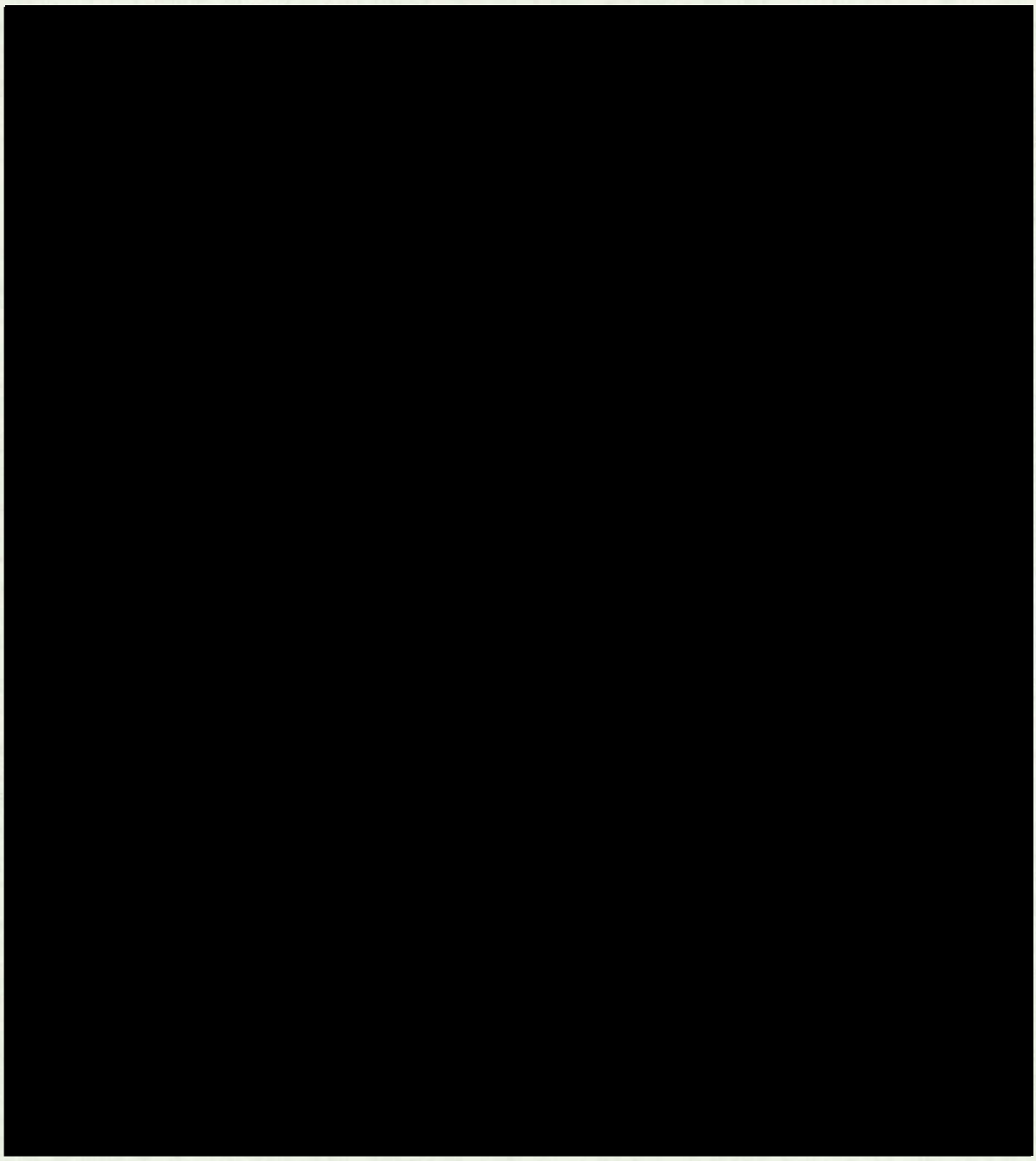
The test procedure involves the measurement of light transmittance against time. Observations are also made concerning the characteristic smoking or burning patterns, the colour, and the nature of the smoke. The test proceeds until a minimum light-transmittance value is reached. The light-transmittance data are then converted to specific optical densities using the relationship:

$$Ds = 132 \log_{10} (100/T)$$

where T is the percentage transmittance. The specific optical density is plotted as a function of time to yield a typical smoke accumulation curve. These curves can vary considerably depending upon conditions

FIGURE 17

N.B.S. smoke chamber assembly



of flaming or smouldering combustion.

There are a number of other types of smoke tests and these have been reviewed and criticised by Rasbash and Phillips[124]. These authors also list the smoke-producing properties of a number of different materials.

1.2.3.4 The Oxygen-Index Test: its development into a standard test method in the study of flammability.

The original concept of a flammability test which directly measures the minimum concentration of gaseous oxidant which will support combustion was due to Wolfhard and his co-workers[125]. Eichhorn[126], and particularly Fenimore, Martin and Jones[127-130] devised a useful research tool for studying the reactions involved in the combustion of polymers and their flammability as a percentage of oxygen in the atmosphere just capable of supporting a flame. It was intended for use in quality control assessments of the effect of flame retardants on the flammability of polymers, and has been discussed by various authors[131,133]. In 1970, Fenimore and Martin's test formed the basis of an American Society of Testing and Materials (ASTM) standard, which extended the applicability of the oxygen index method to encompass strips of self-supporting materials of defined dimensions. The implementation of this ASTM standard has been discussed by Williamson[134]. Ease of operation and reproducibility have contributed to the wide acceptance of the method, and its general versatility has led to the method being adapted by various national and international organisations.

The reproducibility of the results of the tests for flammability of polymers, as obtained by this "oxygen-

index method", has been confirmed by two ASTM trials[135-136] and an International Standards Organisation inter-laboratory trial[137]. These led Nelson and Webb[138] to redefine the original ASTM inter-laboratory precision by suggesting standard deviations of less than 1.0 for materials with an oxygen index less than 21, and not more than 2.2 for materials that exhibit dripping or char formation.

The variation within a laboratory and between laboratories, displayed in the results of the two ASTM "round-robin" trials, has been discussed by Isaacs[131], who claims that it should be possible to determine the oxygen index values of a clean-burning polymer (e.g. poly(methyl methacrylate)), and of an erratic burning material (for example, one that drips and forms char) to within 1% and 4% of the values, respectively. Other similar trials have been conducted by Walker[139] and Murch[140], who conclude that it is possible to determine the oxygen index value of any material to a reasonable degree of accuracy and to be confident that a similar result can be obtained by another operator provided that the same procedure is used.

The particular features of the test which make it useful for research will be dealt with in Section 1.2.3.5. Certain factors need to be mentioned here, however, because they affect the standardization of

the test:

Sample moisture content.

Certain standard methods for assessing the flammability of plastics specify that the sample should be conditioned prior to test, mainly because 'the properties of plastics may alter considerably with changes in temperature and relative humidity, and conditioning of specimens before tests is often required to improve the reproducibility of the test result'[141].

The 1976 version of the ASTM test method recommends that samples for which the oxygen index is suspected of being moisture-sensitive be conditioned at 23°C and 50% relative humidity for 40 hours in the case of samples 7 mm or less in thickness, and for 88 hours under these same conditions for samples of greater thickness. Isaacs[131] has shown that the moisture content of the sample has an important influence on the oxygen index value of certain materials.

Sample dimensions

This parameter was not considered as very important by early workers and it was generally accepted that oxygen index values were independent of the size (within certain limits) of the sample[142,143]. Even as recently as 1976, evidence was produced to support this conclusion[144].

Changes in the dimensions of the sample will alter its cross-section, which will in turn affect the rate of heating of the sample and the way in which it burns, whilst changes in the sample shape would be expected to affect the turbulence induced in the gas flow[145].

Goldblum[132] has investigated the effect of material thickness on the oxygen index of polycarbonates and has concluded, that thinner samples give lower values. Isaacs[135] has also noted that thin samples burn more readily. The question of the effect of sample thickness has been investigated by DiPietro and Stepniczka[143], who have concluded that for nylon-6 and two kinds of polyester, the oxygen index increases with thickness to about 2 mm and thereafter remains virtually constant.

In general the effect of altering the dimensions of the sample is difficult to predict[146], since it depends on the thermal conductivity of the material, the extent of formation of insulating char during combustion, and on other factors such as the inorganic content of the polymer. The oxygen index values of a number of polymers present in various geometric form have been reported[138] and the results for any one material show reasonable agreement, especially in view of the gross differences in sample geometry.

Chimney effects

The effect of chimney diameter has been investigated by Day[146]; oxygen-index values were determined in three chimneys of different diameter but with the same gas velocity and sample size. The results suggest that the oxygen index values of the materials tests are independent of the diameter of the chimney. Walker[139] has reported that constriction of the top of the chimney has no measurable effect on the oxygen index.

The heating of the glass chimney that occurs during combustion[147] probably affects the oxygen index by preheating both the sample and the flowing gas mixture; this will be more pronounced in smaller diameter chimneys. The effect of temperature will be considered in more detail in a later section.

Specific heat of the gas

The oxygen index of any material increases almost linearly as the specific heat of the ambient atmosphere increases[148]. This dependence has been shown to hold for argon, nitrogen and oxygen[129,149]. Such a relationship is indeed to be expected; for the higher the specific heat of the flowing gas entering the column, the lower will be the flame zone temperature at a given oxygen concentration and hence the lower will be the rate of heat transfer back to the sample from the flame. With carbon

dioxide and neon, the oxygen fraction ($[O_2]/[\text{inert gas}]$) rather than the oxygen index ($[O_2]/[O_2] + [\text{inert gas}]$) increases linearly with the heat capacity of the gas. With helium, the oxygen index values are ca. 50% greater than that would be expected. This can be attributed to the very high thermal conductivity of this gas, which conducts heat away from the flame, and thus gives abnormally high values of the oxygen index in much the same way as is found with polymers which drip molten material.

Gas flow rates.

Initial studies by Fenimore et al[130,142,150,151] indicated that flow rates in the range 30-120 mm $s^{-1}$ have little effect on the oxygen index of polymers. DiPietro and Stepniczka[143] also investigated the reproducibility of oxygen index values at different flow rates but their results indicated that oxygen index values for the four polyester mixtures investigated did depend appreciably on flow rate, a maximum value being observed in the particular apparatus used, when the volume flow was equivalent to a linear gas velocity of 40 mm $s^{-1}$. It was also found that the sensitivity to flow rate was enhanced as the fire retardant concentration was increased.

Walker[139] found during his investigations that a 25% variation in gas flow rate had little or no effect on the oxygen index. Kanury[148] and others[130,150,151]

concluded that the gas flow up the chimney must be sufficient to clear the combustion products from the vicinity of the sample, but not so large as to increase the mixing rate between vapprized fuel and air at the leading edge of the flame.

Pressure

The flammability of polymers is usually measured at atmospheric pressure. However, some tests have been carried out under reduced pressure and show that the oxygen-index increases as the pressure is decreased[127]. The effect is not thought to be pronounced enough for any normal fluctuations in atmospheric pressure to affect the results, provided that account of the ambient pressure is taken in calculations of the flow rate.

Temperature

The effects of temperature on oxygen index were first reported by DiPietro and Stepniczka[152] and subsequently by Hendrix et al[147], who noticed a fall in the oxygen index obtained from repeated determinations as the glass chimney surrounding the sample became progressively hotter. As other experiments in which the glass column was deliberately heated to a known temperature[153] showed the effect to be significant, it is clear that the chimney must not be allowed to become hot during routine tests.

DiPietro and Stepniczka[143,154] investigated the effects of both the temperature of the sample and the temperature of the gas stream entering the column. It was concluded that, while the oxygen-index is decreased by raising the temperature of both the gases and the sample, the former is only a secondary effect. The hot gases tend to pre-heat the sample which affects the oxygen-index by facilitating degradation of the polymer and hence providing a greater concentration of fuel than would be provided solely by back diffusion of heat from the flame.

Igniter gas and igniter application time

No specification for the type of igniting gas is given in ASTM D2863, although hydrogen and propane are mentioned as possibilities. There is some evidence to suggest that the results obtained using hydrogen as the igniter gas, and therefore shorter times preceding ignition, lead to more reproducible results. A series of inter-laboratory trials involving fire testing stations has tended to confirm this[139].

In a study on polyethylene, Walker[139] suggests that, in order to obtain reproducible results, the application time of the ignition should be controlled. It should not exceed 60 sec , unless the gas is hydrogen when shorter times may prove adequate. The sample must be thoroughly ignited if an equilibrium is to be achieved between the heat generated by combustion

and the heat lost. If the igniter is applied for too short a time, especially under conditions near those at the oxygen index value, the heat generated by combustion is insufficient to make up the deficit resulting from poor ignition. When the time of igniter application is too long, a sample needs 30-60 sec to reach the equilibrium temperature following removal of the igniter[132].

Sample flow properties

Fenimore and Martin[130] reported that polymer samples that flow or drip during burning can give unexpectedly high oxygen index values since heat is carried away from the combustion zone by the flow of molten material. For such samples, an inert ceramic wick makes it easier to obtain an accurate result. Polymer flow properties, which are related to the molecular weight and to the nature of functional groups within the polymer, have been correlated with the oxygen index values for several nylon-6 polymers[155].

1.2.3.5 The oxygen-index test: Its use in the determination of the mechanism of flame-retardance.

Flame-retardant additives have now been developed to act in the condensed phase to influence thermal degradation of the polymer and in the gas phase to quench the flame reactions. However, for those which function in only one phase, the oxygen-index method offers a means of determining this phase[154].

If the flame-retardant acts in the condensed phase[128], then its action should be unaffected by the nature of the oxidant gas, but should change radically with changes in the polymer structure. Conversely, for a flame-retardant which acts mainly in the gas phase, the effect will be similar on polymers of different structure, but may alter markedly with the nature of the gas supporting combustion.

It is also possible to study the mode of action of gaseous flame-retardants by introducing them into the oxygen-nitrogen mixture upstream from the burning polymer. If the additive normally acts in the gas phase when incorporated into the polymer, then it may still act when introduced upstream, but not so efficiently. If the additive acts in the condensed phase, then it should not affect the burning of the polymer when introduced into the surrounding atmosphere. To verify the presence

of a flame-retardant which inhibits the gas-phase flame reaction, consider the main oxidant-consuming step in the oxidation of hydrogen or hydrocarbon in oxygen and nitrous oxide.

In oxygen the step is

$$O_2 + H\cdot \rightleftharpoons OH^{\cdot} + O^{\cdot}$$

which is a chain-branching reaction. Hence the inhibition of this step would be expected to have a large effect on the rate of oxidation.

In nitrous-oxide the analogous step is:

$$N_2O + H^{\cdot} \rightleftharpoons N_2 + OH^{\cdot}$$

which is not a branching reaction, and its inhibition would clearly have a much smaller effect.

The oxygen-index apparatus is easily modified so that various experiments may be carried out on a stable flame burning above a polymer sample.

### 1.2.4 Fundamental Studies

The burning of organic polymers is a complex process which follows the sequence: (i) all or part of the combustible material is heated from an external source, sufficiently powerful to produce a vapour or a concentration of volatile fragments as a result of decomposition of the polymer; (ii) a sufficient concentration of fuel in the vapour phase will ignite, so that a flame results. This is a high-energy zone in which rapid free radical reactions occur, and is normally of the type known as a 'diffusion' flame, controlled by the rate of diffusion of the gaseous oxidant into the flame zone; the net result is the oxidation of the organic material to oxides of carbon and water, together with some 'cracking' products, which may lead to the formation of soot; (iii) the flame heats the polymer by conduction and radiation and more vapour is formed which perpetuates the cycle; and (iv) some polymers decompose to leave a residue of carbon which cannot be further degraded; if the temperature is high enough, this carbonaceous residue will be oxidised by a surface reaction and will appear to glow or burn in the solid phase, the further oxidation here taking place by a surface reaction.

At any time during the burning of a polymer there is thus a vapour phase in which the actual flame reactions are occurring and a condensed phase, usually

in the form of a surface, which may be partly carbonised, and from which fuel for the gas-phase reactions is being produced[156].

However, from the chemical point of view, there are two important stages involved. One is the pyrolysis of the organic polymer to give volatile combustible products and the other is the burning of these products, mixed with an oxidant, in the gas-phase.

The pyrolysis of organic polymers occurs in three fairly distinct stages. At moderate temperatures, i.e. below about 300°C, functional groups react or are eliminated from the main polymer chain. In some cases, extraneous groups, such as catalyst residues, are split off. In other cases a single species of low molecular weight which formed an integral part of the polymer is eliminated and this may be accompanied by regular changes in the nature of the main polymer chain[157]. Between 300 and 550°C, thermal movement of the polymer chain is sufficiently energetic to cause bond scission in the main structure. This may occur at random sites with the production of polymers of much lower molecular weight and small amounts of volatile species. Alternatively, bond-scission may take place at chain ends and may be followed by "unzipping" with the consequent formation of monomer or very small polymer units. Most polymers can react under certain conditions so that there is some

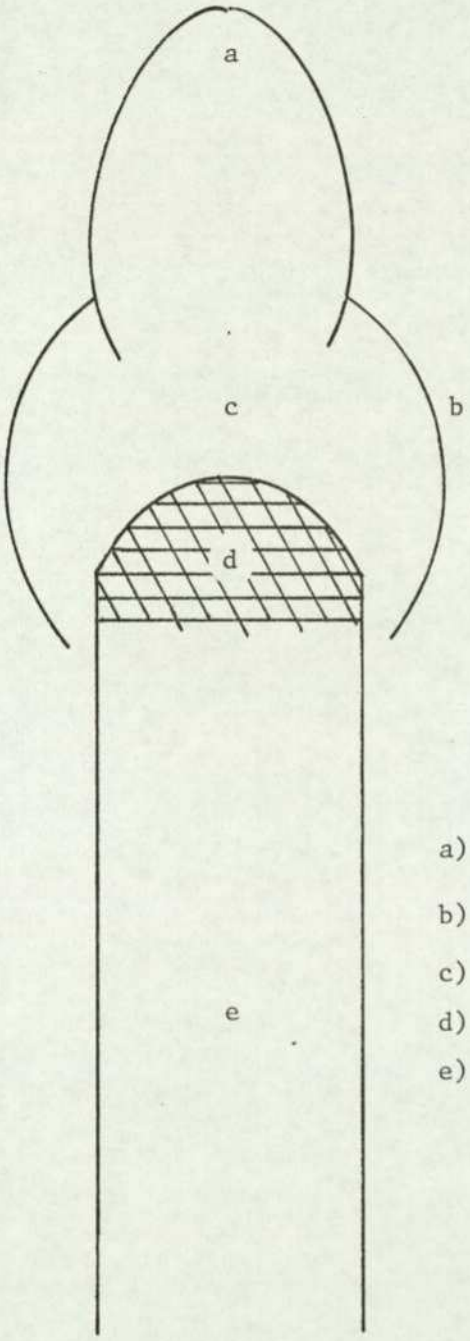
recombination of these highly unsaturated small fragments. This usually results in aromatic or condensed ring structures irrespective of the nature of the original polymer chain[158,159]. The structure eventually becomes increasingly dehydrogenated and, with carbon chain polymers, all elements other than carbon are gradually eliminated, leaving a carbon 'char', the main composition of which depends principally on the temperature reached.

Turning now to the combustion of the volatile decomposition products of the polymer, these generally burn as diffusion flames. In such flames, the combustion process is regulated almost completely by the rate of interdiffusion of oxidant and fuel and there is normally a steady change in gas composition as the flame is traversed.

A wide variation can exist in polymer flames, an idealised flame being shown in Figure 18[160]. This is very similar to the flame on polyethylene burning in air. It consists of five zones (viz. virgin polymer, partially degraded polymer melt, colourless zone, blue zone and yellow sooty cap), four of which can show large variations. Thus the polymer melt may show no signs of the formation or evolution of fuel, or this fuel may be formed from many bubbles in the polymer surface. The generation of char at the surface may vary from negligibly small to relatively large quantities. Furthermore, the char, if formed, may be physically light so that it rests on the molten cone;

FIGURE 18

Burning of a polymeric candle




a) luminous yellow zone

b) blue zone

c) colourless zone

d) partially degraded polymer

e) virgin polymer

or it may be dense so that it causes lumps of material to ablate from the surface. The colourless zone will vary in height, and at the limiting oxygen concentration, it will approximate to the quenching distance for the fuel. The blue cone will also vary in height and is due to various oxidative cracking reactions occurring in the flame. For aromatic polymers the upper zone, yellow or white due to thermal emission from the oxidation of carbon particles, is often capped by a stream of unburnt carbon particles (soot). Certain polymers undergo "flameless burning" or surface oxidation, in which a glowing zone moves down the length of the sample without causing inflammation.

Few studies have been conducted on the diffusion flames of organic polymers. Fenimore and Jones[161] measured the temperatures in flames of polymethyl methacrylate, while Burge and Tipper[162] measured the temperature profiles for polyethylene and polyoxymethylene (Figure 19) in three directions (viz. from above the flame, from the side of the flame and through the base of the flame). Due to the high temperature gradient across the polymer surface and the thermal mass of the thermocouple it was found that the temperatures obtained by probing from above were generally about 50-100$^{o}$ too high. This was cross-checked by determining the temperature in the surface of burning n-eicosane. These results,

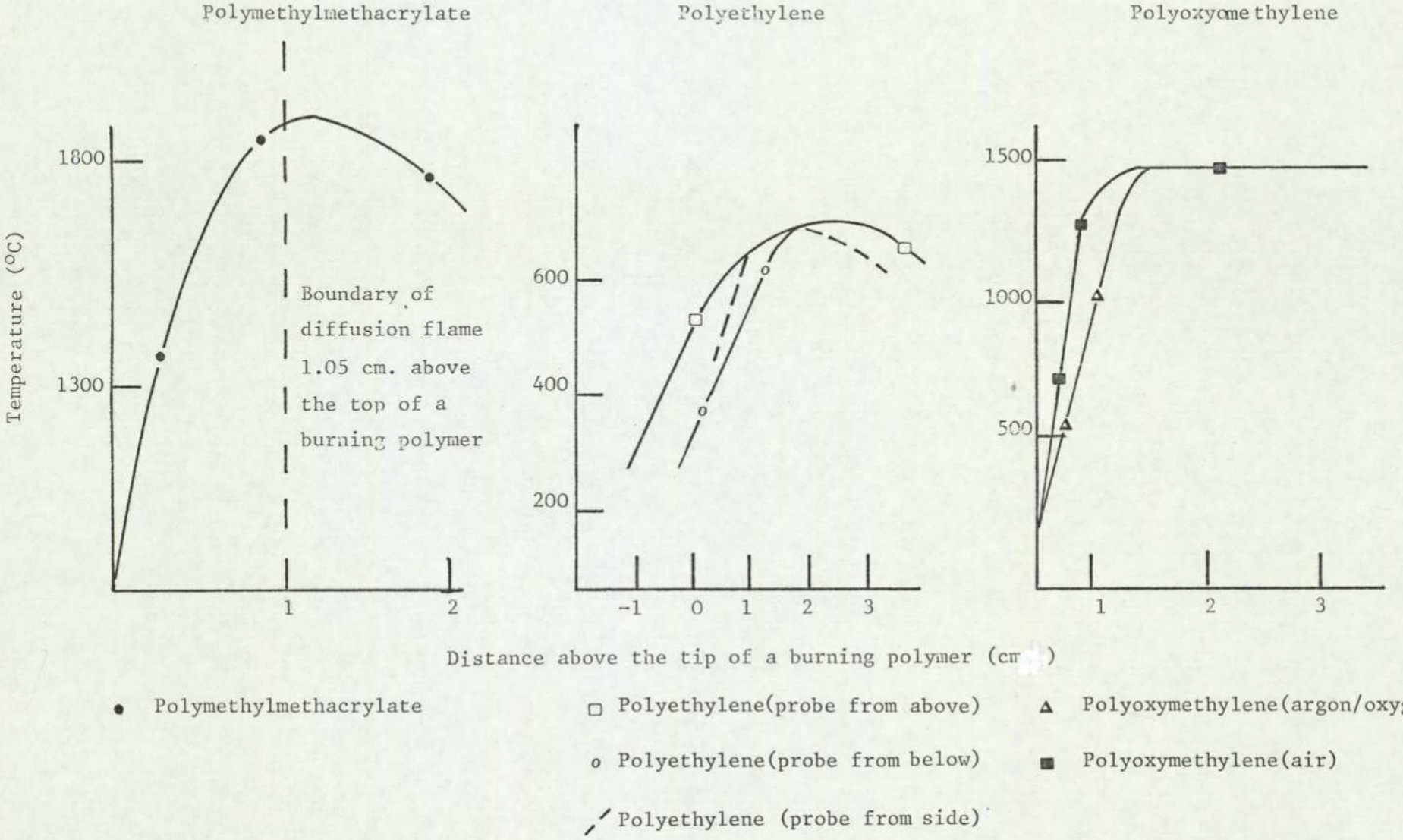



FIGURE 19

Temperature profiles above burning polymers

although in agreement with those of certain other workers, did not correspond well with those of Fenimore and Jones[161], probably because the latter had used argon rather than nitrogen, as an inert gas.

Burge and Tipper[162] and Stuetz et al[158], also measured the change in flame and surface temperature as the oxygen content of the surrounding atmosphere was altered. Work on polyethylene showed that, if the oxygen concentration was doubled, the flame temperatures were unaffected whilst the temperature of the surface was markedly increased.

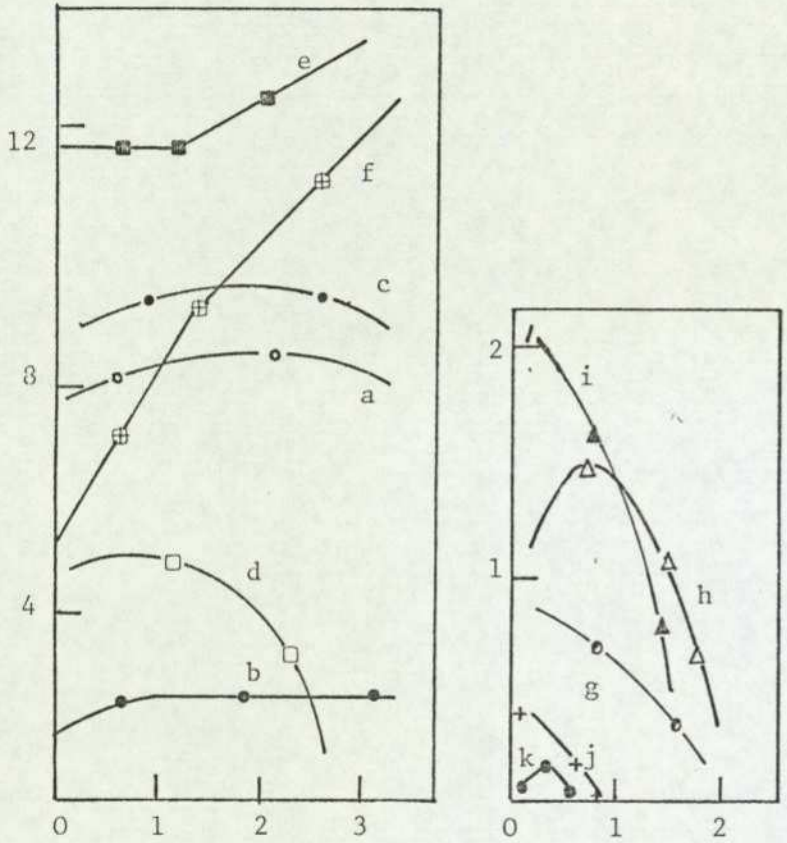
Product profiles may be constructed by withdrawing gas samples from particular positions in the flames and analysing them using gas chromatography. The product profile of polyethylene, taking samples 0.3 cm above the surface, contained roughly equal quantities of carbon monoxide, carbon dioxide and unsaturated hydrocarbons ($C_2$: $C_3$: $C_4$ ≡ 24: 6: 4). Some partial-product profiles for polyethylene are shown in Figure 20.

The thermal decomposition of polymers under oxidative conditions at high temperatures has not received as much attention as their behaviour in inert atmospheres. It is known that the percentage of oxygen in hydrocarbon-oxygen mixtures at elevated temperatures not only reduces the decomposition temperature, but also alters the course of reaction. Hence it is important

FIGURE 20

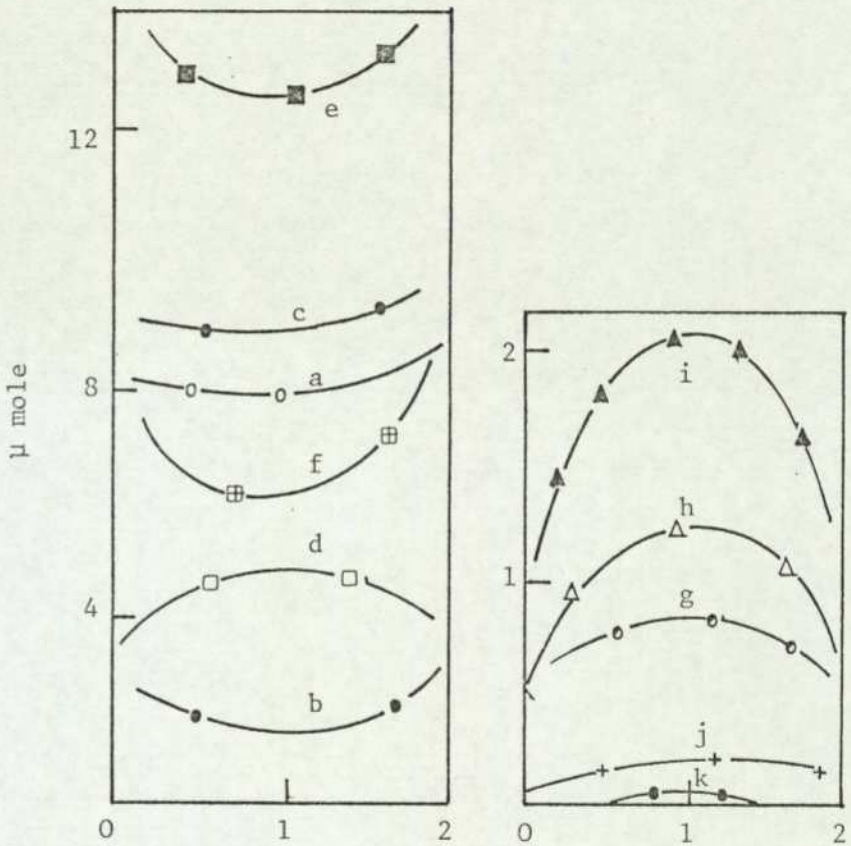
Composition profiles of flames burning above polyethylene.

i) Along central axis of flame




Distance above melt surface (cm.)

ii) Across flame 0.1 cm. above the melt




Distance from one edge of flame (cm.)

a) $N_2$ x 0.1
b) $O_2$
c) $O_2$ consumed x 0.5
d) CO
e) $CO_2$
f) $H_2O$
g) $CH_4$
h) $C_2H_2$
i) $C_2H_4$
j) $C_3H_6$
k) i-$C_4H_8$

to know whether thermal decomposition during polymer combustion is an oxidative or non-oxidative process. Early models of candle-like polymer combustion[160], in surrounding atmospheres of oxygen mixed with various inert gases, suggest that the oxygen from the atmosphere is completely consumed in the flame zone, so that the pyrolysis of the polymer in the condensed phase occurs in the absence of oxygen. This conclusion was derived from the observation that the bottom of the luminous flame zone of a steadily burning candle of polyethylene is at a finite distance from the surface of the polymer melt. The reason for this is that the polymer decomposition products require dilution with atmospheric oxidant before the flammability limits are reached. It is pointed out that, for polymers burning without formation of char, as the oxygen content of the atmosphere is reduced below the critical level, the flame may be extinguished in one of two ways. A polyethylene flame slowly shrinks and the leading edge recedes until, just before extinction, only a small blue flame-cap exists just above the top centre of the sample. On the other hand, with a chlorinated polyethylene containing antimony oxide, only large flames are stable. As the oxygen content is reduced, a violent flicker takes place before the flame is blown off completely. Regardless of the mode of extinction, however, it appears that the stability of the leading edge of the flame is essential

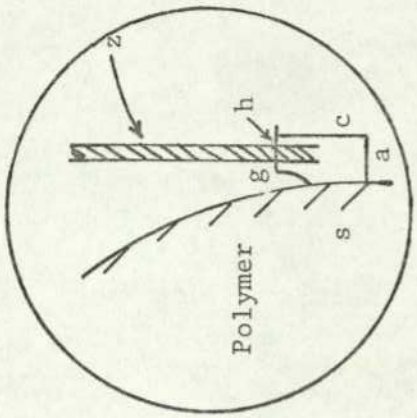
for continuous burning. This concept that the stability of the leading edge is critical and determines the limiting atmosphere in which the flame can be maintained forms the basis of Martin's model for the burning of polymers[160].

For ideal steady-state burning without the formation of solid residue, a control volume is defined as shown in Figure 21. Continuity and steady-state equations for flow across the boundaries of this control volume can then be arranged to give an expression for the ratio, oxygen: inert gas, in terms of parameters which are completely specified by the overall stoichiometry of the flame reaction, flame temperature and heat losses. For a given polymer at the flammability limit, the stoichiometry, flame temperature and molar heat losses are assumed to be independent of the inert gas in the atmosphere. It can then be shown that the ratio of oxygen: inert gas is a linear function of the heat capacity of the inert gas. This is generally found to be the case.

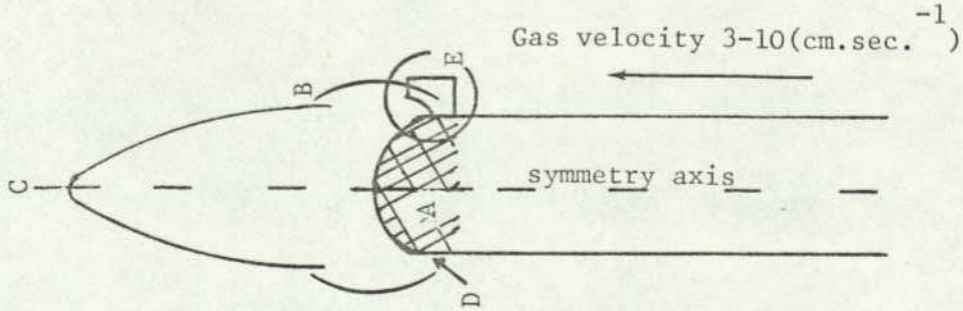
Burge and Tipper[157] have developed a somewhat different concept for the candle-like burning of polymers. Composition profiles were obtained of the gases in the combustion zone, both across and along the axis of the flame. The results suggested that the oxygen concentration, although low, was not zero and that the oxides of carbon and water found in the 1 mm nearest to the polymer surface could have been formed only by a mechanism in which at least part of the

FIGURE 21

Schematic diagram of polymer burning
as defined by Martin[129]




A. molten polymer
B. blue flame zone
C. luminous cap
D. quenching zone at leading edge of flame
E. control volume
a. atmosphere flow-in through surface
c. solid polymer enters through surface
g. flame-gases exit across surface
h. streaming lines in oxidant-inert gas
s. streaming lines in pyrolysis gases
z. visible blue flame

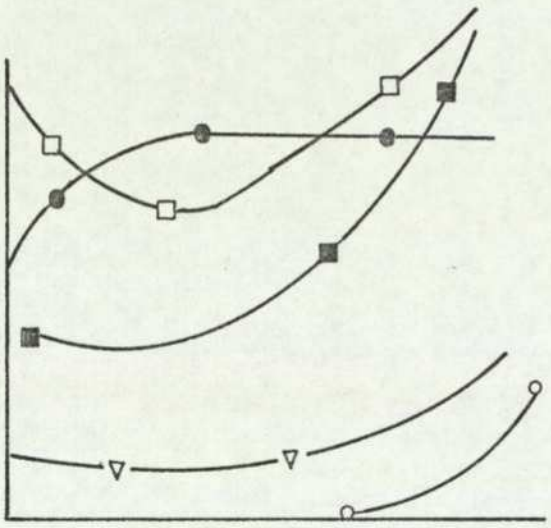


degradation was oxidative. At least 70% of the gas mixture in the flame was found to be nitrogen and it was suggested that the oxygen and nitrogen entered the flame zone by enforced diffusion through the gap between the surface of the polymer and the base of the flame. That the oxygen was then drawn across the surface of the polymer was shown to be consistent with the experimental results[157,162] (Figure 22). It was found that the residence time of the gas-phase oxygen near the surface of the polymer was not sufficient to allow for the formation of the oxidation products[162]. Thus it was concluded that only chemical processes taking part at or just below the surface of the burning materials are important in producing mixtures which pass into the gas phase and give rise to the flame. This is confirmed by the fact that the surface was evidently disturbed and that, when the oxygen concentration in the atmosphere is doubled, the temperature of the surface and the concentration of carbon oxides and water all increased. The concentration of oxygen at the surface showed a slight decrease, thereby confirming its action in the condensed phase.

The rôle of oxygen in the burning of polymers has been clarified by Stuetz et al.[158] who decomposed polypropylene on a thermo balance at relatively low heating rates in atmospheres containing various

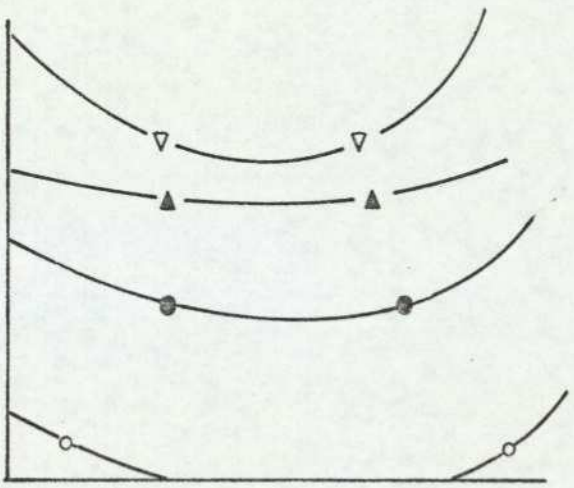
FIGURE 22

Oxygen concentration in flame, on various polymers



Profile up central axis of flame

Concentration of Oxygen (μ mole).



Profile across flame at various heights above polymer surface.

- L.D. Polyethylene - air. 0.1cm.
- L.D. Polyethylene - air. 0.5cm.
- L.D. Polyethylene - 60% oxygen
- HD Polyethylene - air.
- Polymethyl methacrylate
- n-Eicosane

concentrations of oxygen from 0%(pure nitrogen) to 20%. Separate measurements were made of temperatures and composition profiles through both solid and gas phases of burning polypropylene samples;the rates of consumption of the polymer, the flame height and its dependence on the oxygen concentration were investigated and the results complemented those obtained from a comparative study of methane flames.

Sampling and analysis of gases near the burning polymer surface revealed the presence of unchanged oxygen; oxidation products were found in the emerging fuel supply. Neutron activation analysis on slices of burned polymer (that had previously been extinguished by an excess of nitrogen) confirmed the presence of chemically bound oxygen in its surface layers. Extrapolation of these results indicates the presence of 26% oxygen at the surface. Hence a significant proportion of the polymer must undergo oxidative decomposition to carbon dioxide and water.

When the activation energies of decomposition were plotted against oxygen concentration, a significant change was noticed between 0.5 and 1.0% oxygen[158]. This is measured as the equilibrium concentration of oxygen near the surface of the polypropylene sample burning in air. At lower oxygen concentrations, the activation energies rose sharply. Calculation of heat fluxes

in this case showed that about 10% of the heat required for depolymerisation came from the flame and 90% from surface oxidation.

Isaacs[159,163] found that the oxygen index increased with an increase in sample diameter. This confirms the effect of surface oxidation because an increase in cross-sectional burning area reduces the free oxygen concentration near the surface due to the diffusion-controlled access of oxygen to the interface. Recently, however, the rôle of surface oxidation in the production of gaseous fuel during polymer combustion has been studied by radiant pyrolysis techniques[164]. It was found that the pyrolysis rate did not vary with oxygen concentration once a steady state was attained. The production of fuel in small-scale, top-burning polymers therefore involves purely thermal decomposition of the polymer.

Throughout the literature, experimental results on the rôle of oxygen in the burning of polymers seem to agree reasonably well. It is, however, the interpretations which differ[165]. Hence the rôle of oxygen in certain polymers is clearly to promote oxidative decomposition. However, with other polymers, oxygen probably plays little part in the early stages of breakdown and in general its involvement depends heavily on the nature and physical properties of the polymer concerned.

1.2.5 Flame Retardancy: Methods and Mechanisms.

1.2.5.1 Generalised mechanisms of flame-retardant action.

In the combustion of a solid polymer, heat from an external source reaches the polymer and pyrolysis reactions begin to take place in which oxygen may participate, giving rise to volatile, flammable products which diffuse to the surface of the polymer where they mix with air. If heating continues and the temperature reaches a critical value, ignition will take place. If the pyrolysis products and oxygen continue to reach the combustion zone, and if the energy liberated by combustion is sufficiently in excess of heat losses to maintain the ignition temperature, the process becomes self-perpetuating until all the fuel or oxygen has been consumed.

The combustion process, outlined above, is susceptible to interference in a number of ways, any one of which could have a retarding effect.

a) Heat shield: Covering the polymer with a reflecting non-flammable coating may provide an adequate barrier to heat transfer and thus prevent decomposition of the polymer leading to ignition[166,167]. Phosphorus compounds act partly in this way by forming a protective layer of polyphosphoric acids.

b) Dilution of combustion gases: The addition of

38 mole% nitrogen to any air-methane mixture makes the mixture non-flammable by acting as a heat sink; the flame temperature is reduced faster than heat is generated, resulting in cooling and the eventual extinction of the flame[168]. Flame-retardant additives which degrade to give a non-combustible gas blanket (as distinct from other mechanisms) are rare. Certain carbonates evolve $CO_2$, on breakdown. Materials which decompose to give Lewis acids or exclude oxygen or fuel gases from the combustion zone also fall into this category[169].

c) Reduction in overall heat production: If the additive makes a negative contribution to the overall thermal yield during polymer decomposition, it could prevent further combustion.

d) 'Dust' or 'wall' effect : The flame-retarding action of inert dust is widely applied in fire-extinguishing. Heat is consumed in heating dust particles, leading to a lowering of temperature and consequently to extinction of the flame. Heterogeneous chain breaking may also take place by adsorption of active species on the surface of dust particles; this is true especially when the dust consists of metals or certain metal oxides with a high adsorptive capacity for atoms and free radicals[170].

At the wall of a vessel (or at the surface of a solid dust particle) competing interactions such as

$$H^{\cdot} + O_2 \xrightarrow[\text{wall}]{} HO_2^{\cdot}$$

can take place instead of

$$H^{\cdot} + O_2 \longrightarrow HO^{\cdot} + O$$

As the $HO_2^{\cdot}$ radical is relatively unreactive compared with $H^{\cdot}$, $HO^{\cdot}$ and $O^{\cdot}$, these are more likely to diffuse to the "wall" or surface and be deactivated there[171]. When antimony oxide is used as a synergist with halogen compounds, it is first converted to antimony trihalide. The trihalide is then decomposed in the combustion zone giving a fine "fog" of antimony trioxide, and the flame-retardant effect here is at least partly due to the dust effect[166].

e) Chemical inhibition (free radical effect): This is perhaps the most important of the flame-retardant mechanisms because a relatively small proportion of chemical flame-retardant will give rise to a large effect. It also provides indirect evidence for the free-radical chain mechanism of flame propagation.

Certain substances (e.g. halogens or halogen derivatives) strongly affect flame velocity in concengrations as low as 1%. As such small additions do not appreciably change the specific heat or thermal conductivity of the mixture, it seems reasonable to suppose that the compounds added have a direct effect on the course of the reaction[170]. Thus the inhibiting effect of halogen

compounds on hydrocarbon flame reactions is believed to consist in decreasing the concentration of active centres, mainly H atoms as a result of reactions of the type:

$$H^{\cdot} + RX \longrightarrow RH + X^{\cdot}$$

$$\text{or} \quad H^{\cdot} + RX \longrightarrow HX + R^{\cdot}$$

The above processes result effectively in chain termination because very active H atoms are replaced by a much less reactive species such as R or X.

Similarly for $^{\cdot}OH$ :

$$^{\cdot}OH + HBr \longrightarrow HOH + Br^{\cdot}$$

$$Br^{\cdot} + RH \longrightarrow HBr + R^{\cdot}$$

The net result is to replace $^{\cdot}OH$ by a less reactive active species $Br^{\cdot}$ or $R^{\cdot}$.

f) Chemical inhibition (ionic mechanism): Creitz has proposed an ionic mechanism for flame-retardance[172]. Methyl bromide and bromotrifluoromethane were found to be more effective inhibitors when added to the oxygen side of a diffusion flame than when added to the fuel (hydrocarbon) side. In support of this hypothesis it has been shown that flames are displaced by electrical fields. If ions were not involved to a significant extent, the position of the flame would not be affected by the field.

g) Promotion of the formation of incombustible material:

This is not the 'heat shield' mentioned in (a),

which refers to a protective layer on the surface of the polymer. Certain flame-retardants can however promote the formation of solid char rather than volatile pyrolysis products. Nevertheless, in this case the problem remains of glowing combustion of the 'char' which forms a bed of solid fuel, predominantly carbon. Many borates, phosphates and silicates help to suppress this 'afterglow'[173].

1.2.5.2 Some chemical flame-retardant systems.

For various reasons, the following classes of chemical compounds have been added to polymers to impart fire retardance (a) chlorine and bromine compounds (b) phosphorus compounds alone and in conjunction with halogen and nitrogen compounds (c) antimony in conjunction with halogen compounds (d) boric acid and borates and (e) aluminium trioxide and other inert substances. Other compounds have also been proposed for use in specific applications.

(a) Halogen compounds.

The action of halogens is complex and a number of mechanisms have been proposed to explain their flame retardant action. These mechanisms have been extensively reviewed[174-176]. Compounds containing the three heavier halogens (Cl, Br and I) appear to act by destroying the free radicals involved in the combustion process. Fluorine-containing materials, on the other hand, may not exert any chemical inhibiting action. The hydrogen halides are generally effective in the order HI>HBr>HCl>HF, with HF behaving as an inert diluent.

Various theories have been proposed for the flame-retardant action of the halogens. In the gas phase, they may give rise to hydrogen halides which interfere with the chain reactions involved in the combustion

process; for example, they may cause highly active species such as $^{\bullet}OH$ and $H^{\bullet}$ to be replaced by a much less active halogen atom, X, as a result of reactions such as:

$$^{\bullet}OH + HBr \longrightarrow H_2O + Br^{\bullet}$$

$$H^{\bullet} + HBr \longrightarrow H_2 + Br^{\bullet}$$

In other cases, the parallelism between the inhibiting action and the electron-capture efficiency of organo-halogen compounds suggest that the undissociated molecule is involved[177,178].

An interesting alternative to the above mechanism has been proposed by Larsen[174] who points out that, although halogen compounds may take part in gas-phase combustion reactions, this may not he their primary mode of operation. Data for both diffusion flames and pre-mixed flames show that a minimum of 75-80% of halogen is needed to prevent flame propagation. It is thus difficult to understand how a typical halogen containing polymer (with only say 3 to 30 weight % halogen) could inhibit flame propagation in the gas phase. The main function of halogens may therefore be to act as flame retardants by reducing the heat of combustion of the gaseous decomposition products of the polymer. This reduction is such that, in order to sustain a flame, the rate of gasification must be increased by the application of an external heat source.

Chlorine and bromine compounds are however also

capable of acting in the condensed phase. Here they seem to function by alteration of the condensed-phase mechanism to form polymer free radicals. These in turn are capable of either decomposition and chain scission, cross-linking, or reaction with more halogen radicals to form halogenated polymers.

The predominant rôle of bromine compounds in flame retardance is however the gas-phase inhibition of combustion reactions, probably by hydrogen bromide. However, the precise position or stage at which the hydrogen bromide is formed presents much doubt. It has been suggested that the bromine compounds decompose in the condensed phase to form hydrogen bromide, and this must be the case for those compounds which are chemically incorporated into the polymer. However, bromine compounds exist for which vaporisation occurs in preference to breakdown and in these cases the entire additive enters the flame so that the hydrogen bromide is actually formed in the flame. Both Fenimore[130] and Volans[179] claim that the first burst of products in the decomposition of bromine-containing polystyrene is three to seven times richer in bromine than the original polymer. However, it was not possible to distinguish between bromine evolved as hydrogen bromide and that evolved as organic bromo-compounds.

Bromine compounds also act as catalysts for the

decomposition-depolymerisation reaction in many polymers (although not in polyethylene). There seems to be no correlation between those polymers which lose hydrogen bromide specifically in the condensed phase and those which depolymerise more easily. When the concentration of the bromine additive is low, the enhanced pyrolysis produces more products in the gas phase, leading to an acceleration of burning. Delfosse et al[180] found that, when the quantity of halon (polyhalogenated compounds e.g. $CF_2ClBr$, $CF_3Br$) is increased, the enhancement of pyrolysis increases only slowly while the HBr begins to form in increasing quantities owing to the reaction:

$$Br^{\cdot} + RH \longrightarrow HBr + R^{\cdot}$$

($Br^{\cdot}$ being formed by additive destruction). If $OH^{\cdot}$ is the propagating radical, the quenching reaction

$$OH^{\cdot} + HBr \longrightarrow H_2O + Br^{\cdot}$$

then takes place, leading to inhibition of combustion. The retardation varies according to the rate at which HBr is produced from a given substance. Hence, the easier HBr formation, the lower will be the concentration for inhibition. Delfosse concludes that an apparent ambiguity in the action of brominated compounds occurs because two competitive reactions are taking place. To enhance pyrolysis a sufficient radical concentration must be obtained from the additive, even at low concentrations, as a result of the reaction:

$$CX_3Br \longrightarrow CX_3^{\cdot} + Br^{\cdot}$$

$$CX_3^{\cdot} + RH \longrightarrow R^{\cdot} + CX_3H \qquad (RH \text{ is polymer})$$

$R^{\cdot}$ then leads to decomposition through β scission. The energy required to break the C-Br bond is low so that this appears to be the initiation of the unzipping reaction. However, to quench the chain reaction once it has started a large concentration of HBr is required because at this point in the reaction the concentration of $OH^{\cdot}$ radicals increases exponentially.

In the case of chlorine compounds, the principal flame-retarding action may take place in the condensed phase. Thus flame-extinction tends to be of equal efficiency with both oxygen and nitrous oxide as oxidant. The partial product distribution from burning polymers is often altered in the presence of chlorine additives as shown in Table 13. Char formation from chlorinated polyethylene or polyvinyl chloride is much greater than from polyethylene. The fates of the polymer radicals in the condensed phase are as suggested above. Thus chain scission leads to cyclisation and benzene formation, cross-linking leads to char formation, and reaction of the polymer radical with halogen atoms leads to halogenation of the polymer.

Most commercial chlorinated flame-retardants have a high percentage of chlorine. Thus in order to liberate hydrogen chloride, they need to abstract extra hydrogen from the polymers

TABLE 13

Major products formed during the burning of polymers containing chlorine compounds

| Polymer | major Products | Benzene | HCl | Chloro-paraffin |
|---|---|---|---|---|
| Polyethylene | l.m.w. straight chain hydrocarbons | 1% | none | none |
| Chlorinated polyethylene | gradually the degree of branching increased and the degree of unsaturation decreased | 4% | much | none |
| Polyvinyl chloride | - | 10% | much | none |
| Penton ($C_5H_8Cl_2O$) | l.m.w.end in smaller quantity | none | much | 12% |
| Styrene with chlorowax 70 | monomer | little | much | 10% chlorinated monomer |

in which they are used. The strength of this scavenging action can be shown by heating a chlorine compound with hydrocarbon wax. At 260°C the wax is stable on its own more or less indefinitely, but in the presence of the chlorine compound the mass is quickly turned to char.

Combinations of chlorine and bromine have been claimed to be synergistic: it appears rather that their effects are simply additive.

Some halogen compounds which have been shown to have useful flame-retardant properties are shown in Table 14[181].

(b) Phosphorus and its compounds

Inorganic and organic phosphorus compounds are useful fire retardants in many polymers. They are used almost as extensively as halogens. Although the largest single commercial application for phosphorus flame retardants is as platicizers in polyvinyl chloride, their next most important use is in highly oxygenated polymers such as cellulose.

Phosphorus fire retardants and the nature of their fire-retardancy mechanism have been comprehensively reviewed by Lyons[182].

Non-volatile compounds or compounds which are capable of decomposing to produce polyphosphoric acids act in the condensed phase[183]. These acids are then the active species. Thus, on heating tris(t-butyl) phosphate alone,

Table 14

a) Chlorine compounds used as flame retardants

| | |
|---|---|
| Chlorinated paraffins | Perchloropentacyclodecane |
| Chlorendic acid | Tetrachlorophthalic anhydride |
| Hexachloroethane | Decachlorobiphenyl |
| Pentachlorophenol | Vinyl chloroacetate |

Various chlorinated polymers

e.g. Polyvinyl chloride

Polyvinylidene chloride

Chlorinated ethylene

b) Bromine compounds used as flame retardants

| | |
|---|---|
| Pentabromotoluene | Hexabromobenzene |
| Tetrabromobisphenol-A | Tetrabromophthalic anhydride |
| Hexabromocyclohexane | Decabromobiphenyl |
| Pentabromophenol | Tris (2,3-dibromopropyl) phosphate |

Various brominated polymers

e.g. Tribromostyrene

Polyvinyl bromide

Polyvinylidene bromide

2-methyl propene is volatilised and a glassy residue of meta phosphoric acid is formed[184]. Furthermore, the fully neutralised saltsof non-volatile metals are ineffective which suggests that the phosphorus compounds act as precursors for the poly acids mentioned above, which are both strong acids and good dehydration agents. These phosphorus compounds have been used mainly in cellulosic materials where they act by catalysing the formation of char and water vapour at the expense of laevoglucosan, which is the normal fuel species[184].

The phosphorus acids are generated by the thermal decomposition of the alkyl phosphorus ester to an olefin and the corresponding acid. This reaction together with the postulated char-forming dehydration of the cellulose, is shown in the following scheme:

Decomposition

$$R^1CH_2CH_2\text{-}O\text{-}P\text{-} \xrightarrow{\Delta} R^1CH = CH_2 + HO\text{-}P\text{-}$$

$$2HO\text{-}P\text{-} \longrightarrow -P\text{-}O\text{-}P\text{-} + H_2O$$

Esterification and dehydration

$$R\text{-}CH_2\text{-}CH_2\text{-}OH + -P\text{-}O\text{-}P\text{-} \longrightarrow R\text{-}CH_2\text{-}CH_2\text{-}O\text{-}P\text{-}$$

$$R\text{-}CH_2\text{-}CH_2\text{-}O\text{-}P\text{-} \xrightarrow{\Delta} R\text{-}CH{=}CH_2\text{-}P\text{-}OH \longrightarrow \text{char.}$$

In addition to the dehydration mechanism via esterification with a polyphosphoric acid, dehydration may also occur by a single acid-catalysed elimination of water from the

alcohol as indicated below.

$$R\text{-}CH_2\text{-}CH_2OH \xrightarrow{H+} R\text{-}CH_2CH_2\overset{+}{|}OH_2 \longrightarrow R\text{-}CH_2{=}CH_2 + H_2O + H^+$$

The fact that nearly all phosphorus compounds capable of decomposing to acid fragments are effective fire retardants for cellulose and other oxygen-containing polymers is powerful support for such a condensed-phase mechanism.

The high efficiency of phosphorus fire retardants in polyurethane foams[185,186] has also been suggested to be the result of acidic decomposition products which then promote the formation of a structurally stable insulating char. The flammability of such foams is reduced, therefore, by several effects, the most important of which are: the reduction of flammable fuel by the increase in relatively non-flammable char; insulation of the foam from the thermal effects of the flame; and coating of the char with non-volatile thermally stable polyphosphoric acids which screen the hot carbon from the air.[187] The most important evidence in support of the postulated mechanisms are that: the phosphorus flame-retardants reduce the thermal stability of the polymer[188]; they have relatively little fire-retardant effect on acid-resistant polymers such as polyethylene[189]; and in polyurethanes, they increase the charring tendency under flame conditions[190, 191]. Phosphorus from the retardants is largely or completely retained in the residual char[185,192]. The extensive

literature supporting this mechanism leaves little doubt as to its importance in this system and essentially eliminates gas-phase inhibition as being of any significance.

Despite the considerable evidence for a predominantly condensed-phase mechanism for phosphorus fire-retardants in many polymer systems, phosphorus compounds are efficient gas-phase inhibitors for hydrocarbon flames[193,194] and can be expected to exhibit this type of fire-retardancy in some systems[195]. Fire-retardancy in phosphorus-halogen systems is believed to occur in both the condensed and gaseous phases[196]. Lyons[182] attempted to determine whether an additive or synergistic effect predominated from data obtained with a number of polymer systems. A distinct synergism appears to exist for polyolefins, polyacrylates and epoxy resins, while for polyacrylonitrile there is synergism for bromine but not for chlorine. Weil[197] has recently reviewed the literature on phosphorus-halogen systems and has concluded that there are no reliable data to support synergism. Some authors have misapplied the term "synergist" by using it to refer to any beneficial additive, disregarding the question of whether the effect is greater than additive. Hindersinn and Witschard[195] have also critically considered the possibility of phosphorus-halogen combinations and agree that there is no compelling evidence for synergism. The additivity of phosphorus and halogen fire-retardant effects, on the

other hand, seems to be definitely established over a wide range of concentrations and for many polymer systems.

The use of phosphorus and bromine in the same molecule as e.g. tris(2,3-dibromopropyl) phosphate is perhaps the most useful approach, as it helps to get the best possible utilization of the halogen when the flame-retardant molecule breaks down[198]. However, there is insufficient experimental evidence available at this time to propose any single mechanism for phosphorus-halogen flame retardancy.

c) Antimony trioxide and other metal oxides.

Antimony trioxide by itself has been found to be a very poor flame retardant[199]. However the importance of antimony compounds in enhancing the flame-retardant effect of halogens in polymeric compositions was first recognised during the second World War when a combination of antimony trioxide and chlorinated paraffin was developed at Columbia University as a fire-retardant finish for cotton fabrics[200]. Several mechanisms have been suggested for the high efficiency of the antimony-halogen combination. Little[200] originally suggested that hydrogen chloride, thermally evolved in the presence of a flame, reacted in situ with the antimony trioxide to produce SbOCl which was postulated as the active flame-retardant intermediate on account of its effectiveness as a free-radical trap. It may also facilitate generation of halogen atoms which interfere with normal free-radical flame-propagation

reactions. Rhys and Cleaver[201] suggested that the formation of SbOCl or $SbCl_3$ simply delayed the escape of halogen from the flame, thus increasing its efficiency as a free radical chain inhibitor.

A few examples of condensed-phase reactions have also been reported. Reid and Heighway-Bury[202] suggested that the antimony-halogen composition acts as a dehydration catalyst in the condensed phase to promote charring of cellulose at low temperatures. Einhorn[203] reported that the antimony-halogen combination enhanced and strengthened char development in unsaturated polyester resin laminates, when exposed to fire conditions.

On the basis of the above observations, Pitts[204] concluded that there are two distinct fire-retardant effects for antimony-halogen compositions, namely the free-radical termination of gas-phase flame reactions, and solid phase charring as a result of catalysed decomposition of the condensed phase. The importance of each to the total fire-retardant effect will depend upon the chemical structure of the substrate in which the fire retardants are being used. Hindersinn and Witschard's[195] recent review substantiates the above conclusion.

Pitts[204] suggested a mechanism involving the initial reaction of antimony trioxide, in situ or otherwise, with the hydrogen halide evolved by

decomposition of the halogen compound, producing antimony oxychloride (SbOCl) as the key intermediate. It was suggested that this product decomposed via the series of endothermic reactions listed below to yield antimony trichloride with partial regeneration of antimony trioxide. The trichloride was considered to be the primary flame retardant[181,204-208]. Although there is considerable independent evidence substantiating the formation of antimony trichloride on heating chlorine-antimony compositions, there is little or no direct evidence substantiating SbOCl as a necessary part of the mechanism. Thermal decomposition reactions of antimony oxychloride are shown in the equations below:

$$5\ SbOCl_{(s)} \xrightarrow{245^{\circ}-280^{\circ}C} Sb_4O_5Cl_{2(s)} + SbCl_{3(g)}$$

$$4\ Sb_4O_5Cl_{2(s)} \xrightarrow{410^{\circ}-475^{\circ}C} 5Sb_3O_4Cl_{(s)} + SbCl_{3(g)}$$

$$3\ Sb_3O_4Cl \xrightarrow{475^{\circ}-565^{\circ}C} 4Sb_2O_3 + SbCl_{3(g)}$$

$$Sb_2O_{3(s)} \xrightarrow{658^{\circ}C} Sb_2O_{3(l)}$$

Fenimore and Jones[196] have suggested a predominantly gas-phase mechanism for the flame retardancy of antimony oxide in chlorinated polyethylene using the oxygen index method. In the absence of chlorine, the oxygen index was unchanged as the antimony oxide content was increased, nor were appreciable quantities of antimony volatilised, as indicated by 95% retention of antimony in the burned

residue; the oxygen index levels off at a Cl/Sb ratio of 3:1, while only 25% of the antimony remained in the residue; the nitrous oxide index is unchanged over a wide range of antimony oxide concentrations indicating that the fire-retardant efficiency depended on the nature of the oxidant-gas mixture. The levelling of the oxygen index of antimony-containing chlorinated polyethylene at a Cl/Sb ratio of 3 indicates that antimony trichloride is the active fire-retardant intermediate. Learmonth and Thwaite[187] have identified antimony trichloride as a volatile product when 50:50 mixtures of poly(vinyl chloride) or chlorinated wax with antimony oxide were heated to 310°C. Studies were also made of the effect of various metal-halogen systems on the extinction of toluene-oxygen flames; the inhibiting efficiency increased with ease of gaseous oxidation of the halogen compound in the flame. It was thus concluded that the antimony trichloride is the most likely species to be formed initially - and that this is subsequently oxidized in the flame to antimony trioxide, fine particles of which catalyse the recombination of chain propagating free radicals. Benbow and Cullis[209] have studied the effect of antimony oxide and various halogenated compounds in the flame-retardance of polystyrene. The reactions occurring during the decomposition of halogenated flame-retardants and their interaction with antimony oxide are almost thermoneutral; the trichloride is thus probably the active

species. Hastie[210] recently investigated the effect of antimony tribromide on the reactions of premixed fuel-rich methane flames using a mass spectrometric technique; the antimony bromide concentration decreased rapidly in the preflame zone to essentially zero in the flame reaction zone. Concurrently the concentrations of hydrogen bromide, bromine atoms, antimony atoms and SbO increased, reaching maxima in the reaction zone. It was thus concluded that the primary inhibiting function of the antimony tribromide was to provide hydrogen bromide early in the flame as an active inhibitor while it also provides SbO as a catalyst for three body recombinations of H,O and OH in the flame zone. Brauman et al[211-214] concluded that the primary function of the halogen is to transport the otherwise non-volatile antimony to the gas phase as $SbX_3$ via an in situ interaction of the halogen compound with antimony oxide. The antimony trihalide appears to be the effective volatile species which inhibits the flame reactions regardless of whether it enters the flame from the fuel or air side.

Despite this strong evidence of a gas-phase inhibition mechanism of antimony-halogen combinations, evidence supporting a condensed-phase mechanism has also been reported. Abu-Isa[215] studied the decomposition of chlorinated polyethylene in both nitrogen and oxygen atmospheres with and without antimony trioxide present. In the absence of antimony oxide, a chlorinated polyethylene

containing ca 5%Cl lost HCl fourteen times faster than a compound containing 35%Cl in nitrogen, but only three times faster in oxygen. When antimony oxide was present, the dehydrochlorination rates in nitrogen and oxygen were equal. Furthermore, weight loss from the pure polymer was found to be due entirely to direct removal of hydrogen chloride, while in the presence of antimony less than half the weight loss could be attributed to HCl, and 85% of the antimony was volatilised at 150°C. These observations strongly suggest that the antimony is acting in the condensed phase.

Recent work, reviewed by Hindersinn and Witschard[195], has indicated that the effect of various halogen-antimony oxide combinations on the oxygen index of thermoplastics varies widely according to the chemical structure of the base polymer. The oxygen index of fire-retardant thermoplastics compositions containing various ratios of decabromobiphenyl oxide and antimony oxide was shown to vary widely from a maximum at a bromine-to-antimony ratio of 10:1 in high-impact polystyrene to 10:7 in ABS copolymer. This indicates the importance of polymer structure in fire-retardancy behaviour, and implies a significant condensed-phase contribution to fire retardancy in hydrocarbon polymers by halogen-antimony systems.

A number of other antimony compounds have been used in flame retardant compositions. These include organo-antimony compounds which are effective in the absence of

halogens but are expensive and hydrolytically unstable; sodium antimonate, which is known to produce less smoke and have less effect on the opacity of the polymer than the trioxide; and antimony phosphate, which is useful in that it reduces afterglow. Antimony sulphides and oxychlorides have also been used as flame-retardants. However, the trioxide remains the most efficient flame retardant for use with a halogen source.

Studies have been made on the flame-retardant effect of the elements adjacent to antimony in Group V of the Periodic Table, namely, arsenic and bismuth. However, the oxides of arsenic and bismuth tend to be less efficient, more expensive, and, in the former case, more toxic than antimony oxide[182].

A number of other metal oxides have been found useful either alone or in combination with $Sb_2O_3$ and halogens. The performance of $Sb_2O_3$ when applied to cotton is said to be improved by adding $Fe_2O_3$[216] or $SnO_2$[200]. These have a catalytic influence on the thermal degradation of the organic halogen compound[200]. MgO has been found to reduce the smoke-forming tendency of chlorinated allylic polymers[217]. Magnesium hydroxide also reduces the level of smoke when incorporated as part of the filler for polyester sheets[218]. Zinc oxide has varying degrees of flame-retardant efficiency when used with chloroparaffins in coatings[219]. Both ZnO[219] and $Fe_2O_3$[182] are claimed to accelerate the

decomposition of the chloroparaffin.

The use of $TiO_2$, in conjunction with $Sb_2O_3$ and a halogen compound, is an effective flame retardant for polyurethanes[220]. The temperature of decomposition of the halogen compound (e.g. PVC) appears to be lowered and this enhances the flame-retardant action on the basis of the "right place at the right time" theory.

In 1972, Touval[221] claimed that hydrated stannic oxide, is as effective a flame retardant as $Sb_2O_3$ when incorporated in conjunction with a halogen compound into polyethylene, polypropylene and ABS copolymers. Both $Sb_2O_3$ and $SnO_2.H_2O$ apparently react with the halogen compound to form the actual flame-quenching species. Anhydrous stannic oxide does not have a similar effect. The water of hydration in $SnO_2.H_2O$ is, therefore, necessary to enable the tin oxide to behave similarly to antimony oxide.

The more recent literature contains a number of patented flame-retardant compositions, most of which contain antimony trioxide as one component. Takiuchi and Date[222] have studied flame retardance in brominated epoxy and polyester resins containing mixtures of antimony trioxide (<4phr), stannic oxide and zinc oxide in equimolar quantities. Self-extinguishing resins can be prepared using 10% halogen compound, 2% antimony trioxide and 2% stannic oxide. Antimony oxide has also been used (a) in conjunction with

silica or titanium dioxide and a chlorinated paraffin to render polyethylene self-extinguishing[224]; (b) in PVC, with molybdenum dioxide, which acts as a smoke-suppressant[225]; (c) with manganese oxide and zinc oxide to produce flame-retardant polyethylene and PVC for use in electrical cables[226]; and (d) with ferric oxide to confer improved flame retardance on mixtures of ABS copolymers[227]. Various other mixtures of metal oxides with antimony trioxide have been employed to improve the fire performance of polyesters, polyamides and polyurethanes[228-231].

Zinc borate ($2ZnO.3B_2O_3.3.5H_2O$) has been extensively used as a flame-retardant for PVC (see section 1.2.5.1d). In conjunction with aluminium oxide hydrate[232] and antimony oxide[233,234] it has been used to confer flame-retardance on halogenated polymers. Lawson[235] has claimed that mixtures of aluminium oxide trihydrate and zinc oxide exhibit synergistic action in reducing the flammability and smoke-generating properties of PVC. Touval[236,237] has reported the use of mixtures of zinc oxide and magnesium oxide with hydrated stannic oxide as a flame-retardant for PVC, and for polyethylene and ABS copolymers containing Chlorowax S70. Stannic acid ($SnO_2.H_2O$) is now widely used for conferring fire-resistance on fibres[238-240]. Stannic oxide, in conjunction with a chlorinated paraffin or a brominated biphenyl ether decreases the flammability of

polypropylene[241] and epoxy resins[242]. Stannic oxide is not, however, widely used as a flame-retardant for polymers[223]. Although aluminium oxide trihydrate is frequently used in flame-retardant mixtures[243], the monohydrate is not mentioned in the literature. Polymers have also been rendered flame-retardant by incorporation of mixtures of (a) a compound of Fe,Co,Ni,Sn or Sb; (b) an alkali metal halide and (c) a carboxylic acid which may be an integral part of the polymer [244]. A comprehensive list of common metal oxide flame-retardant additives, their trade names, and manufacturers can be found in the Modern Plastics Encyclopedia [245].

Pitts[246] has evaluated a lengthy series of metal oxides as total or partial replacement for $Sb_2O_3$ in a chlorine-containing flexible-urethane-foam formulation at the 15-phr total addition level. The flammability results are listed in Table 15 and indicate that the oxides may be grouped into basically three categories.

Incorporating oxides from the first group proved detrimental, making normally self-extinguishing foams flammable. The second group of metal oxides had virtually no effect on the flame-retardance, while the third group, comprising $Fe_2O_3$, $TiO_2$ and CuO, exhibited a "positive" and quite beneficial effect.

A "positive" effect could be achieved with very small amounts of ferric oxide, suggesting a catalytic, rather

TABLE 15

Flammability of Flexible Urethane Foam Containing ~6.3% Cl, $Sb_2O_3$, and Other Metal Oxides.

| | Flammability[a] | | |
|---|---|---|---|
| Metal Oxides[b] | Rating[c] | Extent of burn(cm) | Burning rate(cm/min) |
| CaO | B | >12.5 | 13.5 |
| MgO | B | >12.5 | 9.3 |
| ZnO | B | >12.5 | 9.0 |
| $MoO_3$ | B | >12.5 | 8.8 |
| $Fe_3O_4$ | B | >12.5 | 6.3 |
| $Fe_2O_3.H_2O$ | B | >12.5 | 6.3 |
| $B_2O_3$ | B | >12.5 | 5.8 |
| $MnO_2$ | S.E. | 8.0 | 8.0 |
| $SiO_2$ | S.E. | 7.0 | 4.5 |
| $CeO_2$ | S.E. | 6.3 | 7.5 |
| $Al_2O_3$ | S.E. | 6.0 | 7.3 |
| None[d] | S.E. | 5.3 | 7.3 |
| $Al_2O_3.3H_2O$ | S.E. | 5.3 | 7.3 |
| $Bi_2O_3$ | S.E. | 5.3 | 7.8 |
| $CuO_2$ | S.E. | 5.3 | 7.8 |
| $SnO_2$ | S.E. | 5.3 | 7.5 |
| SnO | S.E. | 5.3 | 7.5 |
| $As_2O_3$ | S.E. | 5.0 | 7.3 |
| None[e] | S.E. | 4.8 | 7.5 |
| $Fe_2O_3$ | S.E. | 4.5 | 7.8 |
| $TiO_2$ | S.E. | 4.5 | 6.5 |
| CuO | S.E. | 4.3 | 7.5 |

[a]Test according to ASTM D 1692-68.

[b]Each formulation contained 10 phr of $Sb_2O_3$ and 5 phr metal oxide.

[c]Key: B, burning; S.E., self-extinguishing.

[d]Formulation containing 10 phr $Sb_2O_3$ only.

[e]Formulation containing 15 phr $Sb_2O_3$ only.

than a bulk effect[246].

Titanium dioxide, on the other hand, was beneficial, but to a slightly lesser degree than $Fe_2O_3$. $TiO_2$ exhibited a partial replacement effect that proved to be more bulk in nature than catalytic. Finally, CuO behaved more like $Fe_2O_3$ than $TiO_2$; catalytic quantities were sufficient to enhance the flame-retardant effect of $Sb_2O_3$.

Benbow and Cullis[247] have observed at least seven different types of behaviour when various metal oxides were heated with halogen compounds. Most of these ((i)-(v)) gave readily reproducible results but the others ((vi) and (vii)) show much more random behaviour.

(i) Inert oxides : Oxides of aluminium, boron (anhydrous and hydrated), chromium (III), niobium (V), nickel, thorium, titanium and zirconium were not volatilised when heated with various halogen compounds. These oxides also did not affect the decomposition of the halogen compounds.

(ii) Catalytic oxides: Cobalt (II) oxide and iron (III) oxide, although not themselves volatilised, caused a complete change in the decomposition mechanism and catalysed the breakdown of the halogen wax.

(iii) Oxides forming involatile halides: Silver oxide appears unique in that less than the theoretical quantity of the material is volatilised when heated with

a halogen compound. It inhibits the antimony/halogen reaction by successfully competing with antimony oxide for the hydrogen halide released in the condensed phase from the organic halogen compound.

(iv) Partially volatilised oxides: The anhydrous oxide of tin (IV) is partially volatilised when heated with chlorinated wax.

(v) Reactive oxides: Oxides of bismuth, copper(II) lead (II) and zinc are completely volatilised as the corresponding halides when heated with chlorinated wax. However, of these, only bismuth oxide and zinc oxide were found to be useful partial replacements for antimony oxide.

(vi) Oxides in low oxidation states: Vanadium (III) and vanadium (IV) oxides behave as relatively inert oxides until a temperature is reached when the metal oxide begins to absorb oxygen from the gas stream. This results in a gain in weight generally at temperatures such as to mask the later stages of decomposition of the halogen compound.

(vii) Oxides of oxidising acids: Chromium (VI) oxide and manganese(VII) oxide violently oxidise chlorinated wax at a readily reproducible temperature. However, the extent of oxidation depends on the efficiency of mixing of the metal oxide with the halogen

compound. Owing to the explosive nature of these oxidation reactions, the use of these metal oxides as flame retardants was not further investigated.

d) Boron

The use of sodium borates and boric acid as flame retardants in cellulosic materials has long been recognised and boron compounds are also well known to be effective flame retardants in other polymers[248,249]. The use of zinc borates, particularly FIREBRAKE® ZB, has found increasing acceptance in recent years in a variety of organic polymer systems. Although a good deal of information is available on the efficiency of borate based flame-retardants in various polymer systems, little has been published on their mode of action. In the case of cellulosic materials, inorganic borates on heating may form a glassy skin that excludes oxygen and hence prevents further propagation of combustion. The sequence of reactions is summarised as follows:

$$2H_3BO_3 \xrightarrow[-2H_2O]{130\text{-}200^{\circ}C} 2HBO_2 \xrightarrow[-H_2O]{260\text{-}270^{\circ}C} B_2O_3$$

Above 325°C, $B_2O_3$ soften to a glass and becomes fluid enough to flow at 500°C. The physical coating of a glassy matrix is not the sole mechanism. Inorganic boron compounds appear also to promote char formation by a mechanism similar to that of phosphorus compounds incorporated into cellulose.

For many years, hydrated zinc borates have been used as flame retardants in a variety of applications particularly in paint compositions and intumescent coatings[250]. Various stoichiometries have been found useful. However, many of these compositions (containing mixtures of various zinc borates, free boric acid and zinc oxide)[250] are said to lose water at relatively low temperatures, thus causing processing problems when used in polymeric materials. Recently a new crystalline hydrate of zinc borate with the stoichiometry $2ZnO.3B_2O_3$, known as Firebrake ZB (U.S. Borax), has been shown to retain its water of hydration up to 250°C, well above the curing temperatures for most polymers. It is claimed that this new zinc borate is an effective and economical replacement for the now relatively expensive $Sb_2O_3$ in poly(vinyl chloride), polyesters and to some extent polyolefins.

It is assumed that zinc borates act as flame retardants by forming a protective glass matrix at the burning surface of a flammable substrate just as borax-boric acid mixtures probably do. The suitability of zinc borates as partial or total replacements for $Sb_2O_3$ has led to the suggestion that they ultimately combine with halogens from the halogenated polyesters during the burning process. Zinc oxychloride and zinc chloride, both known flame retardants, would thus be generated and act as the real flame retardants[251]. No proof is available to date to indicate whether this is so. Woods[249]

claims to have observed synergism with combinations of antimony oxide and Firebrake ZB in PVC and attributes this to the "different modes of action operating in a complementary fashion".

Another inorganic borate often mentioned in conjunction with the hydrated zinc borates is barium metaborate. Suggested as a partial replacement for $Sb_2O_3$, $BaO.B_2O_3.H_2O$ has been used in cottons and polyolefins[252,253]. Other commercially available metaborates, such as $CaO.B_2O_3.2.5H_2O$ and $ZnO.B_2O_3.2H_2O$, have found limited success in the flame retardant market. The literature reveals several other borate compounds that have specific flame-retardant properties; and these have been listed by Pitts[204]. The tetrafluoroborate additives are presumed to undergo thermal decomposition to evolve $BF_3$ and, in the case of the ammonium salt[254] and metal-ammine complexes, HF is evolved as well. In these systems, the boron of the inorganic additive is assumed to exert its flame-retardant action in the gas phase. However, the tetrafluoroborate salts may also act in the condensed phase of the flammable polymer substrate, increasing char formation as all other inorganic borates do.

e) Nitrogen

Several classes of nitrogen compound have been found to be effective synergists for halogenated flame

retardants, especially aliphatic bromine compounds and some phosphorus-containing flame retardants. N-nitroso and N-chloro compounds have shown synergistic action with bromine compounds in polystyrene foam[255,256]. A few quinone imines have shown similar effects. For example, a foam sample containing 2 phr of 1,1,2,2-tetrabromoethane will burn. If the same formulation contains 2 phr of p-quinone oxime, the foam is self-extinguishing in less than 1 sec[257].

Hydrazones, although they are not initiators of free-radical reactions, like certain other nitrogen flame retardants, do show flame-retardant effects. Their action is probably related to their ability to react with oxygen and form peroxides[257].

Such nitrogen-releasing compounds as azobisformide show only small effects on the flammability of polyolefins even at concentrations of up to 10%. This compound decomposes into 65%$N_2$, 32%CO and 3%$CO_2$, liberating 225 $cm^3$ of gas (STP) per gram. Skinner[258] has shown that the flame-quenching effect of nitrogen is about 40% of that of chlorine on hexane-air flames. These nitrogen-releasing compounds may dilute the gaseous mixture in the flame zone so that it no longer lies within the flammable range.

In polymers other than cellulosics, evidence of nitrogen-phosphorus synergism is not very strong, and in

some polymers, such as poly(methyl methacrylate), antagonistic effects have been observed[197].

f) Free-radical initiators

Eichhorn[259,260] first observed the powerful synergistic effect of peroxides with halogens in studies of 1,1,2,2-tetrabromo ethane in polystyrene, with added dicumylperoxide. Other free-radical initiators such as hydroperoxides, azo compounds, dibenzyl compounds, hydrazines and some sulphur compounds were later investigated. Several possible explanations for their action were put forward:

(i) The free-radical-releasing compounds may accelerate decomposition of the halogen compounds so that the products are available as flame-retardant species at a lower temperature.

(ii) The free-radical initiator may react with the halogen compound lowering the temperature at which oxidation of the polymer begins and thus causing simultaneous decomposition of the polymer and halogen compound.

(iii) An additional supply of free-radicals may accelerate the decomposition of the polymer, making available fragments which react with the halogen compound and lengthen the residence time of the halogen in the combustion zone. This would bring about more effective use of the halogen, as occurs with antimony oxide.

Hindersinn[261] suggested however that the free-radical

compounds initiated thermal depolymerisation of the polymer, reducing the melt viscosity of the polymer and thus removing heat from the flame zone as a result of enhanced dripping.

Fenimore et al[262] showed that the flame-retardance of polystyrene containing tris(2,3 dibromopropyl) phosphate was increased by dicumyl peroxide but returned to the original level if dripping was prevented. Rates of evolution of bromine from the polymer were not affected by the peroxide, and introduction of dicumyl peroxide into polymers which do not drip (e.g. polyethylene) reduced the flame-retardancy.

1.2.5.3 Some physical methods of flame-retardance.

a) Aluminium oxide trihydrate.

Aluminium oxide trihydrate (actually, a crystalline aluminium hydroxide) is one of the most commonly used of all flame retardants for organic polymers. It acts efficiently as a heat sink, absorbing a sufficient fraction of the heat flux generated during the burning of a polymer[263] and releasing its water of hydration as steam, which helps to dilute the combustible gases. This property of alumina trihydrate has been known for some time, and has led to its extensive commercial use as a flame-retardant additive in rubber products[264,265] and polyesters[266-272]. Alumina trihydrate has also been used as a flame-retardant for epoxy resins[273-275], urethanes[275], silicone resins[275], neoprene[276], and as a filler for peroxide-cured ethylene-propylene elastomers[277]. However, there are considerably fewer reports on applications in thermoplastics[278-280].

All available information on the flame retardant action of alumina trihydrate points to the endothermic dehydration as the main process by which this compound retards the burning of polymers. There is no evidence of cationic catalysis or inhibition of any of the reactions occurring during burning either before or after dehydration.

There is no substantial evidence for the use of any

other oxide or hydroxide of aluminium with or without a halogen source in flame retardant compositions. Martin and Price[269] have studied the possible use of anhydrous alumina at low filler loadings and found it unsatisfactory. Pitts has claimed that the "presence of hydrated alumina seems to help reduce the flammability, especially when chlorine is present". Lyons[182] has suggested that $AlCl_3$ is probably formed and serves as a dehydration catalyst in the solid phase during burning and as a source of hydrogen chloride in the gas phase. However, current research has failed to find any active $AlCl_3$ species in the burning process or any apparent enhancement of flame-retardance in the presence of a halogen compound.

b) Other inert fillers

Some other inorganic oxides, salts of mineral acids or glass fibres, also act as inert fillers. Like hydrated alumina they are usually added to the polymer primarily to improve certain physical properties, or as pigments, rather than as flame-retardants although most show some degree of flame retardant action. Polymers containing fillers are opaque and often changes have to be made to the polymer structure (e.g. chlorination of polyethylene) in order to accommodate sufficient filler.

Fillers retard the burning of polymers in three main ways. They act as diluents to reduce combustible material available and also act by helping to prevent the temperature

of the polymer from reaching values at which decomposition occurs to give combustible gases. The temperature will be kept down even more effectively if the material decomposes endothermically, or if the products of decomposition have a high latent heat of vaporisation (e.g. water from hydrated calcium sulphate). Thirdly, inorganic fillers accumulate at the surface of the burning polymer and appear to smother the flame by interfering with the heat flux and oxygen supply to the polymer. However, for certain fillers, a standing ash will be formed which retains the shape of the original sample and stabilises the burning by a wick effect.

c) Intumescent coatings

"To intumesce" means "to swell". An intumescent paint is one which, under the action of excessive heat, is converted to a carbonaceous foam which will adhere to the surface, even under the conditions existing in a fire. The substrate is thereby insulated from the heat flux. A paint or coating material can be rendered "intumescent" by incorporating in the formulation an appropriate system which will first react when heated to give a carbonaceous char and then release a gas which will "blow" the char into a rigid foam.

The char is produced by the dehydration of a compound containing several hydroxyl groups (e.g. sugars, starches and polyhydric alcohols). An acid catalyst is required to initiate rapid char formation at relatively low

temperatures, but is added to the initial formulation as a salt : phosphates, borates and sulphates have been used. To be effective, the salt must decompose to give the parent acid at temperatures between 100-200°C.

In order to obtain a foam-like char on the surface, a gas (preferably non-flammable) must be released at the same time as the char is being formed. The decomposition products of the polyol and the precursor of the acid catalyst can give rise to some "blowing", but generally a blowing agent must also be present, (e.g. urea - $CO(NH_2)_2$ - decomposes at ~130°C to give $NH_3$, $CO_2$ and $H_2O$). It is important to "match" the decomposition temperature of the blowing agent with the rest of the flame-retardant system in order to get an efficient system. Although the general principles underlying these systems are well understood, the development of intumescent coatings has relied very much on "trial and error" methods.

(d) Inert gases and vapours

Inert gases produced in situ often provide a heat-sink and cool the flame, by acting as diluents. Polymers which react to liberate inert gases include polycarbonates (carbon dioxide) and certain amino plastics which liberate nitrogen.

(e) Ablative polymers

If incandescent sections of a burning polymer can be

made to disintegrate from the bulk of the material and remove with them much of their associated heat as they leave the combustion zone, then the combustion of the remaining polymer will be delayed.

## 1.3 Analysis of Experiments with Mixtures

A mixture experiment is an experiment in which the response is a function only of the proportions of the components present in the mixture. The general purpose of mixture experimentation is to make possible estimates, through a response surface exploration, of the properties of an entire multi-component system from only a limited number of observations. These observations are taken at preselected combinations of the components in an attempt to determine which of the combinations in some sense maximise the response.

In the mixture problem, the components represent proportions of a mixture. These proportions must be non-negative and, if expressed as fractions of the mixture, they must add up to unity. The factor space containing these components (say k) may then be geometrically represented by the interior and boundaries of a regular (k-1)-dimensional simplex[281]. For example, when k = 3 the factor space consists of the boundary and all interior points of an equilateral triangle, when k = 4, those of a regular tetrahedron and so on. The vertices represent 'mixtures' consisting entirely of one component and the edges and faces (if any) correspond to two and three components respectively.

Scheffe[282] introduced simplex-lattice designs for mixture experiments and developed polynomial models which

have exactly the same number of terms as there are points in the associated designs. The designs, consisting of a symmetrical arrangement of points, are referred to as {k,m}- lattices. The models are characterized by their relatively simple form and thus possess the property that they are easy to use for predicting the response over the simplex factor space.

The number of points, g, required for any lattice except the special cubic, may be computed from the formula:

$$g = \binom{m + k - 1}{m} = \frac{(m + k - 1)!}{m!(k - 1)!} \qquad (15)$$

or $$C^{m + k - 1}_{m}$$

where k is the number of components under consideration and m is an integer related to the spacing of the points and therefore to the number of blends. The proportions of any component are 0, 1/m, 2/m, - - - - -, 1 (giving a total of (m + 1) equally spaced values from 0 to 1), and all possible mixtures with these proportions are used. For the quadratic lattice, the proportions are 0, $\frac{1}{2}$ and 1, so that m = 2. Similarly, m = 3 for the cubic lattice and m = 4 for the quartic lattic. For the special-cubic lattice m = 2 but all possible 1/3, 1/3, 1/3 mixtures are added. The number of points in special-cubic lattices is therefore :

$$g = \frac{k(k+1)}{2} + \frac{k(k-1)(k-2)}{6} \qquad (16)$$

Each {k,m} lattice design is associated with a polynomial model, expressed in canonical form by Scheffé, with exactly the same number of parameters or terms in the polynomial as there are points in the design (see Figures 23,24).

These models are of relatively simple form possessing the property that they are easy to use for predicting the response over the simplex factor space. Thus, for a specified degree of the polynomial and a fixed number of mixture components, the canonical form of the polynomial includes the minimum number of parameters.

The general first-degree polynomial for expressing a dependent variable y in terms of k variables $x_1$, $x_2$, $x_3$ . . . . ., $x_k$ (omitting the error term) is,

$$y = \beta_o + \sum_i^k \beta_i x_i \qquad (17)$$

where the βs are unknown parameters to be estimated. The corresponding {k,1}- canonical polynomial can be written as,

$$y = \beta_o \sum_i^k \nu x_i + \sum_i^k \beta_i x_i = \sum_i^k \nu x_i \qquad (18)$$

where $\nu_i = \beta_o + \beta_i$, $i = 1, 2, 3, \ldots k$.

The general second-degree polynomial has the terms,

$$y = \beta_o + \sum_{i=1}^k \beta_i x_i + \sum_{i \leq j}^k \sum^k \beta_{ij} x_i x_j \qquad (19)$$

FIGURE 23

Special Cubic: k = 3, m = 2 each point (o) represents a mixture whose components are in proportion to the perpendicular distances to each edge

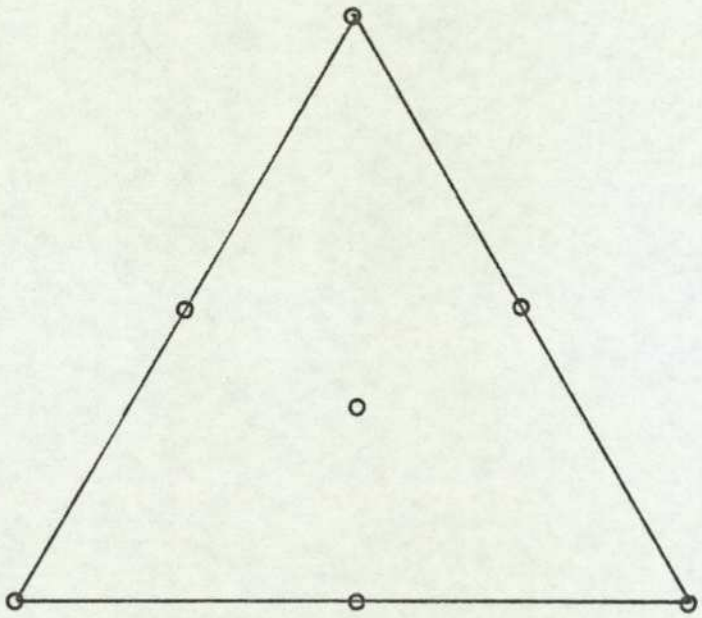
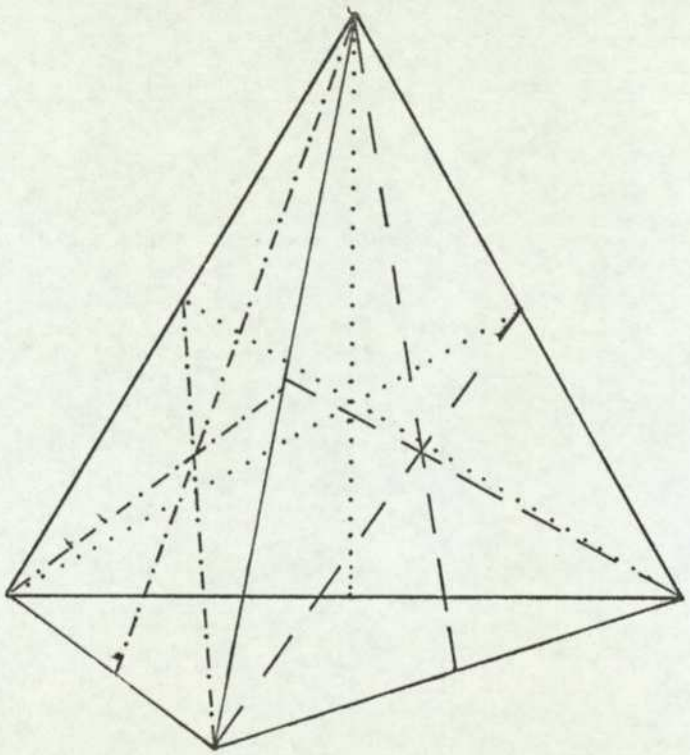


FIGURE 24

Special Cubic: K = 4, m = 2 - Components in proportion to the perpendicular distances from each face.



and the corresponding {k,2} polynomial can be written as:

$$y = \sum_{i}^{k} \gamma_i x_i + \sum_{i=j}^{k} \sum \gamma_{ij} x_i x_j \qquad (20)$$

where $\gamma_i = \beta o + \beta_i + \beta_{ii}$, $1 \leq i \leq k$ and $\gamma_{ij} = \beta_{ij} - \beta_{ii} - \beta_{jj}$, $1 \leq i \leq j \leq k$.

The model (20) can also be written as:

$$y = \sum_{i}^{k} \gamma_i x_i^2 + \sum_{i<j} \sum \delta_{ij} x_i x_j \qquad (21)$$

where $\delta_{ij} = \gamma_{ij} + \gamma_i + \gamma_j$, by multiplying $\Sigma \gamma_i x_i$ in (20) by $\Sigma x_i = 1$. It is possible to derive, the form of a third-order canonical polyonomial in a similar manner.

Equation (20) is appealing to the experimenter owing to the following "uniqueness" property of its terms. The $\gamma_i x_i$ term represents the response to the ith pure component and is unaffected by the response at any vertex other than the ith. The equation $y = \sum_{i=1}^{k} \gamma_i x_i$ therefore represents linear blending. The $\gamma_{ij}$ term expresses the synergism of the mixture system (or in other words, non-linear blending) and the term $\gamma_{ij} x_i x_j$ is affected only by the responses on the edge of the simplex joining the ith and jth vertices.

There are no "degrees of freedom" in this model with which to test "lack of fit" without replicating observations. By replicating observations for a measure of error and augmenting the designs by adding extra points so that such a test can be made, the

design and the analysis lose their simplicity. However, to test the adequacy of the model, particularly in some subsection of main interest, additional points will not only allow for checking "lack of fit" but also improve the estimate of variance $(\hat{y})$ in the immediate area of interest. Draper and Lawrence[283,284] were the first to consider both the variance and the bias of the model.

Gorman and Hinman[285] present a clear exposition on the simplex-lattice designs and the polynomial models of Scheffé[281]. They also extend the canonical polynomials to include the quartic, as does Lambrakis[286] in an alternative design.

By displaying contours of the variance of the estimate of the response of a three-component system using quadratic, cubic and quartic terms, Gorman and Hinman recognise that the precision of the estimate of the response varies greatly over the simplex. Apart from this non-uniformity of precision, however, the lattice method is effective for three-component systems in order to depict response surfaces by drawing response contours. This is evident from the eight figures contained in their paper[285].

Gorman and Hinman state that one should use the canonical polynomials with caution, when the data cover only a small area of the composition space, especially

when using high order models, since these polynomials were derived primarily to be used over the entire lattice. Extensive work on the inadequacy of these models over subspaces of the simplex lattice can be found in papers by Gorman[287], Kurotori[288], McLean and Anderson[289], and Thompson and Myers[290].

In Scheffé's lattice designs, for a three component system, only one constitutent is present at a vertex mixture and two at any point on the boundary. Although data on pure components are generally taken to check assumptions and measure properties of the response prior to using the component in mixtures, there are times when only mixtures consisting of all components simultaneously are meaningful. The designs then consist only of interior points of the simplex. These are presented by Draper and Lawrence[283,284] using a thirteen point design.

Krol[291] presents the results of a three-component experiment where ratios of the components are used. Krol, uses a factorial arrangement similar to that of Kentworthy[292] except that the ratios are transformed to logarithms.

When constraints in the form of lower bounds are placed on the proportions of one or more of the components, Kurotori[288] shows how to transform linearly the constrained components in order to generate new components, which are themselves mixtures. The design space of the new

components is a simple homomorphic transformation of the original simplex space. Kurotori[288] uses three extra points to check "lack of fit" for the special cubic model and employs a computerised plotting technique to illustrate the response curves.

Lattice designs, in general, give a complete coverage of the lattice but are characterized by their coverage of the boundaries at the expense of the interior points. The interior designs of Draper and Lawrence[283,284], Lambrakis[286] and Thompson and Myers[290] improve on this situation if the interest is concentrated on the interior to the boundaries. The canonical polynomials are simple to use for estimation and prediction purposes and the short answer to the use of statistical designs is "that we can save ourselves a lot of money and effort by quite simple devices"[293].

# 2 EXPERIMENTAL

## 2.1 Materials

### 2.1.1 Polymers

Two polymers were used in this work, namely high density polyethylene HD ELTEX® B4002 (Solvay); and an acrylonitrile-butadiene-styrene copolymer ABS UGIKRAL RA®, both supplied by Produits Chimiques Ugine Kühlmann. The physical and chemical properties of these polymers are shown in Table 16.

### 2.1.2 Additives

#### 2.1.2.1 Halogen Compounds

Two halogen-containing flame retardants were used in this work, namely a solid chlorinated paraffin ELECTROFINE® S70; and decabromobiphenyl ADINE® 0102, both supplied by Produits Chimiques Ugine Kühlmann. The physical and chemical properties of these compounds are shown in Table 17.

#### 2.1.2.2 Metal oxides

The metal oxides used in this work included: antimony (III) oxide "Timmonex® Red Star", supplied by Anzon Ltd; copper (II) oxide, iron (III) oxide, molybdenum (VI) oxide and zinc (II) oxide, obtained from B.D.H. Ltd; and the three aluminium oxides

Table 16

The physical and chemical properties of the polymers.

| | | |
|---|---|---|
| POLYETHYLENE : | | HD ELTEX B4002 (Solvay) |
| Density, at 23°C | | 0.950 $g.cm^{-3}$ |
| Melt index, load Skg(Mls) : | | 1.200 g.10 $min^{-1}$ |
| Modulus of elasticity, at 23°C | : | 12,500 $Kg.cm^{-2}$ |
| Vicat softening point, load 1 kg | : | 127°C |
| Deflection temperature under load | : | 80°C |
| ACRYLONITRILE-BUTADIENE-STYRENE : | | UGIKRAL RA (P C U K) |
| Specific gravity | : | 1.05 $g.cm^{-3}$ |
| Flexural modulus of elasticity | : | 2400 MPa |
| Rockwell hardness | : | 113 scale R |
| Vicat softening point at 0.98 daN | : | 102°C |

Variation in weight(%)in

| | | |
|---|---|---|
| 10%HCl | : | 0.32 |
| 10%$HNO_3$ | : | 0.48 |
| 10%$H_2SO_4$ | : | 0.38 |
| 10%NaOH | : | 0.43 |
| 10%$Na_2CO_3$ | : | 0.48 |

Table 17

The physical and chemical properties of the halogen compounds.

Electrofine S70 solid chlorinated paraffin: (P C U K)

Composition : mixture of long chain chlorinated hydrocarbons

| | |
|---|---|
| Chlorine content(%) | 70 |
| Appearance | white powder |
| Specific gravity at 20°C | 1.60-1.63 |
| Softening point(°C)(Ring and Ball method) | 95-105 |
| Residual $CCl_4$(%) | <0.5 |
| Stability to heat-HCl(4 hours at 175°C) (% HCl evolved) | <0.08 |
| Stability to heat-colour(2 hours at 160°C) | remains yellow in molten state |
| Flammability | non-inflammable |
| Toxicity | non-toxic |
| Solubility | insoluble in water and alcohols. |

Adine 0102 decabromobiphenyl : (P C U K )

| | |
|---|---|
| Bromine content(%) | 83-85 |
| Appearance | light beige crystalline powder |
| Particle size(μ) | <150 |
| Melting point (°C) | 370-375 |
| Thermal stability : | |
| decomposition point(°C) | 395 |
| sublimation temperature (°C) | about 350 |
| Water content (%) maximum | 0.2 |
| Toxicity : | |
| oral and cutaneous LD50 = <5g/kg | (on rats) |
| Solubility | very low solubility in most solvents |

$Al_2O_3$ (BACO CA130), $Al_2O_3.H_2O$ (BACO CERA HYDRATE) and $Al_2O_3.3H_2O$ (BACO FRF5 and FRF20) were donated by British Aluminium Chemicals Ltd. All these oxides were used without prior purification. The two tin oxides, viz. tin(II) oxide and β-stannic acid, were prepared in the laboratory as described below:

(a) Tin(II) oxide

A suitable quantity of tin(II) chloride dihydrate was dissolved in the smallest possible volume of hot concentrated hydrochloric acid, and a solution of sodium carbonate was carefully added until the mixture became alkaline. The white tin(II) oxide hydrate which settled out was heated for 2-3 hours in the supernatant liquid, thus causing quantitative conversion to blue-black, lustrous anhydrous tin(II) oxide. The product was purified by washing it several times with water and was then dried at 110°C. The thermal behaviour of this compound was investigated using thermogravimetric analysis. On being heated in air, it is slowly oxidised to $SnO_2$ between 280 and 912°C with a maximum rate of oxygen uptake of 2.7% $min^{-1}$ at 560°C.

(b) Tin(IV) oxide hydrate (β-stannic acid)

An excess of concentrated nitric acid was poured over pure granulated tin in a deep porcelain dish, and the mixture was heated on a water bath with repeated additions of fresh acid. After being cooled, most of the nitric

acid was decanted. The powdered precipitate of β-tin(IV) oxide hydrate was digested several times with cold water and washed on a filter until the wash water was free from nitric acid. The product was then dried at $40^{o}$ in an oven. The water content and thermal behaviour of this compound were determined by thermogravimetry.

(c) Aluminium (III) oxide monohydrate

Pure aluminium ribbons were covered with a layer of amalgam by dipping them in 0.1M solution of $HgCl_2$. The ribbons were then boiled with water. The α-AlOOH obtained was separated by decantation and dried over $CaCl_2$. The thermal behaviour of this compound was determined by thermogravimetry.

2.1.2.3 Other metal compounds

Ammonium molybdate, ammonium tetraborate and talc ($Mg_3H_2(SiO_3)_4$) were also used in this work. These were obtained from B.D.H. Ltd. and were used without further purification. The three aluminium oxychlorides studied were supplied by Produits Chimiques Ugine Kühlmann, Centre of Research, Grenoble.

2.1.2.4 Stabilisers, antioxidants and lubricants

Various additives were needed in small quantities to prevent the atmospheric oxidation of the polymer and to improve their flow properties during milling. These additives are shown in Table 18.

2.1.3 Gases

Air, oxygen and nitrogen (oxygen-free), supplied by British Oxygen Company, were used without further purification.

Table 18

Stabilisers, antioxidants and lubricants used during the milling of polymer samples.

| Generic Name | | Trade Name | | Supplier |
|---|---|---|---|---|
| Lead dibasic phosphite | - | Stavinor PR12® | - | Rhône Poulenc |
| Lead dibasic stearate | - | Stavinor DB30® | - | Rhône Poulenc |
| Di-tert-butyl p-cresol | - | Ionol® | - | Organo Syntheses |
| Stearic Acid | - | - | - | British Drug Houses |
| Glycerol monostearate | - | - | - | Britsh Drug Houses |

## 2.2 Apparatus

### 2.2.1 The thermobalance

Thermoanalytical studies of the degradation and oxidation of the polymers and of the extents of interaction between various metal oxides and halogen compounds were made using a Mettler "Thermoanalyser 2" thermobalance. This apparatus makes it possible to obtain a continuous record of weight, rate of weight change and temperature while the sample is heated under one of five different temperature programmes in any desired atmosphere. Simultaneous differential thermal analysis (DTA) measurements can also be made.

The balance mechanism is located directly below the furnace and is of the beam-substitution type. A change in the sample mass causes a beam deflection which changes the output current of a photoelectric scanning system. The imbalance in photodiode current is amplified and passed through a coil attached to the balance beam which produces the restoring force. The current in the coil is used to measure the sample mass. The balance is designed to weigh samples of up to 16g. and has three sensitivity ranges, 0-1000mg., 0-100mg. and 0-10mg. respectively. A weight expansion unit provides greater accuracy by electronic amplification of the weight signal by a factor of ten. An accuracy of $\pm$ 0.2% of the range can be attained for all three

ranges of sample mass.

The expanded weight signal is electronically differentiated to provide the first derivative of sample weight. The most sensitive range available on the thermogravimetric (TG) unit is 0.5 $mg.min^{-1}$. for full-scale deflection. The accuracy of the instrument is $\pm$ 0.4% in the differential thermogravimetry (DTG) range.

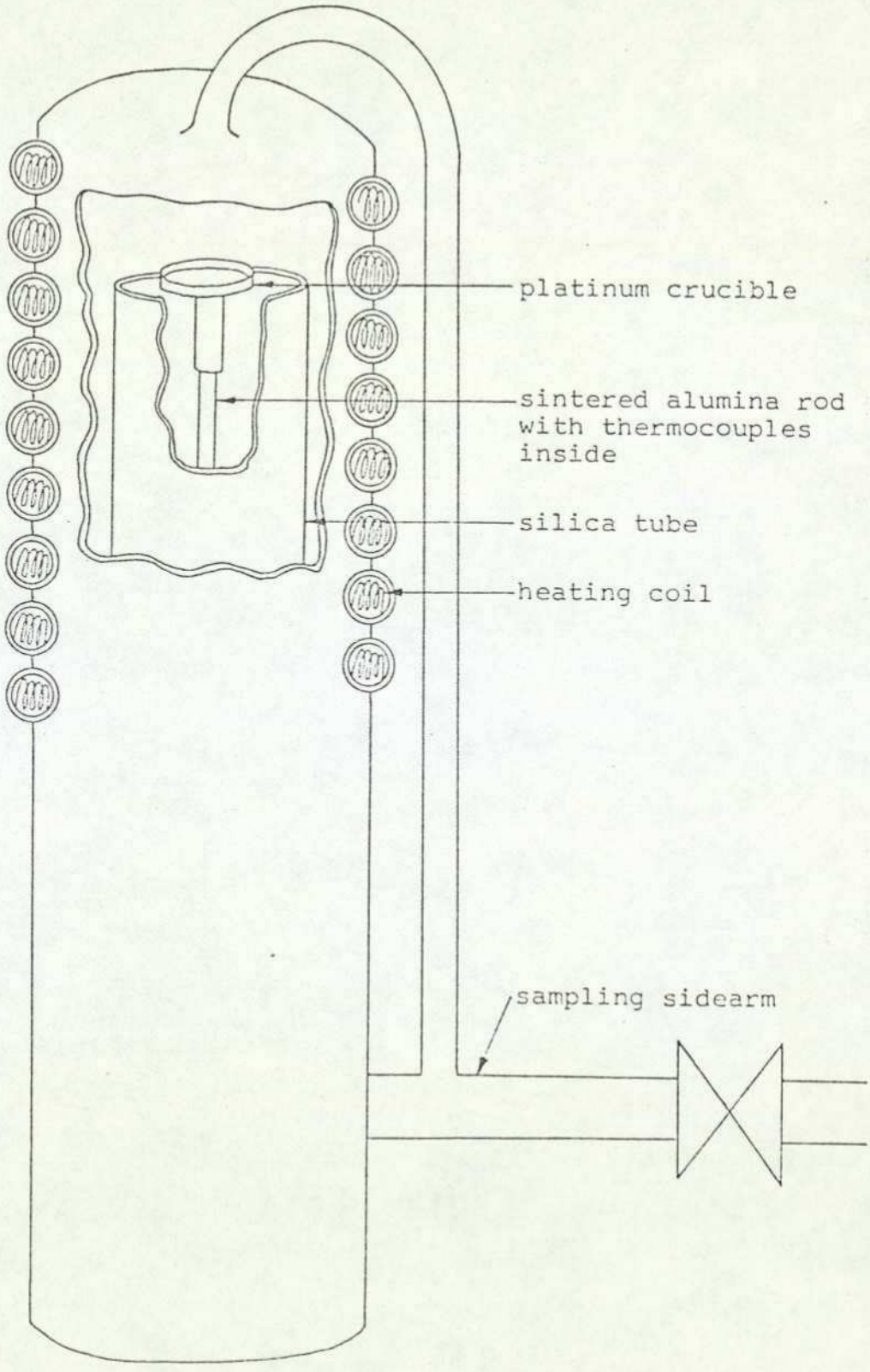
Temperature measurements are carried out by means of a Pt/10%Rh thermocouple. The hot junction is located underneath and in contact with the crucible. Temperatures can be measured with an accuracy of $\pm 2.5^{o}$ at $100^{o}C$ and $\pm$ $2.0^{o}$ at $500^{o}C$.

The DTA unit has six ranges, 20, 50, 100, 200, 500 and 1000μV. An accuracy of $\pm$ 0.2% over the range can be attained for all six ranges.

The furnace tube is of quartz and is surrounded by a reflecting shield. The heating element consists of a non-inductively wound Kanthal wire filament inside a bifilar quartz spiral (see Figure 25). The furnace may be heated from 25 to $1025^{o}C$ at a pre-selected heating rate of between 1 and $20^{o}.min.^{-1}$ or $100^{o}.min^{-1}$. The temperature programme control gives quite accurately linear heating rates. The skew on a heating rate of $5^{o}.min.^{-1}$ does not exceed $\pm$ $1.1^{o}.min.^{-1}$.

FIGURE 25

Bifilar quartz spiral furnace



The five temperature programmes available are as follows:

(i) From ambient temperatures, the furnace may be heated to a pre-selected upper limit and then turned off, when it cools down to room temperature.

(ii) The furnace may be heated to the upper temperature limit and the temperature may be kept there for isothermal work.

(iii) The temperature may be cycled between two pre-set limits.

(iv) The temperature may be lowered from an initially high value to a pre-set lower limit and kept steady.

(v) The temperature may be lowered as in (iv), but when the lower limit is reached, the furnace is switched off and cools to ambient temperatures without control.

Sample holder geometry and composition are of great importance in thermal analysis. Two matched flat-bottomed Pt/10%Rh crucibles were used; these were 8mm. in diameter and had a short straight wall rising vertically from the bottom of the crucible. The crucibles were supported on a sintered four-hole capillary tube which had a cross-piece 270mm. from

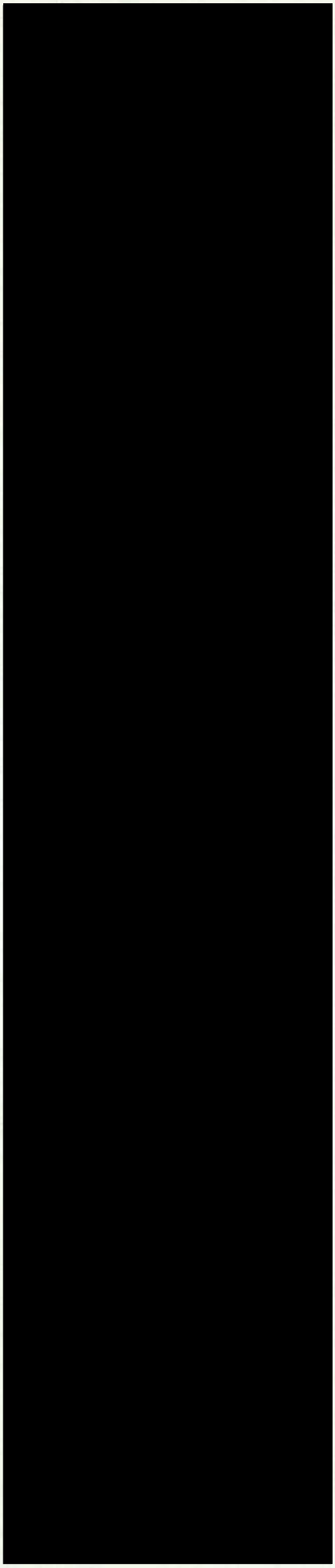
the end, bearing two short alumina pegs 11 mm. apart. Special metal bands, which have no influence on the accuracy of weighing, were used to connect the thermocouple leads from the crucible holder to the fixed balance housing (see Figure 26).

The flow of gas through the furnace is controlled by a pressure-regulating valve and the flow rate is metered by a "rotameter". The passage of gas between the balance housing and the reaction area is shielded by a metal baffle which rests in a socket on top of the balance housing when the crucible holder is in position. This prevents any substance which may fall from the crucible from entering and contaminating the balance housing.

The limits of error stated in this Section for the various channels, with the sole exception of the temperature channel, are lower than those which can be obtained on most other commercial thermobalances. However, although the data points can be read off the recorder chart to a high degree of accuracy, this is impaired by base-line drifts caused by defects inherent in the instrument design. The base-line drift in the weight channel is caused by buoyancy effects due to the heating. In some other commercial thermobalances this has been overcome by use of two matched furnaces, one for each arm of the balance, and by symmetrical

FIGURE 26

Crucible holder for DTA



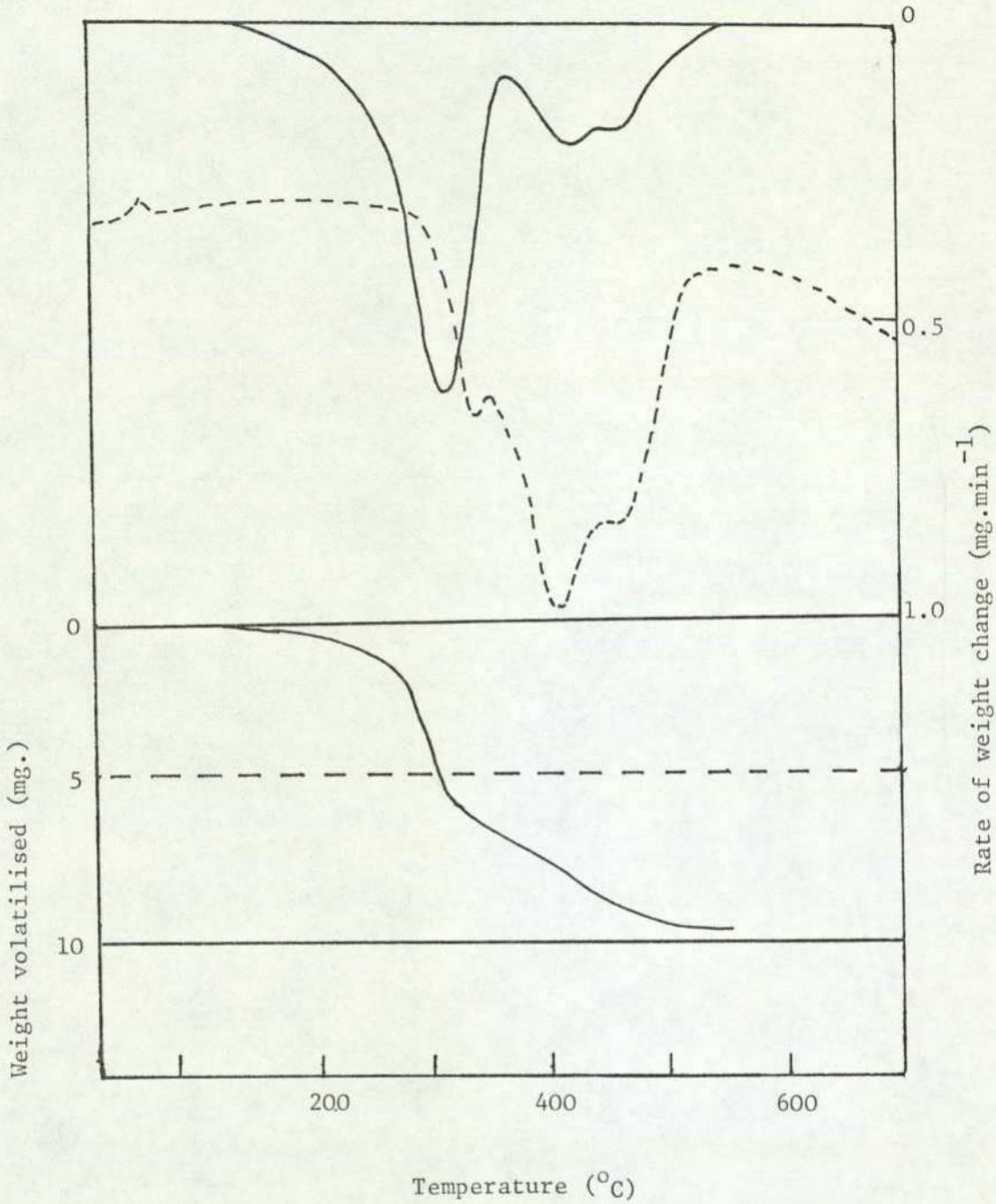
design of the balance. In the Mettler "Thermo-analyser 2" thermobalance, base-line drift finishes by the time the sample reaches approximately 120°C. The amount of such drift can be as much as 0.15mg., which corresponds to 1.66%, in a sample of 9mg. weight.

Base-line drift also occurs on the DTA channel, which leads to errors in calculations of the peak areas of thermal changes. Because the sample is supported on a long rod inside the furnace, it is impossible to align the crucible with the axis of the furance. As a result there is a difference in temperature between the sample and reference crucibles, which causes the base-line drift. High rates of heating increase the effect significantly. Base-line drift in DTA would be reduced if a furnace with a more even temperature distribution were used.

A 12-channel, 6-point dot recorder simultaneously traces in different coloured inks, the temperature curve, the two weight traces (natural and expanded), the differential of the weight trace and the DTA trace. The dot intervals of the tracings were chosen so that each curve, according to its gradient, had the optimum point density. When these points are later joined up, a series of curves and lines are obtained. Figure 27 shows the degradation curves obtained when, a sample of electrofine S70 was heated in a slowly flowing

FIGURE 27

The thermogravimetric analysis of Electrofine S70




- - - D. T. A. trace

atmosphere of air at a rate of $5^{o}$ $min^{-1}$. Block schematic diagrams of the balance mechanism and of the recording and electric systems are shown in Figures 28 and 29 respectively.

FIGURE 28

Block schematic diagram of the
balance mechanism

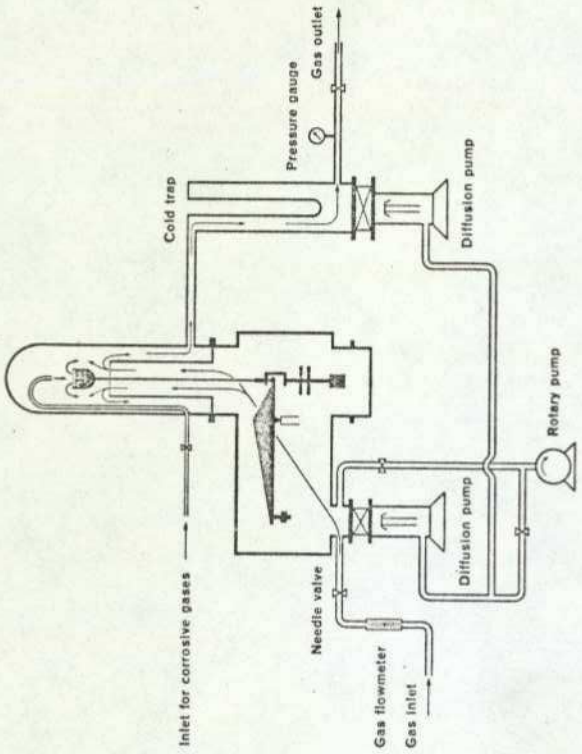
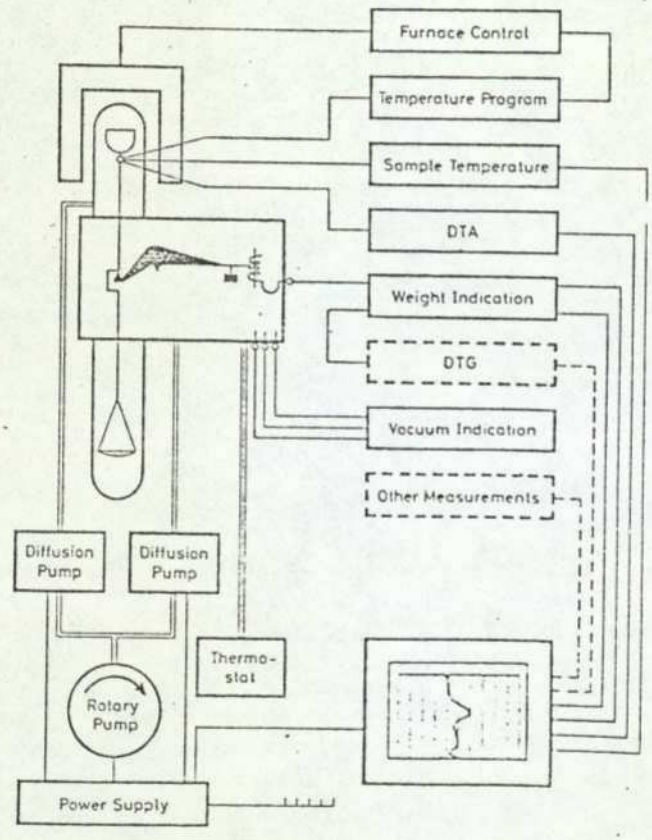


FIGURE 29

Block schematic diagram of the balance mechanism

and the recording and electric systems



2.2.2 Oxygen-Index apparatus.

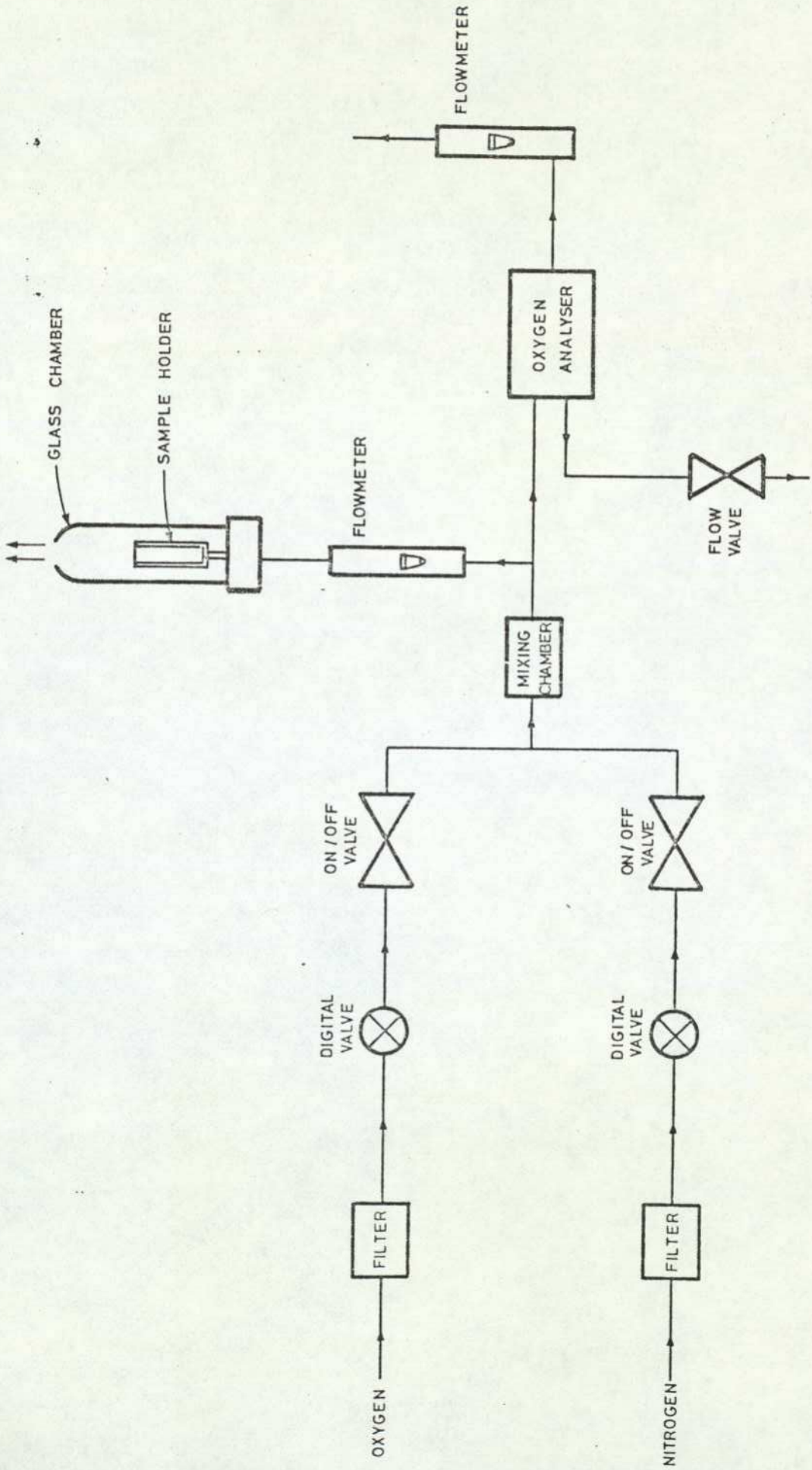
The Stanton Redcroft limiting oxygen-index equipment, designed to meet ASTM D 2863-70 (entitled "Standard method of test for flammability of plastics using the oxygen index method") was used in this work.

The right-hand side of the equipment houses the gas lines. The layout is shown schematically in Figure 30. Two gas inlets at the rear of the instrument lead to two filters fitted with numerical controls. This enabled the needle valves to be set very precisely. An ON-OFF lever is situated adjacent to each control needle valve in each gas line. The two separate pipes merge at a mixing chamber to give a homogeneous combined gas flow. The main portion (ca 99.5%) passes directly to the principal indicating flowmeter which is calibrated to read from 0-25 $dm^3$ $min.^{-1}$ for air. From the flowmeter the gas passes directly to the mesh at the base of the test column. The small by-pass flow (ca 0.5%) goes directly to the paramagnetic oxygen analyser which produces direct digital readout of the percentage oxygen in the gas mixture. The instrument was connected up to cylinders of oxygen and nitrogen via a two-stage regulator and supply pressures of 25 p.s.i. were employed in order to achieve the required flow rates during the test.

The test column on the limiting oxygen-index

FIGURE 30

Schematic layout of the oxygen index apparatus



equipment is a heat-resistant glass column which rests in a casting designed with special entry ports so that the entering gas gives a laminar flow up the column(see Figure 31). At the base of the column is a perforated metal screen in order to catch any fragments or burning droplets formed during combustion of the polymer samples. The standard sample holder is situated at the centre of the column.

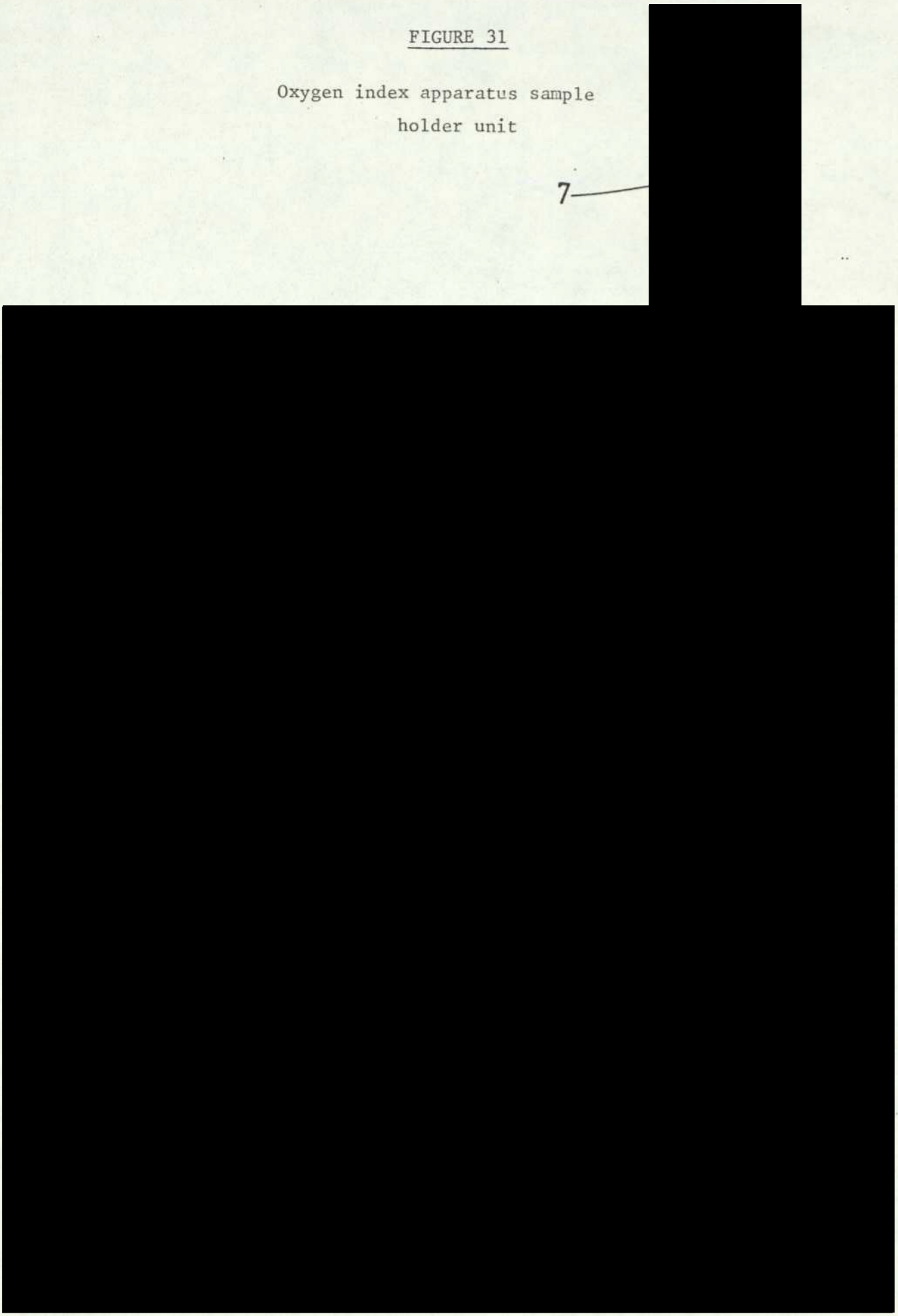
The burner is a 150mm long copper tube attached to a natural gas supply; a standard 25mm flame was used to ignite the samples.

2.2.3 Mass Spectrometer

Mass spectra were obtained with a Kratos MS30 mass spectrometer coupled to a DS50L data handling system. Samples of flame retardant containing polymers were heated in the source of the mass spectrometer and the volatile products were analysed.

FIGURE 31

Oxygen index apparatus sample holder unit



## 2.3 Procedure

### 2.3.1 Preparation of polymer samples

The metal oxides, halogen compounds, stabilisers, antioxidants and lubricants were weighed out prior to incorporation into the polymer. A "Ruth Schwabenthan" two-roll mill was used for this purpose. In the case of ABS copolymer, the weighed flame retardant, 0.5phr antioxidant (Ionol) and 0.5phr lubricant (stearic-acid) were thoroughly mixed with the powdered resin and milled into a "homogeneous" crêpe, by a hand-rolling technique, over a period of ten minutes. The temperatures of the front and back rollers were $170^{o}$ and $165^{o}C$ respectively. For polyethylene, which was in pellet form, the resin was initially milled into a crêpe and the flame retardant, 1phr lead dibasic phosphite, 0.2phr lead dibasic stearate stabilisers and 0.5phr lubricant (glycerol monostearate) were then carefully incorporated into it using a hand rolling technique. The temperature of the two rollers was $10^{o}$ lower than that used for ABS.

An electrically-operated, electrically-heated hydraulic press capable of attaining temperatures up to $220^{o}C$ and pressures up to $5.5 \times 10^{6}$ Pa was used to mould the final test specimens. The cold press used to keep the specimens flat as they cooled was a hand-operated "fly-press" capable of withstanding the

pressures required. The stainless steel moulds were of dimensions 0.3 x 15.2 x 15.2 cm. The crêpes were sandwiched between two "Melinex" sheets, placed in the mould and heated for 5 min at atmospheric pressure at 210°C. The mould was then compressed at $5.5 \times 10^6$ Pa for a further 5 min and then cooled, under pressure, to room temperature.

2.3.2 Procedure for thermal analysis

Thermal analysis runs were carried out in flowing atmospheres of air and nitrogen at a heating rate of $5^{o}$. $min^{-1}$. A gas flow rate of 60 $cm^{3}$. $min^{-1}$ was used; this was sufficiently large to stop the back-diffusion of degradation products into the balance housing and small enough to avoid production of signal noise on the TG and DTG channels. Sample weights of 8-10mg. were used in studies of the effects of various metal oxides on the degradation of the two polymers and the interaction of metal oxides and halogen compounds. In the case of a powdered flame-retardant composition, the sample was spread evenly over the crucible surface. The polymers were cut from films of about 0.1 mm. thickness to a size which just fitted the crucible. The effects due to the geometrical arrangement of the sample on the crucible and of sample size are kept to a minimum. The "range shift" on the DTG panel was manual. A sensitivity of 1 $mg.min^{-1}$ per full scale deflection was used except in cases where polymers were involved. Under these conditions, a sensitivity of 2 $mg.min^{-1}$ had to be employed in order to trace the complex weight changes taking place.

The results of thermogravimetric and DTA runs were printed on the 25 cm wide chart of a six-point "dot" recorder. The data obtained were read off the chart

by hand.

It should be noted that DTA is not an "operator-sensitive technique" and all discrepancies can be explained by differences in procedure, instrument design and sample properties. Wendlandt[294] lists the following sample characteristics which affect the shape of DTA curves: (i) particle size, (ii) thermal conductivity, (iii) heat capacity, (iv) packing density, (v) swelling or shrinking, (vi) mass of sample, (vii) nature of diluents and (viii) degree of crystallinity. It is impossible to choose a suitable reference material for use in DTA studies of the oxidative thermal degradation of polymers because, as the degradation proceeds, so the composition of the polymer, and hence its heat capacity changes. In all the work done, no reference material was used.

### 2.3.3 Measurement of oxygen-index

A Stanton Redcroft critical oxygen index apparatus, designed to meet ASTM D2863-70 specifications was used to test the flammability of the polymer composites.

The gases were used with no prior treatment at cylinder outlet pressures of $1.7 \times 10^5$ Pa. The combination of the mixing chamber and the mesh at the bottom of the chimney gave adequate mixing of the gases even at very high flow rates.

The oxygen concentration was measured with a paramagnetic oxygen analyser producing an electrical signal which allowed direct digital read-out of the limiting oxygen index to a high accuracy. Samples of dimensions 0.3 x 1.3 x 10 2 cm, as specified for the test[295], were ignited for fifteen seconds (or until a stable flame was attained on top of the polymer candle) with a 2.5 cm natural gas flame under controlled oxygen + nitrogen atmospheres. The oxygen concentration in which a candle of polymer burned for a period of three minutes was recorded. The average of four such readings was then recorded as the limiting oxygen index of the polymer sample.

# 3 RESULTS

## 3.1 Thermogravimetric experiments

### 3.1.1 General

The commercially important synergism between antimony oxide and halogen compounds, thought to be due at least in part to gas-phase flame-poisoning reactions, has been shown to involve volatilisation of the antimony solely as the trihalide in an exothermic reaction[296]. Studies of the thermal decomposition of halogen compounds have shown that their synergistic flame-retardant action in conjunction with antimony is related to their mode of decomposition or volatilisation.

For the major part of this work, a chlorinated wax (Electrofine S70) was used, which decomposes quantitatively to liberate hydrogen chloride in the condensed phase when heated above 350°C. With this material, the extent of volatilisation of the metal oxide depends only on its ability to react with the liberated hydrogen halide and on the boiling point of the metal halide formed. In the presentation of data describing the action of flame-retardant additives in polymers, plots are often given of "weight-fraction of material remaining" against "temperature of sample". The "stability temperatures" obtained in this way are highly dependent on such factors as sample size, shape of the containing vessel, rate of heating, nature of the gaseous atmosphere and rate of flow of gas

over the sample. When the halogen additive is heated in a polymer matrix or mixed with metal oxide powder, the apparent "stability temperature", defined as the temperature of maximum rate of additive-loss from the sample, is also dependent on the nature of the matrix, and on the surface area of the powder.

Comprehensive studies have been made of the volatilisation and decomposition, in air, of various metal oxides and mixtures of metal oxides with halogen flame retardant additives on their own and when incorporated into polymers to study their possible combined interactions and joint effects on the thermal decompositions of the polymers.

3.1.2 Metal oxides

Antimony (III) oxide, when heated in air, does not lose weight below 700°C. In flowing nitrogen, however, all the metal oxide is converted to more easily volatilised metal at ca.670°C:

$$2\ Sb_2O_3 \rightleftharpoons 4\ Sb + 3O_2$$

Anhydrous tin (IV) oxide, when heated in air to 750°C, neither loses nor gains weight. No phase transitions or melting points are observed on the DTA curve.

β-tin (IV) oxide hydrate exhibits three distinct dehydration steps, as shown in Figure 32. On being heated, the white powder turns green-black around 310°C, but above 550°C it once more becomes white but now has a greenish tint. The two major steps where water is lost are at 155°C-350°C (7% - maximum rate ca. 3.5% $min^{-1}$ at 305°C) and 350°C - 660°C (3% - maximum rate ca. 8% $min^{-1}$ at 380°C). (Table 19).

Anhydrous black tin (II) oxide is oxidized to tin (IV) oxide between 280°C and 912°C with a maximum rate of oxygen uptake of 2.7% $min^{-1}$ at 560°C (Table 19).

Dry commercial aluminium oxide trihydrate ( $Al_2O_3.3H_2O$ ) is quite stable at temperatures below 205°C and at atmospheric pressure. Between 205 and 220°C however decomposition starts to occur. On being heated to 780°C, the compound loses 33.5% of its initial weight in three

TABLE 19

The thermal analysis of hydrated metal oxides

| Metal Oxide | $SnO_2$ | AlOOH[a] | AlOOH[b] | $Al_2O_3.3H_2O$ |
|---|---|---|---|---|
| Weight-fraction of M.O. volatilised (%) | 10.0 | 26.7 | 15.7 | 33.5 |
| First weight-loss reaction | | | | |
| Weight-fraction volatilised (%) | 7.0 | 3.1 | 1.0 | 3.4 |
| Temperature range ($^{o}C$) | 155-350 | 97-110 | 239-422 | 205-235 |
| Max. rate of volatilisation (% $min^{-1}$) | 3.5 | 6.7 | 7.0 | 25.8 |
| Temperature of max. rate ($^{o}C$) | 305 | 106 | 375 | 222 |
| Second weight-loss reaction | | | | |
| Weight-fraction volatilised (%) | 3.0 | 16.7 | 14.4 | 27.2 |
| Temperature range ($^{o}C$) | 350-660 | 207-321 | 415-650 | 235-424 |
| Max. rate of volatilisation (% $min^{-1}$) | 8.0 | 16.4 | 10.9 | 23.4 |
| Temperature of max. rate ($^{o}C$) | 380 | 266 | 512 | 273 |
| Third weight-loss reaction | | | | |
| Weight-fraction volatilised (%) | | 6.9 | 0.3 | 2.9 |
| Temperature range ($^{o}C$) | | 321-500 | 703-765 | 424-599 |
| Max. rate of volatilisation (% $min^{-1}$) | | 4.1 | 10.8 | 8.8 |
| Temperature of max. rate ($^{o}C$) | | 379 | 7.43 | 494 |

a: laboratory prepared sample

b: commercial sample

stages. It first decomposes to give alumina and water vapour:

$$2Al(OH)_3 \longrightarrow Al_3O_3 + 3H_2O$$

This reaction is endothermic to the extent of ca. 1.4 kJ per gram of aluminium hydroxide. Figure 33 shows the differential thermal analysis (DTA) curves of two samples of aluminium hydroxide differing in particle size, the rate of heating being $5^{-o}$ $min^{-1}$. Most of the water vapour is evolved over the temperature range 200-400°C. For the coarser material (BACO FRF 5), there are three distinct peaks, whereas for the finer material the first and third peaks are much smaller. The first peak, which is observed at about 230°C, is ascribed to the conversion of the trihydrate to the monohydrate (Boehmite)[297]:

$$Al(OH)_3 \longrightarrow AlOOH + H_2O$$

A second peak is found at about 299°C and corresponds to the direct conversion of the trihydrate to an activated (chi) alumina:

$$2Al(OH)_3 \longrightarrow Al_2O_3(chi) + 3H_2O$$

The third broad endothermic peak at about 530°C is due to the conversion of the monohydrate, formed at lower temperatures, to a transition (gamma) alumina:

$$2ALOOH \longrightarrow Al_2O_3(\gamma) + H_2O$$

Decomposition via the monohydrate occurs under particular hydrothermal conditions, which can exist in the centre of large crystals of the trihydrate. As the percentage of coarse material decreases, the likelihood of these conditions existing diminishes. Therefore, a slightly greater percentage of water vapour will be evolved from fine particles of aluminium oxide trihydrate.

The mechanism of decomposition of aluminium oxide monohydrate is completely different from that of the trihydrate. Laboratory-produced α-AlOOH decomposes below 500°C to lose 26.7% of its initial weight in three stages. About 3.1% moisture is lost below 110°C; 16.7% of the dry weight is volatilised between 207 and 321° (with a maximum rate of 16.4% $min^{-1}$ at 266°C) and a further 6.9% is lost between 321 and 500°C (with a maximum rate of 4.1% $min^{-1}$ at 379°C). The third stage is the only endothermic reaction. A commercial sample of this monohydrate ($Al_2O_3.H_2O$) loses a total of 15.7% of its initial weight below 675°C, the only major loss being 14.4% from 415 to 650°C (with a maximum rate of 10.9% $min^{-1}$ at 512°C). The theoretical water loss from this material is ca. 15.0%. The dehydration stage is only moderately endothermic; and is certainly less so than for the trihydrate (Table 19).

Anhydrous alumina ($Al_2O_3$) does not lose weight below 950°C.

The mechanism of decomposition of the three aluminium oxychlorides (Echantillon 3847, 3848 and 3849) is difficult to interpret as their exact chemical composition is not known. The results are best treated in visual form as in Figures 34, 35 and 36. There is some difficulty in understanding the results due to the uncertainty of the effect of physically adsorbed moisture. The fact that the DTA curves show three, six and five stages respectively suggest that these materials are chemically quite different, although each loses about 50% of its initial weight on being heated to 960°C.

Iron (III) oxide, when heated alone in air, steadily gains weight at the rate of slightly over 1% per 100° rise in temperature, gaining a total of ca 10% between 25 and 900°C.

Zinc (II) oxide remains unchanged when heated up to 600°C; it is then slowly oxidised.

Similarly copper (II) oxide shows no change in weight between 25 and 650°C. Its weight subsequently increases by ca.1.7% up to 900°C.

When heated alone, ammonium molybdate and ammonium tetraborate decompose by multi-stage processes (Figure 37). No further attempt was made to study their decomposition reactions.

### 3.1.3 Halogen compounds

Electrofine S70, a chlorinated wax with a chlorine content of 70% w/w, decomposes quantitatively in the condensed phase, liberating hydrogen chloride. More than 99% of the weight of material originally present can be accounted for by the sum of hydrogen chloride plus carbonaceous residue. On being further heated in air, this residue is burnt off the crucible below 550°C, in a reproducible reaction, whilst in nitrogen it undergoes a slow weight loss (SWL) (Figure 37).

Adine 0102, deca-bromobiphenyl, containing 84% w/w bromine, volatilises quantitatively, when heated, without decomposition. It partially sublimes, and this obscures the melting point, which occurs, for a 100mg. sample, at about 385°C ($\pm$ 0.5°C). For these samples, ca. 35% of the material has already volatilised by sublimation below this temperature, and such sublimation leads to deposition of as much as 10% of crystalline decabromobiphenyl on the crucible holder. The later volatilisation of this material gives the appearance of an extra stage in the decomposition.

Tables 20 and 21 show the temperature of maximum rate of reaction ($T_{max}$), and the weight fraction of material volatilised (W.F.), for each stage during the degradation of the chlorinated wax S70 (Table 20) and of the Adine 0102

TABLE 20

The temperature of the maximum rate of weight-loss ($T_{max}$), and the weight fraction of material volatilised (W.F.) when chlorinated was S70 is heated under various experimental conditions.

| Sample size (mg) | Gas | Main degradation stage | | Carbon burn-off | | Total W.F.(%) volatilised |
|---|---|---|---|---|---|---|
| | | $T_{max}$ (°C) | W.F. % | $T_{max}$ (°C) | W.F. % | |
| Samples heated at $5^{o}C\ min^{-1}$ | | | | | | |
| 10 | Air | 322 | 67.2 | 517 | 29.0 | 99.3 |
| 10 | $N_2$ | 309 | 65.7 | SWL | 29.8 | 99.6 |
| 80 | Air | 336 | 66.4 | 539* | 29.1 | 99.5 |
| 80 | $N_2$ | 321 | 65.6 | SWL | 30.0 | 99.6 |
| Samples heated at $2^{o}C\ min^{-1}$ | | | | | | |
| 80 | Air | 307 | 67.9 | 49.6 | 29.4 | 98.8 |
| 80 | $N_2$ | 303 | 68.1 | SWL | 28.9 | 98.8 |

SWL - slow weight loss - in nitrogen the carbon is not burnt-off the crucible

* - carbon burnt-off exothermically.

TABLE 21

The temperature of the maximum rate of weight-loss ($T_{max}$), and the weight-fraction of material volatilised (W.F.) when decarbromobipheyl is heated under various experimental conditions

| Sample size (mg) | Gas | Main volatilisation stage | | Total W.F. (%) volatilised |
|---|---|---|---|---|
| | | $T_{max}$ (°C) | W.F.* % | |
| Samples heated at 5°C $min^{-1}$ | | | | |
| 10 | Air | 398 | 97.1 | 99.2 |
| 10 | $N_2$ | 399 | 96.5 | 99.4 |
| 100 | Air | 456 | 90.1 | 99.5 |
| 100 | $N_2$ | 460 | 88.8 | 99.8 |
| Samples heated at 2°C $min^{-1}$ | | | | |
| 100 | Air | 427 | 90.0 | 99.9 |
| 100 | $N_2$ | 421 | 88.6 | 99.7 |

*The differences in these weight-fractions is due to condensation of material on the crucible holder (see text).

(Table 21). The accuracy of the results varies with the mode of decomposition of the additives studied. In Table 20, typical of a condensed phase decomposition process, the values of W.F. are remarkably constant, whilst those of $T_{max}$ vary by 10-15° with the same experimental conditions. In Table 21, which is representative of additives which volatilise without decomposition, the values of $T_{max}$ are reproducible to $\pm 3^{o}C$, whilst those of W.F. exhibit a more random variation.

The chlorinated wax S70 is more stable in air than in nitrogen and, when the flow rates of both gases are increased, $T_{max}$ is not significantly effected. There is also little change in the $T_{max}$ value when the rate of heating is decreased from $5^{o}$ $min^{-1}$ to $2^{o}$ $min^{-1}$.

Experiments with Adine 0102 in nitrogen and air, give identical results. However, at high gas-flow rates, $T_{max}$ is lowered as volatilisation is facilitated and a similar change is noticed when the rate of heating is reduced from $5^{o}$ $min^{-1}$ to $2^{o}$ $min^{-1}$.

The various stages in the decomposition of S70 and Adine 0102 are shown in Table 22.

TABLE 22

The thermal analysis of Electrofine S70 and Adine 0102

| | S70 | Adine |
|---|---|---|
| Total weight-fraction volatilised(%) | 98.8 | 99.8 |
| Main weight loss reaction | | |
| Weight-fraction volatilised(%) | 67.8 | 99.8 |
| Temperature range ($^{o}$C) | 150-350 | 175-425 |
| Max. rate of volatilisation(% min.$^{-1}$) | 9.3 | 11.5 |
| Temperature of max. rate ($^{o}$C) | 307 | 420 |
| Carbon 'burn-off' reactions | | |
| Total weight-fraction volatilised(%)* | 31.0 | - |
| Temperature range ($^{o}$C) | 350-508 | - |
| First stage | | |
| Weight-fraction volatilised(%)* | 18.2 | - |
| Max. rate of volatilisation(% min.$^{-1}$) | 5.9 | - |
| Temperature of max. rate ($^{o}$C) | 429 | - |
| Temperature of"max.heat of reaction"($^{o}$C) | 429 | - |
| Second stage | | |
| Weight-fraction volatilised(%)* | 12.8 | |
| Max. rate of volatilisation(% min.$^{-1}$) | 5.0 | |
| Temperature of max. rate ($^{o}$C) | 450 | |

### 3.1.4. Metal Oxides + Halogen compounds

#### 3.1.4.1 Mixtures of halogen compounds and single metal oxides

Mixtures of antimony (III) oxide and chlorinated wax S70 volatilise in up to four stages (Table 23). The major interaction takes place in the main weight loss stage between 219 and 355°C, when antimony oxide is converted to antimony trichloride.

$$Sb_2O_3 + 6HCl \longrightarrow 2SbCl_3 + 3H_2O$$

When a stoichiometrically insufficient amount of chlorinated wax is used, the main weight loss reaction occurs in a single stage; the interaction is quantitative, so that no additional evolution of hydrogen chloride takes place. When the chlorinated wax is in excess, the main weight loss stage is divided into two fairly rapid reactions. The first is the conversion of the oxide to the trichloride and the second, the extent of which increases with the weight of S70 in the sample, is the evolution of hydrogen chloride from the unchanged wax. The reactions are moderately exothermic and hence the frequently postulated endothermic breakdown of antimony oxychloride in the condensed phase is highly unlikely. The maximum rate of the main reaction is ca. 18% $min^{-1}$ at ca. 300°C. The carbon 'burn-off" reactions occur in two stages between 335 and 900°C and are probably due to some

TABLE 23

Thermal analysis of mixtures of $Sb_2O_3$ and S70

| Ratio of $Sb_2O_3$ to S70(w/w): | 0:1 | 1:1 | 1:2 | 1:3 | 1:4 |
|---|---|---|---|---|---|
| Weight-fraction of M.O.volatilised(%): | - | 80.2 | 88.4 | 99.1 | 98.7 |
| Total W.F. of mixture volatilised(%):* | 98.8 | 176.8 | 144.2 | 132.1 | 123.4 |
| Theor. W.F. volatilisable (%): | 100.0 | 195.8 | 150.0 | 133.3 | 125.0 |
| First main weight-loss reaction. | | | | | |
| Weight-fraction volatilised(%): | 67.8 | 64.6 | 43.3 | 47.2 | 44.5 |
| Weight-fraction vol. (% of S70)(%):* | 67.8 | 137.2 | 64.9 | 62.9 | 55.6 |
| Temperature range ($^{o}$C)C | 150-350 | 219-355 | 222-305 | 169-303 | 234-306 |
| Max. rate of volatilisation(%.min$^{-1}$): | 9.3 | 18.2 | 19.6 | 11.6 | 21.8 |
| Temperature of max. rate ($^{o}$C): | 302 | 302 | 296 | 380 | 295 |
| Second main weight-loss reaction. | | | | | |
| Weight-fraction volatilised(%): | - | - | 35.4 | 27.4 | 28.3 |
| Weight-fraction vol. (% of S70) (%):* | - | - | 53.1 | 36.5 | 35.4 |
| Temperature range ($^{o}$C): | - | - | 305-355 | 303-335 | 306-365 |
| Max. rate of volatilisation (%.min$^{-1}$): | - | - | 15.3 | 8.9 | 15.0 |
| Temperature of max. rate ($^{o}$C): | - | - | 308 | 320 | 319 |
| Carbon 'burn-off' reactions. | | | | | |
| Total weight-fraction volatilised(%): | 31.0 | 18.5 | 17.5 | 24.3 | 27.1 |
| Total W.F. volatilised (% of S70)(%):* | 31.0 | 39.7 | 26.3 | 32.4 | 33.9 |
| Temperature range ($^{o}$C): | 305-508 | 355-488 | 355-528 | 355-900 | 365-900 |
| (a) First stage. | | | | | |
| Weight-fraction volatilised(%): | 18.2 | 15.1 | 17.5 | 22.8 | 21.9 |
| Weight-fraction vol. (% of S70)(%):* | 18.2 | 32.4 | 26.3 | 30.4 | 27.4 |
| Max. Rate of volatilisation(%.min$^{-1}$): | 5.4 | 10.0 | 6.8 | 20.8 | 10.9 |
| Temperature of max. rate ($^{o}$C): | 429 | 445 | 479 | 488 | 520 |
| Temperature of max. endothermicity($^{o}$C): | 429 | 425 | 461 | 488 | 509 |
| (b) Second stage. | | | | | |
| Weight-fraction volatilised(%): | 12.8 | 3.4 | - | 1.6 | 5.4 |
| Weight-fraction vol. (% of S70)(%):* | 12.8 | 7.3 | - | 2.0 | 6.8 |
| Max. rate of volatilisation(%.min$^{-1}$): | 5.0 | 7.0 | - | 3.5 | 7.8 |
| Temperature of max. rate ($^{o}$C): | 450 | 523 | - | 660 | 827 |

interaction between the $SbCl_3$ and the carbon residue.

For quantitative volatilisation of tin (II) oxide by conversion to $SnCl_2$, 100 mg of S.70 should react with 129.1 mg SnO to form and volatilise 180.3 mg of $SnCl_3$. The observed interaction between SnO (II) oxide and S70 is thus not quantitative (Table 24). When heated on its own, SnO is slowly oxidised to $SnO_2$ between 280 and 912°C with a maximum rate of oxygen uptake of 2.7% $min^{-1}$ at 560°C. Thus the extensive weight-loss when SnO is heated with S70 must be wholly attributable to the interaction of the two materials when S70 is in excess. The optimum interaction takes place with a molar ratio of 2SnO:3S70. A total weight-fraction of 164.1% is volatilised largely in the main weight loss stage, and no interaction appears to occur in the carbon 'burn-off' stage. Comparison of the total weight-fraction of sample actually volatilised with the maximum theoretical weight-fraction which could be volatilised, showed that, with all mixtures containing excess S70 (SnO:S70 ratios > 1:1.3 w/w), ca. 85% of the mixture was volatilised. Hence, SnO interacts quite strongly with S70 but the reaction does not appear to take place stoichiometrically. This may be attributed to the weight gained during oxidation. The thermal analysis of SnO and Adine 0102 mixtures indicates that a lowering of the temperature of decomposition of Adine occurs. This is followed by a weight-gain, which is due to partial oxidation of the remaining SnO.

TABLE 24

Thermal analysis of mixtures of SnO and S70

| Ratio of SnO to S70(w/w): | 0:1 | 1:8 | 1:3 | 2:5 | 1:2 | 1:1 | 3:2 | 1:0 |
|---|---|---|---|---|---|---|---|---|
| Weight-fraction of M.O.volatilised(%): | - | 82.9 | 77.2 | 82.3 | 64.9 | 26.6 | 10.0 | 1.2 |
| Total W.F. of mixture volatilised(%):* | 98.8 | 110.4 | 125.7 | 132.9 | 132.5 | 126.6 | 112.5 | - |
| Theor. W.F. volatilisable (%): | 100.0 | 112.5 | 133.3 | 140.0 | 150.0 | 200.0 | 229.2 | - |
| First main weight-loss reaction. | | | | | | | | |
| Weight-fraction volatilised(%): | 67.8 | 29.9 | 53.9 | 58.6 | 68.1 | 48.0 | 7.8 | 0.9 |
| Weight-fraction vol. (% of S70) (%):* | 67.8 | 33.3 | 71.9 | 83.6 | 102.2 | 96.0 | 19.5 | - |
| Temperature range ($^{o}$C): | 150-350 | 191-260 | 223-285 | 185-293 | 145-343 | 234-317 | 209-283 | 72-197 |
| Max. rate of volatilisation(%.min$^{-1}$): | 9.3 | 18.7 | 29.3 | 22.8 | 39.1 | 25.7 | 21.5 | 5.9 |
| Temperature of max. rate ($^{o}$C): | 302 | 236 | 263 | 273 | 282 | 275 | 276 | 133 |
| Second main weight-loss reaction. | | | | | | | | |
| Weight-fraction volatilised(%): | - | 41.1 | 18.6 | 15.2 | - | - | 26.3 | 0.3 |
| Weight-fraction vol. (% of S70)(%):* | - | 46.2 | 24.8 | 21.5 | - | - | 65.8 | - |
| Temperature range ($^{o}$C): | - | 260-347 | 285-361 | 293-365 | - | - | 283-363 | 197-235 |
| Max. rate of volatilisation(%.min$^{-1}$): | - | 12.8 | 4.3 | 3.3 | - | - | 7.3 | 22.2 |
| Temperature of max. rate ($^{o}$C): | - | 312 | 307 | 317 | - | - | 287 | 224 |
| Carbon 'burn-off' reactions. | | | | | | | | |
| Total weight-fraction volatilised(%): | 31.0 | 27.1 | 21.8 | 20.0 | 20.2 | 15.3 | 11.0 | - |
| Total W.F.volatilised(% of S70)(%):* | 31.0 | 30.5 | 29.1 | 28.3 | 30.3 | 30.6 | 27.5 | - |
| Temperature range ($^{o}$C): | 350-508 | 347-530 | 361-516 | 365-527 | 346-524 | 317-554 | 363-598 | - |
| (a) First stage. | | | | | | | | |
| Weight-fraction volatilised(%): | 18.2 | 9.5 | 21.8 | 20.0 | 20.2 | 15.3 | 11.0 | - |
| Weight-fraction vol. (% of S70)(%):* | 18.2 | 10.7 | 29.1 | 28.3 | 30.3 | 30.6 | 27.5 | - |
| Max. Rate of volatilisation(%.min$^{-1}$): | 5.4 | 8.9 | 8.3 | 8.5 | 6.7 | 6.7 | 8.3 | - |
| Temperature of max. rate ($^{o}$C): | 429 | 387 | 476 | 472 | 471 | 477 | 486 | - |
| Temperature of Max. endothermicity($^{o}$C): | 429 | 414 | 461 | 464 | 472 | 468 | 486 | - |
| (b) Second stage. | | | | | | | | |
| Weight-fraction volatilised(%): | 12.8 | 17.6 | - | - | - | - | - | - |
| Weight-fraction vol. (% of S70)(%):* | 12.8 | 19.8 | - | - | - | - | - | - |
| Max. rate of volatilisation (%.min$^{-1}$): | 5.0 | 7.2 | - | - | - | - | - | - |
| Temperature of max. rate ($^{o}$C): | 450 | 471 | - | - | - | - | - | - |

When tin(IV) oxide hydrate is heated with S70 (in $SnO_2$:S70 molar ratios of 1:2, 2:3 and 2:5) the total weight-fractions volatilised (based on total loss of S70 = 100%) are 183%, 122% and 114% respectively (Table 25). The interactions take place principally in the main weight loss stage rather than during carbon 'burn-off'. Thus about 30% of the weight-fraction (expressed as a percentage of S70) is volatilised in the carbon burn-off stage, even though the reaction occurs at a higher temperature than with S70 alone. The decomposition takes place in three distinct stages (Figure 32). The first stage is equivalent to the loss of hydrogen chloride from the chlorinated wax. The second stage, a shoulder on the first rate of weight-change peak, is presumably due to volatilisation of $SnCl_4$ formed during the first stage, and the final stage is the carbon 'burn-off' reaction. With a mixture of molar ratio $3SnO_2$:2S70, interaction takes place in both the main and carbon 'burn-off' reactions. The reaction between $SnO_2$ and Adine occurs in two distinct stages. The first weight-loss stage can be attributed to the volatilisation of Adine coupled with the evolution of water of hydration from $SnO_2$. There is some indication that the first weight-loss reaction is in fact two reactions occurring simultaneously; this could be due to further evolution of bromine. The carbon 'burn-off' is a slow reaction

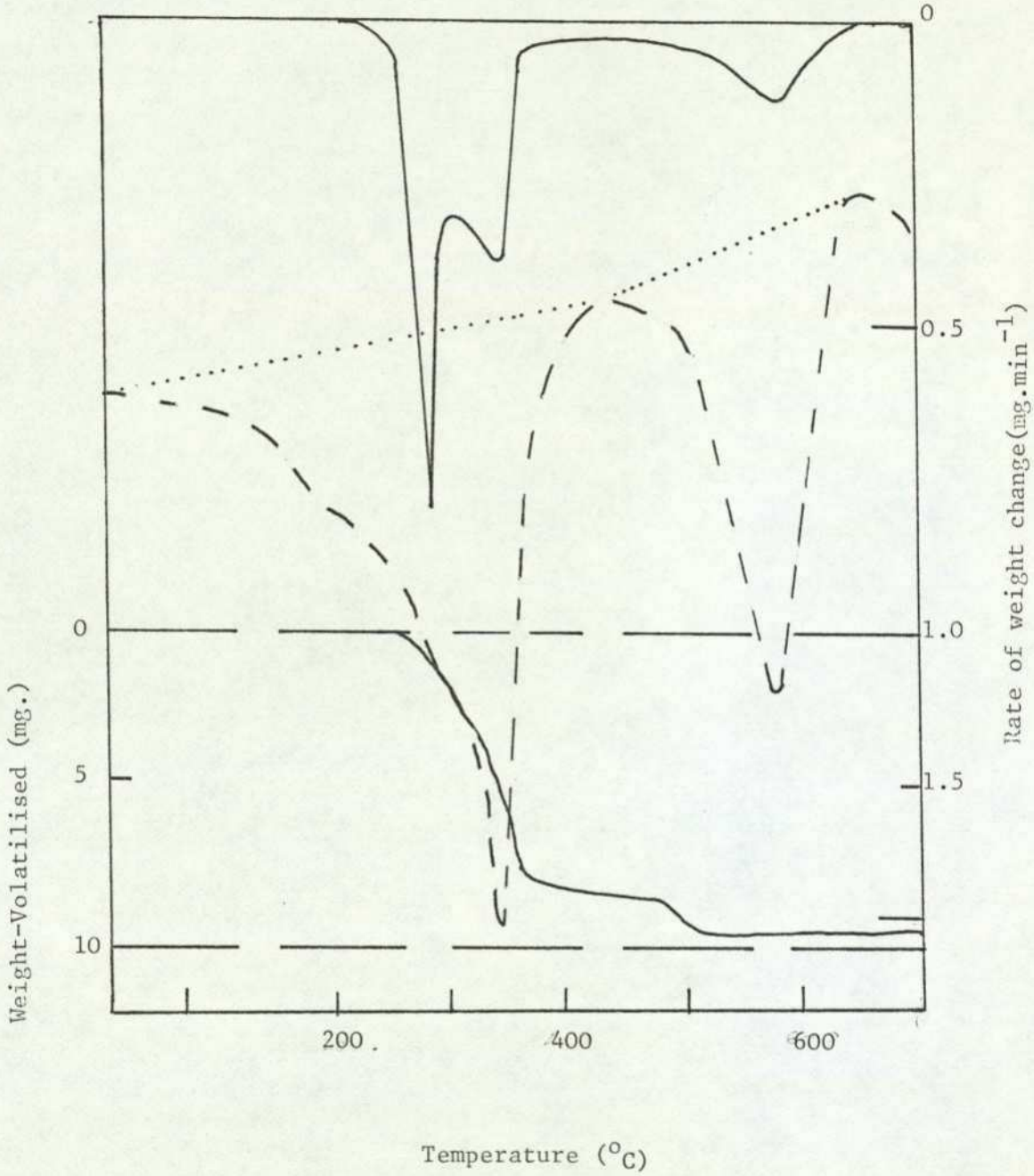
TABLE 25

Thermal analysis of mixtures of $SnO_2$ and S70

| Ratio of $SnO_2$ to S70 (w/w): | 0:1 | 2:5 | 1:2 | 2:3 | 1:1 | 3:2 | 1:0 |
|---|---|---|---|---|---|---|---|
| Weight-fraction of M.O.volatilised(%): | - | 43.8 | 44.0 | 50.2 | 56.6 | 83.9 | 23.2 |
| Total W.F. of mixture volatilised(%):* | 98.8 | 131.4 | 122.0 | 133.0 | 141.9 | 162.2 | - |
| Theor. W.F. volatilisable(%): | 100.0 | 140.0 | 150.0 | 166.7 | 174.1 | 174.1 | - |
| First main weight-loss reaction. | | | | | | | |
| Weight-fraction volatilised (%): | 67.8 | 40.3 | 61.7 | 62.5 | 54.5 | 48.9 | 2.7 |
| Weight-fraction vol. (% of S70)(%):* | 67.8 | 56.4 | 91.4 | 104.2 | 108.9 | 122.3 | - |
| Temperature range (°C): | 150-350 | 155-311 | 168-361 | 153-365 | 142-355 | 159-340 | 37-76 |
| Max. rate of volatilisation(%.min$^{-1}$): | 9.3 | 11.9 | 12.0 | 10.4 | 11.4 | 11.4 | 12.0 |
| Temperature of max. rate (°C): | 302 | 292 | 301 | 292 | 289 | 282 | 59 |
| Second main weight-loss reaction. | | | | | | | |
| Weight-fraction volatilised(%): | - | 22.2 | - | - | - | - | 3.0 |
| Weight-fraction vol. (% of S70)(%):* | - | 31.3 | - | - | - | - | - |
| Temperature range (°C): | - | 311-360 | - | - | - | - | 76-136 |
| Max. rate of volatilisation(%.min$^{-1}$): | - | 9.4 | - | - | - | - | 8.3 |
| Temperature of max. rate (°C): | - | 322 | - | - | - | - | 99 |
| Carbon 'burn-off'reactions. | | | | | | | |
| Total weight-fraction volatilised(%): | 31.0 | 21.4 | 20.6 | 17.6 | 16.6 | 16.0 | 17.5 |
| Total W.F. volatilised (% of S70)(%):* | 31.0 | 30.0 | 30.5 | 29.3 | 33.2 | 40.0 | - |
| Temperature range (°C): | 350-508 | 360-538 | 361-541 | 365-528 | 355-529 | 340-514 | 136-788 |
| (a) First stage. | | | | | | | |
| Weight-fraction volatilised(%): | 18.2 | 21.4 | 20.6 | 17.6 | 16.6 | 16.0 | 17.5 |
| Weight-fraction vol. (% of S70)(%):* | 18.2 | 30.0 | 30.5 | 29.3 | 33.2 | 40.0 | - |
| Max. Rate of volatilisation (%.min$^{-1}$): | 5.4 | 5.9 | 6.6 | 8.2 | 7.8 | 5.1 | 2.0 |
| Temperature of max. rate (°C): | 429 | 492 | 481 | 492 | 490 | 462 | 310 |
| Temperature of max. endothermicity(°C): | 429 | 478 | 482 | 484 | 490 | 424 | 261. |
| (b) Second stage. | | | | | | | |
| Weight-fraction volatilised(%): | 12.8 | - | - | - | - | - | - |
| Weight-fraction vol. (% of S70)(%):* | 12.8 | - | - | - | - | - | - |
| Max. rate of volatilisation (%.min$^{-1}$): | 5.0 | - | - | - | - | - | - |
| Temperature of max. rate (°C): | 450 | - | - | - | - | - | - |

FIGURE 32

The interaction of Electrofine S70 with $SnO_2$.



similar to that of Adine when heated alone; it is clear that the residual carbon does not react with $SnO_2$.

The decomposition of aluminium oxide monohydrate and S70 takes place in two stages and is very similar to the decomposition of pure S70 (Table 26). There is little interaction between α-AlOOH and S70 when present in a 1:1 molar ratio. The two weight-loss stages are observed at 150-325°C and 352-534°C. With excess S70, there is no apparent interaction during either stage. The carbon 'burn-off' becomes a prolonged single-stage decomposition when α-AlOOH is present, although the DTA trace consists of a number of short exothermic reactions due probably to the effects of powdered α-AlOOH on the 'burn-off' reaction. The weight-fraction volatilised in the main weight loss stage is slightly higher than that of S70 alone and is due to the loss of water from the monohydrate.

Aluminium oxide trihydrate does not influence the decomposition of the chlorinated wax. The total weight-fraction volatilised is equivalent to the sum of that due to the loss of water from the trihydrate and that from the breakdown of the chlorinated wax. There is no evidence to suggest that aluminium trichloride is formed. (Table 27).

The decomposition of anhydrous alumina and S70 takes place in two stages, not unlike that of S70 when heated

TABLE 26

Thermal analysis of mixtures of AlOOH and S70

| Ratio of AlOOH to S70(w/w): | 0:1 | 1:1 | 2:5 | 1:5 | 1:8 | 1:0 |
|---|---|---|---|---|---|---|
| Weight-fraction of M.O.volatilised(%): | - | 54.4 | 29.2 | 16.9 | 7.8 | 26.7 |
| Total W.G. of mixture volatilised(%):* | 98.8 | 120.9 | 111.2 | 103.2 | 101.0 | - |
| Theor. W.F. volatilisable)%): | 100.0 | 138.4 | 138.4 | 119.2 | 112.8 | - |
| First main weight-loss reaction. | | | | | | |
| Weight-fraction volatilised(%): | 67.8 | 20.4 | 54.8 | 61.1 | 66.2 | 3.1 |
| Weight-fraction vol. (% of S70) (%):* | 67.8 | 40.8 | 75.9 | 72.8 | 74.7 | - |
| Temperature range ($^{o}$C): | 150-350 | 148-301 | 150-325 | 163-361 | 158-382 | 30-105 |
| Max. rate of volatilisation(%.min$^{-1}$): | 9.3 | 9.1 | 13.1 | 12.8 | 11.7 | 8.9 |
| Temperature of max. rate ($^{o}$C): | 302 | 286 | 325 | 319 | 327 | 48 |
| Second main weight-loss reaction. | | | | | | |
| Weight-fraction volatilised(%): | - | 22.8 | - | - | - | 16.7 |
| Weight-fraction vol. (% of S70)(%):* | - | 45.8 | - | - | - | - |
| Temperature range($^{o}$C): | - | 301-372 | - | - | - | 207-321 |
| Max. rate of volatilisation (%.min$^{-1}$): | - | 18.2 | - | - | - | 16.4 |
| Temperature of max. rate ($^{o}$C): | - | 330 | - | - | - | 266 |
| Carbon 'burn-off' reactions. | | | | | | |
| Total weight-fraction volatilised(%): | 31.0 | 18.0 | 26.0 | 25.5 | 23.3 | 6.9 |
| Total W.F. volatilised (% of S70)(%):* | 31.0 | 36.0 | 37.0 | 30.4 | 26.3 | - |
| Temperature range ($^{o}$C): | 350-508 | 372-549 | 352-534 | 361-560 | 382-556 | 321-494 |
| (a) First stage. | | | | | | |
| Weight-fraction volatilised(%) | 18.2 | 18.0 | 26.7 | 25.5 | 23.3 | 6.9 |
| Weight-fraction vol. (% of S70)(%):* | 18.2 | 36.0 | 37.0 | 30.4 | 26.3 | - |
| Max. Rate of volatilisation (%.min$^{-1}$): | 5.4 | 5.5 | 4.8 | 5.0 | 6.1 | 4.1 |
| Temperature of max. rate ($^{o}$C): | 429 | 483 | 455 | 463 | 486 | 379 |
| Temperature of max. endothermicity($^{o}$C): | 429 | 483 | 455 | 483 | 492 | 426 |
| (b) Second stage. | | | | | | |
| Weight-fraction volatilised (%) | 12.8 | - | - | - | - | - |
| Weight-fraction vol. (% of S70)(%):* | 12.8 | - | - | - | - | - |
| Max. rate of volatilisation(%.min$^{-1}$): | 5.0 | - | - | - | - | - |
| Temperature of max. rate ($^{o}$C): | 450 | - | - | - | - | - |

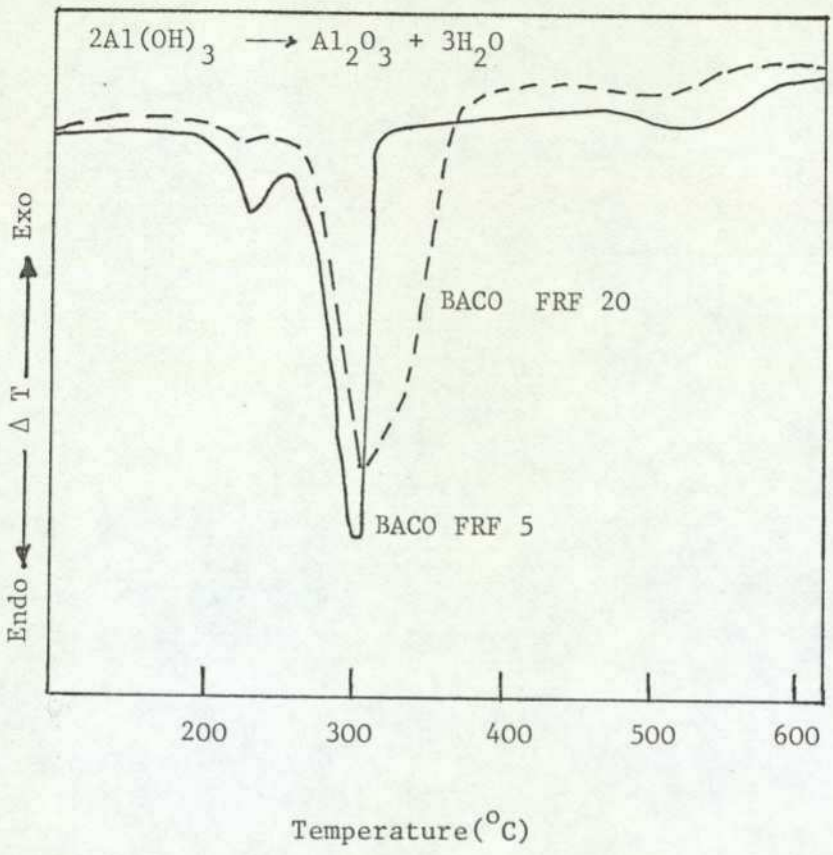
TABLE 27

Thermal analysis of mixtures of metal oxides and S70

| Metal Oxide | $Fe_2O_3$ | ZnO | $MoO_3$ | CuO | $Al_2O_3$. | AlOOH | $Al_2O_3.3H_2O$ | Talc |
|---|---|---|---|---|---|---|---|---|
| Ratio of M.O. to S70(w/w): | 1:2 | 1:2 | 1:2 | 1:2 | 1:2 | 2:5 | 2:5 | 1:2 |
| Weight-fraction of M.O.volatilised(%): | 64.0 | 99.7 | 86.7 | 74.8 | 61.4 | 79.2 | 83.2 | 63.7 |
| Total W.F. of mixture volatilised(%):* | 96.0 | 149.8 | 130.1 | 112.2 | 92.1 | 111.2 | 116.5 | 95.6 |
| Theor. W.F.volatilisable(%): | 150.0 | 150.0 | 150.0 | 150.0 | 150.0 | 140.: | 140.0 | 150.0 |
| First main weight-loss reaction. | | | | | | | | |
| Weight-fraction volatilised(%): | 37.2 | 29.3 | 32.3 | 37.5 | 43.6 | 54.8 | 54.7 | 44.8 |
| Weight-fraction vol.(% of S70)(%):* | 55.8 | 33.4 | 48.5 | 56.3 | 65.5 | 75.9 | 76.6 | 67.2 |
| Temperature range (°C): | 125-300 | 197-326 | 197-275 | 140-340 | 220-378 | 150-325 | 185-380 | 203-380 |
| Max. rate of volatilisation(%.$min^{-1}$): | 11.6 | 39.6 | 30.2 | 21.1 | 24.9 | 13.1 | 9.1 | 23.5 |
| Temperature of max. rate (°C): | 228 | 266 | 223 | 264 | 325 | 325 | 330 | 316 |
| Second main weight-loss reaction. | | | | | | | | |
| Weight-fraction volatilised(%): | 22.9 | 67.6 | 19.9 | 37.3 | - | - | - | - |
| Weight-fraction vol. (% of S70)(%):* | 34.4 | 101.4 | 29.9 | 56.0 | - | - | - | - |
| Temperature range (°C): | 300-392 | 326-680 | 275-342 | 340-600 | - | - | - | - |
| Max. rate of volatilisation(%.$min^{-1}$): | 15.6 | 12.4 | 30.5 | 11.6 | - | - | - | - |
| Temperature of max. rate (°C): | 345 | 492 | 312 | 395 | - | - | - | - |
| Carbon 'burn-off' reactions. | | | | | | | | |
| Total weight-fraction volagilised(%): | 3.9 | - | * | - | 17.8 | 26.7 | 28.5 | 18.9 |
| Total W.F.volatilised(% of S70)(%):* | 5.9 | - | - | - | 26.7 | 37.0 | 39.9 | 28.4 |
| Temperature range (°C) | 392-560 | - | - | - | 378-540 | 352-534 | 380-540 | 380-570 |
| (a) First stage. | | | | | | | | |
| Weight-fraction volatilised(%): | 3.9 | - | 18.8 | - | 17.8 | 26.7 | 28.5 | 18.9 |
| Weight-fraction vol. (% of S70)(%):* | 5.9 | - | | - | 26.7 | 37.0 | 39.9 | 28.4 |
| Max. rate of volatilisation(%.$min^{-1}$): | 18.4 | - | 15.6 | - | 19.5 | 4.8 | 6.6 | 16.9 |
| Temperature of max. rate (°C): | 464 | - | 395 | - | 497 | 455 | 492 | 510 |
| Temperature of max. endothermicity(°C): | 464 | - | - | - | 518 | 455 | 500 | 517 |
| (b) Second stage. | | | | | | | | |
| Weight-fraction volatilised(%): | - | - | 15.7 | - | - | - | - | - |
| Weight-fraction vol. (% of S70)(%):* | - | - | | - | - | - | - | - |
| Max. rate of volatilisation(%.$min^{-1}$): | - | - | 16.0 | - | - | - | - | - |
| Temperature of max. rate (°C): | - | - | 750 | - | - | - | - | - |

FIGURE 33

The differential thermal analysis of aluminium oxide trihydrate



alone. The two weight-loss stages are observed at 220-325°C and 378-540°C and are similar to those for the decomposition of aluminium oxide monohydrate when heated with chlorinated wax (Table 27). There is no detectable interaction between the metal oxide and the halogen source but the halogen compound is completely volatilised.

The thermo-analytical traces obtained when chlorinated wax was heated with the three samples of aluminium oxychloride (Echantillon 3947, 3948 and 3949) are shown in Figures 34, 35 and 36 respectively. The decompositions of these samples, when heated alone, were very complicated. The total weights volatilised from equimolar mixtures of aluminium oxychloride and chlorinated wax are shown in Table 28. Thus, both from the individual reaction stages and from the total weights volatilised, there appears to be little or no interaction between the aluminium oxychlorides and the chlorinated wax.

When a mixture of iron(III)oxide and S70 in a ratio of 1:2 w/w was heated, the decomposition of the chlorinated wax took place at a much lower temperature. The ferric oxide not only decreases the temperature of decomposition by ca 40° for each stage, but also alters the mode of decomposition, by slightly suppressing the initial reaction where hydrogen chloride is initially released and

FIGURE 34

The interaction between Electrofine S70 and Echantillon 3947

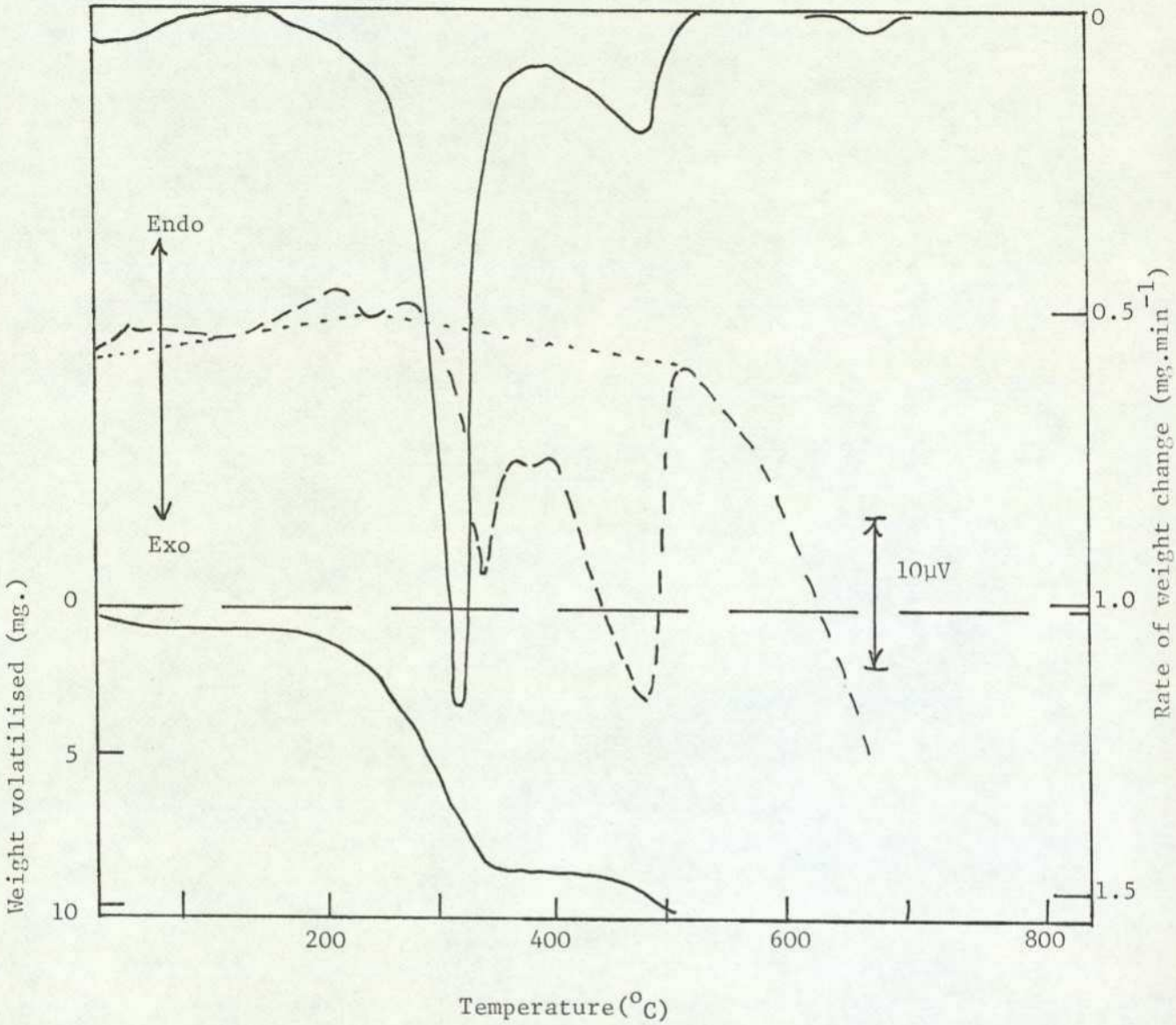


FIGURE 35

The interaction between Electrofine S70 and Echantillon 3948

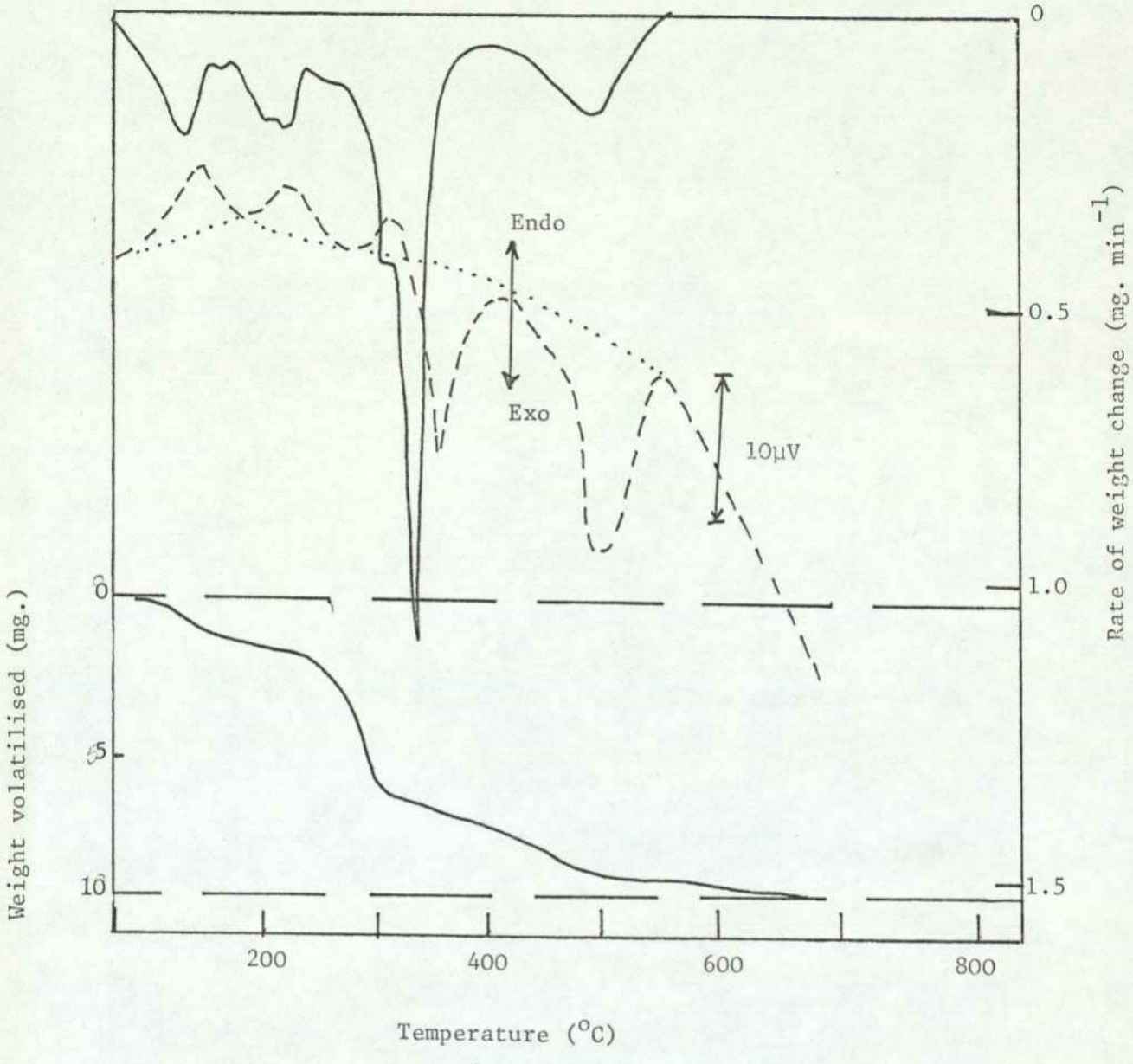


FIGURE 36

The interaction between Electrofine S70 and Echantillon 3949

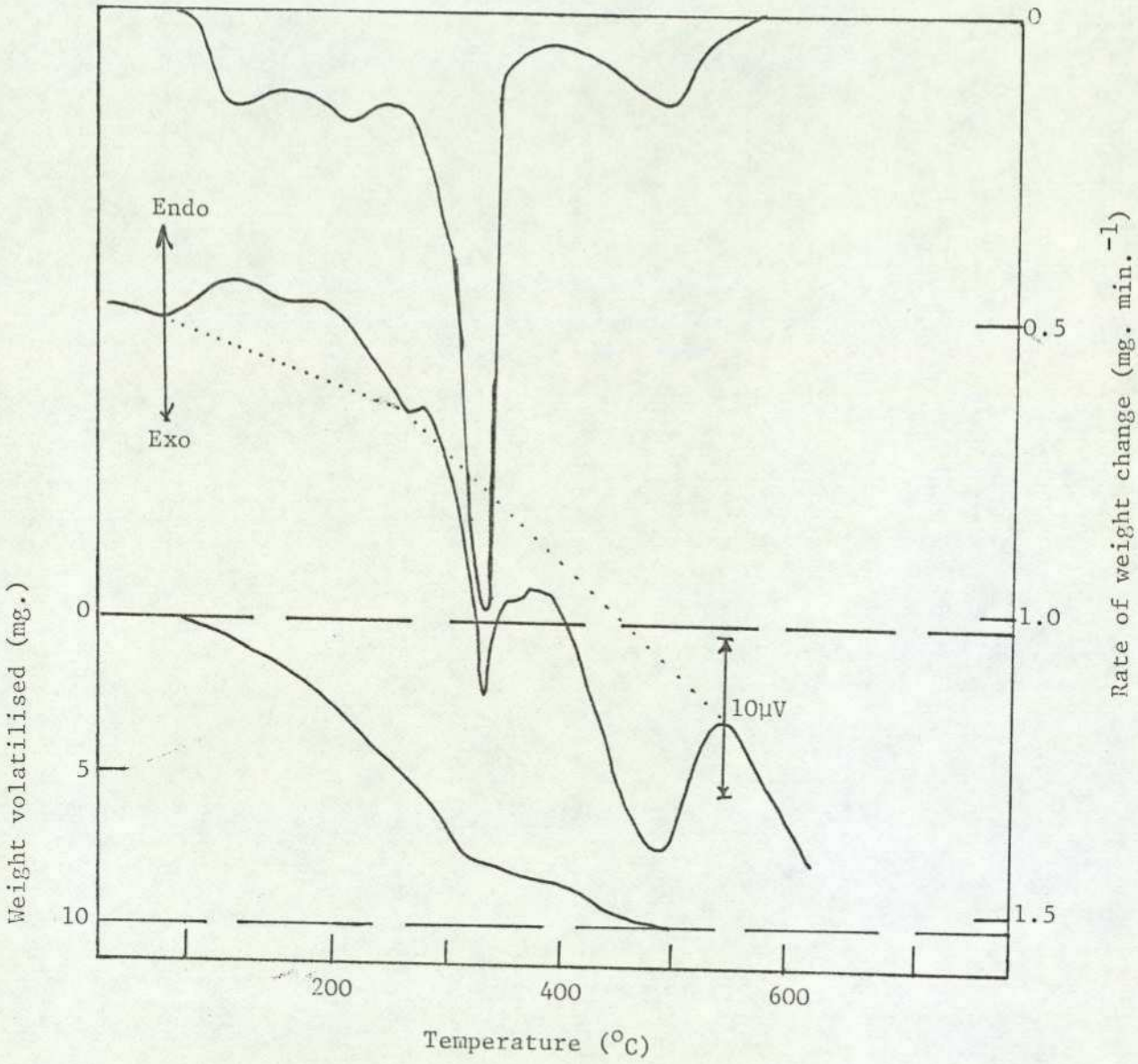


TABLE 28

The thermal analysis of mixtures of aluminium oxychlorides, alone and with chlorinated wax.

| Compound | weight fraction volatilised (%, w/w of S70) | |
|---|---|---|
| | alone | with S70 |
| None | - | 100.0 |
| 3947 | 53.0 | 152.5 |
| 3948 | 56.1 | 157.8 |
| 3949 | 57.6 | 154.0 |

accelerating the second stage of the reaction. The extent of the carbon burn-off stage is also decreased by ca. 10%.

Zinc(II)oxide is completely volatilised when heated with S70. The interaction takes place in two main weight-loss steps between 197-326°C and 326-680°C (Table 27). The second weight-loss in fact consists of three overlapping reactions in which hydrogen chloride and zinc chloride are 'initially volatilised' followed by a small carbon burn-off stage.

Copper(II)oxide when heated with S70 at temperatures below 600°C, does not appear to volatilise as its corresponding halide. Decomposition of copper oxide and S70 takes place in three stages similar to those observed during the decomposition of S70 alone.

The decomposition of molybdenum(VI)oxide and chlorinated wax involves four distinct exothermic reactions. The first stage occurs rather abruptly at 197°C when the mixture loses 32.3% of its initial weight. The second and third stages are observed between 275-342°C and 342-473°C, when amounts corresponding roughly to 19.9 and ca 18.8% of the initial weight are further volatilised (Table 27). There is no apparent carbon burn-off stage and further interaction between the metal oxide and residual carbon takes place above 640°C. The total percentage of metal oxide volatilised is ca 61%.

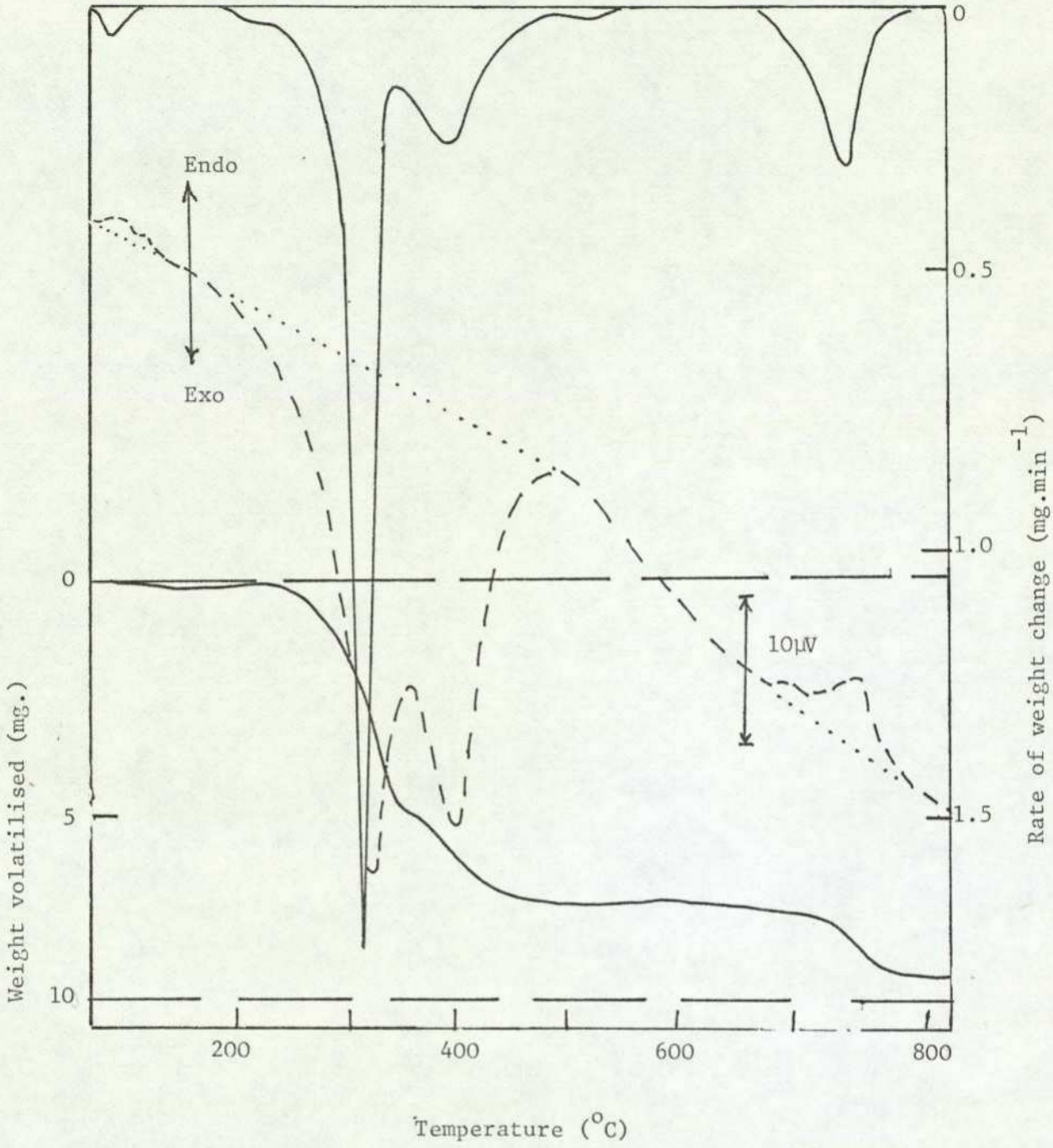
Commercially available Talc was also heated with chlorinated wax. There appeared to be no loss of water, no decomposition of Talc and no interaction between the two compounds.

When ammonium molybdate was heated with chlorinated wax, there was little or no interaction between the salt and the chlorine source. The molybdenum oxide formed as a decomposition product from the molybdate was then volatilised quantitatively from the crucible at about 750°C (Figure 37).

Ammonium tetraborate does not influence the decomposition of chlorinated wax. It loses water of hydration in three small stages, but this appears to have little or no effect on the decomposition of S70.

FIGURE 37

The interaction between Electrofine S70 and ammonium molybdate



3.1.4.2 Mixtures of chlorinated wax S70 and two metal oxides

In these experiments the ratio of metal oxide to S70 was kept constant at 1:2(w/w) and the ratios of the two metal oxides were varied.

$Sb_2O_3$/ZnO reacts with S70 in three stages. The volatilisation of $Sb_2O_3$ and S70 is accompanied by two extensive main weight-loss reactions and almost no interaction in the carbon 'burn-off' stage. In contrast, the reaction of ZnO/$Sb_2O_3$ with S70 takes place with extensive interaction in the first weight-loss stage followed by a smaller interaction in the second weight-loss stage and extensive interaction in the carbon 'burn-off' reaction (Table 29, Figure 39). This excess volatilisation in the carbon 'burn-off' reaction is probably due to volatilisation of $ZnCl_2$ occurring at a higher temperature than that of $SbCl_3$. Pure ZnO and pure $Sb_2O_3$ are known to be fully volatilised as their chlorides when heated separately with an excess of chlorinated wax. The weight fraction of metal oxide mixture volatilised is smaller than the weight fraction of $Sb_2O_3$ and ZnO volatilised when these compounds are heated individually with S70.

$Sb_2O_3$/αAlOOH also reacts with S70 in three stages. The extensive interaction which takes place in two steps in the main weight-loss stage indicates a 'pseudo-synergistic' effect; because α-AlOOH and S70 do not

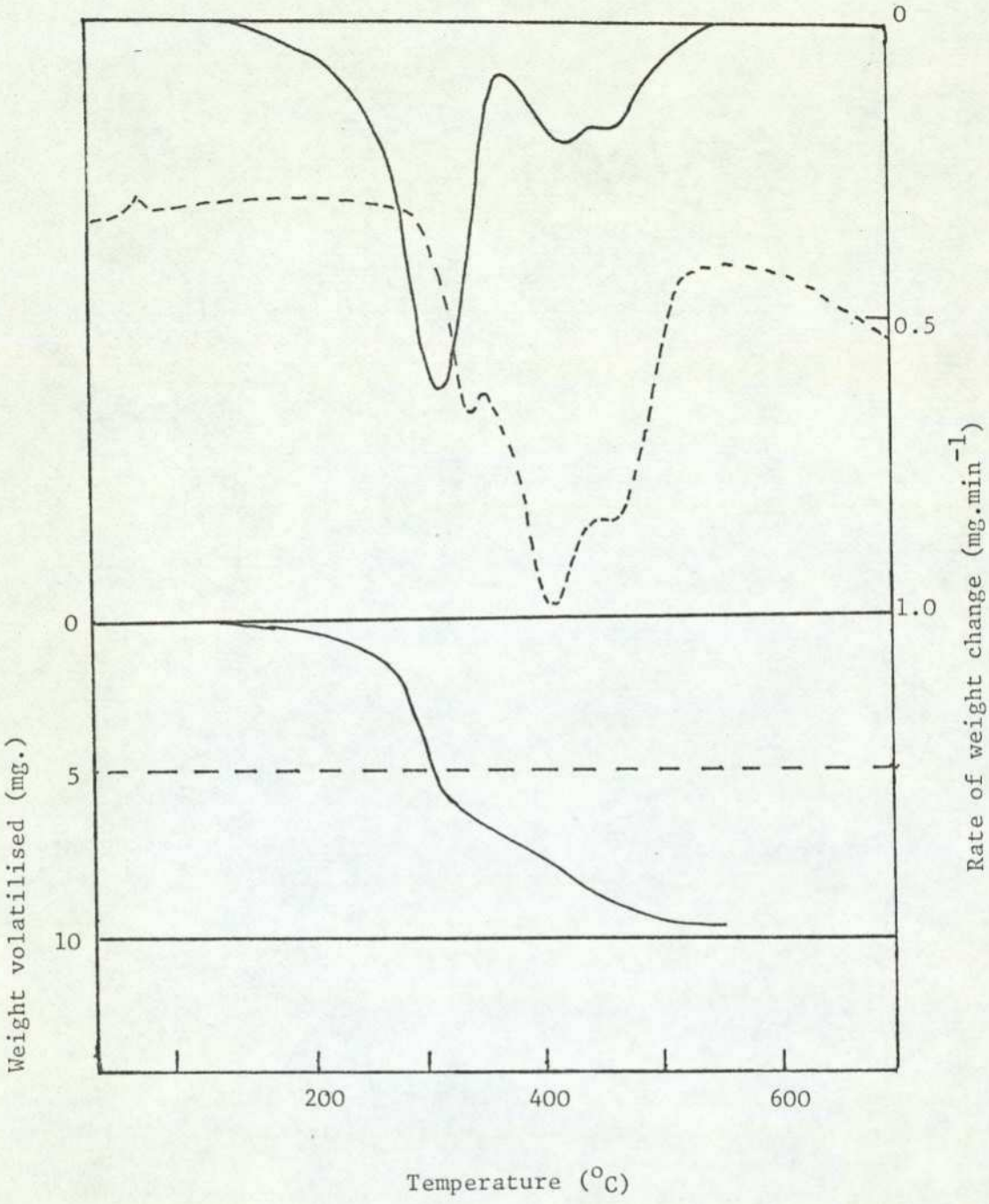
TABLE 29

Thermal analysis of mixtures of $Sb_2O_3$/ZnO and S70

| Ratio of $Sb_2O_3$ to ZnO(w/w): | 1:0 | 4:1 | 2:1 | 3:2 | 1:1 | 2:3 | 1:2 | 1:4 | 1:8 | 0:1 |
|---|---|---|---|---|---|---|---|---|---|---|
| Weight-fraction of M.O.volatilised(%): | 88.4 | 41.4 | 85.4 | 86.6 | 79.2 | 82.3 | 53.5 | 70.3 | 73.8 | 99.7 |
| Total W.F. of mixture volatilised(%):* | 144.2 | 120.7 | 142.7 | 143.3 | 139.6 | 141.1 | 126.8 | 135.2 | 136.9 | 149.8 |
| Theor. of W.F. volatilisable(%): | 150.0 | 150.0 | 150.0 | 150.0 | 150.0 | 150.0 | 150.0 | 150.0 | 150.0 | 150.0 |
| First main weight-loss reaction. | | | | | | | | | | |
| Weight-fraction volatilised(%): | 43.3 | 34.8 | 55.4 | 47.8 | 37.1 | 40.5 | 41.9 | 38.1 | 29.1 | 29.3 |
| Weight-fraction vol. (% of S70)(%):* | 64.9 | 52.2 | 83.1 | 71.7 | 55.7 | 60.8 | 62.9 | 57.2 | 43.7 | 43.9 |
| Temperature range (°C): | 222-305 | 181-287 | 175-284 | 177-276 | 180-275 | 181-276 | 177-319 | 183-333 | 180-295 | 197-326 |
| Max. rate of volatilisation(%.min$^{-1}$): | 19.7 | 40.0 | 37.2 | 15.9 | 17.2 | 24.1 | 14.9 | 11.3 | 23.9 | 39.6 |
| Temperature of max. rate (°C): | 308 | 266 | 249 | 256 | 252 | 247 | 258 | 255 | 255 | 266 |
| Second main weight-loss reaction. | | | | | | | | | | |
| Weight-fraction volatilised(%): | 35.4 | 11.9 | 8.2 | 15.3 | 15.9 | 11.4 | - | - | - | 67.6 |
| Weight-fraction vol. (% of S70)(%):* | 53.1 | 17.9 | 12.3 | 22.9 | 23.9 | 17.0 | - | - | - | 101.4 |
| Temperature range (°C): | 305-355 | 287-325 | 284-325 | 276-342 | 275-323 | 276-321 | - | - | - | 326-680 |
| Max. rate of volatilisation (%.min$^{-1}$): | 15.3 | 21.8 | 7.4 | 4.5 | 17.8 | 4.9 | - | - | - | 12.4 |
| Temperature of max. rate (°C): | 308 | 300 | 290 | 284 | 292 | 290 | - | - | - | 492 |
| Carbon 'burn-off' reactions. | | | | | | | | | | |
| Total weight-fraction volatilised(%): | 17.5 | 33.7 | 31.5 | 32.4 | 40.0 | 42.2 | 42.6 | 52.0 | 62.1 | - |
| Total W.F. volatilised(% of S70)(%):* | 26.3 | 50.6 | 47.3 | 48.6 | 60.0 | 63.2 | 63.9 | 78.0 | 93.2 | - |
| Temperature range (°C): | 355-528 | 325-432 | 321-520 | 342-500 | 323-600 | 325-495 | 319-500 | 333-580 | 295-840 | - |
| (a) First stage. | | | | | | | | | | |
| Weight-fraction volatilised(%): | 17.5 | 33.7 | 31.5 | 32.4 | 40.0 | 25.9 | 17.3 | 16.7 | 29.0 | - |
| Weight-fraction vol. (% of S70)(%):* | 26.3 | 50.6 | 47.3 | 48.6 | 60.0 | 63.2 | 26.0 | 25.1 | 43.5 | - |
| Max. rate of volatilisation (%.min$^{-1}$): | 6.9 | 7.9 | 14.6 | 7.8 | 6.7 | 5.1 | 8.4 | 7.1 | 18.2 | - |
| Temperature of max. rate (°C): | 479 | 424 | 418 | 425 | 428 | 414 | 403 | 400 | 442 | - |
| Temperature of max. endothermicity(°C): | 461 | 418 | 402 | 415 | 422 | 404 | 389 | 385 | 380 | - |
| (b) Second stage. | | | | | | | | | | |
| Weight-fraction volatilised(%): | - | - | - | - | - | 16.3 | 25.3 | 35.3 | 33.1 | - |
| Weight-fraction vol. (% of S70)(%):* | - | - | - | - | - | 24.5 | 38.0 | 53.0 | 49.7 | - |
| Max. rate of volatilisation (%.min$^{-1}$): | - | - | - | - | - | 5.0 | 8.6 | 8.2 | 19.7 | - |
| Temperature of max. rate (°C): | - | - | - | - | - | 447 | 443 | 475 | 475 | - |

FIGURE 38

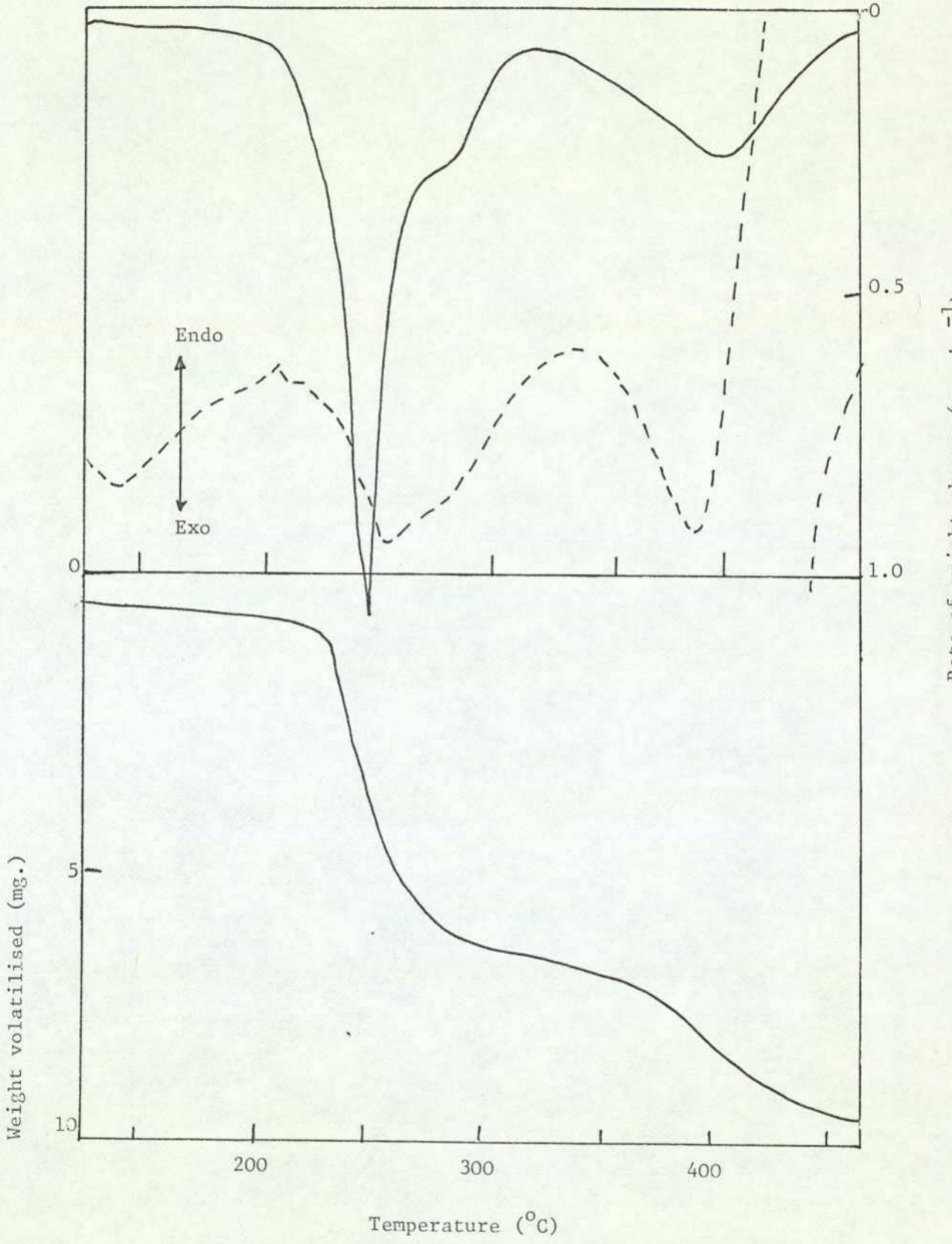
The thermogravimetric analysis of Electrofine S70




- - - D. T. A. trace

FIGURE 39

The interaction of $Sb_2O_3$ with ZnO during the decomposition of Electrofine S70



normally react with each other (Table 30). Thus the presence of $Sb_2O_3$ and the water of hydration from the αAlOOH facilitates the reaction of the antimony compound with S70, especially when $Sb_2O_3$ is in excess. The weight fraction of metal oxide volatilised is larger with $Sb_2O_3$ than with mixtures of α-AlOOH and SnO or $SnO_2$ (see below).

When $Sb_2O_3/Fe_2O_3$ is heated in a molar ratio greater than 1:0.2, the interaction with S70 takes place in three stages. The behaviour is similar to that observed during the decomposition of S70 when it is heated with $Sb_2O_3$ alone, but the weight loss takes place at a much lower temperature (Table 31). However, when $Sb_2O_3$ and $Fe_2O_3$ in a ratio of 1:0.1 are heated with S70, decomposition takes place in two stages and the weight fraction of metal oxide volatilised increases. Thus, with increasing quantities of $Fe_2O_3$ present, the initial temperature of decomposition and/or interaction of the $Sb_2O_3$/S70 system is lowered by up to 80°C. The extent of chemical reaction of $Sb_2O_3$ with S70 is slightly decreased, but there is increased interaction in the carbon 'burn-off' stage, where the ferric oxide strongly catalyses the reaction of the carbon with oxygen from the air, making the reaction very exothermic. Its overall effect is to reduce the total weight of $Sb_2O_3$ volatilised.

$Sb_2O_3/SnO$, when heated in a molar ratio of 1:1 with excess S70, decomposes the wax in two stages; the total

TABLE 30

Thermal analysis of mixtures of $Sb_2O_3$/ALOOH and S70

| Ratio of $Sb_2O_3$ to ALOOH (w/w) | 1:0 | 4:1 | 5:2 | 2:1 | 3:2 | 1:1 | 2:3 | 1:4 | 0:1 |
|---|---|---|---|---|---|---|---|---|---|
| Weight-fraction of M.O.volatilised(%): | 88.4 | 76.0 | 66.8 | 68.2 | 45.7 | 51.7 | 47.2 | 36.2 | 54.4 |
| Total W.F. of mixture volatilised(%):* | 144.2 | 138.1 | 133.4 | 134.5 | 132.0 | 125.8 | 123.6 | 118.1 | 120.9 |
| Theor. W.F. volatilisable (%): | 150.0 | 150.0 | 150.0 | 150.0 | 150.0 | 150.0 | 150.0 | 150.0 | 138.4 |
| First main weight-loss reaction. | | | | | | | | | |
| Weight-fraction volatilised (%): | 43.3 | 52.0 | 47.4 | 48.0 | 26.7 | 34.7 | 41.5 | 12.6 | 20.4 |
| Weight-fraction vol. (% of S70)(%):* | 64.9 | 78.0 | 71.7 | 72.1 | 40.1 | 52.1 | 62.3 | 18.9 | 40.8 |
| Temperature range (°C): | 222-305 | 173-321 | 146-326 | 178-315 | 176-281 | 166-293 | 172-324 | 159-270 | 148-301 |
| Max. rate of volatilisation(%. $min^{-1}$): | 19.7 | 17.3 | 9.4 | 9.7 | 16.6 | 6.7 | 12.3 | 9.1 | 9.1 |
| Temperature of max. rate (°C)% | 296 | 309 | 302 | 296 | 268 | 261 | 283 | 237 | 286 |
| Second main weight-loss reaction. | | | | | | | | | |
| Weight-fraction volatilised(%) | 35.4 | 18.7 | 22.2 | 21.7 | 41.1 | 27.6 | 21.7 | 44.4 | 22.8 |
| Weight-fraction vol. (% of S70)(%):* | 53.1 | 28.1 | 33.3 | 32.6 | 61.7 | 41.4 | 32.6 | 66.6 | 45.6 |
| Temperature range (°C): | 305-355 | 321-358 | 316-372 | 315-358 | 281-359 | 293-351 | 324-370 | 270-370 | 301-372 |
| Max. rate of volatilisation(%.$min^{-1}$): | 15.3 | 37.0 | 9.3 | 8.6 | 19.7 | 8.2 | 32.5 | 16.6 | 18.6 |
| Temperature of max. rate (°C): | 308 | 327 | 321 | 324 | 322 | 320 | 334 | 333 | 330 |
| Carbon 'burn -off' reactions. | | | | | | | | | |
| Total weight-fraction volatilised(%): | 17.5 | 21.3 | 19.3 | 19.7 | 14.1 | 21.6 | 19.1 | 21.7 | 18.0 |
| Total W.F. volatilised (% of S70) (%):* | 26.3 | 32.0 | 28.9 | 29.6 | 21.2 | 32.4 | 28.7 | 32.6 | 36.0 |
| Temperature range (°C): | 355-528 | 358-556 | 372-540 | 358-530 | 359-510 | 351-532 | 370-563 | 370-530 | 372-549 |
| (a) First stage. | | | | | | | | | |
| Weight-fraction volatilised (%): | 17.5 | 21.3 | 19.3 | 19.7 | 14.1 | 21.6 | 19.1 | 21.7 | 18.0 |
| Weight-fraction vol. (% of S70)(%):* | 26.3 | 32.0 | 28.9 | 29.6 | 21.2 | 32.4 | 28.7 | 32.6 | 36.0 |
| Max. Rate of volatilisation(%.$min^{-1}$): | 6.9 | 5.1 | 5.0 | 5.6 | 8.7 | 6.1 | 4.8 | 5.3 | 5.6 |
| Temperature of max. rate (°C): | 479 | 486 | 492 | 471 | 471 | 481 | 483 | 487 | 482 |
| Temperature of max. endothermicity (°C): | 461 | 473 | 478 | 463 | 459 | 469 | 467 | 474 | 470 |
| (b) Second stage. | | | | | | | | | |
| Weight-fraction volatilised (%): | - | - | - | - | - | - | - | - | - |
| Weight-fraction vol. (% of S70) (%):* | - | - | - | - | - | - | - | - | - |
| Max. rate of volatilisation (%.$min^{-1}$): | - | - | - | - | - | - | - | - | - |
| Temperature of max. rate (°C): | - | - | - | - | - | - | - | - | - |

TABLE 31

Thermal analysis of mixtures of $Sb_2O_3/Fe_2O_3$ and S70

| Ratio of $Sb_2O_3$ to $Fe_2O_3$ (w/w): | 1:0 | 10:1 | 4:1 | 2:1 | 3:2 | 2:3 | 1:4 | 0:1 |
|---|---|---|---|---|---|---|---|---|
| Weight-fraction of M.O. volatilised(%): | 88.4 | 83.8 | 65.5 | 49.6 | 37.7 | - | - | 64.0 |
| Total W.F. of mixture volatilised(%):* | 144.2 | 137.7 | 126.2 | 116.5 | 111.3 | 89.4 | 84.1 | 96.0 |
| Theor. W.F. volatilisable (%): | 150.0 | 145.5 | 140.0 | 133.3 | 130.0 | 120.0 | 110.0 | 150.0 |
| First main weight-loss reaction. | | | | | | | | |
| Weight-fraction volatilised(%): | 43.3 | 72.3 | 39.5 | 46.4 | 40.7 | 35.0 | 29.5 | 37.2 |
| Weight-fraction vol.(% of S70)(%):* | 64.9 | 105.2 | 55.3 | 61.9 | 52.9 | 42.0 | 32.5 | 55.8 |
| Temperature range (°C): | 222-305 | 173-338 | 147-274 | 142-258 | 140-256 | 125-235 | 140-226 | 125-300 |
| Max. rate of volatilisation(%.min$^{-1}$) | 19.7 | 27.3 | 16.5 | 23.8 | 26.8 | 24.5 | 13.0 | 11.6 |
| Temperature of max. rate (°C): | 296 | 293 | 264 | 235 | 234 | 215 | 203 | 228 |
| Second main weight-loss reaction. | | | | | | | | |
| Weight-fraction volatilised(%): | 35.4 | - | 27.6 | 13.9 | 18.7 | 10.0 | 10.7 | 22.9 |
| Weight-fraction vol. (% of S70)(%):* | 53.1 | - | 38.6 | 18.5 | 24.3 | 12.0 | 11.8 | 34.4 |
| Temperature range (°C): | 305-355 | - | 274-332 | 258-314 | 256-312 | 235-274 | 226-275 | 300-392 |
| Max. rate of volatilisation(%.min$^{-1}$): | 15.3 | - | 15.9 | 10.7 | 29.9 | 24.7 | 24.8 | 15.6 |
| Temperature of max. rate (°C): | 308 | - | 281 | 271 | 270 | 241 | 233 | 345 |
| Carbon 'burn-off' reactions. | | | | | | | | |
| Total weight-fraction volatilised(%): | 17.5 | 22.3 | 23.1 | 27.1 | 26.2 | 29.5 | 36.2 | 3.9 |
| Total W.F. volatilised(% of S70)(%):* | 26.3 | 32.5 | 32.3 | 36.1 | 34.1 | 35.4 | 39.8 | 5.9 |
| Temperature range (°C): | 355-528 | 367-419 | 332-540 | 314-563 | 312-483 | 274-520 | 275-530 | 392-560 |
| (a) First stage. | | | | | | | | |
| Weight-fraction volatilised(%): | 17.5 | 22.3 | 23.1 | 27.1 | 26.2 | 29.5 | 36.2 | 3.9 |
| Weight-fraction vol. (% of S70)(%):* | 26.3 | 32.5 | 32.3 | 36.1 | 34.1 | 35.4 | 39.8 | 5.9 |
| Max. rate of volatilisation (%.min$^{-1}$): | 6.9 | 16.7 | 16.4 | 14.9 | 8.3 | 10.6 | 7.0 | 18.4 |
| Temperature of max.rate (°C): | 479 | 416 | 400 | 382 | 355 | 380 | 326 | 464 |
| Temperature of max. endothermicity(°C): | 461 | 419 | 393 | 376 | 330 | 343 | 321 | 464 |
| (b) Second stage. | | | | | | | | |
| Weight-fraction volatilised (%): | - | - | | | | | | |
| Weight-fraction vol. (% of S70)(%): | - | - | | | | | | |
| Max. rate of volatilisation (%.min$^{-1}$): | - | - | | | | | | |
| Temperature of max. rate (°C): | - | - | | | | | | |

weight-fraction volatilised is 148.3% and the interactions occur at 215-359°C and 371-572°C. The carbon 'burn-off' reaction takes place at a higher temperature and this accounts for a more exothermic reaction (Table 32).

When $\underline{Sb_2O_3/SnO_2}$ hydrate are heated with S70, the water of crystallisation is not given off in a separate stage but is lost in the main stage of the reaction at 174-368°C, which is a much slower, more exothermic process. The carbon 'burn-off' reaction occurs in the same temperature range as that for β-$SnO_2$ hydrate and S70, viz. 368-522°C (Table 32).

$\underline{Sb_2O_3/MoO_3}$ is the binary metal oxide system which undergoes least interaction with S70 in both stages (Table 32). The main weight loss occurs at 200-348°C and the carbon 'burn-off' reaction takes place at 348-476°C. The results are similar to those obtained with $Fe_2O_3$, suggesting some effect, although the temperatures at which the interactions occur are not reduced.

$\underline{Sb_2O_3/CuO}$ react with S70 only in the main weight loss stage which occurs between 188-336°C. Here volatile halides are formed and volatilised (Table 32).

$\underline{Sb_2O_3/(NH_4)_6Mo_7O_{24}.4H_2O}$ does not react with S70. The thermogravimetric trace shows two distinct weight-loss stages. The total weight lost corresponds to a complete volatilisation of the chlorinated wax and some

TABLE 32

Thermal analysis of mixtures of $Sb_2O_3$/metal oxides and S70

| Metal Oxide | SnO | $SnO_2$ | $Fe_2O_3$ | AlOOH | ZnO | $MoO_3$ | CuO | AM |
|---|---|---|---|---|---|---|---|---|
| Ratio of M.O. to S70 (w/w): | 1:1.1 | 1:1.3 | 1:1.5 | 1:1.5 | 1:1.3 | 1:1.6 | 1:1.6 | 1:1 |
| Ratio of M.O. to S70 (molar): | 1:1 | 1:1 | 1:1 | 1:1 | 1:1 | 1:1 | 1:1 | - |
| Weight-fraction of M.O.volatilised(%): | 53.4 | 58.7 | 58.0 | 75.4 | 76.3 | 57.6 | 58.3 | 72.7 |
| Total W.F.of mixture volatilised(%):* | 148.3 | 145.8 | 138.5 | 150.8 | 158.8 | 137.5 | 142.0 | 109.1 |
| Theor. W.F. volatilisable (%): | 211.1 | 228.4 | 250.4 | 248.1 | 225.8 | 225.5 | 226.3 | 150.0 |
| First main weight-loss reaction. | | | | | | | | |
| Weight-fraction volatilised(%): | 63.0 | 67.6 | 61.0 | 75.1 | 65.9 | 67.9 | 62.5 | 58.4 |
| Weight-fraction vol.(% of S70)(%):* | 119.7 | 120.3 | 101.6 | 125.8 | 118.3 | 111.6 | 112.0 | 87.6 |
| Temperature range (°C): | 215-359 | 174-368 | 136-310 | 181-368 | 169-346 | 200-348 | 188-336 | 212-345 |
| Max. rate of volatilisation(%.min$^{-1}$): | 41.9 | 18.1 | 8.1 | 15.8 | 12.0 | 10.7 | 21.3 | 43.5 |
| Temperature of max. rate (°C): | 290 | 310 | 236 | 310 | 284 | 295 | 292 | 303 |
| Second main weight-loss reaction. | | | | | | | | |
| Weight-fraction volatilised (%): | - | - | - | - | - | - | - | 14.3 |
| Weight-fraction vol. (% of S70)(%):* | - | - | - | - | - | - | - | 21.5 |
| Temperature range (°C): | - | - | - | - | - | - | - | 345-515 |
| Max. rate of volatilisation(%.min$^{-1}$): | - | - | - | - | - | - | - | 11.6 |
| Temperature of max. rate (°C): | - | - | - | - | - | - | - | 406 |
| Carbon 'burn-off' reactions. | | | | | | | | |
| Total weight-fraction volatilised(%): | 14.9 | 14.3 | 22.2 | 15.0 | 23.6 | 15.5 | 17.0 | - |
| Total W.F. volatilised (% of S70)(%):* | 28.3 | 25.4 | 37.0 | 25.1 | 42.4 | 25.5 | 30.5 | - |
| Temperature range (°C): | 371-512 | 368-522 | 310-475 | 368-516 | 346-543 | 348-476 | 336-538 | - |
| First stage. | | | | | | | | |
| Weight-fraction volatilised (%): | 14.9 | 14.3 | 22.2 | 15.0 | 23.6 | 15.5 | 17.0 | - |
| Weight-fraction vol. (% of S70)(%):* | 28.3 | 25.4 | 37.0 | 25.1 | 42.4 | 25.5 | 30.5 | - |
| Max. rate of volatilisation (%.min$^{-1}$): | 10.0 | 6.3 | 8.5 | 10.1 | 5.8 | 9.2 | 12.6 | - |
| Temperature of max. rate (°C): | 452 | 465 | 351 | 465 | 426 | 402 | 439 | - |
| Temperature of max. endothermicity(°C): | 451 | 448 | 346 | 454 | 413 | 398 | 395 | - |

AM : $(NH_4)_6Mo_7O_{24}.4H_2O$

loss due to either the volatilisation of antimony trichloride or the loss of water and ammonia from the molybdate (Table 32).

β-$SnO_2$ hydrate/ZnO interacts with S70 in a three-stage reaction (Table 33). When ZnO is in stoichiometric excess, water of hydration is evolved from $SnO_2$ hydrate at 150-165°C and this helps to promote considerably interactions in the β-$SnO_2$/ZnO/S70 system. When $SnO_2$ is in excess, the maximum weight fraction of metal oxide volatilised is ca. 60.4%. This compares with ca 45.6% for $SnO_2$ heated with S70 alone. As the proportion of ZnO is increased, the interactions generally occur with an increase in the maximum rate of volatilisation for each stage of reaction. The maximum weight fraction of metal oxide volatilised with excess ZnO increases to ca. 99% with pure ZnO and is ca. 86.6% with a $2SnO_2$:5ZnO mixture (w/w). There is increasing interaction in the carbon 'burn-off' stage, presumably due to the rapid volatilisation of $ZnCl_2$ formed from the ZnO. This work has shown that $ZnCl_2$ volatilises at a higher temperature than $Sb_2O_3$ or $SnO_2$.

β-$SnO_2$ hydrate/αAlOOH reacts with S70 in three stages (Table 34). The individual stages are not very distinct and indicate that these reactions occur almost simultaneously. Two small weight losses are also observed at about 130 and 154°C; these may be attributed to the loss of water from the

TABLE 33

Thermal analysis of mixtures of $SnO_2$/ZnO and S70

| Ratio of $SnO_2$ ZnO (w/w) | 1:0 | 8:1 | 4:1 | 2:1 | 3:2 | 1:1 | 2:3 | 1:2 | 2:5 | 1:4 | 1:8 | 0:1 |
|---|---|---|---|---|---|---|---|---|---|---|---|---|
| Weight-fraction of M.O.volatilised(%): | 44.0 | 62.6 | 57.6 | 53.6 | 64.7 | 42.4 | 55.8 | 70.3 | 86.6 | 63.6 | 57.4 | 99.7 |
| Total W.F. of mixture volatilised(%):* | 122.0 | 130.9 | 128.8 | 126.8 | 132.4 | 121.2 | 127.9 | 135.2 | 143.3 | 131.8 | 128.7 | 149.8 |
| Theor. W.F.volatilisable (%): | 150.0 | 150.0 | 150.0 | 150.0 | 150.0 | 150.0 | 150.0 | 150.0 | 150.0 | 150.0 | 150.0 | 150.0 |
| First main weight-loss reaction. | | | | | | | | | | | | |
| Weight-fraction volatilised(%): | 61.7 | 24.7 | 23.1 | 22.3 | 32.1 | 26.4 | 29.7 | 11.6 | 24.5 | 26.4 | 20.6 | 29.3 |
| Weight-fraction vol. (% of S70)(%):* | 91.4 | 37.1 | 34.7 | 33.5 | 48.2 | 39.6 | 44.6 | 17.4 | 36.8 | 39.6 | 30.9 | 43.9 |
| Temperature range (°C): | 168-361 | 149-270 | 147-275 | 215-276 | 138-292 | 210-280 | 156-286 | 278-312 | 165-305 | 177-277 | 156-295 | 197-326 |
| Max. rate of volatilisation(%.min$^{-1}$): | 12.8 | 13.0 | 23.3 | 7.4 | 15.4 | 11.2 | 16.2 | 12.9 | 22.7 | 19.8 | 24.5 | 39.6 |
| Temperature of max. rate (°C): | 301 | 258 | 262 | 256 | 268 | 266 | 259 | 259 | 267 | 261 | 261 | 266 |
| Second main weight-loss reaction. | | | | | | | | | | | | |
| Weight-fraction volatilised(%): | - | 33.7 | 32.2 | 29.4 | 18.2 | 14.3 | 13.3 | 11.6 | 14.5 | 7.3 | 10.3 | 67.6 |
| Weight-fraction vol.(% of S70)(%):* | - | 50.1 | 48.3 | 44.1 | 27.3 | 21.5 | 20.0 | 17.4 | 21.8 | 11.0 | 15.5 | 101.4 |
| Temperature range (°C): | - | 270-333 | 275-338 | 276-340 | 292-332 | 280-327 | 282-330 | 278-312 | 305-401 | 277-315 | 295-388 | 326-680 |
| Max. rate of volatilisation(%.min$^{-1}$): | - | 14.1 | 17.0 | 8.8 | 9.4 | 7.8 | 6.6 | 6.7 | 9.0 | 38.2 | 15.7 | 12.4 |
| Temperature of max. rate (°C): | - | 300 | 299 | 300 | 307 | 282 | 294 | 285 | 385 | 283 | 371 | 492 |
| Carbon 'burn-off' reactions. | | | | | | | | | | | | |
| Total weight-fraction volatilised(%): | 20.6 | 29.1 | 30.5 | 32.8 | 37.9 | 40.1 | 42.2 | 48.2 | 56.6 | 54.1 | 54.9 | - |
| Total W.F.volatilised (% of S70)(%):* | 30.5 | 43.7 | 45.8 | 49.2 | 56.9 | 60.2 | 63.6 | 72.3 | 84.9 | 81.2 | 82.4 | - |
| Temperature range (°C): | 361-541 | 333-490 | 338-554 | 340-535 | 332-557 | 327-577 | 330-484 | 312-514 | 401-472 | 315-536 | 388-527 | - |
| (a) First stage. | | | | | | | | | | | | |
| Weight-fraction volatilised(%): | 20.6 | 29.1 | 30.5 | 32.8 | 37.9 | 40.1 | 42.2 | 48.2 | 40.6 | 17.4 | 54.9 | - |
| Weight-fraction vol. (% of S70)(%):* | 30.5 | 43.7 | 45.8 | 49.2 | 56.9 | 60.2 | 63.6 | 72.3 | 60.9 | 26.1 | 82.4 | - |
| Max. Rate of volatilisation(%.min$^{-1}$): | 6.6 | 6.3 | 7.8 | 7.5 | 10.5 | 6.9 | 7.4 | 6.0 | 8.7 | 9.8 | 4.6 | - |
| Temperature of max. rate (°C): | 481 | 435 | 451 | 338 | 435 | 435 | 431 | 428 | 456 | 398 | 461 | - |
| Temperature of max.endothermicity(°C): | 482 | 429 | 439 | 324 | 416 | 443 | 416 | 405 | 435 | 428 | 418 | - |
| (b) Second stage. | | | | | | | | | | | | |
| Weight-fraction volatilised (%): | - | - | - | - | - | - | - | - | 16.3 | 36.7 | - | - |
| Weight-fraction vol.(% of S70)(%):* | - | - | - | - | - | - | - | - | 24.5 | 55.1 | - | - |
| Max. rate of volatilisation(%.min$^{-1}$): | - | - | - | - | - | - | - | - | 7.6 | 8.2 | - | - |
| Temperature of max. rate (°C): | - | - | - | - | - | - | - | - | 481 | 453 | - | - |

TABLE 34

Thermal analysis of mixtures of $SnO_2$/AlOOH and S70

| Ratio of $SnO_2$ to AlOOH (w/w) | 1:0 | 5:2 | 2:1 | 3:2 | 1:1 | 2:3 | 1:4 | 0:1 |
|---|---|---|---|---|---|---|---|---|
| Weight-fraction of M.O. volatilised(%): | 44.0 | 41.8 | 45.2 | 45.7 | 35.5 | 63.8 | 24.1 | 58.4 |
| Total W.F. of mixture volatilised(%):* | 122.0 | 120.9 | 122.6 | 122.8 | 117.5 | 131.9 | 112.0 | 122.4 |
| Theor. W.F. volatilisable(%): | 150.0 | 150.0 | 150.0 | 150.0 | 150.0 | 150.0 | 150.0 | 150.0 |
| First main weight-loss reaction. | | | | | | | | |
| Weight-fraction volatilised(%): | 61.7 | 29.7 | 25.5 | 21.0 | 19.2 | 65.6 | 52.3 | 20.4 |
| Weight -fraction vol. (% of S70)(%):* | 91.4 | 44.6 | 38.3 | 31.5 | 28.8 | 98.4 | 78.5 | 40.8 |
| Temperature range (°C): | 168-361 | 133-300 | 135-303 | 127-289 | 213-288 | 204-357 | 233-363 | 148-301 |
| Max. rate of volatilisation(%.min$^{-1}$): | 12.8 | 7.1 | 6.4 | 5.5 | 10.7 | 13.4 | 10.6 | 9.1 |
| Temperature of max. rate (°C): | 301 | 290 | 290 | 278 | 267 | 314 | 322 | 286 |
| Second main weight-loss reaction. | | | | | | | | |
| Weight-fraction volatilised(%): | - | 30.5 | 36.0 | 39.0 | 38.7 | - | - | 22.8 |
| Weight-fraction vol. (% of S70)(%):* | - | 45.8 | 54.0 | 58.5 | 57.8 | - | - | 45.6 |
| Temperature range (°C): | - | 300-372 | 303-374 | 289-367 | 289-369 | - | - | 301-372 |
| Max. rate of volatilisation(%.min$^{-1}$): | - | 9.4 | 9.4 | 10.8 | 10.0 | - | - | 18.2 |
| Temperature of max. rate (°C): | - | 321 | 330 | 327 | 324 | - | - | 330 |
| Carbon 'burn-off' reactions. | | | | | | | | |
| Total weight-fraction volatilised(%): | 20.6 | 20.3 | 20.2 | 22.0 | 20.6 | 22.3 | 22.4 | 18.0 |
| Total W.F. volatilised (% of S70)(%):* | 30.5 | 30.5 | 30.3 | 33.0 | 30.9 | 33.5 | 33.6 | 36.0 |
| Temperature range (°C): | 361-541 | 372-529 | 374-553 | 367-552 | 369-550 | 357-620 | 363-604 | 372-549 |
| (a) First stage. | | | | | | | | |
| Weight-fraction volatilised (%): | 20.6 | 20.3 | 20.2 | 22.0 | 20.6 | 22.3 | 22.4 | 18.0 |
| Weight-fraction vol. (% of S70)(%):* | 30.5 | 30.5 | 30.3 | 33.0 | 30.9 | 33.5 | 33.6 | 36.0 |
| Max. rate of volatilisation (%.min$^{-1}$): | 6.6 | 5.5 | 4.9 | 7.6 | 6.0 | 8.6 | 4.6 | 6.9 |
| Temperature of max. rate (°C): | 481 | 488 | 492 | 482 | 490 | 510 | 547 | 483 |
| Temperature of max. endothermicity(°C): | 482 | 468 | 492 | 466 | 485 | 504 | 526 | 483 |

two hydrated oxides. However, these weight losses are not quantitatively very significant. The total weight fraction volatilised is ca. 122% on average and the weight fraction of metal oxide volatilised is an additive linear function of the individual weight fractions of metal oxide volatilised when heated with S70. This indicates that little or no interaction occurs between the two metal oxides. Furthermore, there is no interaction in the carbon 'burn-off' stage, which is consistent with the results obtained when these metal oxides are heated individually with S70.

$\underline{\beta\text{-}SnO_2 \text{ hydrate}/Fe_2O_3}$ reacts with S70 to liberate water of hydration from the $\beta$-$SnO_2$ at 124-163°C (Table 35). The main weight-loss reaction occurs at a much lower temperature than with any mixture of a metal oxide with $\beta$-$SnO_2$ hydrate, viz. 163-289°C. This is due to the catalytic effect of $Fe_2O_3$ on the decomposition of the S70. There are indications of further interaction between the compounds at 289-475°C.

$\underline{\beta\text{-}SnO_2 \text{ hydrate}/SnO}$ reacts with S70 in two main stages, and there is no evidence of further interaction in the carbon 'burn-off' stage (Table 36). Although the total weight fraction volatilised increases with the proportion of $SnO_2$ present, this may be due to the loss of water of hydration. These metal oxides have an antagonistic effect on the decomposition of S70.

TABLE 35

Thermal analysis of mixtures of $SnO_2$/metal oxides and S70

| Metal Oxide | SnO | $Fe_2O_3$ | AlOOH | ZnO | $MoO_3$ | CuO |
|---|---|---|---|---|---|---|
| Ratio of M.O. to S70 (w/w): | 1:1.3 | 1:1.8 | 1:2 | 1:1.6 | 1:2 | 1:1.6 |
| Ratio of M.O. to S70 (molar): | 1:1 | 1:1 | 1:1 | 1:1 | 1:1 | 1:1 |
| Weight-fraction of M.O. volatilised(%): | 41.0 | 77.9 | 47.6 | 84.2 | 17.9 | 42.7 |
| Total W.F. of mixture volatilised(%):* | 131.6 | 120.8 | 124.6 | 136.8 | 109.5 | 127.5 |
| Theor. W.F. volatilisable(%): | 225.9 | 282.3 | 299.4 | 254-5 | 291.9 | 255.7 |
| First main weight-loss reaction. | | | | | | |
| Weight-fraction volatilised(%): | 56.9 | 3.8 | 62.3 | 3.3 | 53.5 | 53.0 |
| Weight-fraction vol. (% of S70)(%):* | 102.1 | 5.7 | 93.5 | 5.0 | 81.4 | 87.0 |
| Temperature range (°C): | 127-338 | 124-163 | 215-367 | 145-214 | 154-339 | 152-325 |
| Max. rate of volatilisation(%.min$^{-1}$): | 25.9 | 35.0 | 11.9 | 24.0 | 12.5 | 13.8 |
| Temperature of max. rate (°C): | 276 | 156 | 312 | 202 | 281 | 289 |
| Second main weight-loss reaction. | | | | | | |
| Weight-fraction volatilised(%): | - | 42.3 | - | 46.5 | - | - |
| Weight-fraction vol. (% of S70)(%):* | - | 65.5 | - | 76.6 | - | - |
| Temperature range (°C): | - | 163-289 | - | 214-331 | - | - |
| Max. rate of volatilisation(%.min$^{-1}$): | - | 7.3 | - | 9.7 | - | - |
| Temperature of max. rate (°C): | - | 246 | - | 270 | - | - |
| Carbon 'burn-off' reactions. | | | | | | |
| Total weight-fraction volatilised(%): | 17.0 | 31.8 | 20.2 | 34.4 | 18.4 | 24.6 |
| Total W.F. volatilised(% of S70)(%):* | 30.5 | 49.2 | 30.5 | 56.7 | 27.9 | 40.4 |
| Temperature range (°C): | 338-528 | 289-475 | 367-526 | 331-554 | 339-478 | 325-540 |
| First stage. | | | | | | |
| Weight-fraction volatilised(%): | 17.0 | 31.8 | 20.2 | 34.4 | 18.4 | 24.6 |
| Weight-fraction vol. (% of S70)(%):* | 30.5 | 49.2 | 30.5 | 56.7 | 27.9 | 40.4 |
| Max. rate of volatilisation (%.min$^{-1}$): | 4.5 | 8.7 | 5.8 | 6.5 | 10.9 | 13.7 |
| Temperature of max. rate (°C): | 447 | 377 | 462 | 429 | 411 | 395 |
| Temperature of max. endothermicity(°C): | 417 | 342 | 452 | 411 | 411 | 383 |

TABLE 36

Thermal analysis of mixtures of $SnO/SnO_2$ and S70

| Ratio of SnO to $SnO_2$(w/w): | 1:0 | 4:1 | 4:3 | 1:1 | 3:4 | 2:3 | 1:4 | 0:1 |
|---|---|---|---|---|---|---|---|---|
| Weight-fraction of M.O. volatilised(%): | 64.9 | 52.9 | 21.8 | 54.4 | 63.0 | 65.7 | 36.9 | 45.6 |
| Total W.F. of mixture volatilised(%):* | 132.5 | 126.4 | 110.9 | 127.2 | 131.5 | 132.9 | 118.5 | 122.0 |
| Theor. W.F. volatilisable(%): | 150.0 | 150.0 | 150.0 | 150.0 | 150.0 | 150.0 | 150.0 | 150.0 |
| First main weight-loss reaction. | | | | | | | | |
| Weight-fraction volatilised(%): | 68.1 | 53.6 | 56.9 | 48.2 | 41.1 | 44.1 | 27.8 | 61.7 |
| Weight-fraction vol. (% of S70)(%):* | 102.2 | 80.4 | 85.4 | 72.3 | 61.7 | 66.2 | 41.7 | 91.4 |
| Temperature range (°C): | 195-343 | 121-283 | 127-338 | 150-292 | 143-283 | 150-297 | 168-269 | 168-361 |
| Max. rate of volatilisation(%.$min^{-1}$): | 39.1 | 28.5 | 25.9 | 26.2 | 25.7 | 20.3 | 16.3 | 12.8 |
| Temperature of max. rate (°C): | 282 | 264 | 279 | 270 | 270 | 276 | 255 | 301 |
| Second main weight-loss reaction. | | | | | | | | |
| Weight-fraction volatilised(%): | - | 10.9 | - | 16.2 | 25.4 | 22.8 | 31.0 | - |
| Weight-fraction vol. (% of S70)(%):* | - | 16.4 | - | 24.3 | 38.1 | 34.2 | 46.5 | - |
| Temperature range (°C): | - | 283-335 | - | 292-348 | 283-348 | 297-358 | 269-354 | - |
| Max. rate of volatilisation(%.$min^{-1}$): | - | 22.1 | - | 4.5 | 4.8 | 7.7 | 15.1 | - |
| Temperature of max. rate (°C): | - | 287 | - | 301 | 300 | 312 | 291 | - |
| Carbon 'burn-off' reactions. | | | | | | | | |
| Total weight-fraction volatilised(%): | 20.2 | 19.8 | 17.6 | 20.4 | 21.1 | 21.6 | 19.1 | 20.6 |
| Total W.F. volatilised (% of S70)(%):* | 30.3 | 29.7 | 25.5 | 30.6 | 31.7 | 32.4 | 28.7 | 30.5 |
| Temperature range (°C): | 346-524 | 335-530 | 338-528 | 348-500 | 347-512 | 358-538 | 354-540 | 361-541 |
| First stage | | | | | | | | |
| Weight-fraction volatilised(%): | 20.2 | 19.8 | 17.0 | 20.4 | 21.1 | 21.6 | 19.1 | 20.6 |
| Weight-fraction vol. (% of S70)(%):* | 30.3 | 29.7 | 25.5 | 30.6 | 31.7 | 32.4 | 28.7 | 30.5 |
| Max. rate of volatilisation (%.$min^{-1}$?: | 6.7 | 5.8 | 4.5 | 5.9 | 6.4 | 6.9 | 6.0 | 6.6 |
| Temperature of max. rate (°C): | 471 | 482 | 447 | 482 | 482 | 482 | 485 | 481 |
| Temperature of max. endothermicity(°C): | 472 | 476 | 482 | 458 | 456 | 468 | 485 | 482 |

This is probably due to the oxidation of SnO to $SnO_2$ and subsequent conversion of the latter to $SnCl_4$. The maximum rates of volatilisation for each stage of the reaction are similar to those of SnO/S70 although the temperatures of each stage do not correspond with the reaction of either SnO/S70 or $\beta$-$SnO_2$/S70.

$\beta$-$SnO_2$ hydrate/$MoO_3$ does not react significantly with S70 (Table 35). In fact it seems that $MoO_3$ retards the volatilisation of $\beta$-$SnO_2$ as $SnCl_4$. The small interaction which takes place at 154-339°C consists of the evolution mainly of HCl together with some $SnCl_4$; the carbon 'burn-off' stage at 339-478°C is similar to that of S70 alone.

$\beta$-$SnO_2$ hydrate/CuO interacts with S70 in two stages, viz. at 152-325°C and 325-540°C. Although CuO normally forms a volatile halide quite easily, this reaction evidently does not occur when CuO is mixed with $\beta$-$SnO_2$ (Table 35).

SnO/ZnO reacts with S70 in three rather indistinct stages (Table 37). The main-weight loss consists of two superimposed fast reactions. There is, again, an increase in the interaction during the carbon 'burn-off' stage with increasing proportions of ZnO; but these interactions occur at much lower rates than do the reactions between $SnO_2$/ZnO and S70. These are due to the volatilisation of $ZnCl_2$. Although there is an increase in the weight fraction volatilised during carbon 'burn-off' with increasing proportion of ZnO, there is a distinct, but slight, decrease in the weight fraction of metal

TABLE 37

Thermal analysis of mixtures of SnO/ZnO and S70

| Ratio of SnO to ZnO(w/w): | 1:0 | 8:1 | 4:1 | 3:2 | 6:5 | 1:1 | 5:6 | 2:3 | 1:4 | 0:1 |
|---|---|---|---|---|---|---|---|---|---|---|
| Weight-fraction of M.O.volatilised(%): | 64.9 | 83.3 | 71.0 | 74.6 | 87.5 | 83.6 | 80.1 | 78.9 | 73.2 | 99.7 |
| Total W.F. of mixture volatilised(%): | 132.5 | 141.8 | 135.5 | 137.5 | 143.7 | 141.7 | 139.9 | k39.3 | 136.6 | 149.8 |
| Theor. W.F. volatilisable(%): | 150.0 | 150.0 | 150.0 | 150.0 | 150.0 | 150.0 | 150.0 | 150.0 | 150.0 | 150.0 |
| First main weight-loss reaction. | | | | | | | | | | |
| Weight-fraction volatilised(%): | 68.1 | 67.6 | 63.8 | 51.6 | 59.9 | 47.9 | 41.5 | 49.2 | 39.1 | 29.3 |
| Weight-fraction vol.(% of S70)(%):* | 102.2 | 101.4 | 95.7 | 77.4 | 89.9 | 71.9 | 62.3 | 73.8 | 58.7 | 43.9 |
| Temperature range($^{o}$C): | 195-343 | 196-325 | 198-329 | 182-303 | 161-320 | 167-261 | 200-317 | 176-309 | 193-324 | 197-326 |
| Max. rate of volatilisation(%.min$^{-1}$): | 39.1 | 30.9 | 29.1 | 27.5 | 19.5 | 12.4 | 28.4 | 22.5 | 17.7 | 39.6 |
| Temperature of max. rate ($^{o}$C): | 282 | 263 | 260 | 256 | 247 | 249 | 260 | 251 | 251 | 266 |
| Second main weight-loss reaction. | | | | | | | | | | |
| Weight-fraction vol.(% of S70)(%):* | - | - | - | - | - | 10.3 | 14.7 | - | - | 67.6 |
| Weight-fraction vol. (% of S70)(%):* | - | - | - | - | - | 15.5 | 22.1 | - | - | 101.4 |
| Temperature range ($^{o}$C): | - | - | - | - | - | 261-308 | 317-408 | - | - | 326-680 |
| Max. rate of volatilisation(%.min$^{-1}$): | - | - | - | - | - | 1.4 | 2.6 | - | - | 12.4 |
| Temperature of max. rate ($^{o}$C): | - | - | - | - | - | 282 | 398 | - | - | 492 |
| Carbon 'burn-off' reactions. | | | | | | | | | | |
| Total weight-fraction volatilised(%): | 20.2 | 26.9 | 26.6 | 39.9 | 35.9 | 36.3 | 37.2 | 43.8 | 52.1 | - |
| Total W.F.volatilised(% of S70)(%):* | 30.3 | 40.4 | 39.9 | 59.9 | 53.9 | 54.5 | 55.8 | 65.7 | 78.2 | - |
| Temperature range ($^{o}$C): | 346-524 | 325-513 | 329-527 | 303-512 | 320-500 | 308-500 | 408-700 | 309-480 | 324-519 | - |
| (a) First stage. | | | | | | | | | | |
| Weight-fraction volatilised(%): | 20.2 | 26.9 | 26.6 | 39.9 | 35.9 | 36.3 | 20.3 | 23.9 | 13.1 | - |
| Weight-fraction vol. (% of S70)(%):* | 26.8 | 40.4 | 39.9 | 59.9 | 53.9 | 54.5 | 30.8 | 35.9 | 19.7 | - |
| Max. rate of volatilisation(%.min$^{-1}$): | 6.7 | 4.3 | 5.4 | 5.4 | 5.8 | 5.7 | 6.2 | 4.6 | 6.9 | - |
| Temperature of max. rate ($^{o}$C): | 471 | 461 | 441 | 431 | 415 | 419 | 440 | 409 | 384 | - |
| Temperature of max. endothermicity($^{o}$C): | 472 | 454 | 420 | 389 | 405 | 391 | 443 | 388 | 384 | - |
| (b) Second stage. | | | | | | | | | | |
| Weight-fraction volatilised(%): | - | - | - | | | | 16.7 | 19.9 | 39.0 | - |
| Weight-fraction vol. (% of S70)(%):* | - | - | - | | | | 25.1 | 29.9 | 58.5 | - |
| Max. rate of volatilisation (%.min$^{-1}$): | - | - | - | | | | 12.3 | 5.4 | 7.7 | - |
| Temperature of max. rate ($^{o}$C): | - | - | - | | | | 458 | 437 | 450 | - |

oxide volatilised. The optimum ratio is around 6SnO:5ZnO(w/w) at which ca. 87.5% of the metal oxide is volatilised.

SnO/αAlOOH reacts with S70 in three distinct, but small stages (Table 38). There is no evidence of loss of water from α-AlOOH and, unlike the carbon 'burn-off' reaction found with $Sb_2O_3$, only a single-stage exothermic reaction occurs. There is little evidence of any interaction between the two metal oxides.

SnO/$Fe_2O_3$, when heated with S70, reacts at much lower temperatures than do other mixtures containing SnO (Table 39). The main weight loss reaction occurs at 128-284°C; the carbon 'burn-off' reaction is observed at 284-487°C and is very exothermic. Since $Fe_2O_3$ acts as a catalyst, the material volatilised (125.4%) consists mainly of $SnCl_2$ and HCl; the above weight fraction is high when compared with that found during the volatilisation of SnO and S70 on their own.

SnO/$MoO_3$ does not seem to volatilise the S70 when these oxides are mixed together even though they form volatile oxides when heated individually with S70.

SnO/CuO reacts with S70 to volatilise $SnCl_2$, $CuCl_2$ and HCl in two stages; the main reaction takes place at 166-314°C and the carbon 'burn-off' reaction occurs at 314-545°C. The weight fraction of metal oxide

TABLE 38

Thermal analysis of mixtures of SnO/ALOOH and S70

| Ratio of SnO to ALOOH (w/w) | 1:0 | 4:1 | 2:1 | 3:2 | 1:1 | 2:3 | 1:4 | 0:1 |
|---|---|---|---|---|---|---|---|---|
| Weight-fraction of M.O.volatilised(%): | 64.9 | 55.4 | 60.0 | 62.4 | 53.2 | 50.6 | 22.7 | 54.4 |
| Total W.F.of mixture volatilised(%):* | 132.5 | 127.5 | 130.0 | 131.1 | 126.8 | 125.3 | 111.3 | 120.9 |
| Theor. W.F.volatilisable(%): | 150.0 | 150.0 | 150.0 | 150.0 | 150.0 | 150.0 | 150.0 | 138.4 |
| First main weight-loss reaction. | | | | | | | | |
| Weight-fraction volatilised(%): | 68.1 | 38.5 | 53.8 | 50.9 | 45.4 | 36.0 | 20.5 | 20.4 |
| Weight-fraction vol. (% of S70)(%):* | 102.2 | 57.8 | 80.7 | 76.4 | 68.1 | 54.0 | 30.8 | 40.8 |
| Temperature range (°C): | 195-343 | 175-285 | 160-280 | 160-280 | 159-290 | 143-282 | 160-266 | 148-301 |
| Max. rate of volatilisation(%.min$^{-1}$): | 39.1 | 30.7 | 18.9 | 18.1 | 13.7 | 11.1 | 20.8 | 9.1 |
| Temperature of max. rate (°C): | 282 | 263 | 253 | 256 | 256 | 251 | 240 | 286 |
| Second main weight-loss reaction. | | | | | | | | |
| Weight-fraction volatilised(%): | - | 13.9 | 11.3 | 15.5 | 20.3 | 25.9 | 32.8 | 22.8 |
| Weight-fraction vol. (% of S70)(%):* | - | 20.9 | 17.0 | 23.3 | 30.5 | 38.9 | 49.2 | 45.6 |
| Temperature range (°C): | - | 285-350 | 280-340 | 280-348 | 290-380 | 282-354 | 266-367 | 301-372 |
| Max. rate of volatilisation(%.min$^{-1}$): | - | 20.5 | 18.9 | 4.2 | 4.5 | 6.7 | 14.1 | 18.6 |
| Temperature of max. rate (°C): | - | 293 | 301 | 301 | 310 | 314 | 310 | 338 |
| Carbon 'burn-off' reactions. | | | | | | | | |
| Total weight-fraction volatilised(%): | 20.2 | 32.3 | 21.5 | 21.0 | 18.9 | 21.6 | 20.9 | 18.0 |
| Total W.F. volatilised (% of S70)(%):* | 30.3 | 48.5 | 32.3 | 31.5 | 28.4 | 32.4 | 31.4 | 36.0 |
| Temperature range (°C): | 346-524 | 350-560 | 340-538 | 348-538 | 380-571 | 354-548 | 367-590 | 372-549 |
| First stage. | | | | | | | | |
| Weight-fraction volatilised(%): | 20.2 | 32.3 | 21.5 | 21.0 | 18.9 | 21.6 | 20.9 | 18.0 |
| Weight-fraction vol. (% of S70)(%):* | 30.3 | 48.5 | 32.3 | 31.5 | 28.4 | 32.4 | 31.4 | 36.0 |
| Max. rate of volatilisation (%.min$^{-1}$): | 6.7 | 4.9 | 5.4 | 7.0 | 7.5 | 6.6 | 9.3 | 6.9 |
| Temperature of max. rate (°C): | 471 | 489 | 477 | 486 | 492 | 487 | 500 | 483 |
| Temperature of max. endothermicity(°C): | 472 | 489 | 450 | 480 | 492 | 487 | 497 | 483 |

volatilised is however not very significant (Table 39).

$\underline{ZnO/NH_4HB_4O_7.3H_2O}$ reacts with chlorinated wax in two main stages. The first weight loss between 175-350°C is due to three simultaneous exothermic reactions and ca 28.6% of the initial weight is volatilised. The second stage consists of two overlapping reactions and corresponds to the loss of hydrogen chloride and zinc chloride at 472 and 494°C. The total percentage weight of mixture volatilised was 78.2% which may be compared with a theoretical weight loss of 83% if none of the ammonium metaborate were volatilised; this thus indicates only minor interaction between the above system and the chlorine source (Table 40).

TABLE 39

Thermal analysis of mixtures of SnO/metal oxides and S70

| Metal Oxide: | $Fe_2O_3$ | AlOOH | ZnO | $MoO_3$ | CuO |
|---|---|---|---|---|---|
| Ratio of M.O. to S70 (w/w): | 1:1.6 | 1:1.9 | 1:1.2 | 1:1.7 | 1:1.2 |
| Ratio of M.O. to S70(Molar): | 1:1 | 1:1 | 1:1 | 1:1 | 1:1 |
| Weight-fraction of M.O.volatilised(%): | 40.4 | 62.1 | 58.9 | 38.1 | 27.5 |
| Total W.F. of mixture volatilised(%):* | 125.4 | 132.9 | 142.4 | 122.8 | 129.3 |
| Theor. W.F. volatilised(%): | 259.2 | 287.3 | 220.5 | 267.9 | 221.6 |
| First main weight-loss reaction. | | | | | |
| Weight-fraction volatilised(%): | 49.2 | 65.8 | 52.6 | 57.2 | 45.9 |
| Weight-fraction vol. (% of S70)(%):* | 80.1 | 100.9 | 96.3 | 91.3 | 83.6 |
| Temperature range (°C): | 128-284 | 160-329 | 176-318 | 189-328 | 166-314 |
| Max. rate of volatilisation(%.min$^{-1}$): | 13.2 | 22.9 | 41.8 | 29.9 | 25.5 |
| Temperature of max. rate (°C): | 228 | 257 | 274 | 263 | 278 |
| Second main weight-loss reaction. | | | | | |
| Weight-fraction volatilised(%): | - | - | - | - | - |
| Weight-fraction vol. (% of S70)(%):* | - | - | - | - | - |
| Temperature range (°C): | - | - | - | - | - |
| Max. rate of volatilisation(%.min$^{-1}$): | - | - | - | - | - |
| Temperature of max. rate (°C): | - | - | - | - | - |
| Carbon 'burn-off' reactions. | | | | | |
| Total weight-fraction volatilised(%): | 27.8 | 21.0 | 28.8 | 19.7 | 22.1 |
| Total W.F. volatilised(% of S70)(%):* | 45.3 | 32.2 | 52.7 | 31.4 | 40.3 |
| Temperature range (°C): | 284-487 | 329-535 | 318-535 | 328-485 | 314-545 |
| First stage. | | | | | |
| Weight-fraction volatilised(%): | 27.8 | 21.0 | 28.8 | 19.7 | 22.1 |
| Weight-fraction vol. (% of S70)(%):* | 45.3 | 32.2 | 52.7 | 31.4 | 40.3 |
| Max. rate of volatilisation(%.min$^{-1}$): | 8.0 | 5.0 | 6.4 | 6.1 | 11.6 |
| Temperature of max. rate (°C): | 338 | 433 | 424 | 379 | 374 |
| Temperature of max. endothermicity(°C): | 420 | 281 | 395 | 379 | 407 |

TABLE 40

Thermal analysis of mixtures of ZnO/$(NH_4)_6Mo_7O_{24}.4H_2O$ and S70

| | | ZnO | ZnO/AM | AM |
|---|---|---|---|---|
| Ratio of M.O. to S70 (w/w): | 0:1 | 1:2 | 1:1:4 | 2:5 |
| Weight-fraction of M.O. volatilised(%): | - | 99.7 | 71.1 | 93.4 |
| Total W.F. of mixture volatilised(%):* | 98. | 149.8 | 106.7 | 130.8 |
| Theor. W.F. volatilisable(%): | 100.0 | 150.0 | 150.0 | 140.0 |
| First main weight-loss reaction. | | | | |
| Weight-fraction volatilised(%): | 67.8 | 29.3 | 28.6 | 1.5 |
| Weight-fraction vol.(% of S80)(%):* | 67.8 | 43.9 | 42.9 | 2.1 |
| Temperature range($^{o}$C): | 150-350 | 197-326 | 175-350 | 71-135 |
| Max. rate of volatilisation(%.min$^{-1}$): | 9.3 | 39.6 | 27.5 | 33.1 |
| Temperature of max. rate ($^{o}$C): | 302 | 266 | 272 | 116 |
| Second main weight-loss reaction. | | | | |
| Weight-fraction volatilised(%): | -. | 67.6 | 42.5 | 54.1 |
| Weight-fraction vol. (% of S70)(%):* | - | 101.4 | 63.0 | 81.2 |
| Temperature range ($^{o}$C): | - | 326-680 | 350-700 | 188-354 |
| Max. rate of volatilisation(%.min$^{-1}$): | - | 12.4 | 11.1 | 22.3 |
| Temperature of max. rate ($^{o}$C): | - | 492 | 494 | 328 |
| Carbon 'burn-off' reactions. | | | | |
| Total weight-fraction volatilised(%): | 31.0 | - | - | 37.8 |
| Total W.F. volatilised (% of S70)(%):* | 31.0 | - | - | 52.9 |
| Temperature range ($^{o}$C): | 305-508 | - | - | 354-960 |
| (a) First stage. | | | | |
| Weight-fraction volatilised(%): | 18.2 | - | - | 18.8 |
| Weight-fraction vol. (% of S70)(%):* | 18.2 | - | - | 26.3 |
| Max. rate of volatilisation(%.min$^{-1}$): | 5.4 | - | - | 8.7 |
| Temperature of max. rate ($^{o}$C): | 429 | - | - | 394 |
| Temperature of max. endothermicity($^{o}$C): | 429 | - | - | 391 |
| (b) Second stage. | | | | |
| Weight-fraction volatilised(%): | 12.8 | - | - | 19.0 |
| Weight-fraction vol. (% of S70)(%):* | 12.8 | - | - | 26.6 |
| Max. rate of volatilisation(%.min$^{-1}$): | 5.0 | - | - | 11.1 |
| Temperature of max. rate ($^{o}$C): | 450 | - | - | 775 |

AM : $(NH_4)_6Mo_7O_{24}.4H_2O$

### 3.1.5 Polymers

Thermogravimetric studies of the two virgin polymers were undertaken to form a basis for comparison with polymers containing flame retardant compositions.

In the absence of oxygen, polyethylene is stable up to ca. 250°C where chain-scission is found to take place producing a decrease in molecular weight. At about 360°C, volatile products begin to appear, while at higher temperatures (above 450°C) complete degradation of the polymer occurs (Table 41). In air, the decomposition is initiated at about the same temperature (Table 42). The DTA trace shows the presence of a number of small degradation stages which can be attributed to the various modes of chain-scission and there is a carbon burn-off reaction above ca. 450°C. The reactions are highly exothermic, especially the main degradation. The melting range is between ca. 90-140°C in nitrogen and between ca. 115-130°C in air. No glass transition temperature appears to be indicated in the DTA trace.

On being heated, acrylonitrile-butadiene-styrene (ABS) undergoes two very distinct weight loss stages. The first is between 244-440°C and shows two simultaneous, yet different, chemical decompositions at 409 and 434°C due to the different homopolymers in the blend. The second weight-loss reaction between 440-570°C is a single exothermic degradation stage (Table 42).

TABLE 41

Thermal analysis of the polymer in nitrogen

| | HDPE S70 | ABS ADINE |
|---|---|---|
| Total weight fraction volatilised(%): | 95.5 | 96.5 |
| Temperature range-melting (°C) : | 115-138 | - |
| Initial weight-loss reaction-hydrogen halide : | | |
| Weight-fraction volatilised(%) : | 18.7 | - |
| Temperature range (°C) : | 230-354 | - |
| Temperature of max. rate (°C) : | 290 | - |
| Main weight-loss reactions : | | |
| Weight-fraction volatilised(%) : | 52.7 | 70.7 |
| Number of weight-loss stages : | 5 | 3 |
| (a) Temperature range (°C) : | 404-452 | 194-347 |
| (b) Temperature range (°C) : | - | 347-390 |
| (c) Temperature range (°C) : | - | 390-442 |
| Second weight-loss reaction : | | |
| Weight-fraction volatilised(%) : | 24.1 | 25.8 |
| (a) Temperature range (°C) : | 452-500 | 454-584 |
| (b) Temperature range (°C) : | - | - |

TABLE 42

Thermal analysis of the polymer in air

| | HDPE | ABS |
|---|---|---|
| Total weight fraction volatilised(%): | 97.6 | 96.7 |
| Temperature range-melting ($^{o}$C) : | 92-140 | 95-235 |
| Initial weight-loss reaction-hydrogen halide : | | |
| Weight-fraction volatilised(%) : | 8.8 | - |
| Temperature range ($^{o}$C) : | 223-382 | - |
| Temperature of max. rate ($^{o}$C) : | 338 | - |
| Main weight-loss reactions : | | |
| Weight-fraction volatilised(%) : | 85.1 | 89.3 |
| Number of weight-loss stages : | 2 | 2 |
| (a) Temperature range ($^{o}$C) : | 382-419 | 235-429 |
| (b) Temperature range ($^{o}$C) : | 419-468 | 429-464 |
| (c) Temperature range ($^{o}$C) : | - | - |
| Second weight-loss reaction : | | |
| Weight-fraction volatilised(%) : | 3.7 | 7.4 |
| (a) Temperature range ($^{o}$C) : | 468-526 | 464-640 |
| (b) Temperature range ($^{o}$C) : | - | - |

### 3.1.6 Polymer + Halogen

The addition of chlorowax 70 to polyethylene appears to delay the initial decomposition of the polymer. On melting, some hydrogen chloride is releasedbetween 230 and 354°C. The decomposition by numerous chain-scission reactions takes place between 404 and 452°C and the cross-linked carbonaceous char is then burnt off between 452 and 500°C (Table 43). The residue at this temperature is about 4.5% of the original weight of the sample and can be burnt off the crucible at a higher temperature.

The course of the decomposition of ABS is also altered when Adine is incorporated into it. The distinct initial weight loss reaction now consists of three simultaneous changes occurring at a much lower temperature between 194 and 442°C (Table 43). The carbon burn-off reaction is extended to 584°C and ca. 96.5% of the total weight of the sample is lost. This is identical to the weight lost by ABS alone.

### 3.1.7 Polymer + Halogen + Single Metal Oxide

#### 3.1.7.1 General

Various metal oxide/halogen systems, which were incorporated into the polymers, were heated at $5^{o}$ $min^{-1}$ up to ca. 650°C. In general they lost 90% of their original weight and this shows that some metal oxide was not volatilised.

TABLE 43

Thermal analysis of the polymer/halogen system

| | HDPE | ABS |
|---|---|---|
| Total weight fraction volatilised(%): | 97.4 | 96.5 |
| Temperature range-melting ($^{o}$C) : | 112-137 | - |
| Initial weight-loss reaction-hydrogen halide : | | |
| Weight-fraction volatilised(%) : | 14.8 | - |
| Temperature range ($^{o}$C) : | 230-366 | - |
| Temperature of max. rate ($^{o}$C) : | 266 | - |
| Main weight-loss reactions : | | |
| Weight-fraction volatilised(%) : | 54.7 | 78.3 |
| Number of weight-loss stages : | 3 | 1 |
| (a) Temperature range ($^{o}$C) : | 366-394 | 244-440 |
| (b) Temperature range ($^{o}$C) : | 394-398 | - |
| (c) Temperature range ($^{o}$C) : | 398-420 | - |
| Second weight-loss reaction : | | |
| Weight-fraction volatilised(%) : | 27.9 | 18.2 |
| (a) Temperature range ($^{o}$C) : | 420-450 | 440-571 |
| (b) Temperature range ($^{o}$C) : | 450-496 | - |

3.1.7.2 In polyethylene (HDPE)

The decomposition of polyethylene involves a number of types of bond scission. Since thermogravimetric studies of these samples were not accompanied by any evolution gas analysis, the decomposition is discussed only in generalised terms.

The addition of $Sb_2O_3$ to the HDPE/S70 system does not greatly alter the decomposition trace. However, an additional peak at 427°C indicates the release of $SbCl_3$ and this has been confirmed by mass spectrometric analysis (MS30/DS20 system). The carbon burn-off due to the presence of a metal is also indicated by a sharp peak within the carbon burn-off rate of weight change trough.

The main decomposition in the presence of SnO takes place between 350 and 482°C and is highly exothermic (Table 44). There is an extensive loss of weight of ca. 98.6%, which indicates some synergistic interaction between the halogen and the metal oxide. However, no metal halide species was detected.

The decomposition of $SnO_2$ is less complex. There is an initial loss of HCl between 210 and 320°C, followed by a number of insignificant reactions and two distinct fast reactions. A total of 92.3% is volatilised.

Although ZnO is completely volatilised as its chloride in the presence of S70, only 93.3% of the sample is lost

TABLE 44

Thermal analysis of HDPE/S70/metal oxide systems

| | $Sb_2O_3$ | SnO | $SnO_2$ | ZnO | $Fe_2O_3$ | $Al_2O_3$ | AlOOH | $Al_2O_3.3H_2O$ | $(NH_4)_6Mo_7O_{24}$ |
|---|---|---|---|---|---|---|---|---|---|
| Total weight fraction volatilised(%): | 95.1 | 98.6 | 92.3 | 93.3 | 91.2 | 90.2 | 93.3 | 91.8 | 93.7 |
| Temperature range-melting ($^oC$) : | 126-138 | 120-139 | 120-136 | 124-136 | 120-134 | 120-135 | 120-135 | 120-135 | 124-136 |
| Initial weight-loss reaction-hydrogen halide : | | | | | | | | | |
| Weight-fraction volatilised(%) : | 18.8 | 20.4 | 15.6 | 8.9 | 8.8 | 14.5 | 13.1 | - | 17.1 |
| Temperature range ($^oC$) : | 250-347 | 210-350 | 210-320 | 206-320 | 192-300 | 229-316 | 230-366 | - | 240-342 |
| Temperature of max. rate ($^oC$) : | 302 | 270 | 266 | 265 | 235 | 280 | 276 | - | 290 |
| Main weight-loss reactions : | | | | | | | | | |
| Weight-fraction volatilised(%) : | 76.3 | 78.2 | 76.7 | 84.4 | 82.4 | 75.7 | 80.2 | 66.2 | 76.6 |
| Number of weight-loss stages : | 3 | 5 | 5 | 5 | 3 | 3 | 2 | 4 | 5 |
| (a) Temperature range ($^oC$) : | 347-356 | 350-432 | 425-500 | 414-495 | 400-485 | 406-430 | 420-460 | 220-454 | 412-436 |
| (b) Temperature range ($^oC$) : | 356-490 | 432-468 | - | - | - | 430-442 | 460-500 | - | 436-470 |
| (c) Temperature range ($^oC$) : | - | 468-482 | - | - | - | 442-470 | - | - | 470-500 |
| Second weight-loss reaction : | | | | | | | | | |
| Weight-fraction volatilised(%) : | - | - | - | - | - | - | - | - | - |
| (a) Temperature range ($^oC$) : | - | - | - | - | - | - | - | 25.6 | - |
| (b) Temperature range ($^oC$) : | - | - | - | - | - | - | - | 454-570 | - |

when this compound is heated in air. The decomposition is similar to that of HDPE/$SnO_2$/S70 (Figure 40) and hence one is tempted to deduce that the metal oxide has little or no effect on the degradation of the polymer.

$\underline{Fe_2O_3}$ catalyses the decomposition of the polymer. The temperature of decomposition is reduced to 192°C and 91.2% of the sample is volatilised up to a temperature of 500°C.

The thermogravimetric traces of the decomposition of HDPE/S70 containing the three oxides of alumina are very different to the other samples. The decomposition in the presence of $\underline{Al_2O_3}$ is highly exothermic and there are two distinct weight losses in the main degradation stage between 420 and 500°C. The slightly endothermic reaction due to the loss of water from $\underline{AlOOH}$ appears to decrease the exothermicity of the main degradation of the polymer, while the highly endothermic release of water vapour from $\underline{Al_2O_3}.\underline{3H_2O}$ totally alters the degradation pattern of polyethylene/chlorowax 70 (Figure 41).

The complex degradation of $(NH_4)_6Mo_7O_{24}.4H_2O$ also shows a different trend in the thermal degradation of this polymer/halogen system.

FIGURE 40

The weight loss/rate of weight change traces for the polyethylene/ Electrofine S70/metal oxide systems

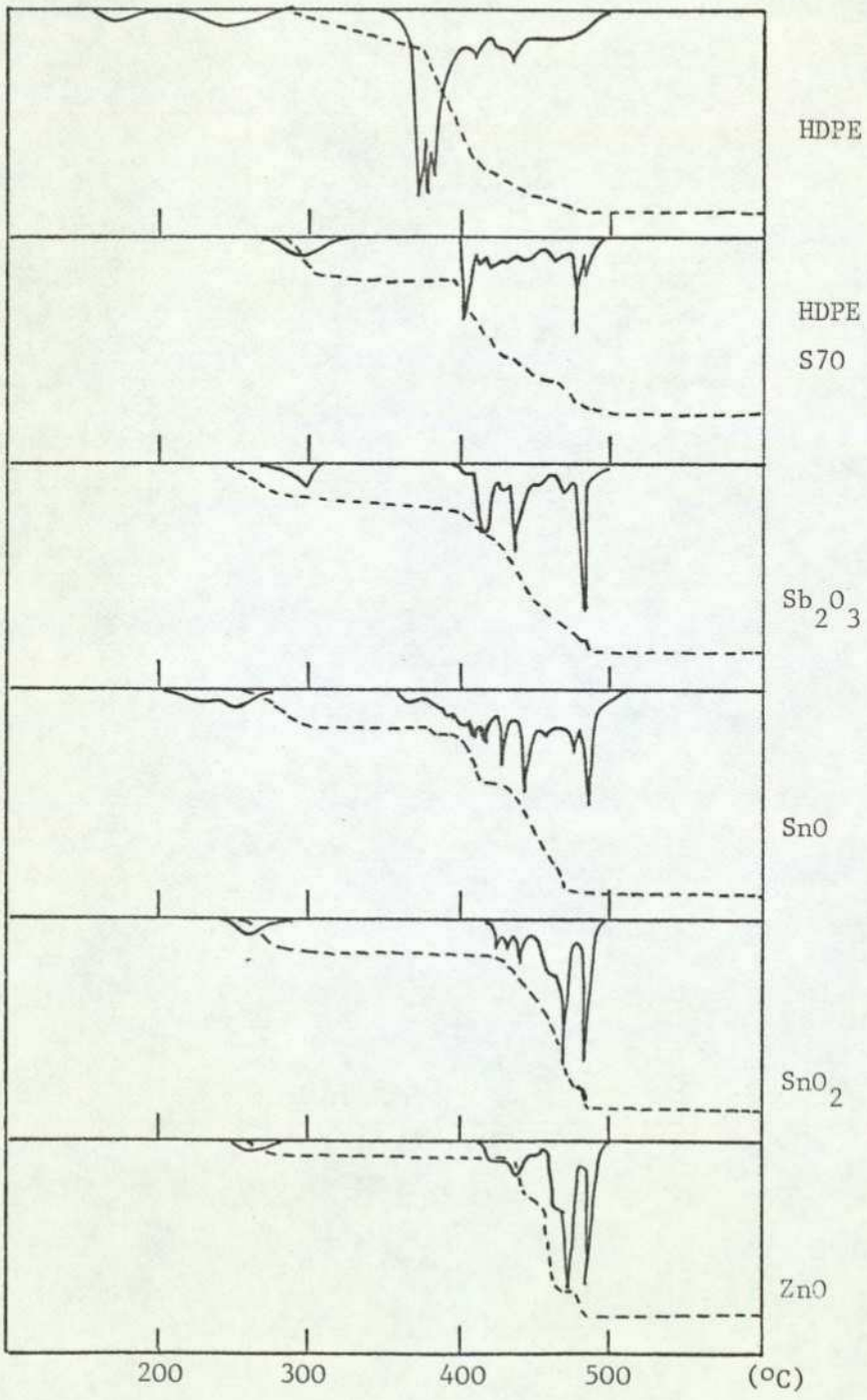
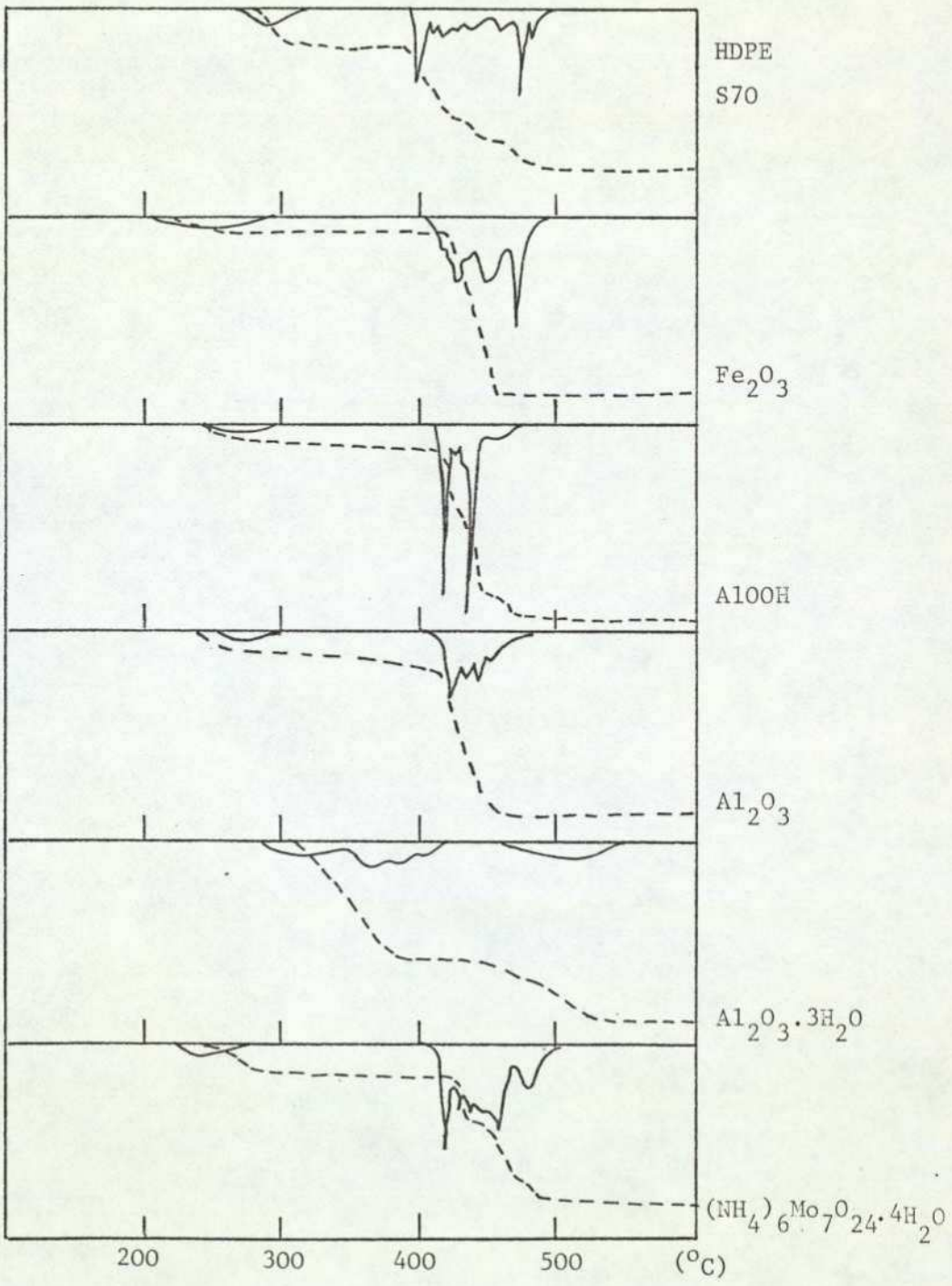


FIGURE 41

The weight loss/rate of weight change traces for the polyethylene/Electrofine S70/metal oxides systems



3.1.7.3 In acrylonitrile-butadiene-styrene (ABS)

The rate of weight change traces for samples of ABS containing Adine and various metal oxides show no common trend (Figures 42 and 43).

The addition of $Sb_2O_3$ initiates decomposition at a lower temperature of 200°C and a total of four distinct stages are observed. The initial decomposition involves the loss of HBr and $SbBr_3$ and this has been confirmed by mass spectrometry.

The decomposition due to the presence of SnO and $SnO_2$ appears to be very similar. A total of 91.9 and 91.0% respectively of the initial weight is lost.

There are a number of small weight changes in the sample containing ZnO (Figure 42). The initial stage is very exothermic and appears to be due to the volatilisation of HBr and some $ZnBr_2$. The second stage is a highly complex multi-stage degradation.

The catalytic action of $Fe_2O_3$ is evident from the fact that this compound initiates degradation at a much lower temperature (Table 45). The rate of weight change trace shows a number of reactions due to the effect of $Fe_2O_3$ on the various homopolymers in the blend (Figure 43).

The decomposition of the ABS/Adine system in the presence of $Al_2O_3$, AlOOH and $Al_2O_3.3H_2O$ is

FIGURE 42

The weight change/rate of weight change traces for the ABS/Adine/metal oxide system

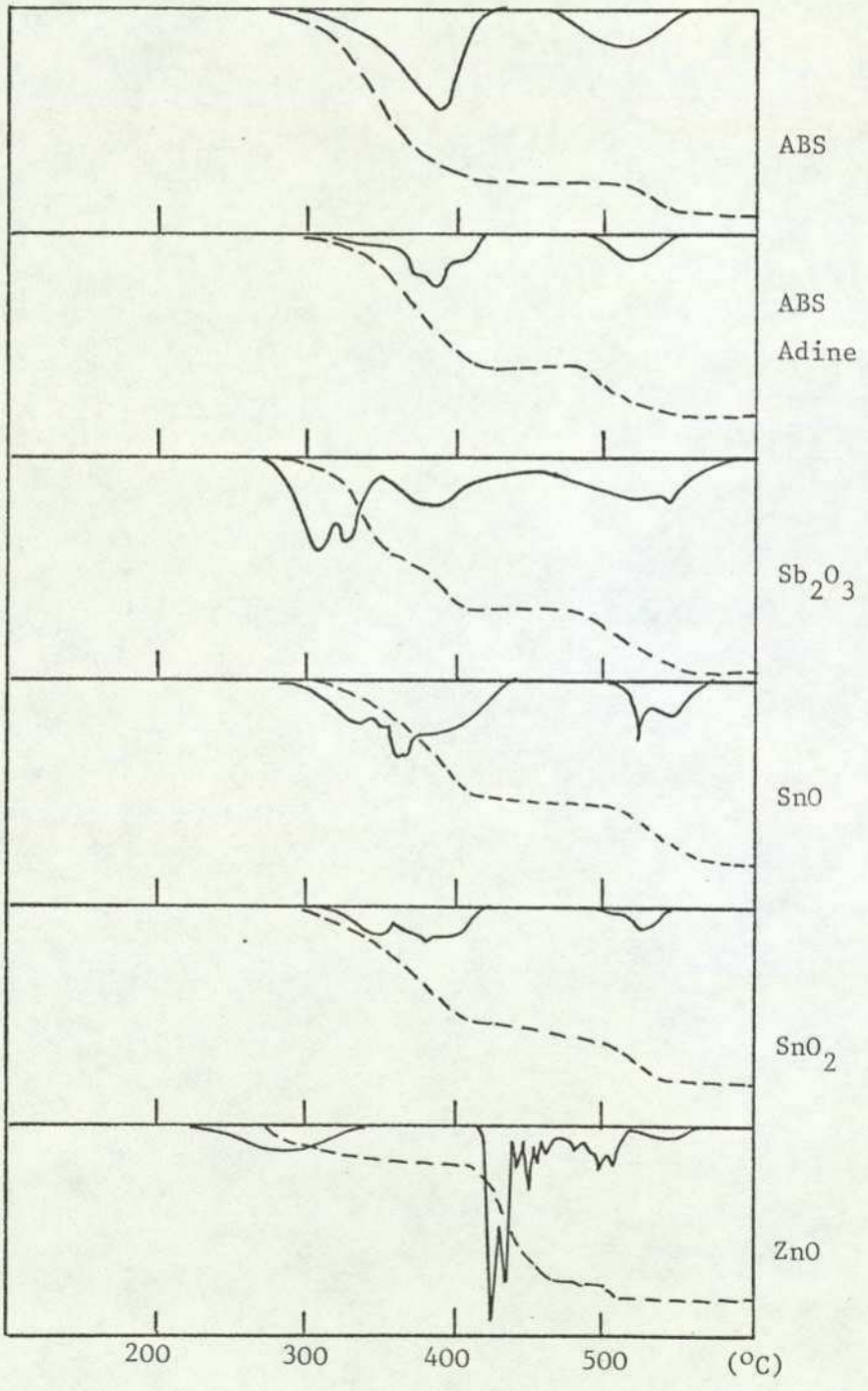


FIGURE 43

The weight change/rate of weight change traces

for the ABS/Adine/metal oxide system

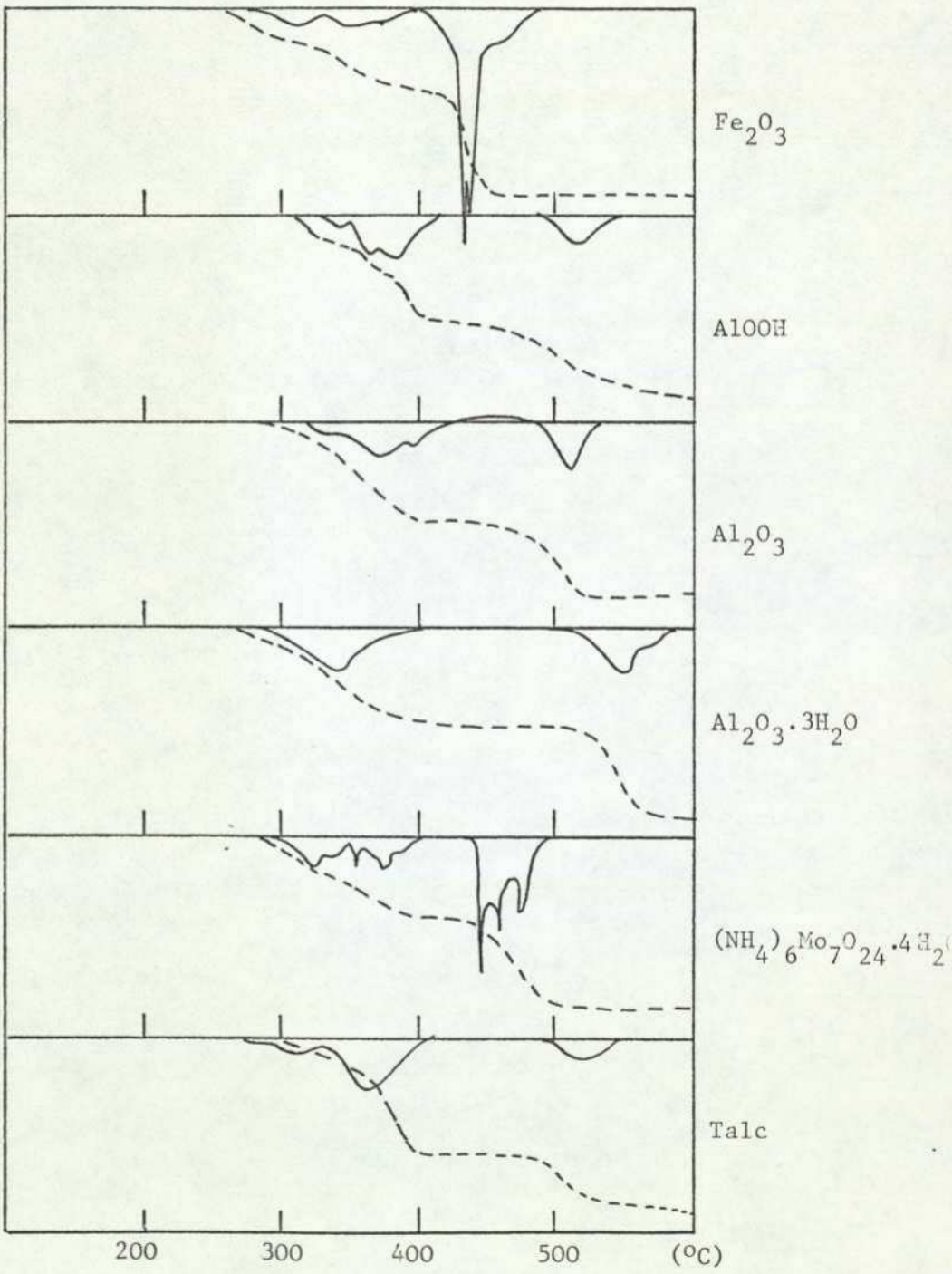


TABLE 45

Thermal analysis of ABS/Adine/metal oxide systems

| | $Sb_2O_3$ | SnO | $SnO_2$ | ZnO | $Fe_2O_3$ | $Al_2O_3$ | AlOOH | $Al_2O_3.3H_2O$ | Talc | $(NH_4)_6Mo_7O_{24}$ |
|---|---|---|---|---|---|---|---|---|---|---|
| Total weight fraction volatilised(%): | 95.8 | 91.9 | 91.0 | 90.7 | 91.0 | 78.4 | 90.6 | 92.6 | 91.3 | 89.1 |
| Temperature range-melting ($^oC$) : | - | - | - | - | - | - | - | - | - | - |
| Initial weight-loss reaction-hydrogen halide : | | | | | | | | | | |
| Weight-fraction volatilised(%) : | 40.4 | - | 23.3 | 21.0 | 15.5 | - | 19.1 | 47.7 | 15.0 | - |
| Temperature range ($^oC$) : | 200-360 | - | 215-356 | 210-370 | 175-332 | - | 240-350 | 235-440 | 244-355 | - |
| Temperature of max. rate ($^oC$) : | 317&324 | - | 342 | 295 | 320 | - | 336 | 350 | 335 | - |
| Main weight-loss reactions : | | | | | | | | | | |
| Weight-fraction volatilised(%) : | 29.3 | 57.9 | 37.1 | 54.7 | 21.6 | 48.1 | 43.6 | 44.9 | 48.6 | 43.1 |
| Number of weight-loss stages : | 1 | 4 | 3 | 7 | 2 | 2 | 2 | 2 | 3 | 5 |
| (a) Temperature range ($^oC$) : | 360-443 | 225-446 | 356-440 | 415-470 | 332-440 | 255-440 | 350-431 | 440-582 | 355-452 | 225-341 |
| (b) Temperature range ($^oC$) : | - | - | - | - | - | - | - | 582-624 | - | 341-418 |
| (c) Temperature range ($^oC$) : | - | - | - | - | - | - | - | - | - | - |
| Second weight-loss reaction : | | | | | | | | | | |
| Weight-fraction volatilised(%) : | 26.1 | 34.0 | 30.6 | 15.0 | 53.9 | 30.3 | 27.9 | - | 25.5 | 48.2 |
| (a) Temperature range ($^oC$) : | 443-532 | 490-615 | 440-585 | 470-560 | 440-492 | 440-551 | 431-575 | - | 452-566 | 418-452 |
| (b) Temperature range ($^oC$) : | 532-600 | - | - | - | - | - | - | - | - | 452-520 |

quite similar. The decomposition is in two major stages between 230-440°C and 440-600°C (Table 45).

When $(NH_4)_6Mo_7O_{24}.4H_2O$ is heated in the ABS/Adine system, two multi-stage reactions appear to take place. The first is between 225 and 418°C followed by a faster reaction between 418 and 520°C (Figure 43).

The decomposition of ABS/Adine containing talc has three distinct stages and is very similar to the decomposition of the ABS/Adine system on its own.

3.1.8 Polymer + Mixed Metal Oxides + Halogen Compound

3.1.8.1 General

When the polymers containing a halogen compound and a mixture of two metal oxides were heated, it becomes evident (from a study of the thermal decomposition of these samples) that certain metal oxides hinder the volatilisation of others. In general, these systems all release some hydrogen halide after the polymer has melted to a viscous mass and this is generally followed by decomposition of the polymer.

3.1.8.2 Polyethylene/halogen/mixed metal oxide systems

When a polyethylene/Electrofine S70/antimony

oxide system containing another metal oxide is heated in air, the polymer melts at ca. 118°C and decomposition generally takes place between 400 and 500°C (Table 46). Hydrogen chloride is released between 220 and 340°C and there is no separate carbon burn-off stage (Figure 44). $Fe_2O_3$ does not appear to lower the temperature of decomposition of the chlorinated wax in the sample; it does however accelerate polymer decomposition and encourages cross-linking to form char by a highly exothermic reaction. AlOOH causes the polymer to undergo a slightly less exothermic decomposition, while $Al_2O_3.3H_2O$ decomposes endothermically to cancel out the highly exothermic decomposition of the polymer. Various antimony/halogen species have been identified using mass spectrometry and there is some possible evidence of aluminium-halogen species when anhydrous alumina is used.

When SnO replaces $Sb_2O_3$, there is no evidence of its interaction with either $Fe_2O_3$ or AlOOH. AlOOH appears to prevent any further interaction between the tin(11)oxide and the chlorinated wax and only 91.7% of the polymer sample is volatilised (Figure 45).

$SnO_2$ and $Fe_2O_3$ also hinder the volatilisation

TABLE 46

Thermal analysis of HDPE/S70/two metal oxide systems

| | $Sb_2O_3$ $SnO_2$ | $Sb_2O_3$ ZnO | $Sb_2O_3$ $Fe_2O_3$ | $Sb_2O_3$ $Al_2O_3$ | $Sb_2O_3$ AlOOH | $Sb_2O_3$ $Al_2O_3.3H_2O$ | $Sb_2O_3$ $(NH_4)_6Mo_7O_{24}$ | SnO ZnO | SnO AlOOH | $SnO_2$ $Fe_2O_3$ |
|---|---|---|---|---|---|---|---|---|---|---|
| Total weight fraction volatilised(%): | 95.6 | 93.3 | 92.9 | 93.5 | 92.7 | 94.3 | 93.2 | 95.3 | 91.7 | 94.5 |
| Temperature range-melting ($^oC$) : | 115-134 | 116-129 | 118-135 | 120-134 | 114-131 | 120-134 | 118-135 | 119-132 | 111-129 | 119-134 |
| Initial weight-loss reaction-hydrogen halide : | | | | | | | | | | |
| Weight-fraction volatilised(%) : | 23.9 | 19.2 | 20.5 | 22.9 | 22.7 | 22.3 | 24.3 | 18.3 | 19.6 | 44.6 |
| Temperature range ($^oC$) : | 137-340 | 207-332 | 222-298 | 250-335 | 235-348 | 230-350 | 235-356 | 204-307 | 214-323 | 260-415 |
| Temperature of max. rate ($^oC$) : | 296 | 291 | 243 | 295 | 303 | 300 | 306 | 250 | 265 | 362 |
| Main weight-loss reactions : | | | | | | | | | | |
| Weight-fraction volatilised(%) : | 71.7 | 74.1 | 72.4 | 70.6 | 70.0 | 72.0 | 69.0 | 77.0 | 72.1 | 49.9 |
| Number of weight-loss stages : | 7 | 5 | 5 | 4 | 8 | 8 | 5 | 3 | 6 | 1 |
| (a) Temperature range ($^oC$) : | 423-500 | 415-500 | 367-476 | 416-506 | 408-510 | 395-500 | 405-492 | 414-495 | 400-500 | 415-505 |
| (b) Temperature range ($^oC$) : | - | - | - | - | - | - | - | - | - | - |
| (c) Temperature range ($^oC$) : | - | - | - | - | - | - | - | - | - | - |
| Second weight-loss reaction : | | | | | | | | | | |
| Weight-fraction volatilised(%) : | | | | | | | | | | |
| (a) Temperature range ($^oC$) : | - | - | - | - | - | - | - | - | - | - |
| (b) Temperature range ($^oC$) : | - | - | - | - | - | - | - | - | - | - |

FIGURE 44

The weight loss/rate of weight change traces for the polyethylene/Electrofine S70/mixed metal oxide systems

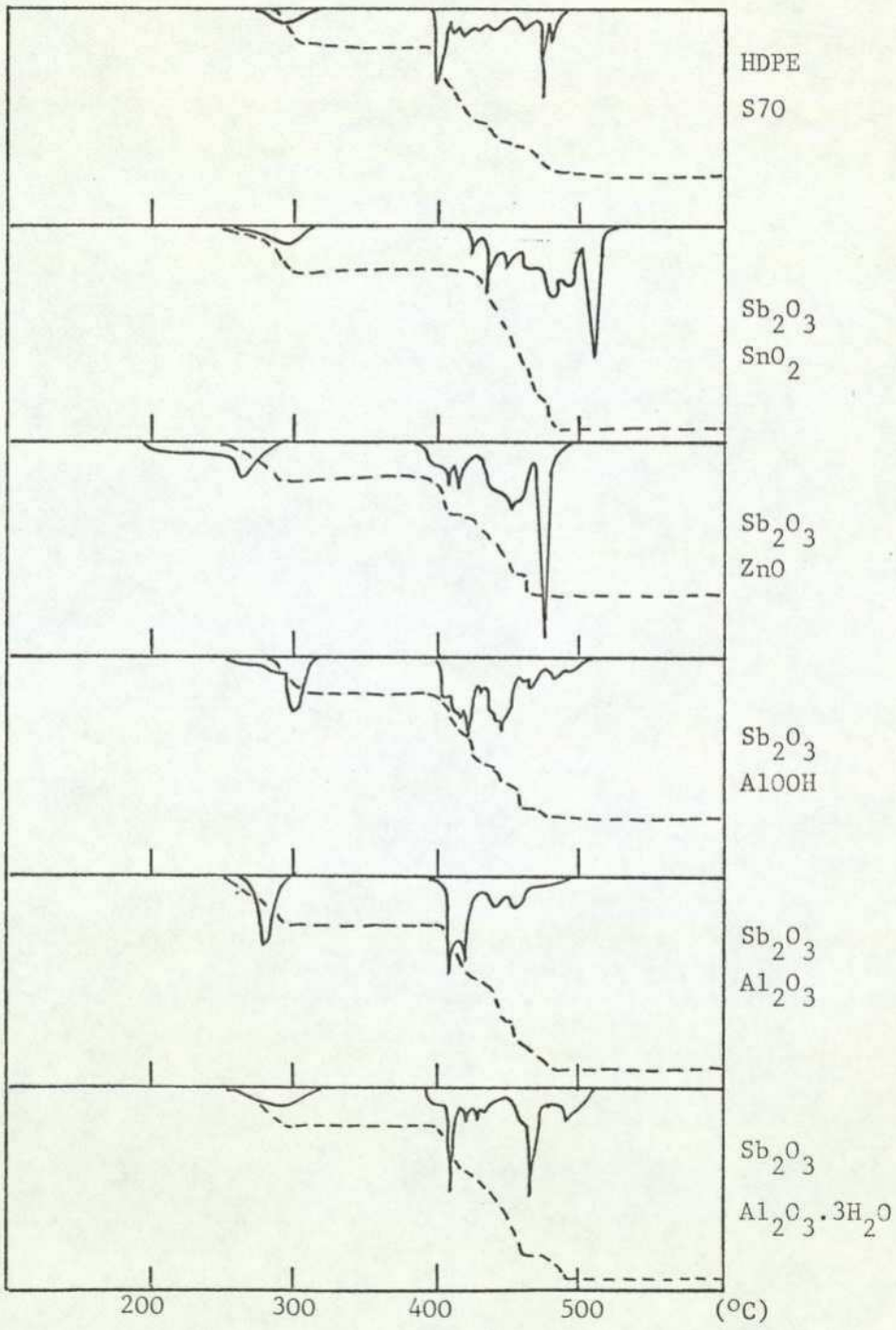
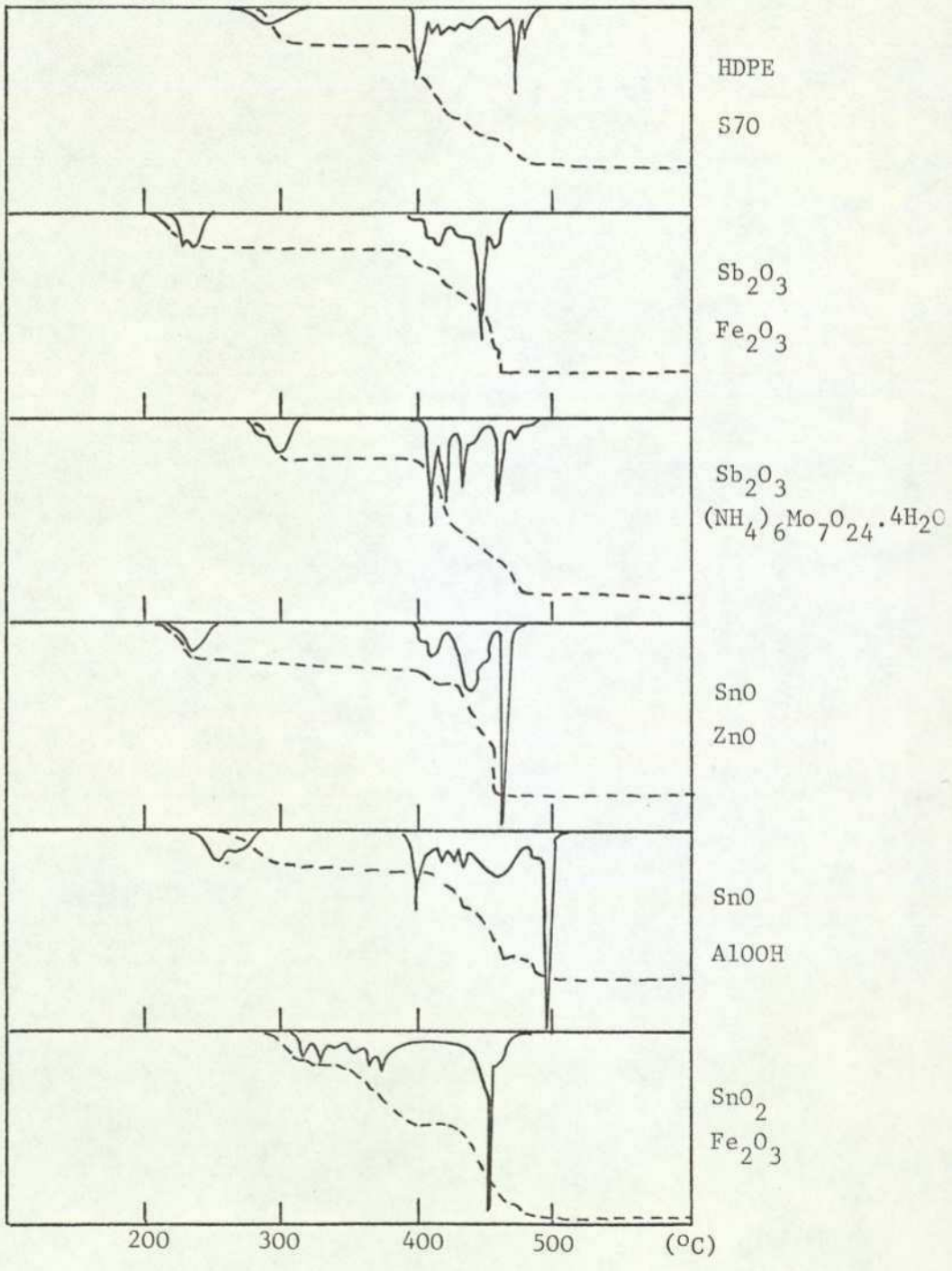


FIGURE 45

The weight loss/rate of weight change traces for the polyethylene/Electrofine S70/mixed metal oxide systems



of the chlorine source. There is no decrease in the temperature of decomposition of these polymers. No carbon burn-off stage is found.

3.1.8.3 ABS/halogen/mixed metal oxide systems

In the ABS/halogen/$Sb_2O_3$ system, SnO definitely retards the volatilisation of $SbCl_3$ (Table 47). Only 78.9% of the sample is volatilised. ZnO, $Fe_2O_3$, AlOOH and anhydrous $Al_2O_3$ all appear either to volatilise as the corresponding halides or to assist the decomposition of the antimony/halogen system or to decompose individually; hence ca. 95% of the weight of the polymer is lost in these samples (Figure 46). Reaction with $Al_2O_3.3H_2O$ is accompanied by the endothermic release of water vapour and this appears to prevent further volatilisation of the metal halide. Antimony bromide and hydrogen bromide have been detected by mass spectrometry for all samples containing $Sb_2O_3$.

The decomposition of the ABS/halogen system, in conjunction with $SnO/Fe_2O_3$, SnO/AlOOH and $SnO_2/Fe_2O_3$, appears to be the sum of their separate decompositions. About 93% of the sample is volatilised between 220 and 600°C (Figure 47) and no metal halide species were identified using mass spectrometric technique (MS30/DS20 system).

TABLE 47

Thermal analysis of ABS/Adine/two metal oxide systems

| | $Sb_2O_3$ $SnO_2$ | $Sb_2O_3$ ZnO | $Sb_2O_3$ $Fe_2O_3$ | $Sb_2O_3$ $Al_2O_3$ | $Sb_2O_3$ AlOOH | $Sb_2O_3$ $Al_2O_3.3H_2O$ | $Sb_2O_3$ $(NH_4)_6Mo_7O_{24}$ | $Sb_2O_3$ Talc | SnO ZnO | SnO AlOOH | $SnO_2$ $Fe_2O_3$ |
|---|---|---|---|---|---|---|---|---|---|---|---|
| Total weight fraction volatilised(%): | 78.9 | 95.4 | 95.0 | 94.8 | 92.7 | 79.6 | 84.9 | 91.8 | 94.2 | 92.8 | 93.0 |
| Temperature range-melting ($^oC$) : | - | - | - | - | - | - | - | - | - | - | - |
| Initial weight-loss reaction-hydrogen halide : | | | | | | | | | | | |
| Weight-fraction volatilised(%) : | 25.9 | 29.6 | 16.1 | 29.0 | 43.7 | 27.7 | 17.9 | 37.5 | 54.0 | 23.8 | 11.3 |
| Temperature range ($^oC$) : | 266-355 | 260-356 | 260-325 | 256-350 | 250-365 | 249-365 | 255-346 | 275-358 | 260-441 | 220-346 | 220-325 |
| Temperature of max. rate ($^oC$) : | 310 | 327 | 306 | 305 | 320 | 324 | 305 | 320 | 340 | 325 | 311 |
| Main weight-loss reactions : | | | | | | | | | | | |
| Weight-fraction volatilised(%) : | 28.7 | 24.0 | 25.7 | 28.4 | 24.6 | 27.8 | 27.2 | 30.3 | 21.6 | 43.4 | 29.9 |
| Number of weight-loss stages : | 1 | 1 | 1 | 4 | 1 | 1 | 1 | 1 | 1 | 3 | 1 |
| (a) Temperature range ($^oC$) : | 355-442 | 356-439 | 325-405 | 350-400 | 365-450 | 365-445 | 345-430 | 385-449 | 441-542 | 346-445 | 325-402 |
| (b) Temperature range ($^oC$) : | - | - | - | - | - | - | - | - | - | - | - |
| (c) Temperature range ($^oC$) : | - | - | - | - | - | - | - | - | - | - | - |
| Second weight-loss reaction : | | | | | | | | | | | |
| Weight-fraction volatilised(%) : | 24.3 | 41.8 | 53.2 | 37.4 | 24.4 | 23.9 | 39.8 | 24.0 | 18.6 | 25.6 | 51.8 |
| (a) Temperature range ($^oC$) : | 442-570 | 439-510 | 405-460 | 480-547 | 450-565 | 445-573 | 430-474 | 449-560 | 542-630 | 445-580 | 402-440 |
| (b) Temperature range ($^oC$) : | - | 510-625 | 460-517 | - | - | - | 474-560 | - | - | - | 440-520 |

FIGURE 46

The weight change/rate of weight change traces for the ABS/Adine/mixed metal oxide systems

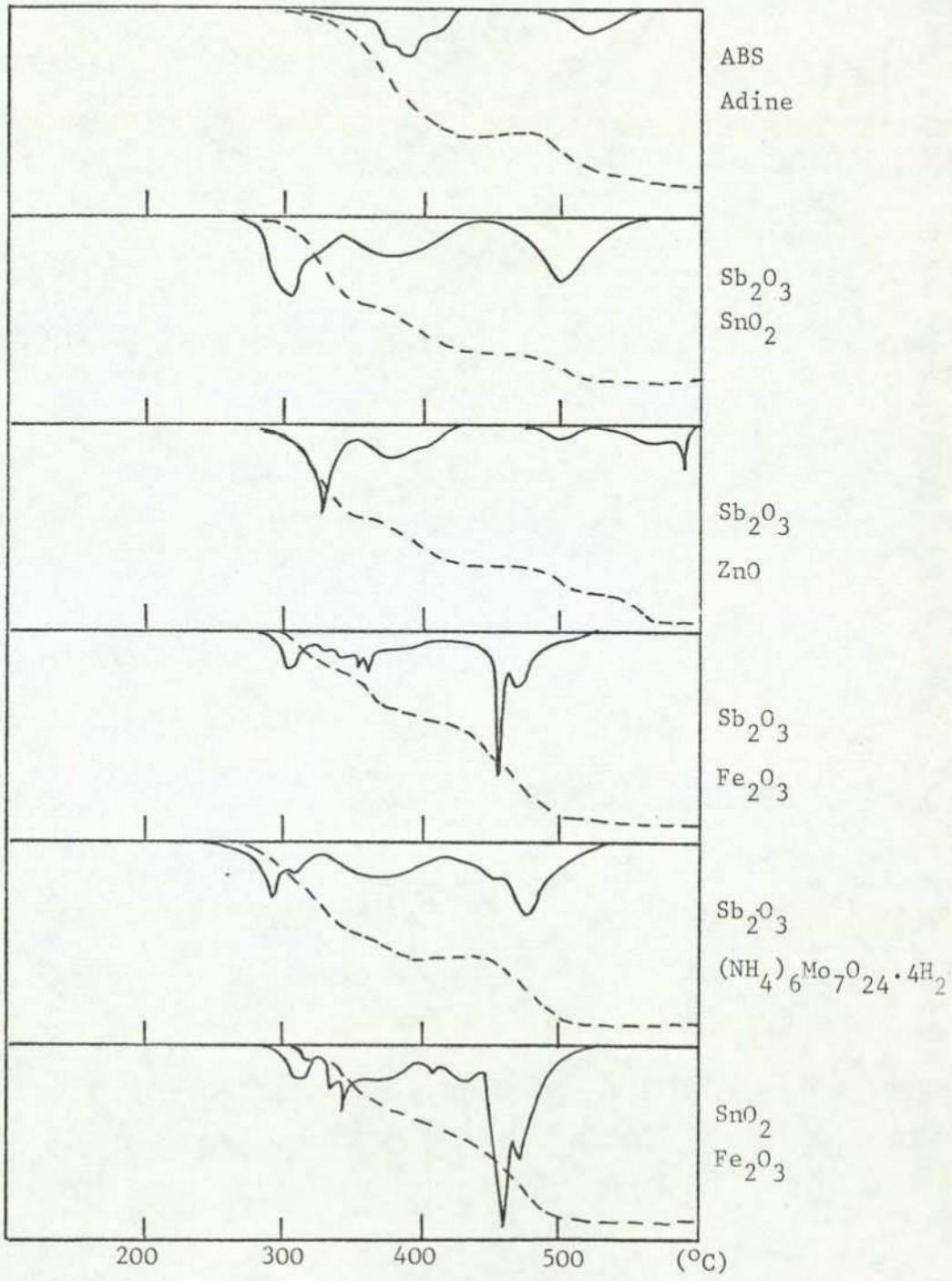
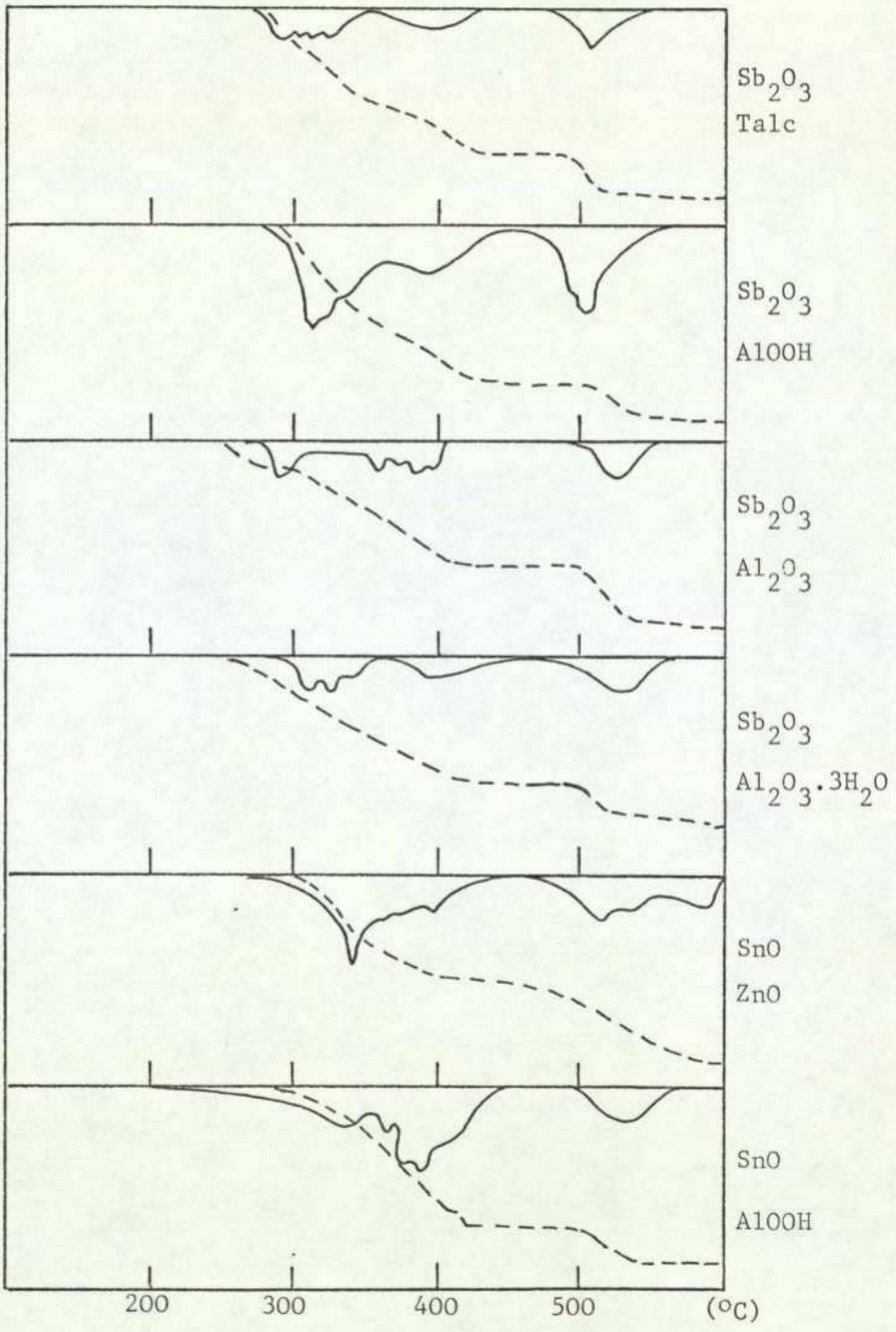


FIGURE 47

The weight change/rate of weight change traces for the ABS/Adine/mixed metal oxide systems



## 3.2 Flammability Measurements

### 3.2.1 The Experimental Designs

The flammabilities of polymer/metal oxide/halogen compound systems was measured using the oxygen-index method. The plotting of these results in the form of triangular diagrams enabled the variation in flammability to be represented pictorially, and the contribution of each component could then be readily deduced. The triangular models also facilitated the prediction of trends in the oxygen-index of any polymer/additive system within the defined limits and thus permitted optimisation of the ratio of flame-retardant compound to polymer, of halogen to metal oxide(s) and of one metal oxide to another.

The design for a three-component system involves the initial estimation of the composition of three boundary mixtures. This is done by consulting the thermal analysis results and choosing three mixtures such that the ternary system covered includes all the possible mixtures that might be of interest.

Now, a simplex lattice design is a set of selected points over the mixture space at which data (responses) are gathered to fit an assumed response equation. A response equation or regression may be linear, quadratic, cubic, special or reduced cubic, quartic, etc. and is intended to describe responses over the mixture space.

Additional responses are gathered at other mixture points which have not contributed to the fitting of the response equation. These responses are used to estimate a "lack-of-fit" error which enables the experimenter to accept or reject the fitted assumed-response equation.

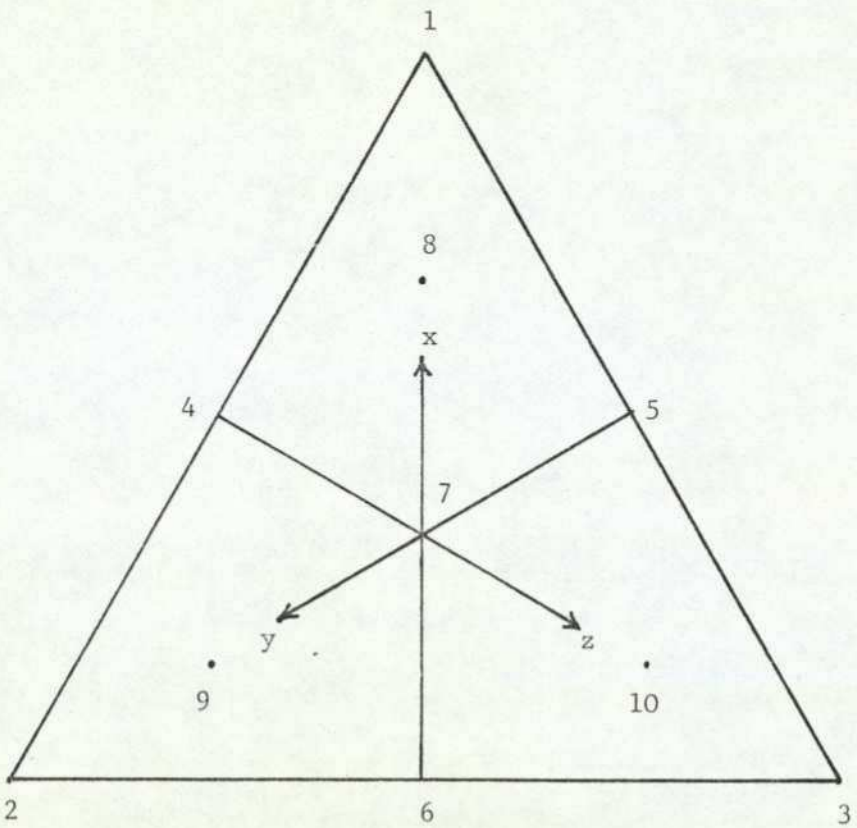
Consider a system with three components $x_i$, $y_i$, and $z_i$, the mixture space of which is the area within an equilateral triangle (Figure 48). The axes of the three components are shown by the arrows. The values of the three components at the three vertices of the simplex lattice design can be linear transformations of

$$x_1 = 1.0\,, \quad y_1 = 0.0\,, \quad z_1 = 0.0$$
$$x_2 = 0.0\,, \quad y_2 = 1.0\,, \quad z_2 = 0.0$$
$$x_3 = 0.0\,, \quad y_3 = 0.0\,, \quad z_3 = 1.0.$$

Once the three boundary compositions, have been determined, the compositions at points 4-10 can be computed using the matrix equation where each row of matrix A represents the coordinates of a mixture from 1 to 10 respectively; matrix B is the transformation matrix governing the lattice space and matrix C represents (in rows) the composition of the three boundary points 1, 2 and 3.

FIGURE 48

The ternary system



| A | | | | B | | | C | | |
|---|---|---|---|---|---|---|---|---|---|
| $a_{11}$ | $a_{12}$ | $a_{13}$ | = | 1 | 0 | 0 | $x_1$ | $y_1$ | $z_1$ |
| $a_{21}$ | $a_{22}$ | $a_{23}$ | | 0 | 1 | 0 | $x_2$ | $y_2$ | $z_2$ |
| $a_{31}$ | - - - - - | | | 0 | 0 | 1 | $x_3$ | $y_3$ | $z_3$ |
| - | - | - | | 1/2 | 1/2 | 0 | | | |
| - | - | - | | 1/2 | 0 | 1/2 | | | |
| - | - | - | | 0 | 1/2 | 1/2 | | | |
| - | - | - | | 1/3 | 1/3 | 1/3 | | | |
| - | - | - | | 2/3 | 1/6 | 1/6 | | | |
| - | - | - | | 1/6 | 2/3 | 1/6 | | | |
| $a_{101}$ | $a_{102}$ | $a_{103}$ | | 1/6 | 1/6 | 2/3 | | | |

The responses (oxygen index values) to the ten points (ten different mixtures with three variables) are then measured experimentally and the theoretical responses at the best points 7, 8, 9 and 10 are determined. The departure of these measured responses from their theoretically predicted values (residuals) are an indication of the adequacy of the fitted response equation.

The coefficients for a quadratic model can be calculated as follows:

$\beta_i = n_i (i = 1, 2, 3)$ where $n_i$ is the ith response

$\beta_{ij} = 4n_{ij} - 2n_i - 2n_j$ where i = 1, 2, 3 and j = 1, 2, 3.

note point 4 is designated by response $n_{12}$

point 5 is designated by response $n_{13}$

point 6 is designated by response $n_{23}$

point 7 is designated by response $n_{123}$

The theoretical oxygen index for a quadratic model is thus

$$OI = \beta_1 x_1 + \beta_2 x_2 + \beta_3 x_3 + \beta_{12} x_1 x_2 + \beta_{13} x_1 x_3 + \beta_{23} x_2 x_3$$

The suitability of the quadratic model is assessed from the residuals at the test points 7, 8, 9 and 10. A"lack-of-fit" error can be calculated and its departure from the estimated variance can be used as evidence of a good fit. If a more complete model is necessary, then a reduced-cubic can be augmented.

$$\beta_{123} = 27n_{123} - 12(n_{12}+n_{13}+n_{23}) + 3(n_1+n_2+n_3)$$

The reduced-cubic equation for the calculation of the predicted oxygen indices at points 8, 9 and 10 is then

$$OI = \beta_1 x_1 + \beta_2 x_2 + \beta_3 x_3 + \beta_{12} x_1 x_2 + \beta_{13} x_1 x_3 + B_{23} x_2 x_3 + \beta_{123} x_1 x_2 x_3$$

Once a model adequate for representing the system at the test points has been found a graphical contour analysis of the responses is computed.

The study of four-component systems, consisting of a mixture of two metal oxides and a halogen compound incorporated into the polymer was carried out using the above mentioned simplex design. Here percentage by weight of the polymer was fixed at 70 and 80% and various ratios of excess halogen compound to the two metal oxides were investigated. The halogen compound was kept in excess to ensure maximum volatilisation of the metal oxides. The percentage composition at the ten points

is shown in Table 48, and the various positions of these compositions can be seen in Figure 49. These systems can also be viewed in three dimensions and give a more accurate picture of the response surfaces in question.

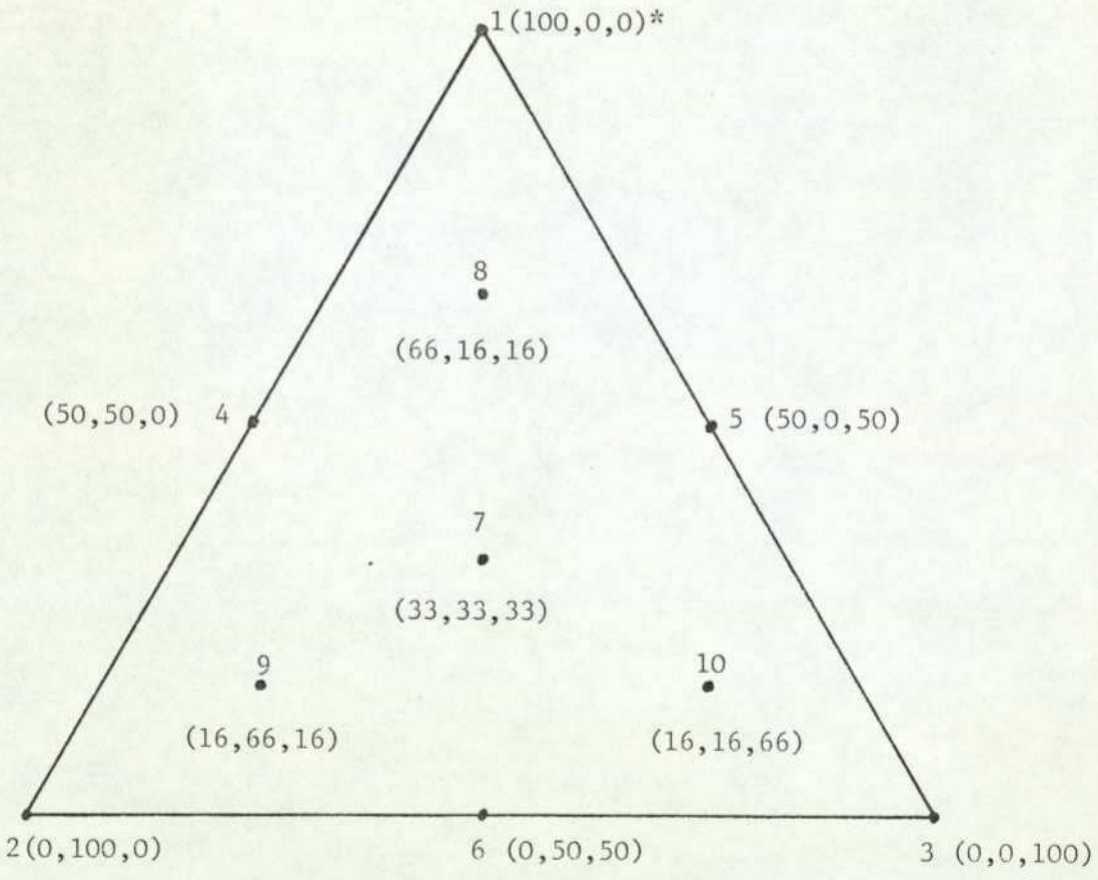
TABLE 48

The percentage composition at various points in the triangular diagrams.

| | 70% polymer | | | 80% polymer | | |
|---|---|---|---|---|---|---|
| | Halogen | M.O.I | M.O.II | Halogen | M.O.I | M.O.II |
| 1 | 30.0 | 0.0 | 0.0 | 20.0 | 0.0 | 0.0 |
| 2 | 15.0 | 15.0 | 0.0 | 10.0 | 10.0 | 0.0 |
| 3 | 15.0 | 0.0 | 15.0 | 10.0 | 0.0 | 10.0 |
| 4 | 22.5 | 7.5 | 0.0 | 15.0 | 5.0 | 0.0 |
| 5 | 22.5 | 0.0 | 7.5 | 15.0 | 0.0 | 5.0 |
| 6 | 15.0 | 7.5 | 7.5 | 10.0 | 5.0 | 5.0 |
| 7 | 20.0 | 5.0 | 5.0 | 13.3 | 3.3 | 3.3 |
| 8 | 25.0 | 2.5 | 2.5 | 16.6 | 1.6 | 1.6 |
| 9 | 17.5 | 10.0 | 2.5 | 11.6 | 6.6 | 1.6 |
| 10 | 17.5 | 2.5 | 10.0 | 11.6 | 1.6 | 6.6 |

FIGURE 49

Triangular Diagram: Component Ratios (percentages)




*(Halogen, Metal Oxide I, Metal Oxide II)

### 3.2.2 Polymers

#### 3.2.2.1 HDPE

Oxygen index values for a number of commercial samples of polyethylene have been quoted on numerous occasions in the literature. The results vary from 16.4 to 19.3[298–299], with an average value of 17.4, which is that obtained by Fenimore and Martin[142]. The oxygen-index of Eltex B 4002 high density polyethylene was found to be 18.5. The polymer sample burned with a steady clean flame which flickered before it died.

#### 3.2.2.2 ABS

The oxygen index of ABS was found to be 18.6. This result is consistent with that of DiPietro and Stepniczka[300] who quote an oxygen index for a sample of high-impact ABS (Uniroyal's Royalite 20)of 18.3. The candle was easy to ignite and burned with a sooty flame and some dripping.

### 3.2.3 Polymer/Halogen compound

The addition of a halogen compound to a polymer generally increases its oxygen index. Increases of between 3 and 6 have been observed in this work. When measurements were made of the oxygen index of HDPE containing various amounts of chlorinated wax, a gradual increase in oxygen index was noticed for samples containing between 10 and 35 phr halogen compound (Figure 50). An oxygen index value of ca 21.4 was then obtained for samples containing between 35 and 50phr halogen (Table 49). No further addition of S70 to the polymer was possible. The samples were easy to ignite, burned with a clean flame and there was some dripping.

A similar pattern was observed for samples of ABS and decabromobiphenyl (Figure 51). A sharp increase in oxygen index was observed from 19.2 for ABS containing 5 phr Adine to 24.2 for samples of ABS containing 35phr Adine. The oxygen index value then levels out at 24.4 for samples containing more than 35phr Adine (Table 50). Only samples containing a maximum of 50phr halogen compound were studied. The polymer candles burned with sooty flames and left a crusty carbonaceous char.

TABLE 49

The Oxygen Index of samples of HDPE polymer containing Electrofine S70

| S70 p.h.r. | Oxygen Index |
|---|---|
| 0 | 18.5 |
| 5 | 18.5 |
| 10 | 18.6 |
| 15 | 19.1 |
| 20 | 20.0 |
| 25 | 20.8 |
| 30 | 20.9 |
| 35 | 21.0 |
| 40 | 21.3 |
| 45 | 22.2 |
| 50 | 21.5 |

FIGURE 50

The Oxygen Index of samples of HDPE Polymer containing Electrofine S70 (chlorinated wax)

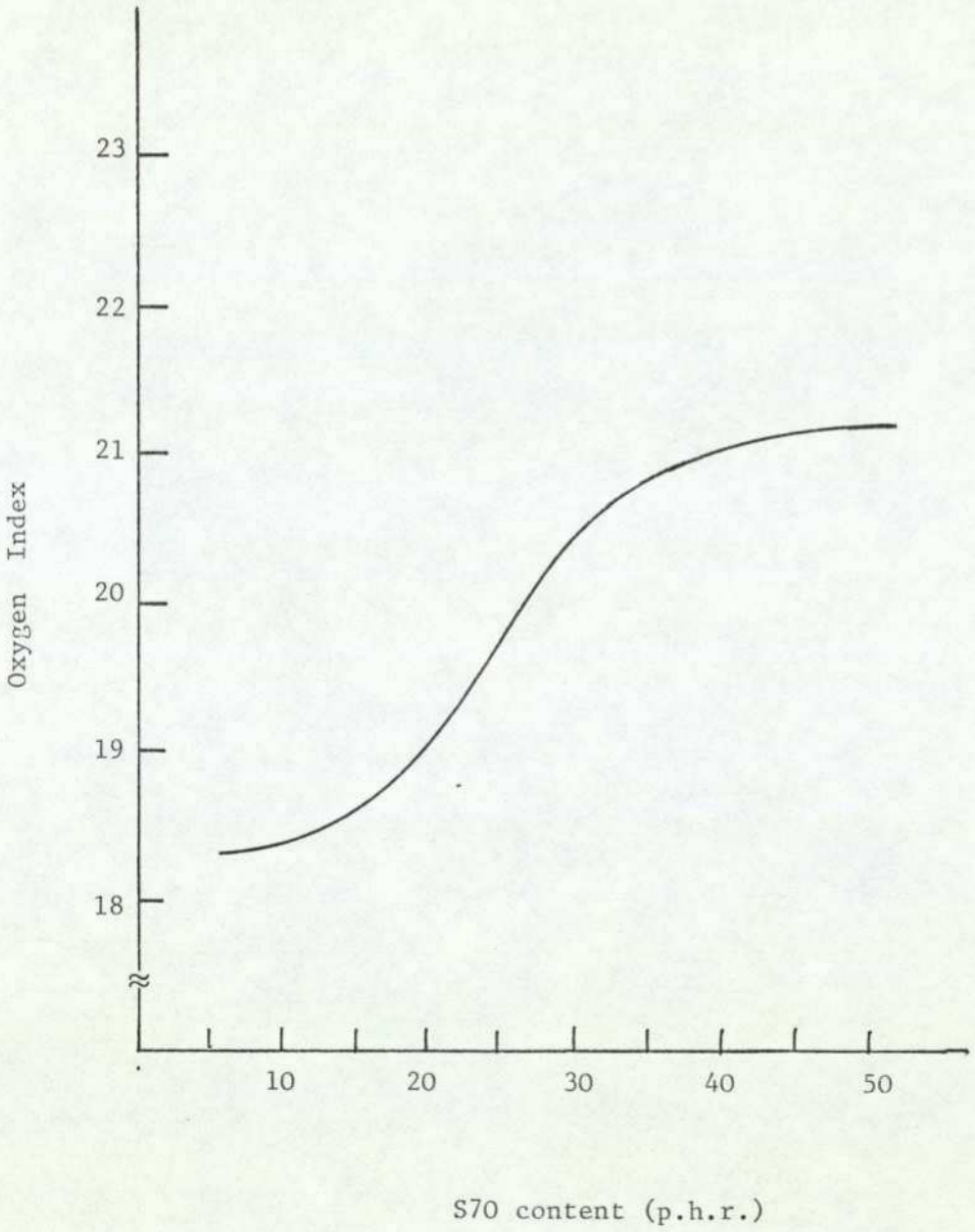


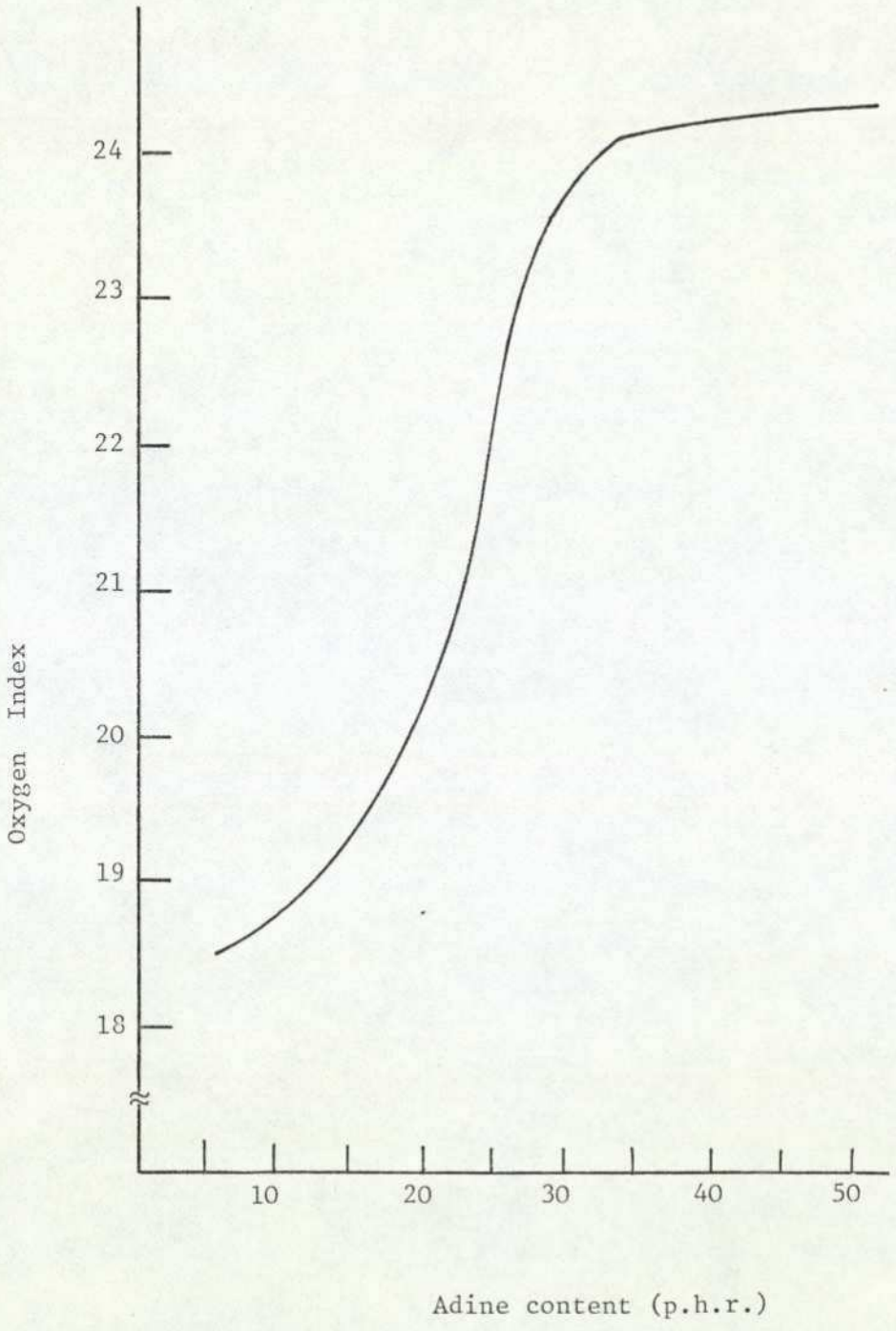
TABLE 50

The Oxygen Index of samples of ABS copolymer containing Adine 0102 (decabromobiphenyl).

| Adine p.h.r. | Oxygen Index |
|---|---|
| 0 | 18.50 |
| 5 | 19.2 |
| 10 | 19.8 |
| 15 | 20.9 |
| 20 | 23.1 |
| 25 | 23.8 |
| 30 | 24.2 |
| 35 | 24.2 |
| 40 | 24.3 |
| 45 | 24.4 |
| 50 | 24.4 |

FIGURE 51

The Oxygen Index of samples of ABS copolymer containing Adine 0102 (decabromobiphenyl)



### 3.2.4 Polymer/Halogen compound/single metal oxide

#### 3.2.4.1 General

In order to discuss any synergism or antagonism between various mixtures of metal oxides and halogen compounds, it is interesting to note that, when a metal oxide is mixed with a halogen compound and incorporated into a polymer, the oxygen index values obtained do not (in general) vary by more than ca.3(Table 51). The synergism between $Sb_2O_3$ and halogens is well known. The increased oxygen index for the $Fe_2O_3$/halogen compound systems has been attributed to the catalytic action of the iron oxide on the formation of char. This system may be classed as synergistic since $Fe_2O_3$, on its own[301], when incorporated in a polymer, does not affect the oxygen index although it does promote polymer degradation. Synergism between $Al_2O_3.3H_2O$ and halogens has also been suggested by some authors[301].

#### 3.2.4.2 Polymer/Halogen compound/$Sb_2O_3$

An initial study of the flammability of antimony (III) oxide, halogen compound and polymer was carried out by a linear loading design. When the weight of $Sb_2O_3$ is kept constant at 7.5phr, the oxygen index of the system increases with the concentration of the halogen compound, and thus with the total weight of additive in the polymer. When the weight of the halogen compound is kept constant at 7.5phr and the weight of $Sb_2O_3$ is varied from 7.5 to

TABLE 51

The Oxygen Index of samples of HDPE and ABS polymers containing metal oxides and halogen compounds.

| Polymer | H D P E | | | | A B S | | | |
|---|---|---|---|---|---|---|---|---|
| Percentage Polymer | 70 | | 80 | | 70 | | 80 | |
| M.O.:Halogen Ratio | 1:1 | 1:3 | 1:1 | 1:3 | 1:1 | 1:3 | 1:1 | 1:3 |
| Metal Oxide | | | | | | | | |
| $Sb_2O_3$ | 25.4 | 25.1 | 25.1 | 24.6 | 30.8 | 34.2 | 26.9 | 28.1 |
| SnO | 21.7 | 21.9 | 22.2 | 22.0 | 24.4 | 27.8 | 23.7 | 25.0 |
| $SnO_2$ | 22.6 | 21.4 | 21.3 | 21.5 | 24.8 | 27.8 | 23.2 | 24.2 |
| ZnO | 20.1 | 21.5 | 19.5 | 20.1 | 24.5 | 24.8 | 22.0 | 22.8 |
| $Fe_2O_3$ | 22.9 | 25.3 | 20.1 | 21.1 | 28.1 | 30.4 | 26.2 | 27.9 |
| $Al_2O_3$ | 19.8 | 20.4 | 19.9 | 20.2 | 27.8 | 27.6 | 24.0 | 24.9 |
| AlOOH | 19.8 | 21.2 | 19.1 | 20.1 | 24.1 | 24.8 | 22.6 | 22.9 |
| $Al_2O_3.3H_2O$ | 21.4 | 21.7 | 19.8 | 20.2 | 23.1 | 24.3 | 21.4 | 22.3 |
| $(NH_4)_6Mo_7O_{24}\cdot 4H_2O$ | 20.8 | 21.6 | 20.6 | 21.2 | 26.7 | 28.7 | 24.1 | 25.0 |
| Talc | - | - | - | - | 25.6 | 27.0 | - | - |

22.5 phr, the oxygen-index changes by less than 1% (Table 52). This suggests that even with 7.5 phr Adine present, the $Sb_2O_3$ is in molar excess. Thus the experiment was repeated with 15 phr halogen compound. The trace obtained thus consisted of two parts. The first was parallel to that obtained for 7.5 $Sb_2O_3$ up to 15 phr. It then levels out and becomes parallel to the original line obtained for 7.5 phr Adine (Figure 52).

Triangular diagrams were also extensively used to study the flammability and synergism in the antimony(III) oxide/halogen compound systems and the simplex designs covered a lattice defined by the following parameters:

a) polymer concentrations varying from 100 to 60%,
b) halogen compound concentrations varying between 0 and 40%, and
c) antimony(III) oxide varying also between 0 and 40%.

The design was subdivided into three smaller sets. It was hoped that the contour maps of the individual designs would indicate a trend similar to that of the full design and match those of adjacent designs.

In the design with coordinates (100,0,0), (80,20,0) and (80,0,20) - where the coordinates are in terms of (ABS, ADINE, $Sb_2O_3$) - it can be seen that there is an optimum ratio below 80% ABS for an oxygen index of around 27.0. Both the quadratic and reduced cubic models predict similar trends and confirm that the maximum

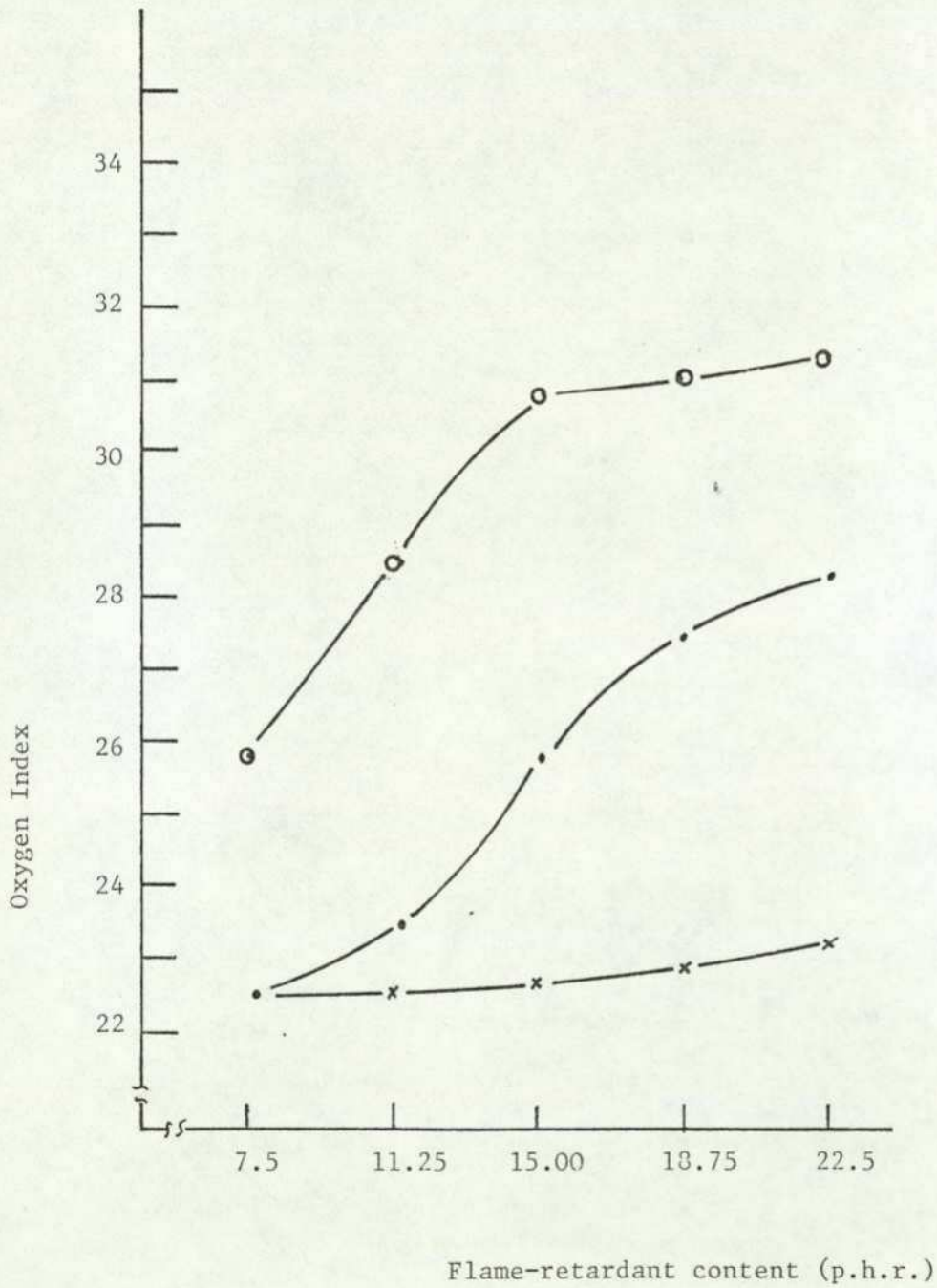
TABLE 52

The Oxygen Index of samples of ABS copolymer containing ADINE 0102 and antimony oxide

| ADINE p.h.r. | $Sb_2O_3$ p.h.r. | Oxygen Index |
|---|---|---|
| 7.50 | 7.50 | 22.5 |
| 11.25 | 7.50 | 23.4 |
| 15.00 | 7.50 | 25.7 |
| 18.75 | 7.50 | 27.3 |
| 22.50 | 7.50 | 28.2 |
| 7.50 | 11.25 | 22.5 |
| 7.50 | 15.00 | 22.6 |
| 7.50 | 18.75 | 22.9 |
| 7.50 | 22.50 | 23.2 |
| 15.00 | 7.50 | 25.7 |
| 15.00 | 11.25 | 28.4 |
| 15.00 | 15.00 | 30.5 |
| 15.00 | 18.75 | 30.8 |
| 15.00 | 22.50 | 30.9 |

FIGURE 52

The Oxygen Index of ABS copolymer containing $Sb_2O_3$ and Adine 0102




× at 7.5 p.h.r. Adine 0102

• at 7.5 p.h.r. $Sb_2O_3$

o at 15 p.h.r. Adine 0102

oxygen-index would be found in the region around (80,15,15). The statistical analysis shows that all the results belong to the same set; and that there is little significant difference between the observed and calculated oxygen-indices for the quadratic and cubic models. In the design with coordinates (60,20,20), (80,20,0) and (80,0,20) the trend is continued by the quadratic model and an optimum oxygen-index of 33.0 can be achieved by a mixture of composition (67,17,16). There is a definite positive correlation and the calculated oxygen-index values for this model are very similar to the measured values. The average deviation for the design with coordinates (60,20,20), (80,20,0) and (60,40,0) is $\pm$1.7 over the measured oxygen index values. However, the cubic model continues the trends indicated by the two previous designs and finally maximises the oxygen index in the region (75,10,15). With a composite of these three designs, together with the area where ABS varies from 80% to 60% along the halogen axis, the trends are found to be consistent with those for the individual composites (Figures 53 and 54). Since this is a generalised illustration, there is a decrease in statistical significance and there exists a larger difference between the observed and calculated oxygen-index results. An optimisation of oxygen-index can be found around the area indicated by the plateau in the region (75,10,15). (Table 53.)

There is less statistical significance for the three

TABLE 53

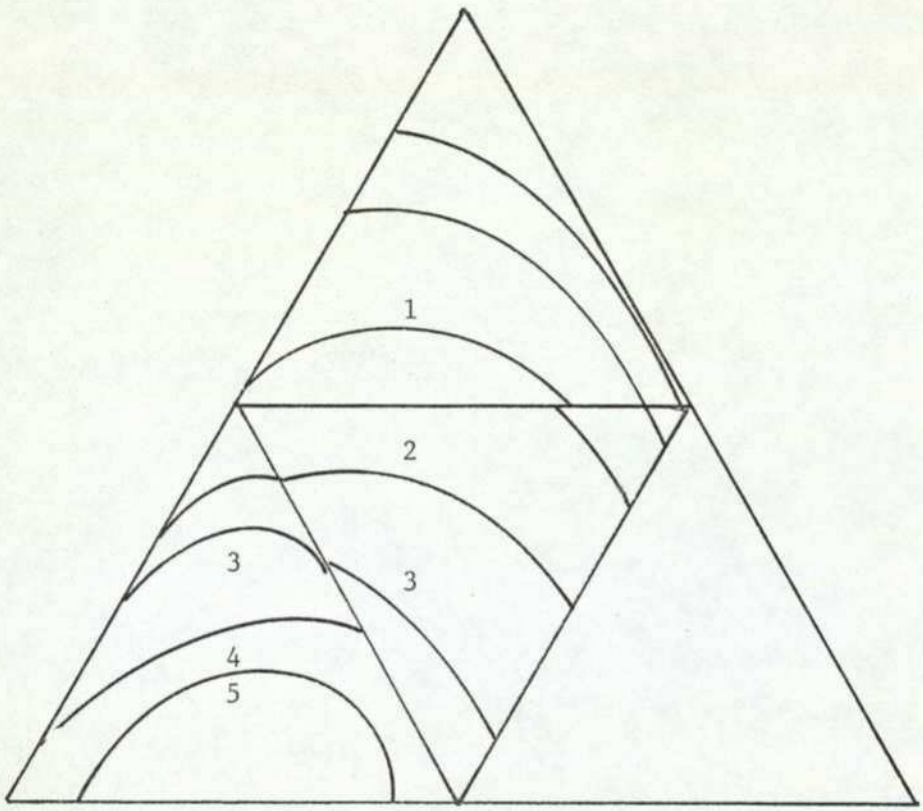
The Oxygen index of samples of ABS containing Adine and $Sb_2O_3$

| Points | ABS % | ADINE % | $Sb_2O_3$ % | Oxygen Index | Points | ABS % | ADINE % | $Sb_2O_3$ % | Oxygen Index |
|---|---|---|---|---|---|---|---|---|---|
| 1 | 100.0 | 0.0 | 0.0 | 18.6 | 1 | 60.0 | 20.0 | 20.0 | 33.1 |
| 2 | 80.0 | 20.0 | 0.0 | 23.6 | 2 | 80.0 | 20.0 | 0.0 | 23.6 |
| 3 | 80.0 | 0.0 | 20.0 | 20.0 | 3 | 80.0 | 0.0 | 20.0 | 20.0 |
| 4 | 90.0 | 10.0 | 0.0 | 21.1 | 4 | 70.0 | 20.0 | 10.0 | 32.2 |
| 5 | 90.0 | 0.0 | 10.0 | 19.6 | 5 | 70.0 | 10.0 | 20.0 | 29.0 |
| 6 | 80.0 | 10.0 | 10.0 | 26.9 | 6 | 80.0 | 10.0 | 10.0 | 26.9 |
| 7 | 86.7 | 6.7 | 6.7 | 22.6 | 7 | 73.3 | 13.3 | 13.3 | 30.4 |
| 8 | 93.3 | 3.3 | 3.3 | 20.3 | 8 | 66.7 | 16.7 | 16.7 | 31.8 |
| 9 | 83.3 | 13.3 | 3.3 | 26.3 | 9 | 76.7 | 16.7 | 6.7 | 29.2 |
| 10 | 83.3 | 3.3 | 13.3 | 21.4 | 10 | 76.7 | 6.7 | 16.7 | 24.6 |

| Points | ABS % | ADINE % | $Sb_2O_3$ % | Oxygen Index | Points | ABS % | ADINE % | $Sb_2O_3$ % | Oxygen Index |
|---|---|---|---|---|---|---|---|---|---|
| 1 | 60.0 | 20.0 | 20.0 | 33.1 | 1 | 100.0 | 0.0 | 0.0 | 18.6 |
| 2 | 80.0 | 20.0 | 0.0 | 23.6 | 2 | 60.0 | 40.0 | 0.0 | 31.4 |
| 3 | 60.0 | 40.0 | 0.0 | 31.4 | 3 | 60.0 | 0.0 | 40.0 | 21.4 |
| 4 | 70.0 | 20.0 | 10.0 | 32.2 | 4 | 80.0 | 20.0 | 0.0 | 23.6 |
| 5 | 60.0 | 30.0 | 10.0 | 34.6 | 5 | 80.0 | 0.0 | 20.0 | 20.0 |
| 6 | 70.0 | 30.0 | 0.0 | 24.4 | 6 | 60.0 | 20.0 | 20.0 | 33.1 |
| 7 | 66.7 | 26.7 | 6.7 | 35.9 | 7 | 73.3 | 13.3 | 13.3 | 30.4 |
| 8 | 63.3 | 23.3 | 13.3 | 31.6 | 8 | 86.7 | 6.7 | 6.7 | 22.6 |
| 9 | 73.3 | 23.3 | 3.3 | 32.0 | 9 | 66.7 | 26.7 | 6.7 | 35.9 |
| 10 | 63.3 | 33.3 | 3.3 | 38.3 | 10 | 66.7 | 6.7 | 26.7 | 26.4 |

FIGURE 53

Triangular composite of three designs in ABS




Key :

1: 26.1

2: 28.0

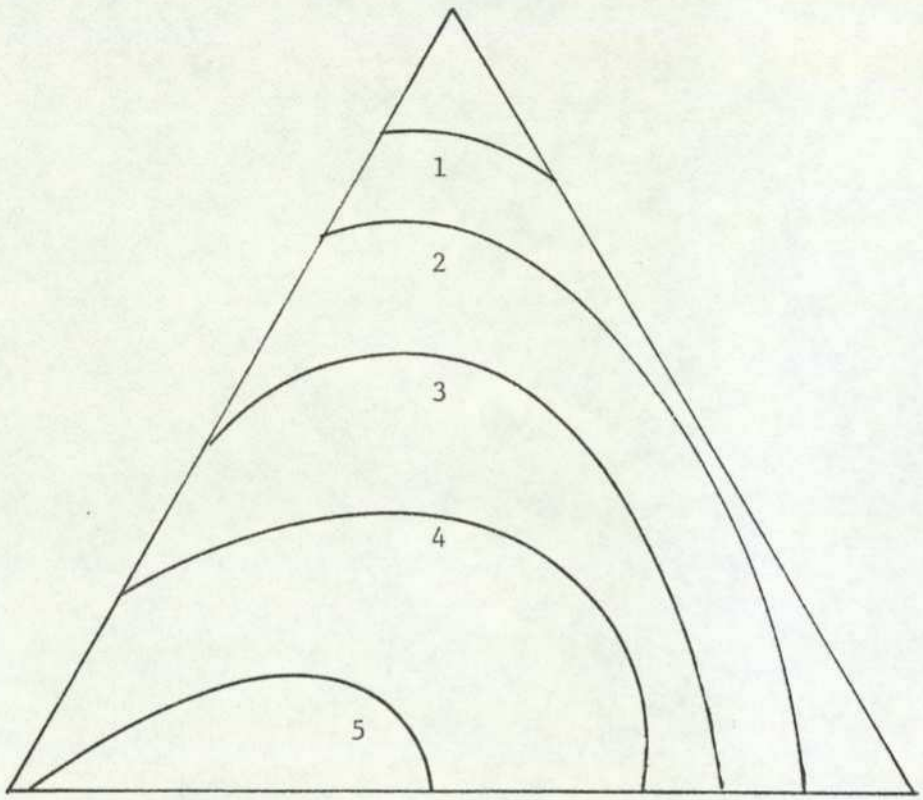
3: 29.8

4: 31.7

5: 33.6

FIGURE 54

Composite of the complete design in ABS




Key :

| | |
|---|---|
| 1 | 20.4 |
| 2 | 22.3 |
| 3 | 26.1 |
| 4 | 29.8 |
| 5 | 33.5 |

subsets in the polyethylene composites. In the design with coordinates (100,0,0), (80,20,0) and (80,0,20) there is only a small range of oxygen-index values between 18.1 and 25.5 and hence, the deviation of $\pm$1.0 in the cubic model is significant. The trend indicates an increase in oxygen-index towards the region around (85,8,7). The quadratic and cubic models for the design contained within the compositions (60,20,20),(80,20,0) and (80,0,20) are pictorially similar and indicate the absence of a plateau of maximum oxygen index (Figures 55 and 56). Similarly, the design with coordinates (60,20,20), (80,20,0) and (60,40,0) does not show any maximisation of oxygen index but indicates an area around (60,30,10) as tending towards higher oxygen index values. The generalised design agrees with the predicted trends and indicates a plateau where the maximum oxygen index is ca. 26.0. (Table 54).

Two other random designs were investigated, one for ABS and the other for polyethylene. The constraints of these designs lay within the original scope of investigation and tended to substantiate further the results obtained (Tables 55 and 56).

TABLE 54

The Oxygen index of samples of HDPE containing S70 and $Sb_2O_3$

| Points | HDPE % | S70 % | $Sb_2O_3$ % | Oxygen Index | Points | HDPE % | S70 % | $Sb_2O_3$ % | Oxygen Index |
|---|---|---|---|---|---|---|---|---|---|
| 1 | 100.0 | 0.0 | 0.0 | 18.5 | 1 | 60.0 | 20.0 | 20.0 | 26.2 |
| 2 | 80.0 | 20.0 | 0.0 | 20.8 | 2 | 80.0 | 20.0 | 0.0 | 20.8 |
| 3 | 80.0 | 0.0 | 20.0 | 18.1 | 3 | 80.0 | 0.0 | 20.0 | 18.1 |
| 4 | 90.0 | 10.0 | 0.0 | 19.7 | 4 | 70.0 | 20.0 | 10.0 | 25.1 |
| 5 | 90.0 | 0.0 | 10.0 | 18.5 | 5 | 70.0 | 10.0 | 20.0 | 22.6 |
| 6 | 80.0 | 10.0 | 10.0 | 25.5 | 6 | 80.0 | 10.0 | 10.0 | 25.3 |
| 7 | 86.7 | 6.7 | 6.7 | 24.3 | 7 | 73.3 | 13.3 | 13.3 | 25.7 |
| 8 | 93.3 | 3.3 | 3.3 | 24.2 | 8 | 66.7 | 16.7 | 16.7 | 24.7 |
| 9 | 83.3 | 13.3 | 3.3 | 24.6 | 9 | 76.7 | 16.7 | 6.7 | 20.8 |
| 10 | 83.3 | 3.3 | 13.3 | 19.2 | 10 | 76.7 | 6.7 | 16.7 | 24.5 |

| Points | HDPE % | S70 % | $Sb_2O_3$ % | Oxygen Index | Points | HDPE % | S70 % | $Sb_2O_3$ % | Oxygen Index |
|---|---|---|---|---|---|---|---|---|---|
| 1 | 60.0 | 20.0 | 20.0 | 26.2 | 1 | 100.0 | 0.0 | 0.0 | 18.5 |
| 2 | 80.0 | 20.0 | 0.0 | 20.8 | 2 | 60.0 | 40.0 | 0.0 | 23.2 |
| 3 | 60.0 | 40.0 | 0.0 | 23.5 | 3 | 60.0 | 0.0 | 40.0 | 21.5 |
| 4 | 70.0 | 20.0 | 10.0 | 25.1 | 4 | 80.0 | 20.0 | 0.0 | 20.8 |
| 5 | 60.0 | 30.0 | 10.0 | 26.6 | 5 | 80.0 | 0.0 | 20.0 | 18.1 |
| 6 | 70.0 | 30.0 | 0.0 | 22.2 | 6 | 60.0 | 20.0 | 20.0 | 26.1 |
| 7 | 66.7 | 26.7 | 6.7 | 25.5 | 7 | 73.3 | 13.3 | 13.3 | 25.7 |
| 8 | 63.3 | 23.3 | 13.3 | 24.8 | 8 | 86.7 | 6.7 | 6.7 | 24.3 |
| 9 | 73.3 | 23.3 | 3.3 | 25.6 | 9 | 66.7 | 26.7 | 6.7 | 25.5 |
| 10 | 63.3 | 33.3 | 3.3 | 25.4 | 10 | 66.7 | 6.7 | 26.7 | 21.7 |

TABLE 55

The Oxygen Index of samples of ABS copolymers containing Adine 0102 and $Sb_2O_3$.

| Points | ABS % | Adine % | $Sb_2O_3$ % | Oxygen Index |
|---|---|---|---|---|
| 1 | 92.0 | 6.0 | 2.0 | 21.9 |
| 2 | 76.0 | 20.6 | 3.4 | 30.2 |
| 3 | 76.0 | 12.0 | 12.0 | 31.2 |
| 4 | 84.0 | 13.3 | 2.7 | 26.4 |
| 5 | 84.0 | 9.0 | 7.0 | 24.8 |
| 6 | 76.0 | 16.3 | 7.7 | 31.6 |
| 7 | 81.3 | 12.9 | 5.8 | 26.7 |
| 8 | 86.7 | 9.4 | 3.9 | 24.3 |
| 9 | 78.7 | 16.7 | 4.6 | 28.4 |
| 10 | 78.7 | 12.4 | 8.9 | 29.2 |

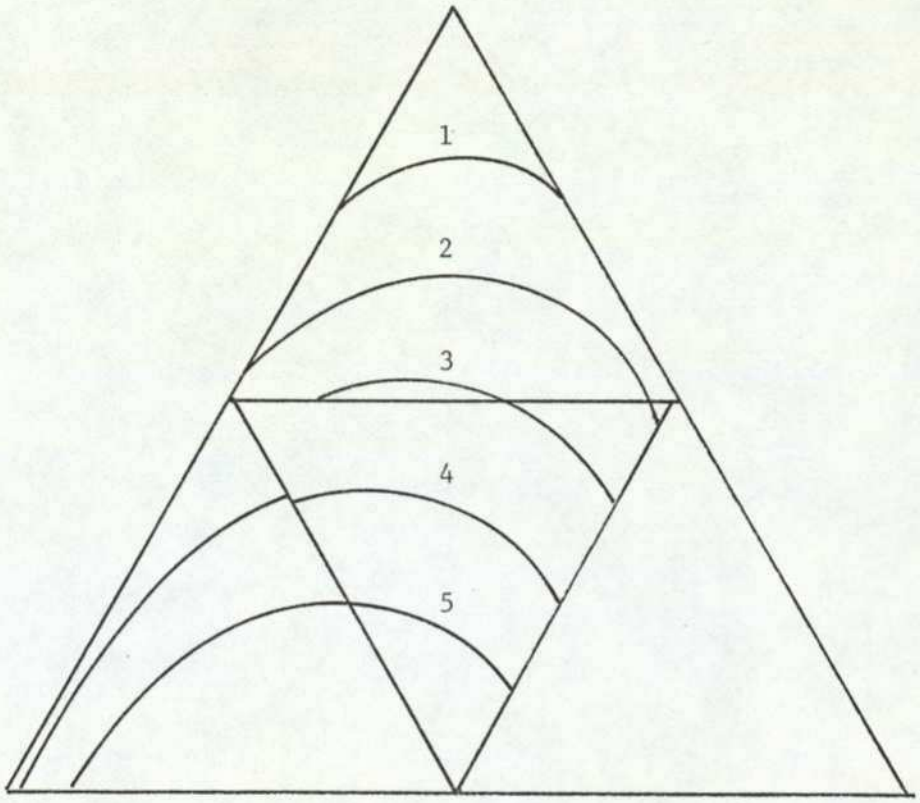
TABLE 56

The Oxygen Index of samples of HDPE containing Electrofine S70 and $Sb_2O_3$.

| Points | HDPE % | S70 % | $Sb_2O_3$ % | Oxygen Index |
|---|---|---|---|---|
| 1 | 85.0 | 11.3 | 3.8 | 24.2 |
| 2 | 72.0 | 24.0 | 4.0 | 25.3 |
| 3 | 72.0 | 16.8 | 11.2 | 25.8 |
| 4 | 78.5 | 17.6 | 3.9 | 24.5 |
| 5 | 78.5 | 14.0 | 7.5 | 24.8 |
| 6 | 72.0 | 20.4 | 7.6 | 25.3 |
| 7 | 76.3 | 17.4 | 6.3 | 24.5 |
| 8 | 80.7 | 14.3 | 4.0 | 24.3 |
| 9 | 74.2 | 20.7 | 5.2 | 25.2 |
| 10 | 74.2 | 17.1 | 8.8 | 25.1 |

FIGURE 55

Triangular composite of three designs in HDPE

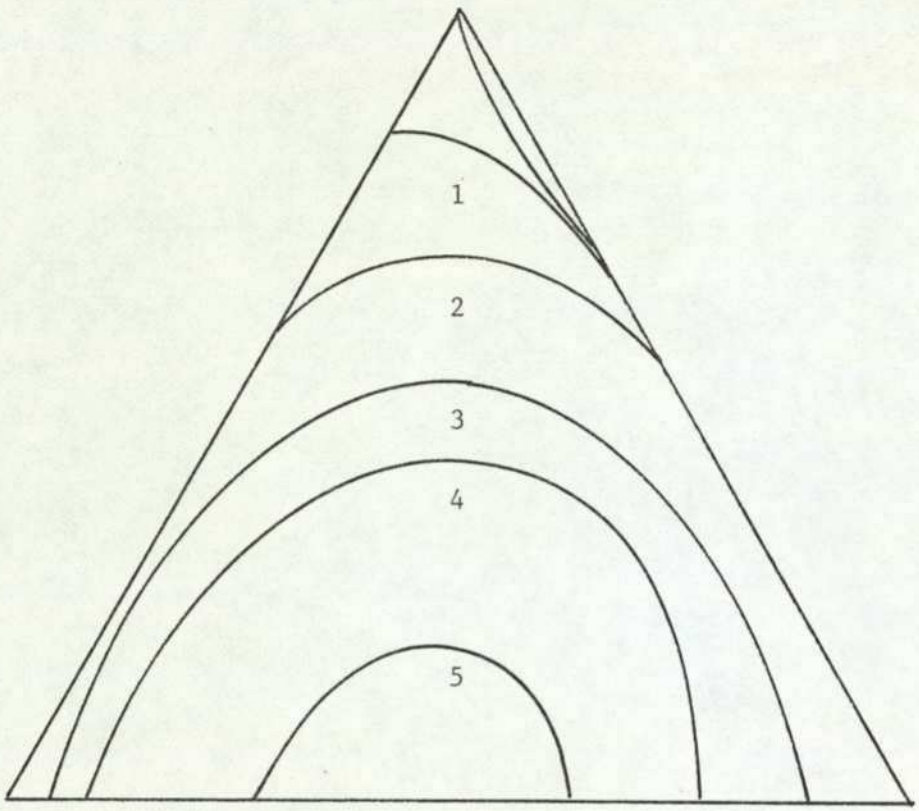



Key :

| | |
|---|---|
| 1 | 20.5 |
| 2 | 21.6 |
| 3 | 22.8 |
| 4 | 24.0 |
| 5 | 25.1 |

FIGURE 56

Composite of the complete design in HDPE




Key :

| | |
|---|---|
| 1 | 20.5 |
| 2 | 21.6 |
| 3 | 22.8 |
| 4 | 24.0 |
| 5 | 25.1 |

3.2.4.3 Polymer/Halogen compound/Oxides of Alumina

a) $Al_2O_3$

When 10 phr of $Al_2O_3$ were incorporated into HDPE together with increasing amounts of chlorinated wax (varying from 5 to 50 phr) there was a steady, but small, increase in the oxygen index (Tables 57 and 58). Similar experiments were carried out using ABS copolymer. In this case, a sudden, almost exponential rise was observed for the oxygen index (Figures 57 and 58). A maximum value of 36.4 was recorded for the sample containing 10 phr $Al_2O_3$ and 50 phr Adine. When the amount of the halogen compound was kept constant and the metal oxide content was increased, there was no change in the oxygen index.

b) AlOOH

An increase in the amount of halogen incorporated with a fixed amount of AlOOH does not show the sharp increase noticed for samples containing $Al_2O_3$. In HDPE, an increase of ca. 3 in the oxygen index is noticed when the Electrofine S70 content is increased from 5 to 50 phr (Tables 57 and 58).

In ABS, this increase in oxygen index is ca. 7.5 and the response is almost linear. ( Figures 57 and 58). An increase in the amount of metal oxide incorporated once again does not alter the oxygen index.

FIGURE 57

The Oxygen index of samples of HDPE containing the oxides of alumina and Electrofine S70

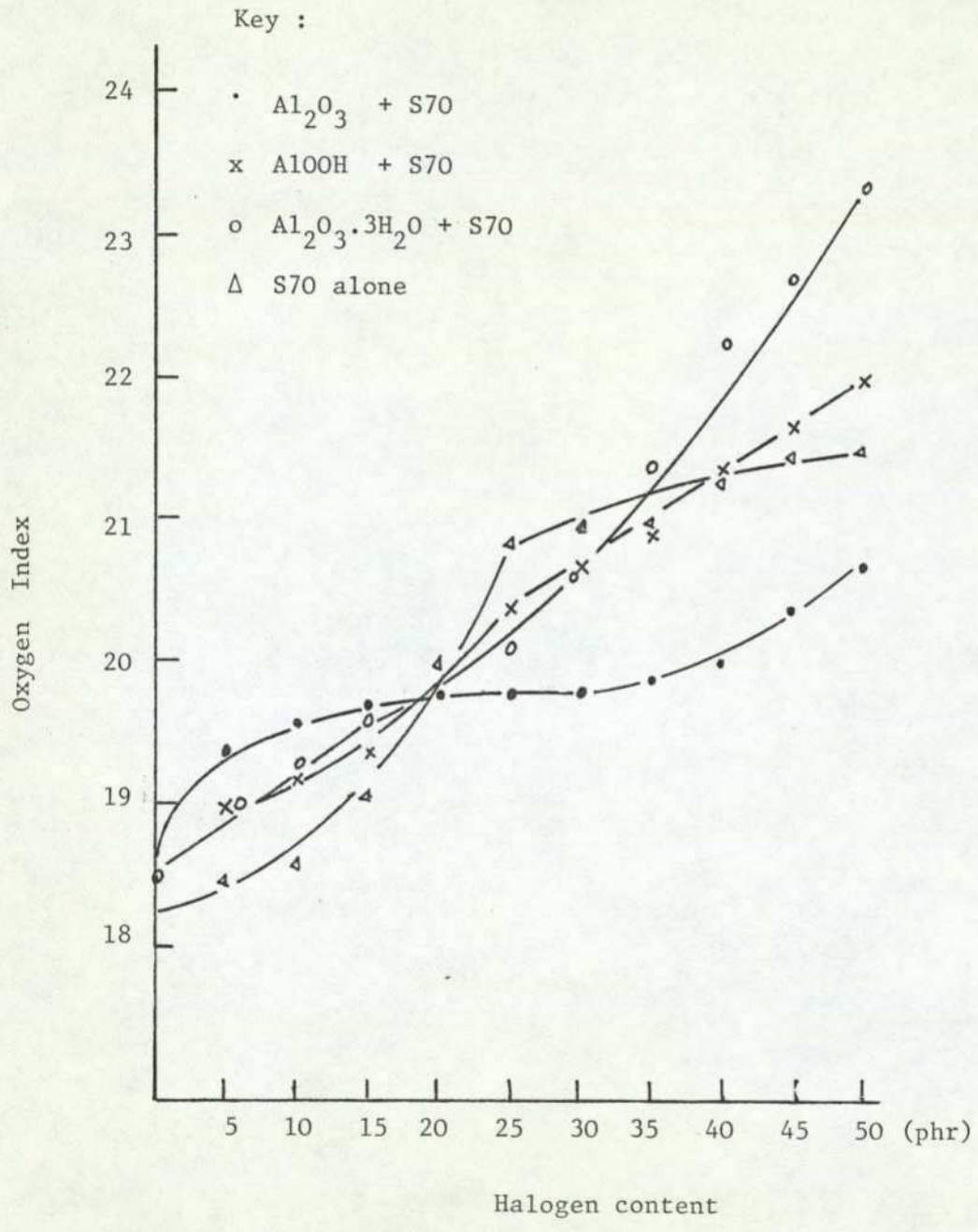


FIGURE 58

The Oxygen Index of samples of ABS containing the oxides of alumina and Adine 0102

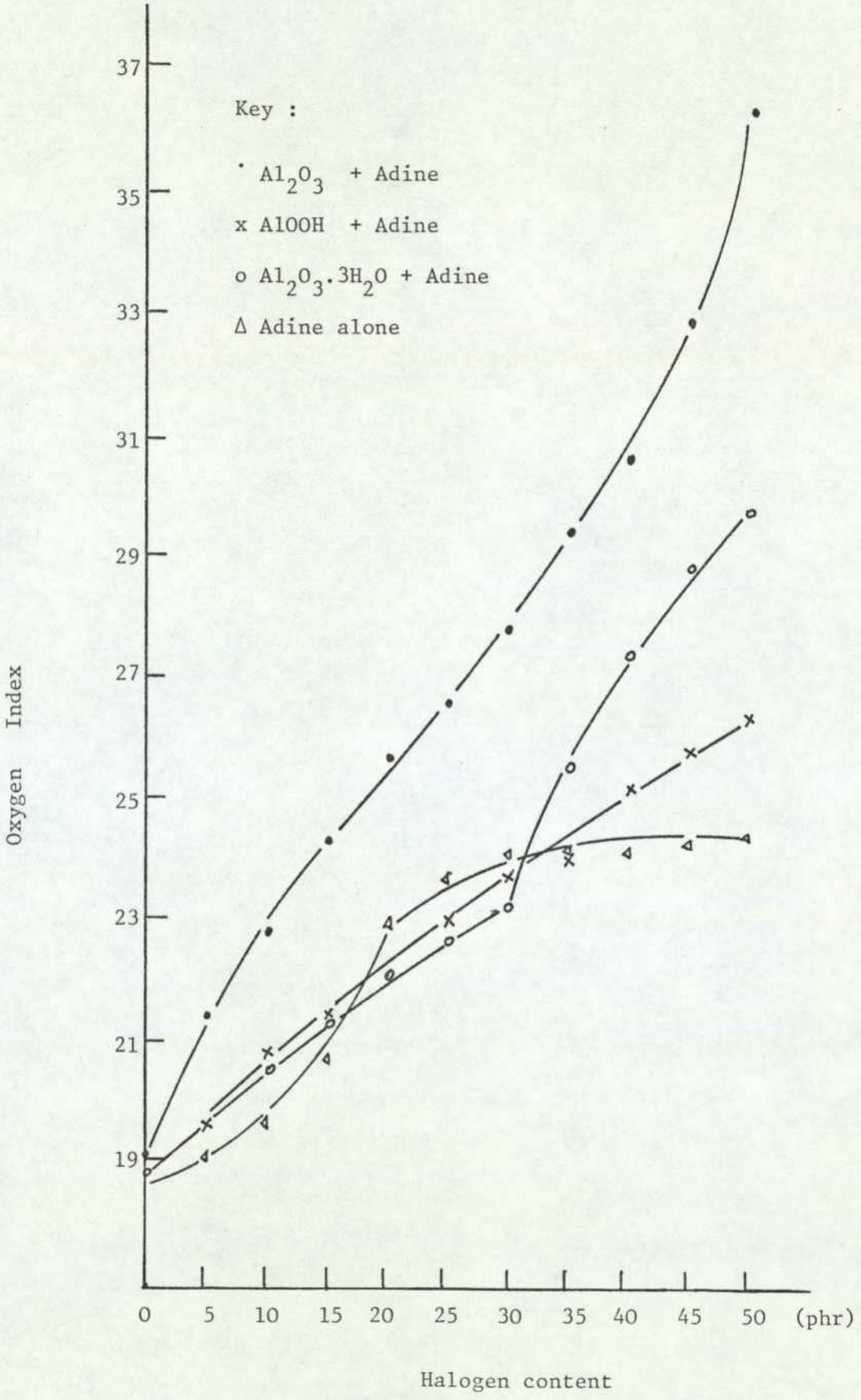


TABLE 57

The Oxygen Index of samples of HDPE polymer containing $Al_2O_3$, AlOOH, $Al_2O_3.3H_2O$ and S70.

| Metal Oxide | Halogen | Oxygen Index | | |
|---|---|---|---|---|
| p.h.r. | p.h.r. | $Al_2O_3$ | AlOOH | $Al_2O_3.3H_2O$ |
| 10 | 0 | 18.5 | 18.6 | 18.6 |
| 10 | 5 | 19.4 | 19.0 | 19.0 |
| 10 | 10 | 19.6 | 19.2 | 19.3 |
| 10 | 15 | 19.7 | 19.4 | 19.6 |
| 10 | 20 | 19.8 | 19.8 | 19.8 |
| 10 | 25 | 19.8 | 20.4 | 20.1 |
| 10 | 30 | 19.8 | 20.7 | 20.9 |
| 10 | 35 | 19.9 | 20.9 | 21.4 |
| 10 | 40 | 20.0 | 21.4 | 22.3 |
| 10 | 45 | 20.4 | 21.7 | 22.7 |
| 10 | 50 | 20.7 | 22.0 | 23.4 |
| 10 | 10 | 19.6 | 19.2 | 19.3 |
| 15 | 10 | 19.4 | 19.2 | 19.4 |
| 20 | 10 | 19.4 | 19.2 | 19.4 |

TABLE 58

The Oxygen Index of samples of ABS copolymer containing $Al_2O_3$, AlOOH, $Al_2O_3.3H_2O$ and Adine.

| Metal Oxide | Halogen | Oxygen Index | | |
|---|---|---|---|---|
| p.h.r. | p.h.r. | $Al_2O_3$ | AlOOH | $Al_2O_3.3H_2O$ |
| 10 | 0 | 19.2 | 18.9 | 18.8 |
| 10 | 5 | 21.5 | 19.7 | 19.7 |
| 10 | 10 | 22.9 | 20.9 | 20.6 |
| 10 | 15 | 24.4 | 21.5 | 21.4 |
| 10 | 20 | 25.8 | 22.2 | 22.2 |
| 10 | 25 | 26.6 | 23.1 | 22.8 |
| 10 | 30 | 27.9 | 23.8 | 23.3 |
| 10 | 35 | 29.5 | 24.1 | 25.6 |
| 10 | 40 | 30.7 | 25.3 | 27.5 |
| 10 | 45 | 33.0 | 25.9 | 29.0 |
| 10 | 50 | 36.4 | 26.4 | 29.9 |
| - | - | - | - | - |
| 10 | 10 | 22.9 | 20.9 | 20.6 |
| 15 | 10 | 22.9 | 20.9 | 20.6 |
| 20 | 10 | 22.9 | 20.9 | 20.6 |

c) $\underline{Al_2O_3 \cdot 3H_2O}$

When 10 phr of $Al_2O_3$ were incorporated into HDPE together with increasing amounts of chlorinated wax, a steady three-stage increase in oxygen index is observed (Figures 57 and 58). In ABS, there is a steady increase of 4.5 up to 30 phr Adine, followed by a sharp increase of 6.6 between 30 and 50 phr Adine. The maximum oxygen index is 29.9. Once again the oxygen index appears to be independent of the amount of metal oxide incorporated (Tables 57 and 58).

3.2.5 Polymer/Halogen compound/Two metal oxides

3.2.5.1 $Sb_2O_3/SnO_2$/halogen compound

Figure 59 shows the variation of oxygen index with the selective amounts of the above 3 compounds for systems containing 70% HDPE. The oxygen index exhibits a maximum between points 2 and 6 which lie along the axis joining the coordinates representing only polymer and metal oxide. The quadratic curve is more statistically significant although the residuals i.e. the difference between the computed and observed oxygen index valves are similar for both the quadratic and reduced cubic models. A similar trend is found for systems containing 80% HDPE but the oxygen index values are somewhat lower (Tables 59 and 60). Extensive reaction of tin(IV) oxide with S70 during milling (which indeed makes incorporation into the polymer almost impossible) suggests that this metal oxide plays little or no part in the flame-retardant action. However, despite doubts about the homogeneity of the samples caused by incorporation difficulties, the measured response appears to be statistically significant. The samples were difficult to ignite as short (10s), ignition times did not allow the flame to stabilise itself. Re-ignition gave inconsistent results so that abnormally long ignition times (45s.) were used. Near the oxygen index, the sample dripped

TABLE 59

The Oxygen index of samples containing HDPE and a 30% mixture of metal oxides and S70

| Points* | $Sb_2O_3$ a | $Sb_2O_3$ b | $Sb_2O_3$ $SnO_2$ | $Sb_2O_3$ ZnO | $Sb_2O_3$ $Fe_2O_3$ | $Sb_2O_3$ $Al_2O_3$ | $Sb_2O_3$ AlOOH | $Sb_2O_3$ ATH [c] | $Sb_2O_3$ AM[d] | SnO ZnO | SnO AlOOH | $SnO_2$ $Fe_2O_3$ |
|---|---|---|---|---|---|---|---|---|---|---|---|---|
| 1 | 22.2 | 22.2 | 22.2 | 22.2 | 22.2 | 22.2 | 22.2 | 22.2 | 22.2 | 22.2 | 22.2 | 22.2 |
| 2 | 24.5 | 25.8 | 25.4 | 25.4 | 25.4 | 25.4 | 25.4 | 25.4 | 25.4 | 21.7 | 21.7 | 22.6 |
| 3 | 24.5 | 25.8 | 22.6 | 20.1 | 22.9 | 29.8 | 19.8 | 21.4 | 20.8 | 20.1 | 19.8 | 22.8 |
| 4 | 25.2 | 26.3 | 25.1 | 25.1 | 25.1 | 25.1 | 25.1 | 25.1 | 25.1 | 21.9 | 21.9 | 21.4 |
| 5 | 25.2 | 26.3 | 21.4 | 21.5 | 25.3 | 20.2 | 21.2 | 21.7 | 21.6 | 21.5 | 21.1 | 25.3 |
| 6 | 25.4 | 25.8 | 25.8 | 22.0 | 25.1 | 24.8 | 25.2 | 25.5 | 25.4 | 21.8 | 22.6 | 23.3 |
| 7 | 25.3 | 26.0 | 24.5 | 25.0 | 26.2 | 25.1 | 25.7 | 25.6 | 24.9 | 23.3 | 24.5 | 22.0 |
| 8 | 24.8 | 26.1 | 22.1 | 24.7 | 27.1 | 26.3 | 25.6 | 25.0 | 23.8 | 23.5 | 24.5 | 27.0 |
| 9 | 25.0 | 26.0 | 25.2 | 25.8 | 26.4 | 24.8 | 25.7 | 25.8 | 25.5 | 23.3 | 24.7 | 23.5 |
| 10 | 25.7 | 26.0 | 22.2 | 23.0 | 24.5 | 24.8 | 25.9 | 25.5 | 23.3 | 23.4 | 23.3 | 23.5 |

Key:

* - The percentage composition at each point is shown in Table 48

a - $Sb_2O_3$ does not substitute the other metal oxide

b - $Sb_2O_3$ substitutes the other metal oxide

c - ATH is the commercial $Al_2O_3.3H_2O$

d - AM is $(NH_4)_6Mo_7O_{24}.4H_2O$

TABLE 60

The Oxygen index of samples containing HDPE and a 20% mixture of metal oxides and S70

| Points* | $Sb_2O_3$ a | $Sb_2O_3$ b | $Sb_2O_3$ $SnO_2$ | $Sb_2O_3$ ZnO | $Sb_2O_3$ $Fe_2O_3$ | $Sb_2O_3$ $Al_2O_3$ | $Sb_2O_3$ AlOOH | $Sb_2O_3$ ATH | $Sb_2O_3$ AM[d] | SnO ZnO | SnO AlOOH | $SnO_2$ $Fe_2O_3$ |
|---|---|---|---|---|---|---|---|---|---|---|---|---|
| 1 | 20.8 | 20.8 | 20.8 | 20.8 | 20.8 | 20.8 | 20.8 | 20.8 | 20.8 | 20.8 | 20.8 | 20.8 |
| 2 | 25.3 | 25.3 | 25.1 | 25.1 | 25.1 | 25.1 | 25.1 | 25.1 | 25.1 | 22.2 | 22.2 | 21.3 |
| 3 | 25.3 | 25.3 | 21.3 | 19.5 | 20.1 | 19.9 | 19.1 | 19.8 | 20.6 | 19.5 | 19.1 | 20.1 |
| 4 | 24.3 | 25.6 | 24.6 | 24.6 | 24.6 | 24.6 | 24.6 | 24.6 | 24.6 | 22.0 | 22.0 | 21.5 |
| 5 | 24.3 | 25.6 | 21.5 | 20.1 | 21.1 | 20.4 | 20.1 | 20.2 | 21.2 | 20.1 | 20.1 | 21.1 |
| 6 | 24.4 | 25.3 | 24.7 | 22.0 | 22.5 | 23.9 | 24.8 | 24.8 | 24.2 | 22.6 | 21.7 | 22.1 |
| 7 | 24.7 | 25.8 | 24.4 | 21.1 | 22.0 | 22.9 | 25.3 | 24.9 | 24.5 | 21.3 | 22.3 | 20.2 |
| 8 | 25.4 | 26.2 | 24.2 | 21.0 | 21.6 | 22.3 | 26.0 | 26.2 | 24.3 | 20.3 | 23.1 | 21.9 |
| 9 | 24.9 | 25.9 | 24.7 | 22.4 | 22.2 | 24.9 | 25.5 | 25.6 | 24.6 | 20.6 | 22.3 | 21.2 |
| 10 | 24.4 | 25.9 | 24.4 | 20.8 | 21.6 | 21.8 | 25.2 | 25.1 | 23.9 | 21.3 | 22.5 | 22.2 |

Key:

* - The percentage composition at each point is shown in Table 48

a - $Sb_2O_3$ does not substitute the other metal oxide

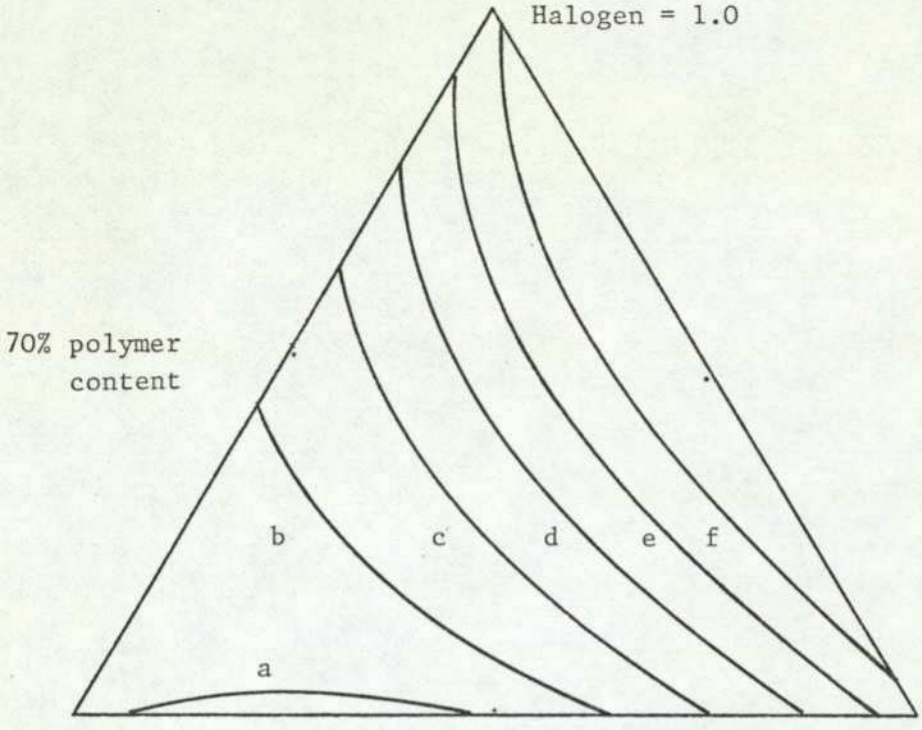
b - $Sb_2O_3$ substitutes the other metal oxide

c - ATH is the commercial $Al_2O_3.3H_2O$

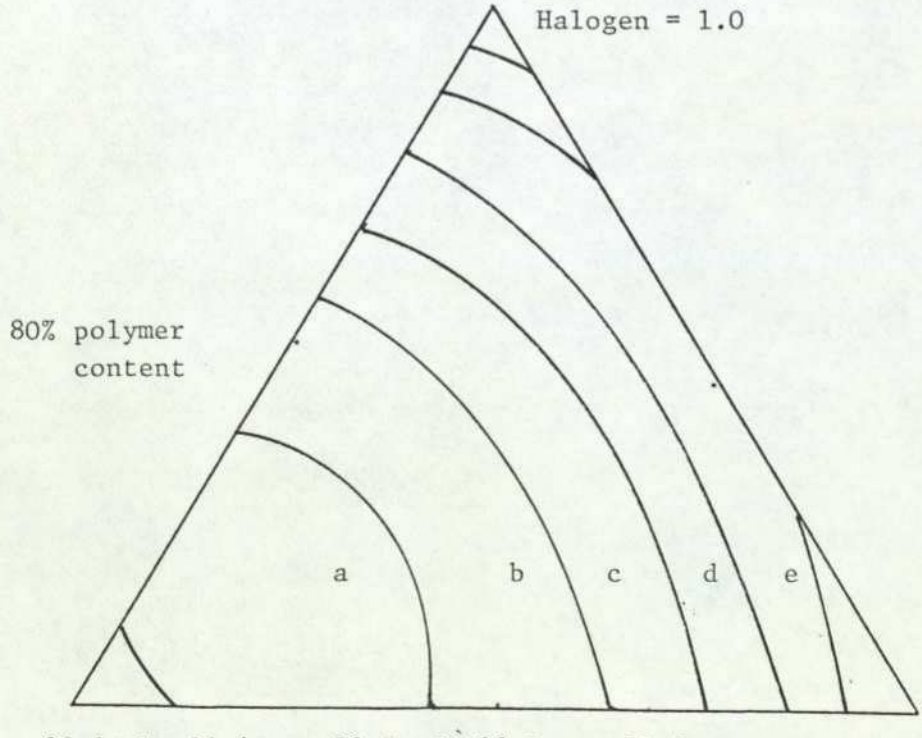
d - AM is $(NH_4)_6Mo_7O_{24}.4H_2O$

FIGURE 59

Oxygen index of three-component systems in HDPE: $Sb_2O_3/SnO_2$/S70




a = 25.8, b = 25.0, c = 24.3, d = 23.6, e = 22.9. f = 22.1




a =25.1, b =24.4, c =23.7, d =23.0, e =22.2.

but the flame generally remained directly above the polymer melt.

With ABS copolymer (Tables 61 and 62) the candle burned with a turbulent sooty flame from under a carbonaceous crust. It was found that, if this crust was removed during the burning process, a lower value was obtained for the oxygen index, especially for mixtures containing 70% of the copolymer. Hence all the results quoted for this material are for samples burning under a crust of char formed in situ. The plots obtained for this same material (Figure 60) show little statistical evidence to support their use, other than pictorially representing the results. With mixtures containing 80% ABS the cubic contours are very significant and the residuals are within the accepted experimental error.

3.2.5.2 $Sb_2O_3$/ZnO/halogen compound

Higher oxygen index values are obtained for compositions containing 70% HDPE than for those with 80% of the polymer. The maximum value is 25.8 at point 9 in the triangular diagram (Tables 59 and 60). The cubic plot (Figure 61) highlights the section of the triangle bounded by points 2, 4, 7 and 9 as being the area of maximum flame-retardance. These cubic contours are statistically significant and the residuals lie within the experimental error margin. At 80% HDPE (Figure 61) the computer plot pinpoints the area where the composition

TABLE 61

The Oxygen index of samples containing 70% ABS and a 30% mixture of metal oxides and Adine

| Points* | $Sb_2O_3$ a | $Sb_2O_3$ b | $Sb_2O_3$ $SnO_2$ | $Sb_2O_3$ ZnO | $Sb_2O_3$ $Fe_2O_3$ | $Sb_2O_3$ $Al_2O_3$ | $Sb_2O_3$ AlOOH | $Sb_2O_3$ ATH [c] | $Sb_2O_3$ AM [d] | $Sb_2O_3$ Talc | SnO ZnO | SnO AlOOH | $SnO_2$ $Fe_2O_3$ |
|---|---|---|---|---|---|---|---|---|---|---|---|---|---|
| 1 | 24.4 | 24.4 | 24.4 | 24.4 | 24.4 | 24.4 | 24.4 | 24.4 | 24.4 | 24.4 | 24.4 | 24.4 | 24.4 |
| 2 | 31.1 | 31.5 | 30.8 | 30.8 | 30.8 | 30.8 | 30.8 | 30.8 | 30.8 | 30.8 | 24.4 | 24.4 | 24.8 |
| 3 | 31.1 | 31.5 | 24.8 | 24.5 | 28.1 | 27.8 | 24.1 | 23.1 | 26.7 | 25.6 | 24.5 | 24.1 | 28.1 |
| 4 | 37.5 | 37.9 | 34.2 | 34.2 | 34.2 | 34.2 | 34.2 | 34.2 | 34.2 | 34.2 | 27.8 | 27.8 | 27.8 |
| 5 | 37.5 | 37.9 | 27.8 | 24.8 | 30.4 | 27.6 | 24.8 | 24.3 | 28.7 | 27.0 | 24.8 | 24.8 | 30.4 |
| 6 | 29.3 | 31.5 | 29.4 | 24.9 | 28.3 | 33.5 | 34.3 | 32.5 | 31.2 | 33.5 | 25.2 | 25.9 | 27.0 |
| 7 | 33.4 | 35.1 | 32.9 | 30.0 | 35.2 | 33.1 | 34.6 | 33.8 | 32.9 | 34.7 | 25.3 | 28.8 | 29.9 |
| 8 | 32.8 | 38.5 | 36.4 | 34.3 | 38.1 | 35.9 | 34.7 | 34.0 | 35.5 | 35.2 | 27.6 | 29.7 | 31.9 |
| 9 | 32.5 | 35.1 | 33.6 | 32.4 | 34.0 | 33.8 | 34.8 | 34.1 | 35.8 | 35.6 | 26.1 | 26.5 | 30.6 |
| 10 | 30.1 | 35.1 | 29.4 | 23.5 | 30.8 | 32.5 | 29.8 | 29.6 | 33.1 | 32.2 | 25.6 | 27.1 | 28.2 |

Key:

* - The percentage composition at each point is shown in Table 48

a - $Sb_2O_3$ does not substitute the other metal oxides

b - $Sb_2O_3$ substitutes the other metal oxides

c - ATH is the commercial $Al_2O_3.3H_2O$

d - AM is $(NH_4)_6Mo_7O_{24}.4H_2O$

TABLE 62

The Oxygen index of samples containing 80% ABS and a 20% mixture of metal oxides and Adine

| Points* | $Sb_2O_3$ a | $Sb_2O_3$ b | $Sb_2O_3$ $SnO_2$ | $Sb_2O_3$ ZnO | $Sb_2O_3$ $Fe_2O_3$ | $Sb_2O_3$ $Al_2O_3$ | $Sb_2O_3$ AlOOH | $Sb_2O_3$ ATH[c] | $Sb_2O_3$ AM[d] | SnO ZnO | SnO AlOOH | $SnO_2$ $Fe_2O_3$ |
|---|---|---|---|---|---|---|---|---|---|---|---|---|
| 1 | 23.6 | 23.6 | 23.6 | 23.6 | 23.6 | 23.6 | 23.6 | 23.6 | 23.6 | 23.6 | 23.6 | 23.6 |
| 2 | 25.8 | 30.2 | 26.9 | 26.9 | 26.9 | 26.9 | 26.9 | 26.9 | 26.9 | 23.7 | 23.7 | 23.6 |
| 3 | 25.8 | 30.2 | 23.2 | 22.0 | 26.2 | 24.0 | 22.6 | 21.4 | 24.1 | 22.0 | 22.6 | 26.2 |
| 4 | 30.4 | 30.4 | 28.1 | 28.1 | 28.1 | 28.1 | 28.1 | 28.1 | 28.1 | 25.0 | 25.0 | 24.2 |
| 5 | 30.4 | 30.4 | 24.2 | 22.8 | 27.9 | 24.9 | 22.9 | 22.3 | 25.0 | 22.8 | 22.9 | 27.9 |
| 6 | 25.8 | 30.2 | 25.8 | 22.2 | 25.5 | 26.0 | 27.0 | 25.0 | 26.2 | 23.7 | 23.3 | 25.2 |
| 7 | 24.6 | 29.3 | 27.2 | 24.5 | 30.3 | 26.5 | 27.2 | 26.6 | 27.7 | 22.5 | 23.5 | 27.3 |
| 8 | 24.2 | 29.2 | 26.6 | 25.8 | 31.2 | 26.3 | 26.4 | 25.7 | 27.6 | 24.2 | 23.7 | 28.1 |
| 9 | 26.6 | 28.9 | 27.3 | 23.4 | 29.4 | 26.3 | 26.9 | 26.2 | 27.2 | 23.9 | 24.8 | 26.7 |
| 10 | 27.0 | 28.9 | 25.4 | 22.5 | 28.6 | 24.6 | 24.1 | 24.3 | 26.7 | 22.8 | 23.4 | 26.5 |

Key:

* - The percentage composition at each point is shown in Table 48

a - $Sb_2O_3$ does not substitute the other metal oxide

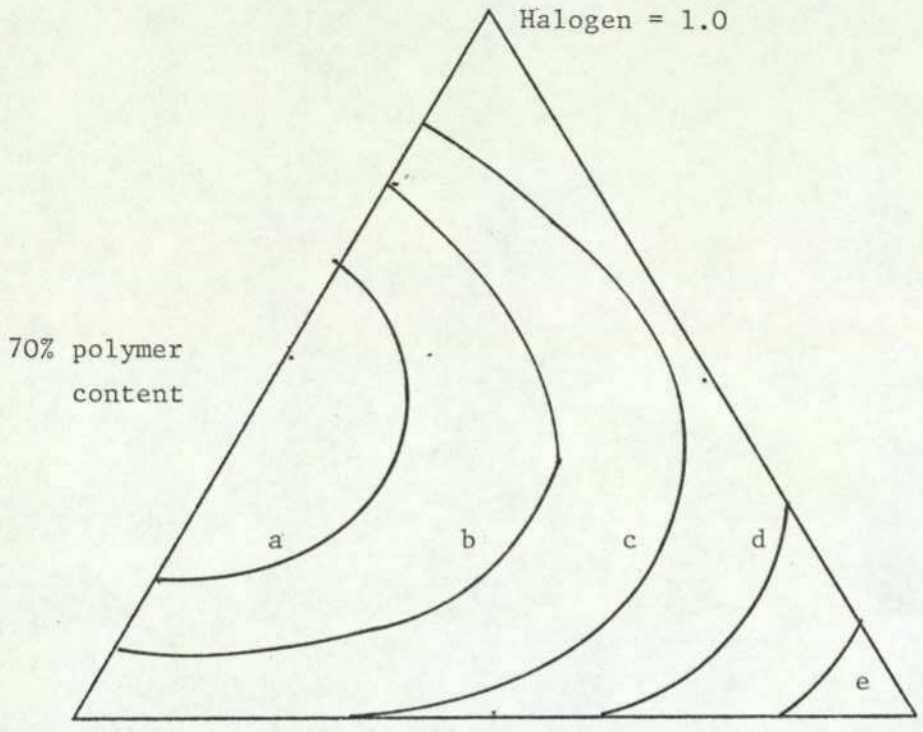
b - $Sb_2O_3$ substitutes the other metal oxide

c - ATH is the commercial $Al_2O_3.3H_2O$

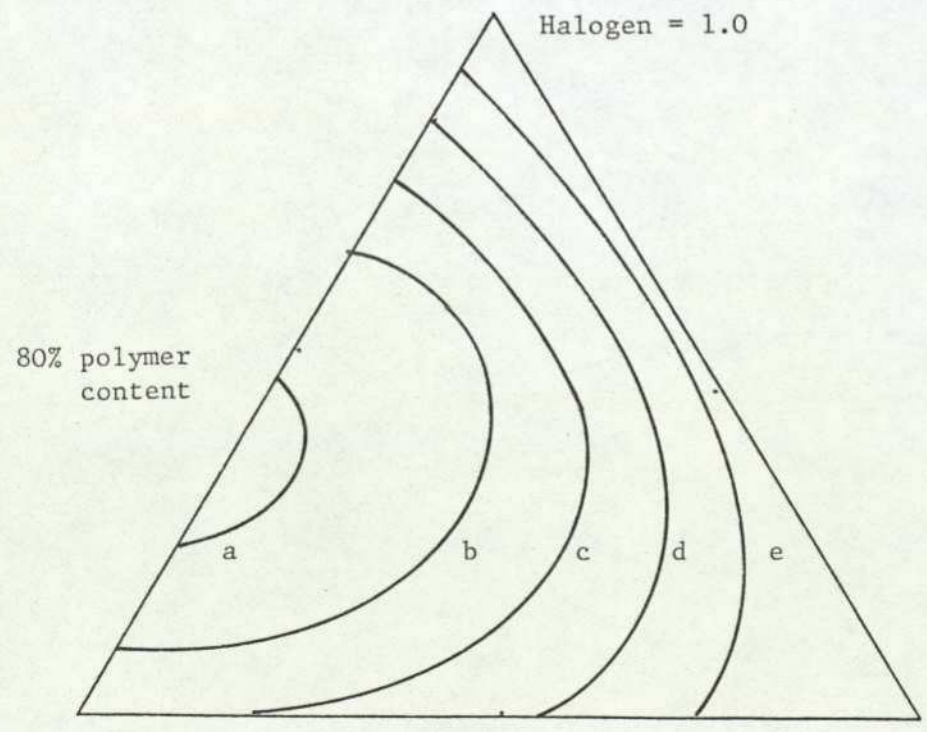
d - AM is $(NH_4)_6Mo_7O_{24}.4H_2O$

FIGURE 60

Oxygen index of three-component systems in ABS: $Sb_2O_3/SnO_2$/Adine



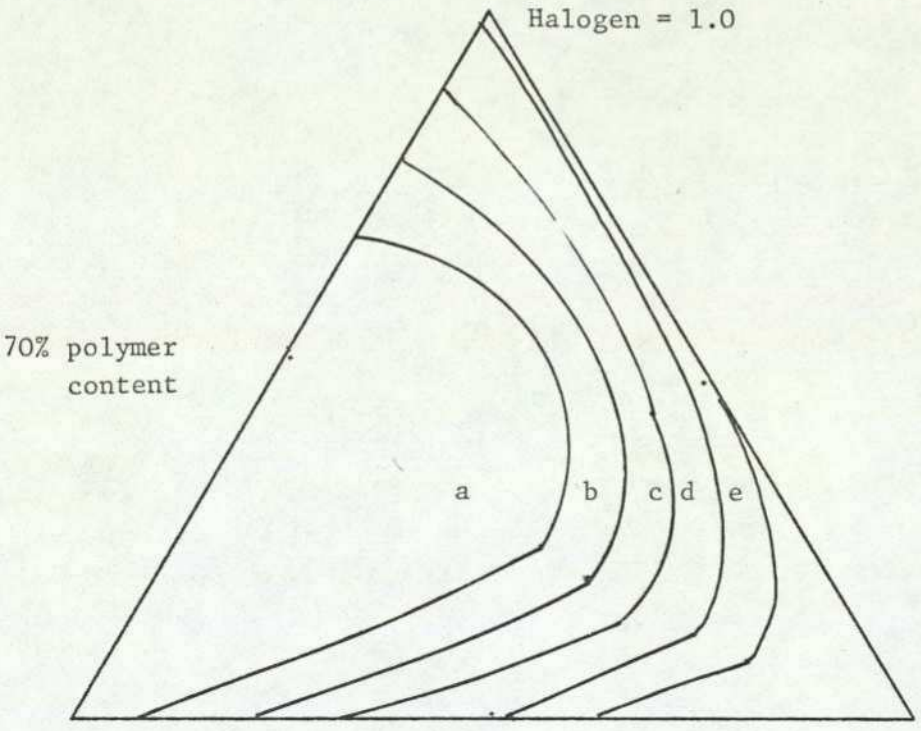

a =34.4, b =32.4, c =30.4, d =28.4, e =26.4.



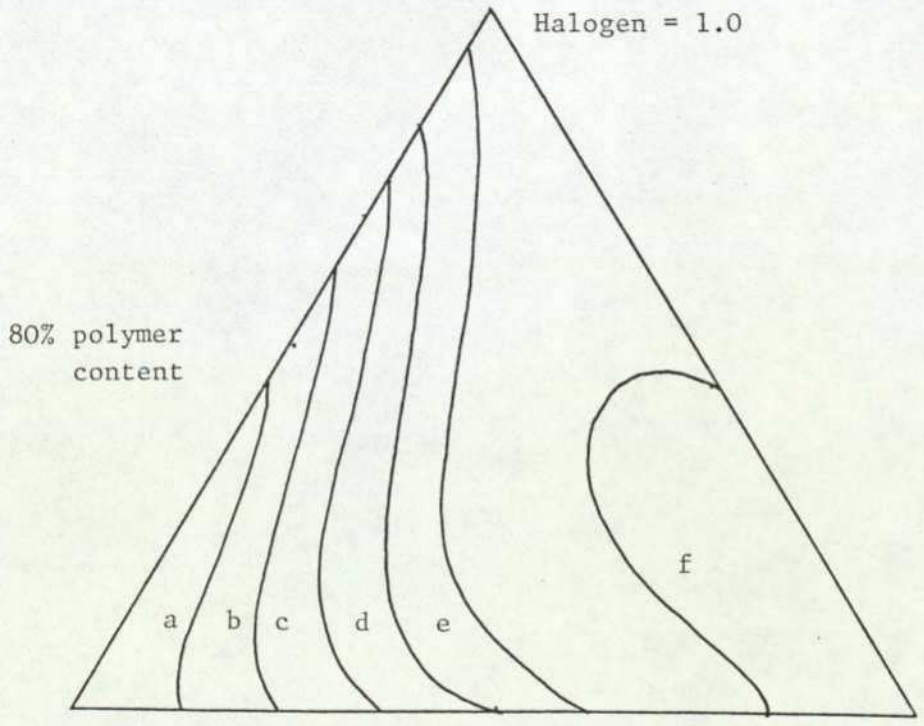

a =28.2, b = 27.4, c =26.5 , d =25.7, e = 24.9.

FIGURE 61

Oxygen index of three-component systems in HDPE: $Sb_2O_3$/ZnO/S70




a =24.8, b =24.0, c =23.2, d =22.4, e = 21.6




a = 24.1, b = 23.4, c = 22.7, d = 22.1, e = 21.4, f = 20.4

is least likely to be useful for flame retardance. The polymer candles burnt with a stable flame after short ignition times. The charred area consisted of a powdery polymeric crust and contained a white residue. When combustion occurred under the oxygen index condition, less dripping was observed although the polymer surface immediately below the flame was a fluid melt. The sample glowed for about 40s. after the flame had extinguished itself.

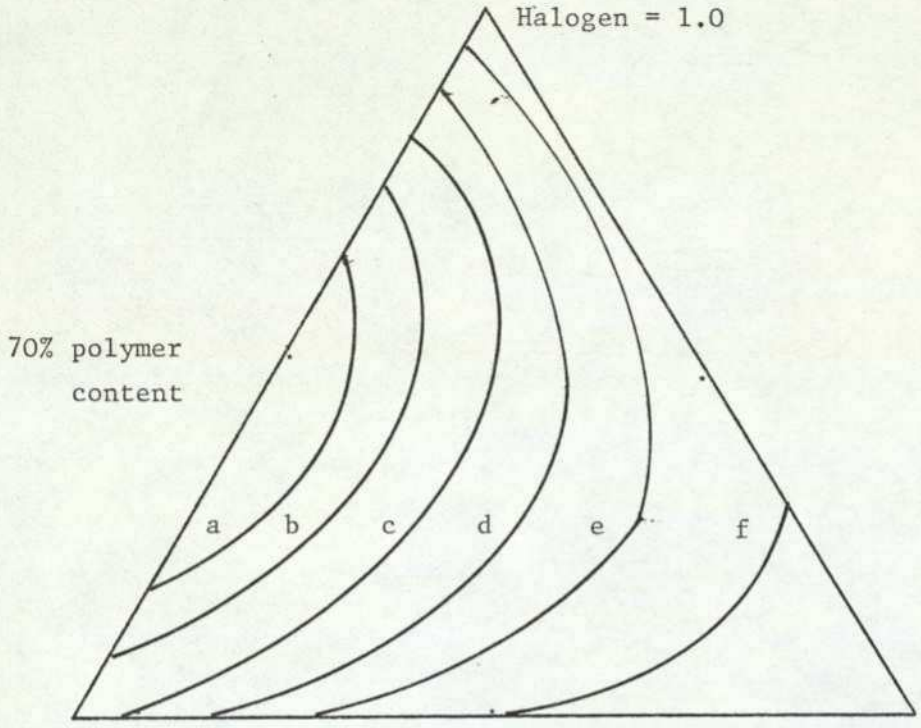
The results with ABS (Tables 61 and 62) show that there is a maximisation of the studied response along the axis, at a point where the $Sb_2O_3$ : Adine ratio is about 1:3. The residuals are $\pm 6$ and therefore significantly higher than the expected statistic error. There is no statistical evidence to support the hypothesis that the response obeys a quadratic or reduced cubic regression; hence the quadratic curves in Figure 62 are used to represent pictorially the trends observed. The samples were easy to ignite and burned with a sooty flame, forming large amounts of carbonaceous crusts. The flame was intensely white and shot out from under the crust as fuel was emitted, in bursts, from the hot polymer. There was little or no glow after extinction of the flame.

3.2.5.3 $Sb_2O_3/Fe_2O_3$/halogen compound

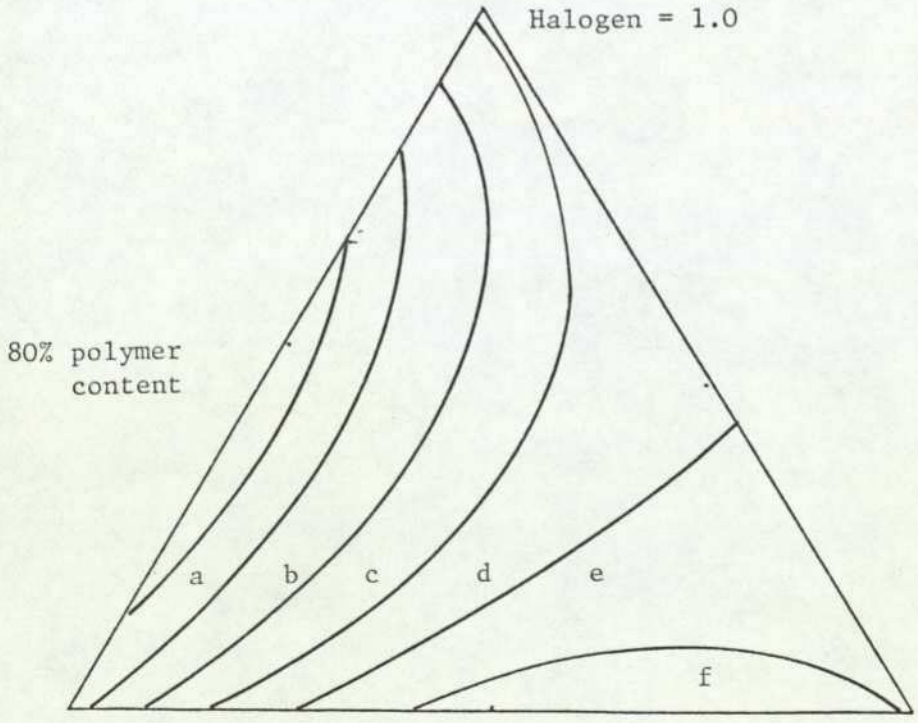
A fairly high oxygen index of 27.1 was recorded for point 8 for the system containing 70% HDPE (Table 59).

FIGURE 62

Oxygen index of three-component systems in ABS: $Sb_2O_3$/ZnO/Adine




a = 34.3, b = 32.5 , c = 30.7, d = 28.9, e = 27.1 f = 25.3



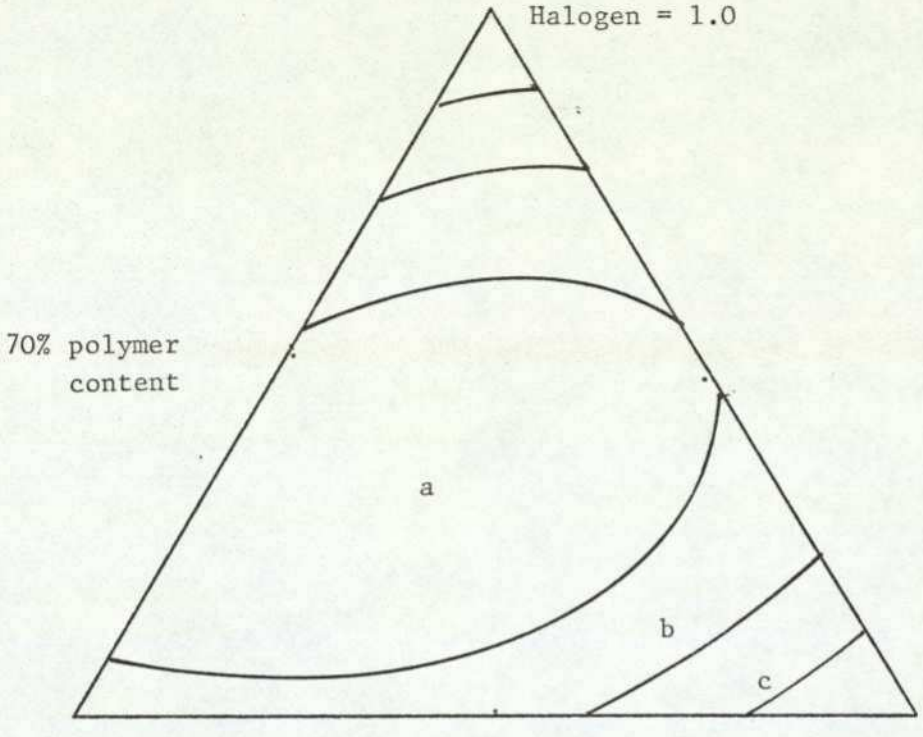

a = 28.1 b = 27.1 , c = 26.1 , d = 25.1, e = 24.1. f = 23.1

The flame-retardant action is improved by the catalytic effect of the iron(III)oxide on the decomposition of the S70, which in turn leads to increased char formation. This, together with residual $Fe_2O_3$, forms a thick crust on top of the burning polymer thus preventing the fuel from feeding the flame. The flame does not travel down the sides of the candle, but tends to be engulfed in the carbonaceous crust. The computer plot of the quadratic regression (Figure 63) indicates an area in the centre of the diagram which is most significant for flame-retardant effectiveness. The trends indicated by the regression analysis of the responses for the compositions containing 80% HDPE indicate that the most significant composition is one that contains $Sb_2O_3$ and halogen with little or no $Fe_2O_3$, thereby confirming the catalytic rôle of the iron oxide in HDPE.

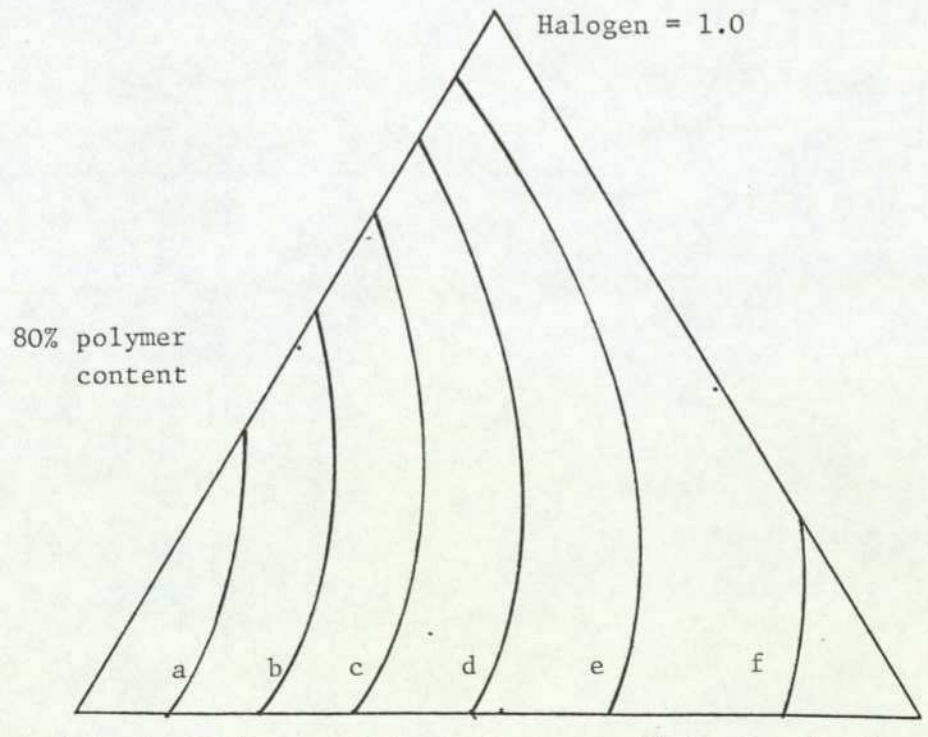
In ABS, an abnormally high oxygen index of 38 is reached at point 8 for the system containing 70% polymer (Tables 61 and 62). This high value is attributed to the fact that char formation in this system occurs so quickly and copiously that the flame has insufficient time to stabilise itself. The virgin polymer candle ignites easily at these high oxygen concentrations but the flame is quickly engulfed by the char. With mixtures containing 80% polymer, similar behaviour is observed. These large variations in response cannot be significantly

FIGURE 63

Oxygen index of three-component systems in HDPE: $Sb_2O_3/Fe_2O_5/S70$




a = 25.7, b =24.8, c =23.9, d = -, e = -.




a =24.1, b =23.4, c =22.7, d =22.1, e = 21.4 f - 20. 8

mapped using a second or third degree regression curve, but the cubic analysis serves as adequate qualitative illustration of the direction of the maximum contour (Figure 64).

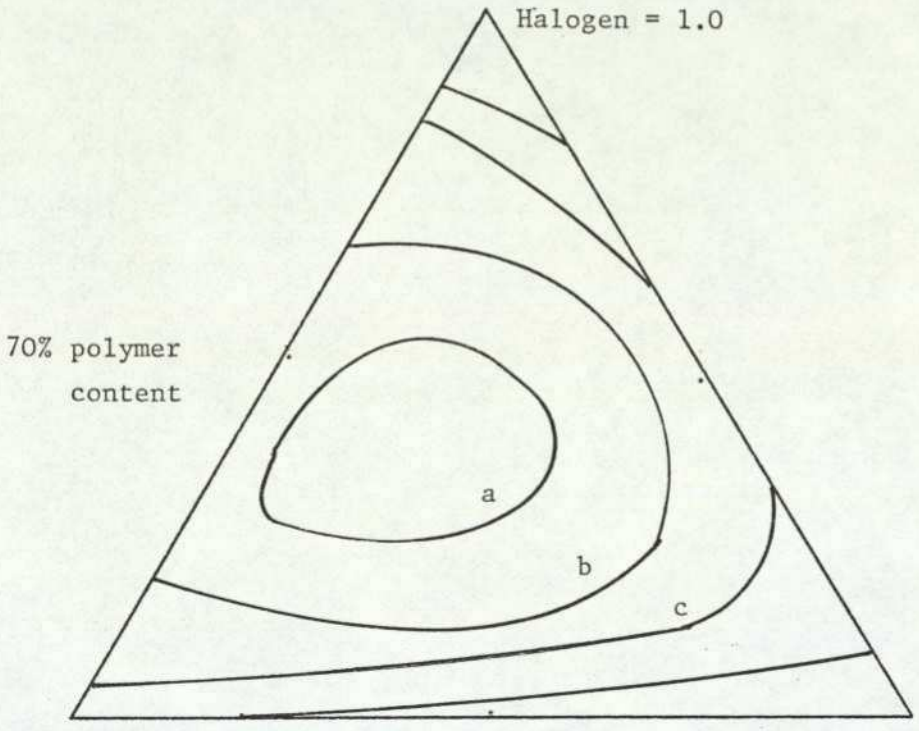
3.2.5.4 $Sb_2O_3$/A100H/halogen compound

The oxygen index values for systems containing 70% HDPE are very similar to those obtained for composites containing only $Sb_2O_3$. The quadratic contours indicate a maximum response in the area around point 9 (Figure 65). The residuals vary between +2.0 and -0.8. The F-test ratio for the quadratic and cubic regression analyses are equal and not significant at the 1% significance level. The quadratic contours for compositions containing 80% HDPE fit well with the response contours at 70% HDPE when viewed in three-dimensions. The candles were difficult to ignite as the ensuing reactions were endothermic and hence required long, sustained ignitions. The flame burned on the top of a fluid melt and there was a slight dripping of the polymer melt. Fuel was transferred via porous channels through the polymer crust.

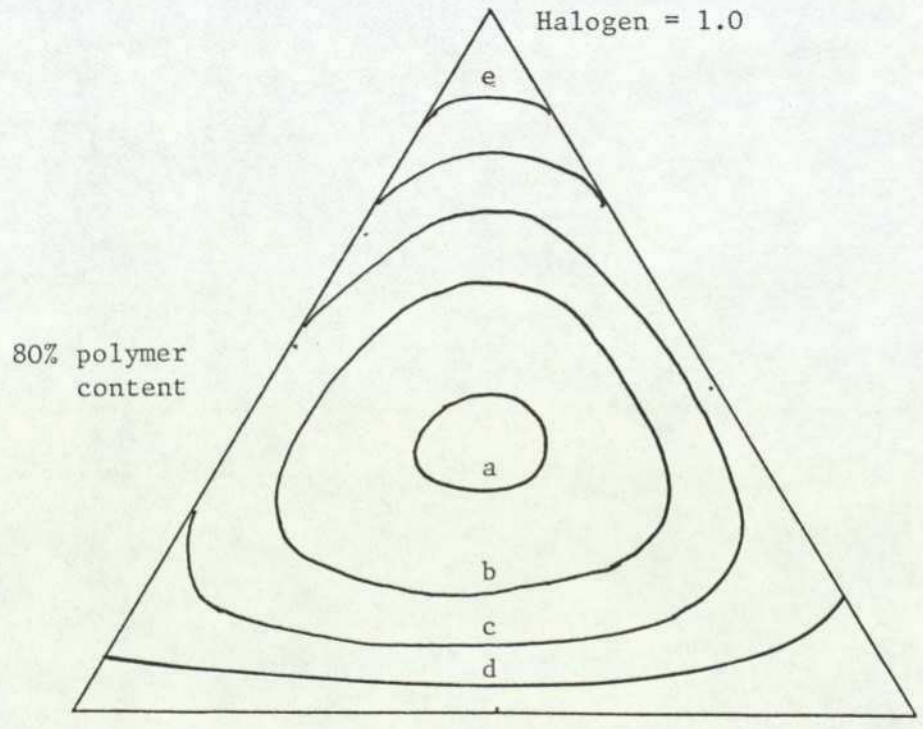
The responses recorded for points 7, 8, 9 and 10 for the system containing 70% ABS indicate a flame-retardant efficiency similar to that of mixtures of $Sb_2O_3$ and Adine. The quadratic regression plot is very significant and highlights the flame-retardant

FIGURE 64

Oxygen index of three-component systems in ABS: $Sb_2O_3/Fe_2O_5$/Adine



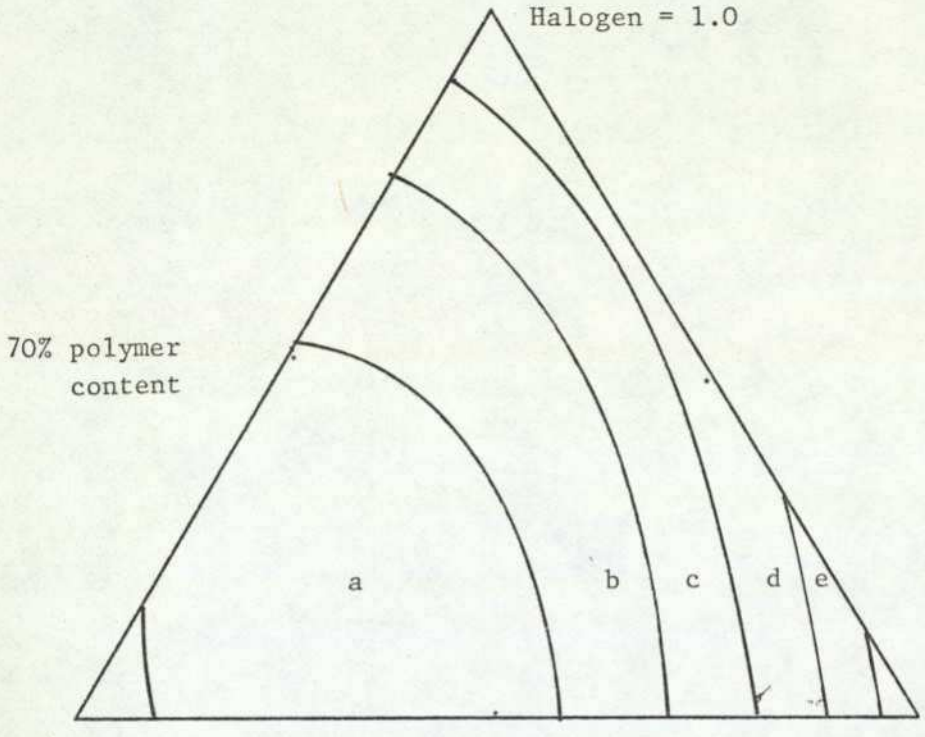

a = 35.9, b = 33.6, c = 31.3, d = 29.0, e = 26.7.



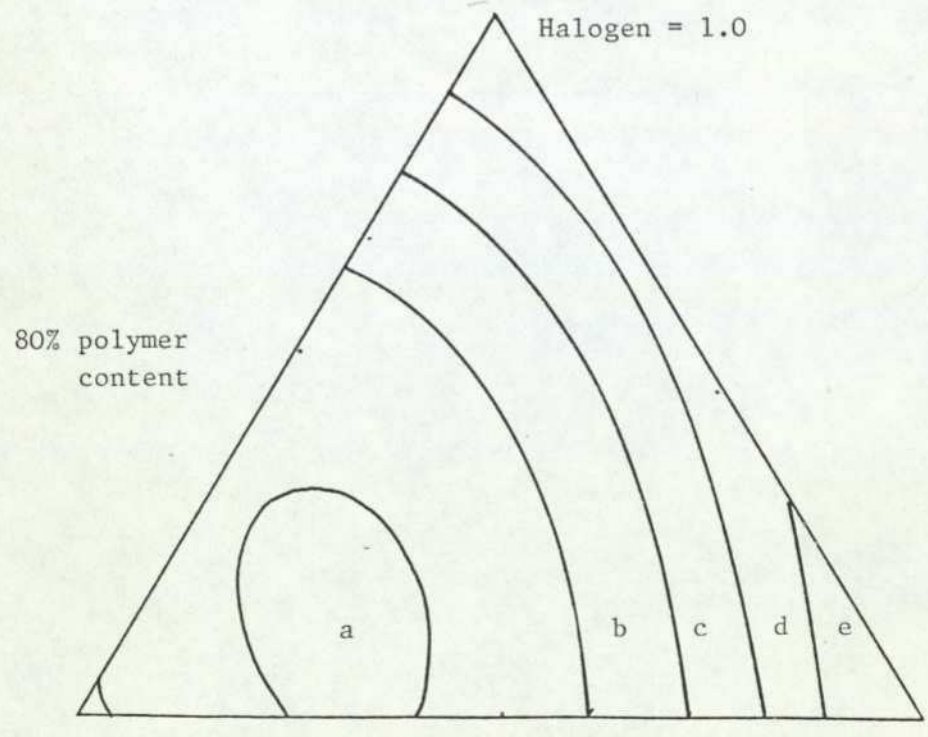

a = 31.2, b = 30.0, c = 28.7, d = 27.4, e = 26.2.

FIGURE 65

Oxygen index of three-component systems in HDPE: $Sb_2O_3$/A100H/S70




a =26.8, b =25.6, c=24.4 , d=23.3, e =22.1.




a =26.0, b =24.8, c =23.7, d = 22.5 e =21.4.

activity in the area between points 4, 7 and 9 (Figure 66). The statistical significance of the quadratic plots for systems containing 70 and 80% ABS is noteworthy and substantiated by residuals of $\pm$ 1.0 at 80% ABS. The candles in this set were easy to ignite. The polymer had tendency to ablate excessively around the oxygen index value especially for systems containing 70% polymer. This explains the slightly higher calculated residuals of + 3.6 to -1.6. The carbonaceous residue was light and fluffy.

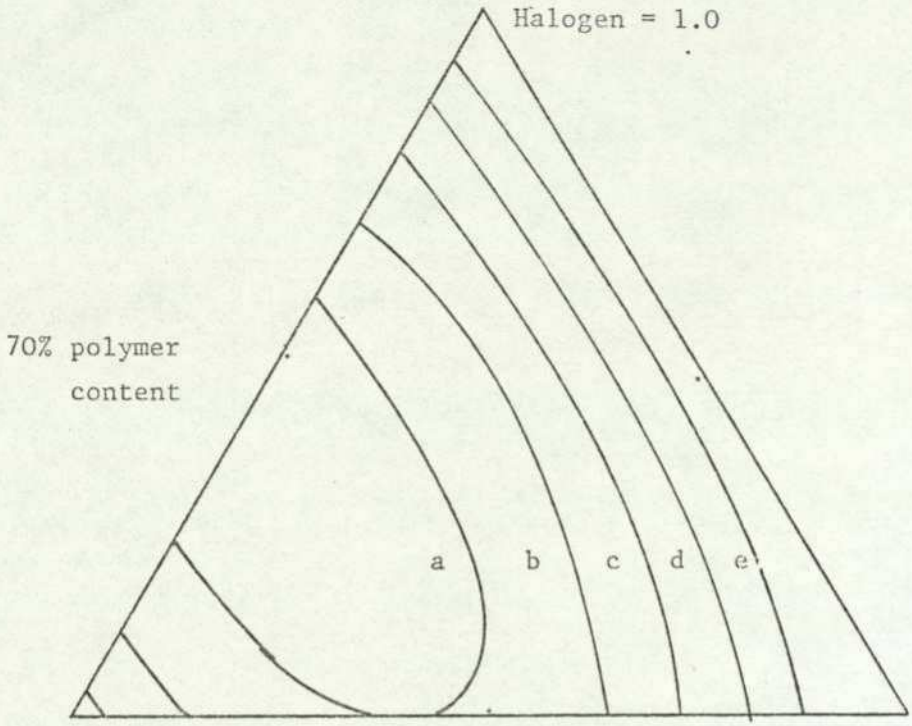
3.2.5.5 $Sb_2O_3/Al_2O_3.3H_2O$/halogen compound

The quadratic and cubic response surfaces for the system containing 70 and 80% HDPE indicate a maximum plateau in the area between points 6, 7 and 9. However, the variance ratio test cautions one against the use of these plots (Figure 67) too literally. The polymer candles burn smoothly, without the formation of much soot. The flame is very cool as the chimney does not heat up appreciably. A large volume of the candle is consumed by the time taken for the candle to extinguish itself under oxygen index conditions. Much flickering is observed before the flame finally dies.

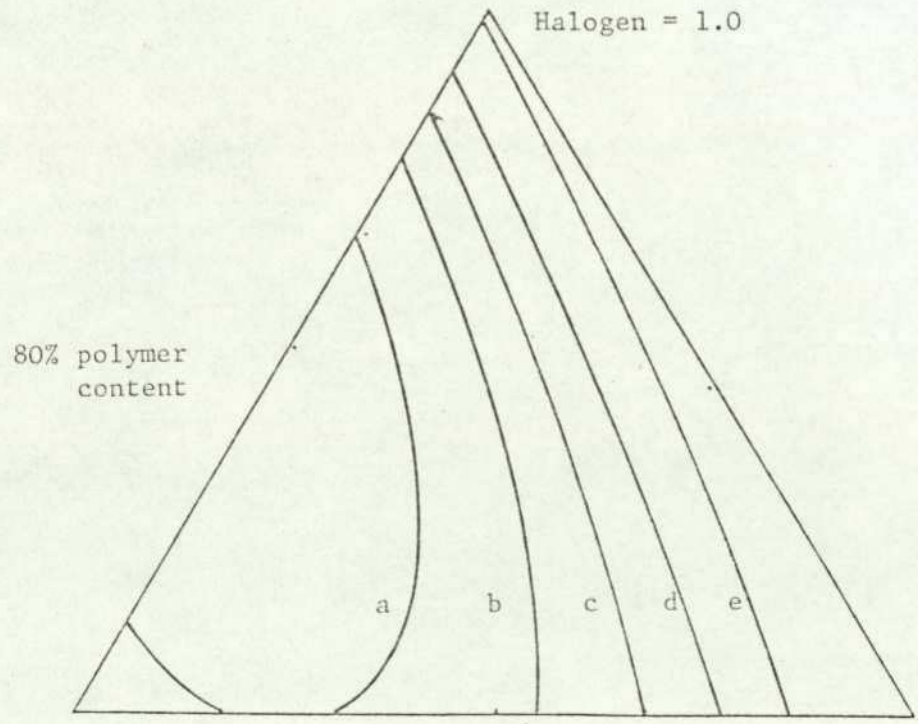
For samples containing 70% ABS, a plateau engulfing points 4, 7 and 9 indicates a maximum oxygen index value of ca. 34.0 in the quadratic response surface plot (Figure 68). The maximum response contour moves towards point 6 for the system containing 80% ABS. The

FIGURE 66

Oxygen index of three-component systems in ABS: $Sb_2O_3$/AlOOH/Adine



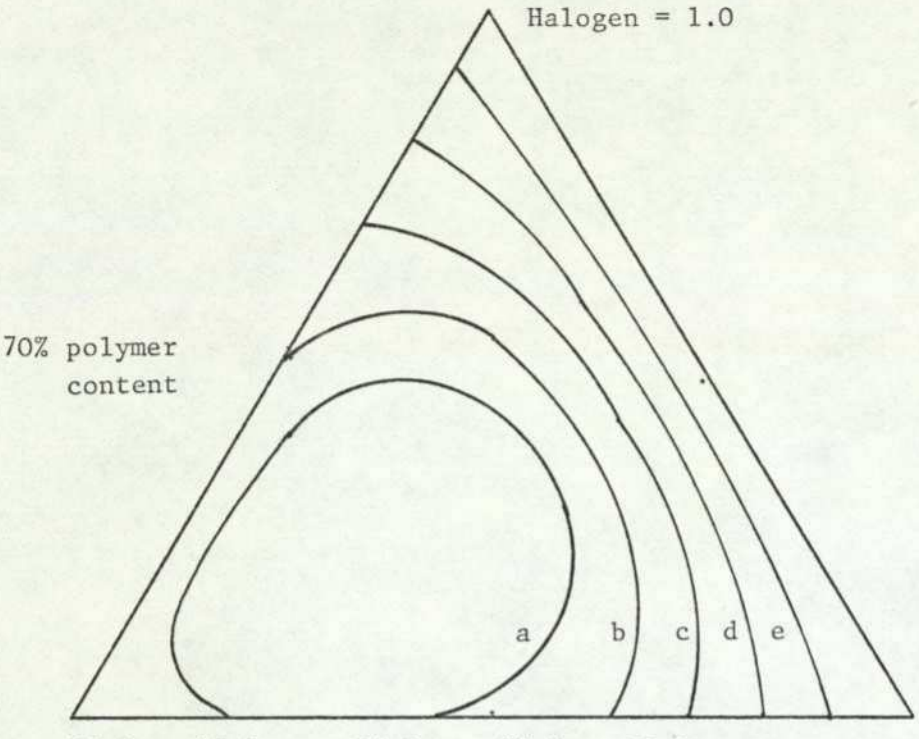

a = 34.8 b = 33.0 c = 31.2 , d = 29.4 e = 27.6



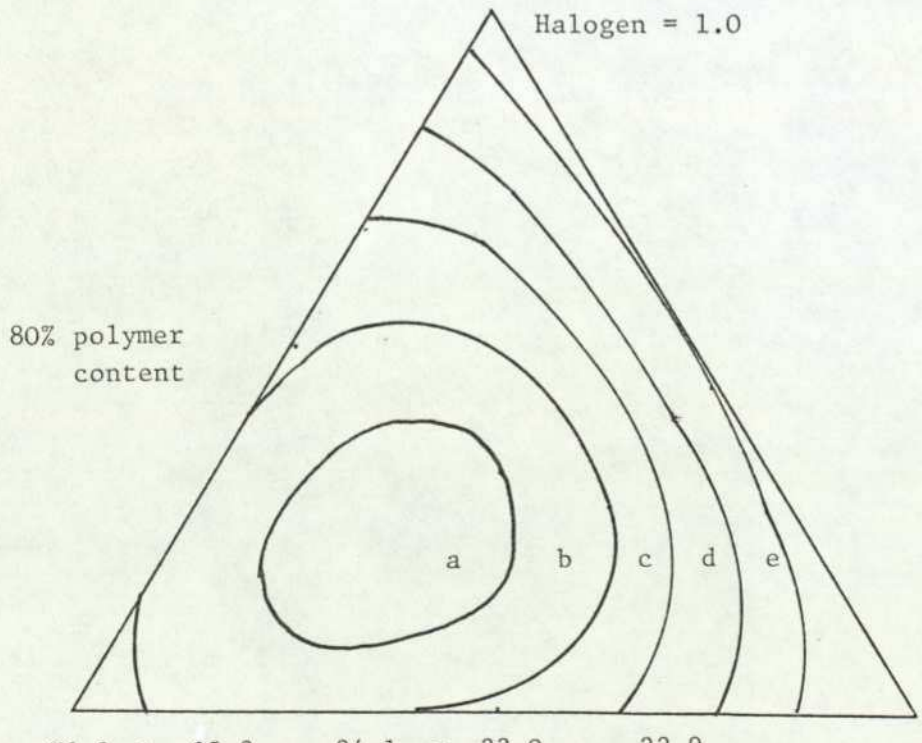

a = 26.5 b = 25.7 , c = 24.9 , d = 24.1, e = 23.4 .

FIGURE 67

Oxygen index of three-component systems in HDPE: $Sb_2O_3/Al_2O_3 \cdot 3H_2O/S70$



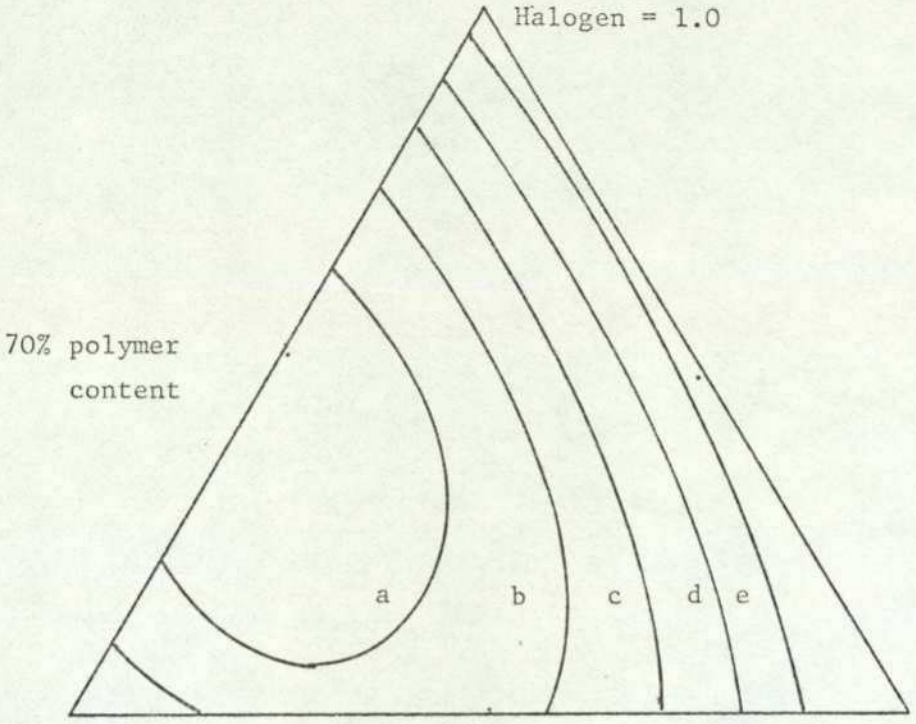

a = 25.8 b =25.1, c = 24.3 d = 23,6e = 22.9



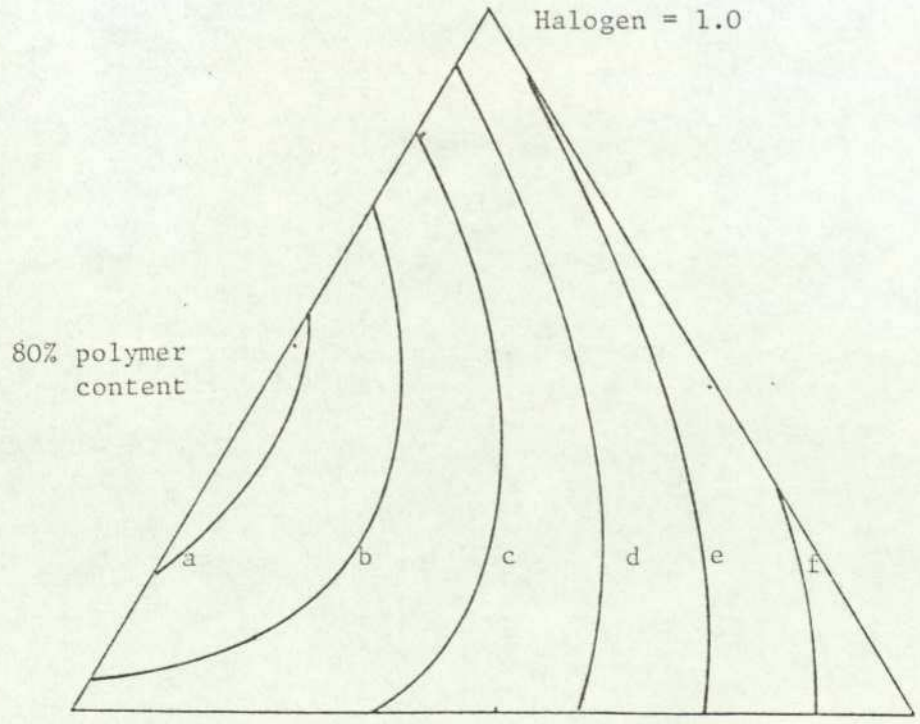

a =26.2, b =25.2, c =24.1, d =23.0, e = 22.9

FIGURE 68

Oxygen index of three-component systems in ABS: $Sb_2O_3/Al_2O_3 \cdot 3H_2O$/Adine




a = 34.2, b = 32.4, c = 30.5, d = 28.7, e = 26.8




a = 28.0 b = 26.9, c = 25.8, d = 24.7, e = 23.6 . f = 22.5

F-test ratio gives a significant indication of minimal error at a significance level of 1%.

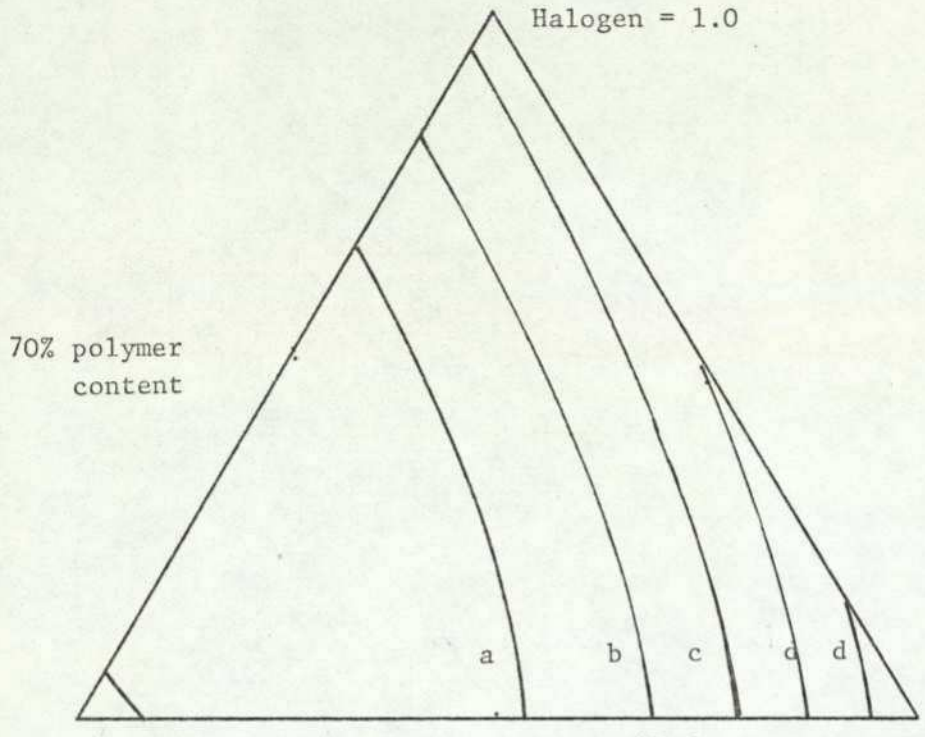
3.2.5.6 $Sb_2O_3/Al_2O_3$/halogen compound

The oxygen index values for samples containing 70% HDPE are much lower than those obtained for the two hydrated aluminium oxides (Tables 59 and 60). Although none of the contours are of statistical significance, the quadratic plot does not suggest that there is any synergism between the two metal oxides or that the flame retardant action is dominated by the antimony/halogen part of the system (Figure 69). The significant oxygen index value of 26.3 is obtained for a mixture of $Sb_2O_3$: $Al_2O_3$:S70 (1:1:10). For samples containing 80% HDPE, significantly lower oxygen index values are obtained. The quadratic plot is extremely signifcant (F-test rates 147.97) and once again indicates no flame retardant action due to the alumina.

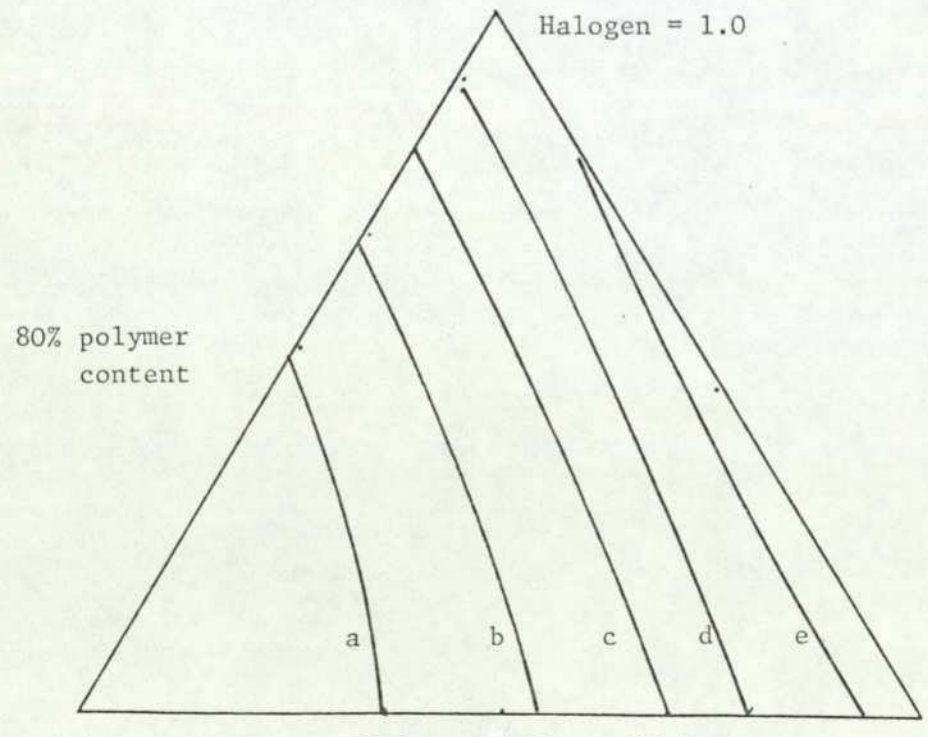
For samples containing 70% ABS, the oxygen index values compare favourably with those obtained for the tri-hydrate/antimony system. The quadratic contours suggest that maximum flame retardant action is found in the region between points 4 and 7 (Figure 70). For samples containing 80% ABS, the oxygen index values are about 10% lower but indicate a similar trend as shown by the quadratic plot.

FIGURE 69

Oxygen index of three-component systems in HDPE: $Sb_2O_3/Al_2O_3$ /S70



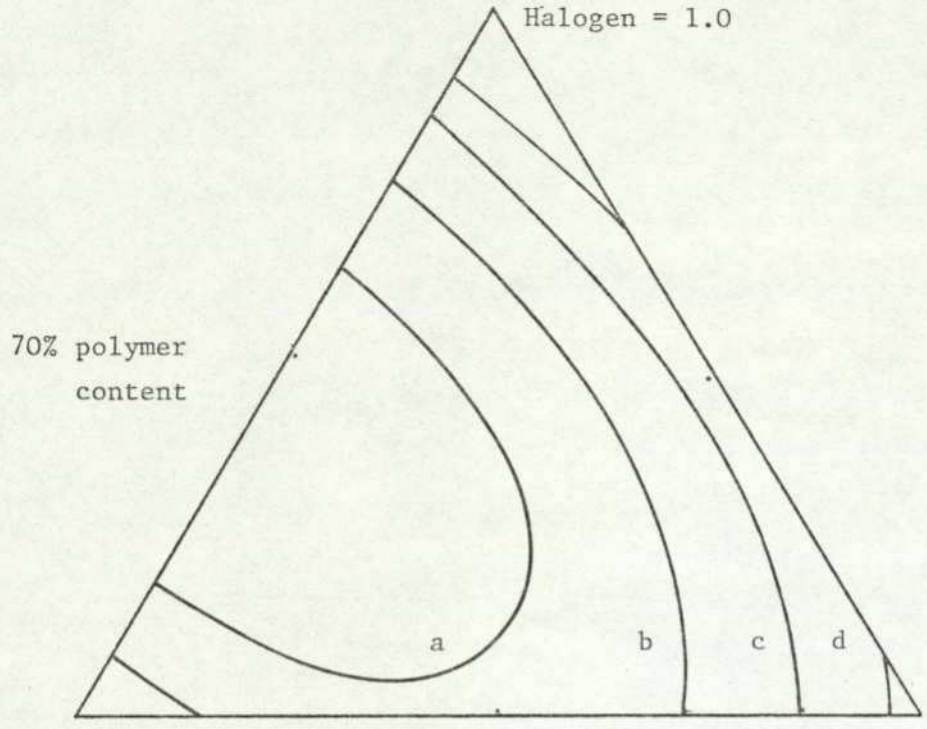

a = 25.1 , b = 24.1, c = 23.1, d = 22.1 e = 21.1



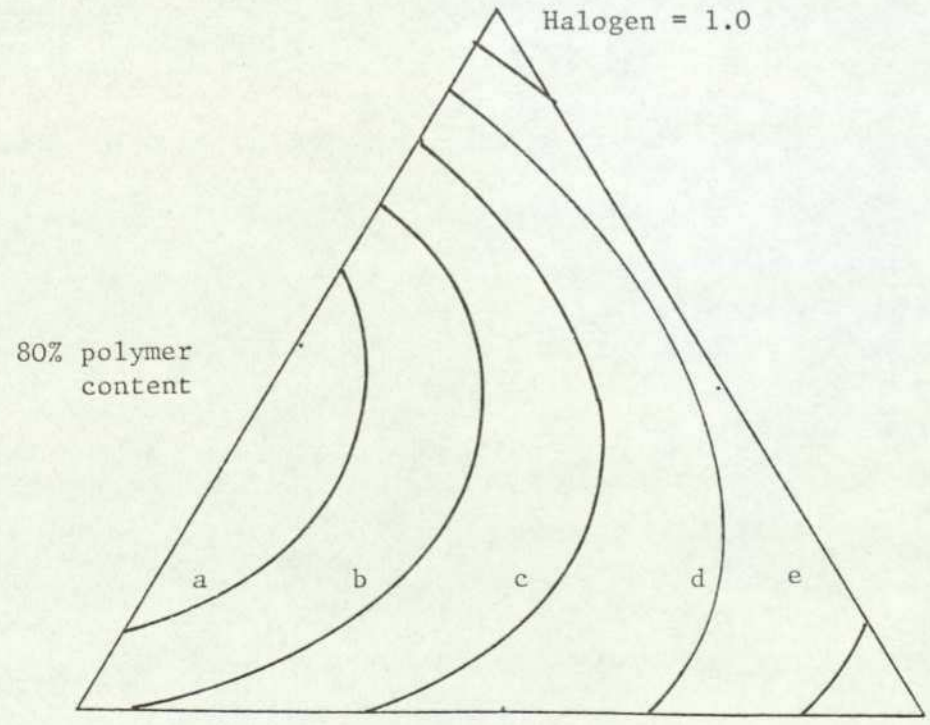

a = 24.5, b = 23.6 , c = 22.6, d = 21.7, e = 20.3

FIGURE 70

Oxygen index of three-component systems in ABS: $Sb_2O_3/Al_2O_3$/Adine




a =34.0, b =32.1, c =30.2, d =28.3, e = - .




a =27.4 b = 26.6, c = 25.8, d =25.1, e = 24.4.

3.2.5.7 $Sb_2O_3$/talc/halogen compound

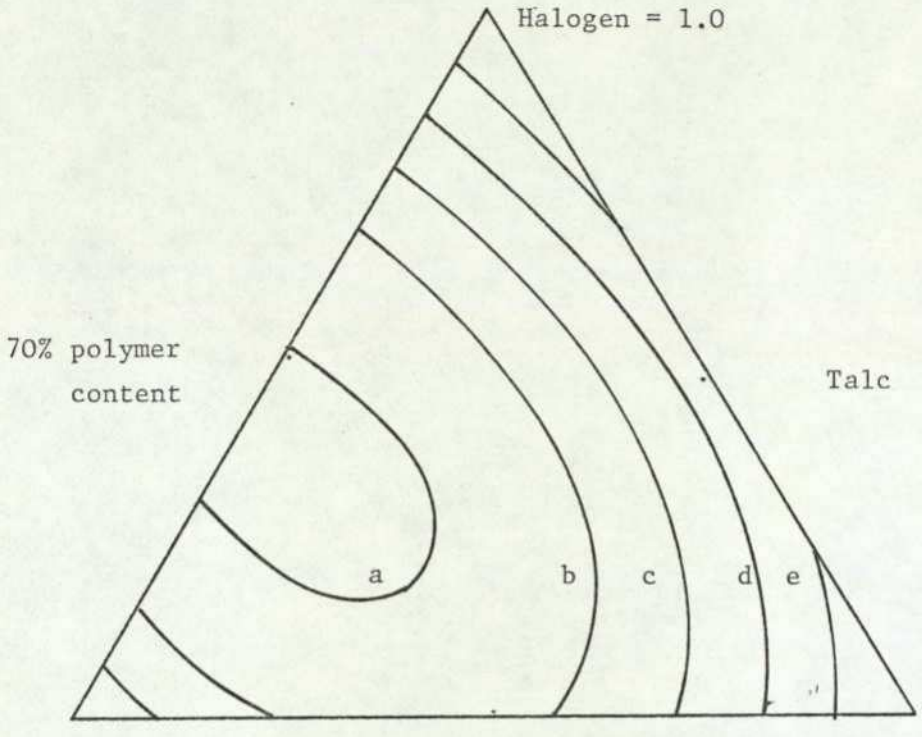
A study of the variations in oxygen index for ABS containing 30% of mixtures of $Sb_2O_3$, talc and Adine showed a flame retardant effect similar to that obtained for $Sb_2O_3$/aluminium oxide/Adine systems. The quadratic contour was similar to that obtained for the antimony/alumina system at the same flame retardant content (Figure 71). A maximum value of 35.6 was obtained for polymer containing 17.5% halogen, 10% antimony oxide and 2.5% talc.

3.2.5.8 $Sb_2O_3$/ammonium molybdate/halogen compound

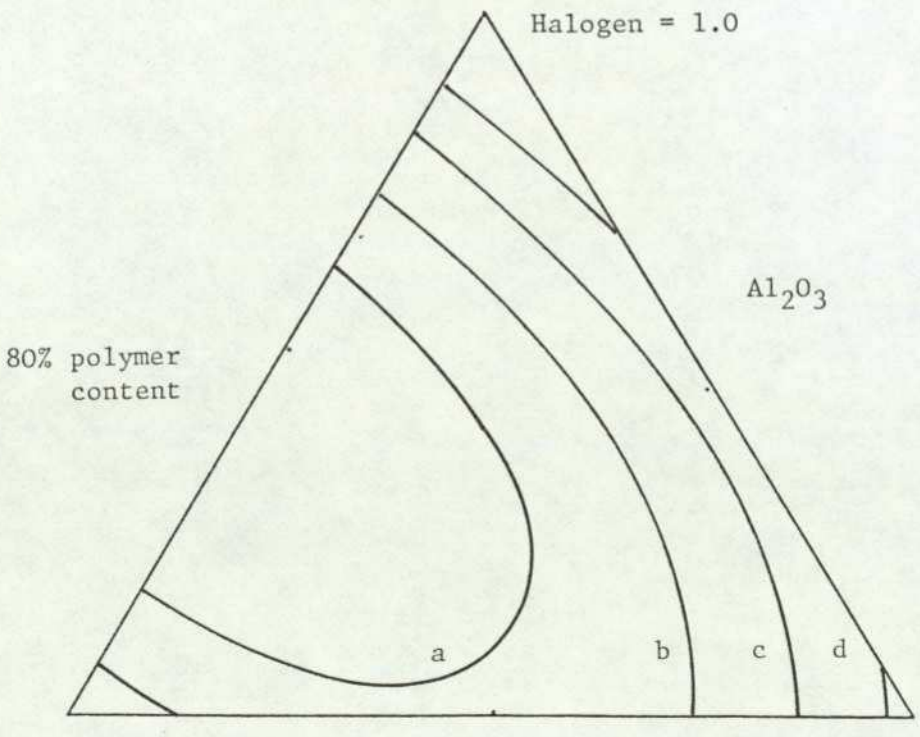
For samples containing 70% HDPE, the cubic regression response surfaces are very significant. The fact that the F-test ratio is 62.29 indicates that the probability of the cubic regression being the best model is greater than 0.995. The residuals are also very small (±0.3). The area around point 9 shows a maximum response contour of ca.25.5 (Figure 72). For samples containing 80% HDPE, the quadratic contours adequately describe the trends. The residuals lie within the experimental error of ±1.0. Again, the area around point 9 shows a maximisation of the response. In these cases, it was found that secondary ignition was necessary for samples when the conditions for combustion corresponded to oxygen mole fractions 1-2 lower than the oxygen index (Tables 59 and 60). The

FIGURE 71

Oxygen index of three-component systems in ABS: $Sb_2O_3$/Talc/Adine



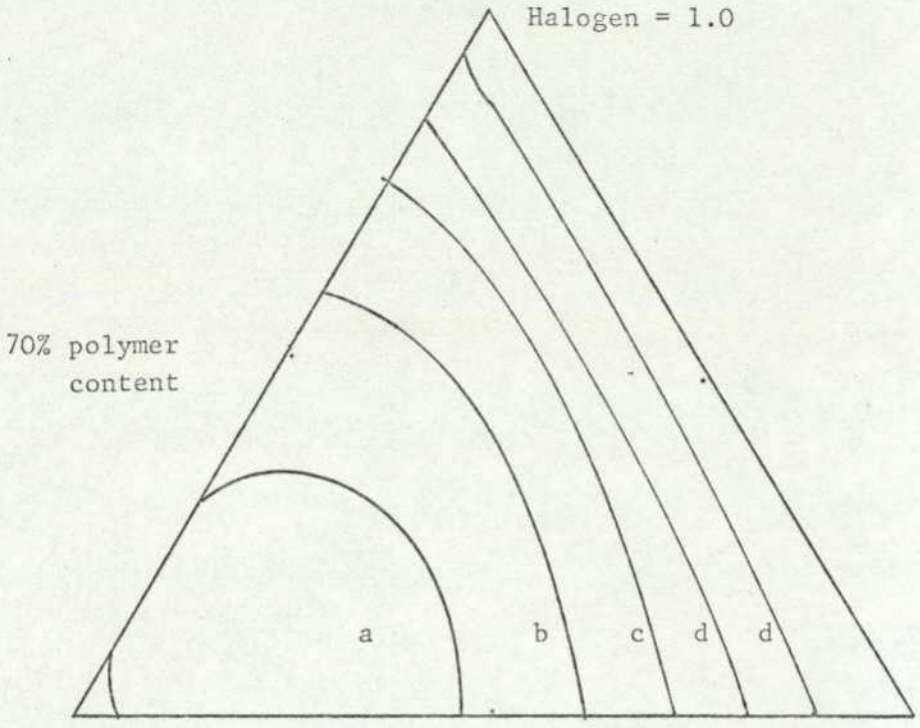

a = 35.7, b = 33.8, c = 31.9, d = 30.0, e = 28.1.



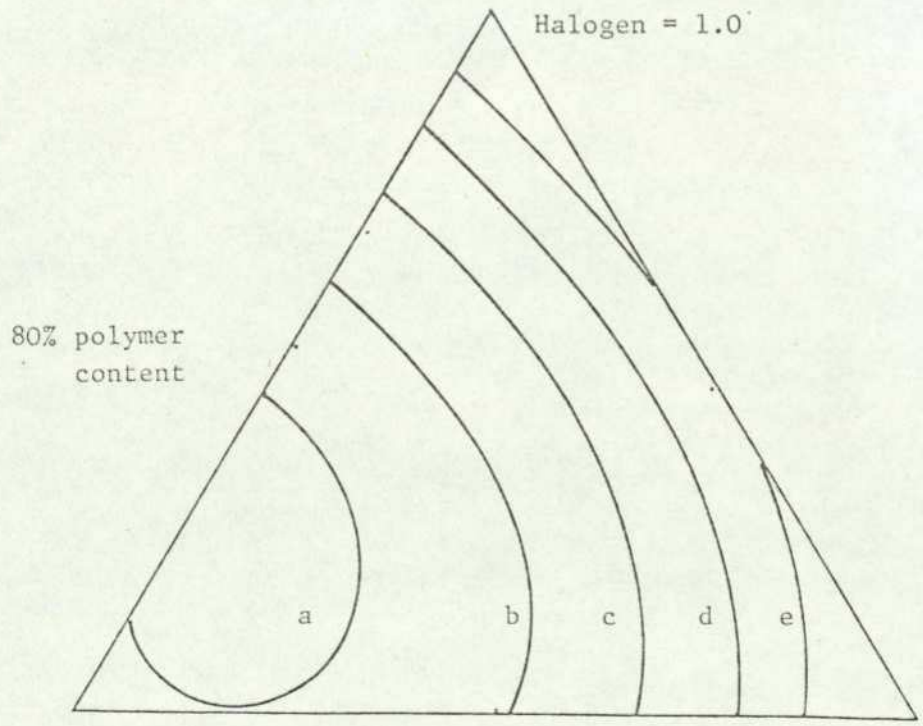

a = 34.0 b = 32.1 , c = 30.2 , d = 28.3, e = - .

FIGURE 72

Oxygen index of three-component systems in HDPE: $Sb_2O_3$/$(NH_4)_6Mo_7O_{24}.4H_2O$/S




a = 25.5 b =24.7, c =23.9, d =23.1 e =22.4,




a =25.1, b =24.4, c =23.6, d = 22.9 e = 22.1

candles burned with a steady flame which had a pronounced blue zone at the bottom.

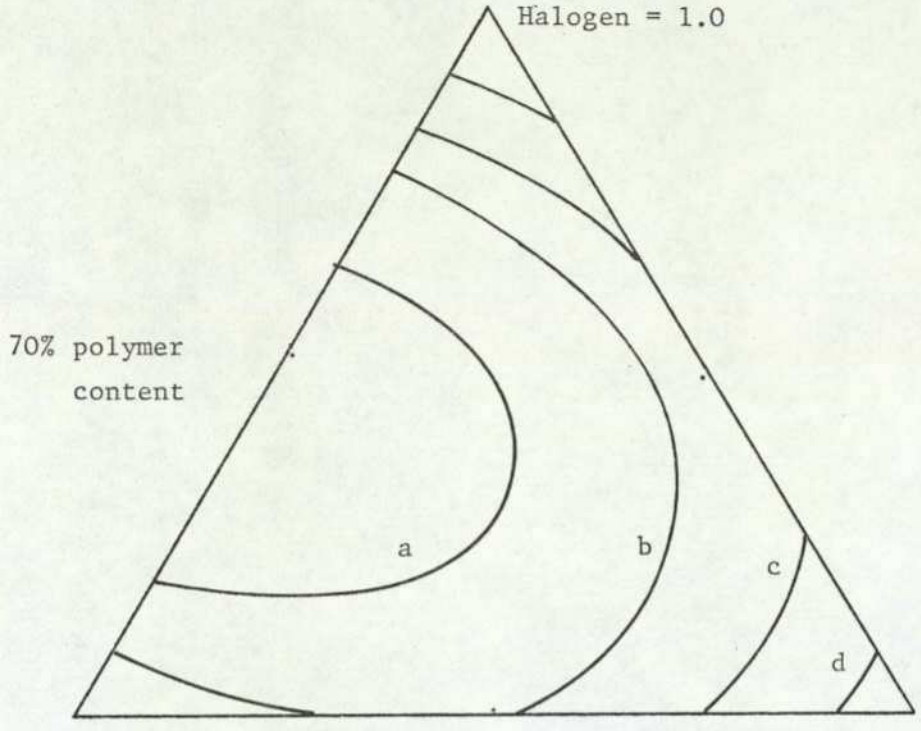
For samples containing 70% ABS, the quadratic contours are used to describe the flame retardant trends. Composites in the area between points 2, 4, 7 and 9 show the greatest flame-retardance potential (Figure 73). Compositions containing 80% ABS can be treated using similar quadratic contours and the residuals are well within the expected error. The polymer candles were easy to ignite and burned vigorously forming a light crusty char, which tended to extinguish the flame. If this char was constantly removed during the burning process, the flame remained on top of the melt at oxygen mole fractions up to 5 lower than the oxygen index. There was also a slight tendency for the candle to ablate under the oxygen index conditions.

3.2.5.9 $SnO_2/Fe_2O_3$/halogen compound

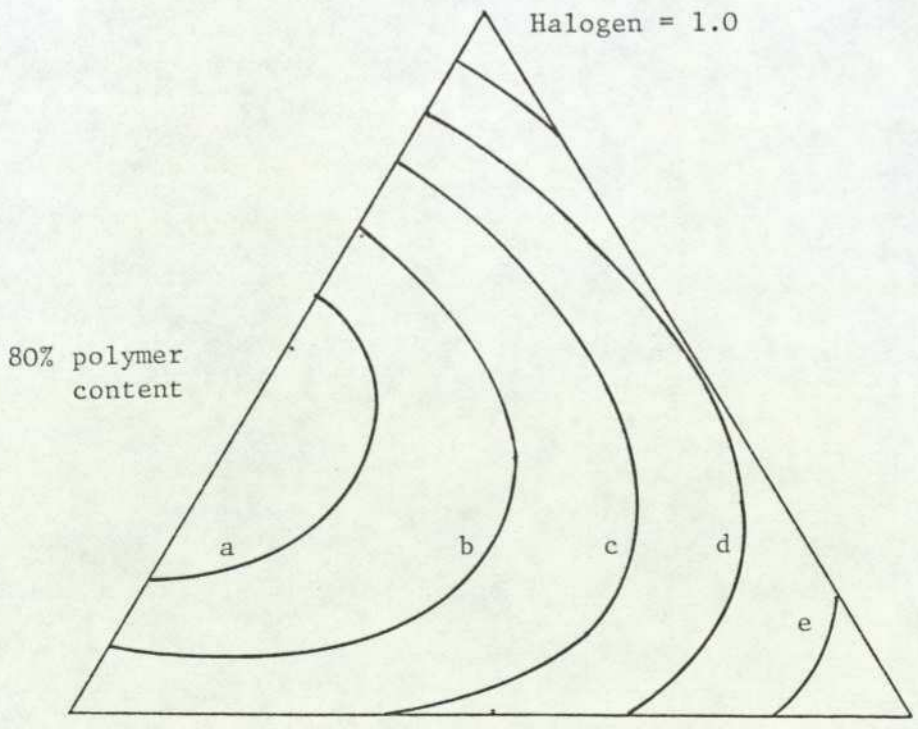
The flame retardant action appears to be due to the formation of a reddish, charred crust on the surface of the polymer. The flame becomes engulfed by a crater of char which is formed very quickly owing to the catalytic action of $Fe_2O_3$ on the decomposition of the polymer. For HDPE the maximum oxygen index is 27.0 at point 8 (Tables 59 and 60). There is little statistical justification for using either the quadratic or the reduced cubic plots, which indicate maximum flame retardant action around point 5

FIGURE 73

Oxygen index of three-component systems in ABS: $Sb_2O_3$/$(NH_4)_6Mo_7O_{24}$/Adine




a =33.7, b =31.8, c =30.0, d =28.1, e = - .




a =28.1 b =27.4 , c =26.6 , d =25.9, e =25.1 .

(Figure 74). For compositions containing 80% HDPE, the cubic plot also indicates a maximum response near the midpoint along the axis joining points 2 and 3.

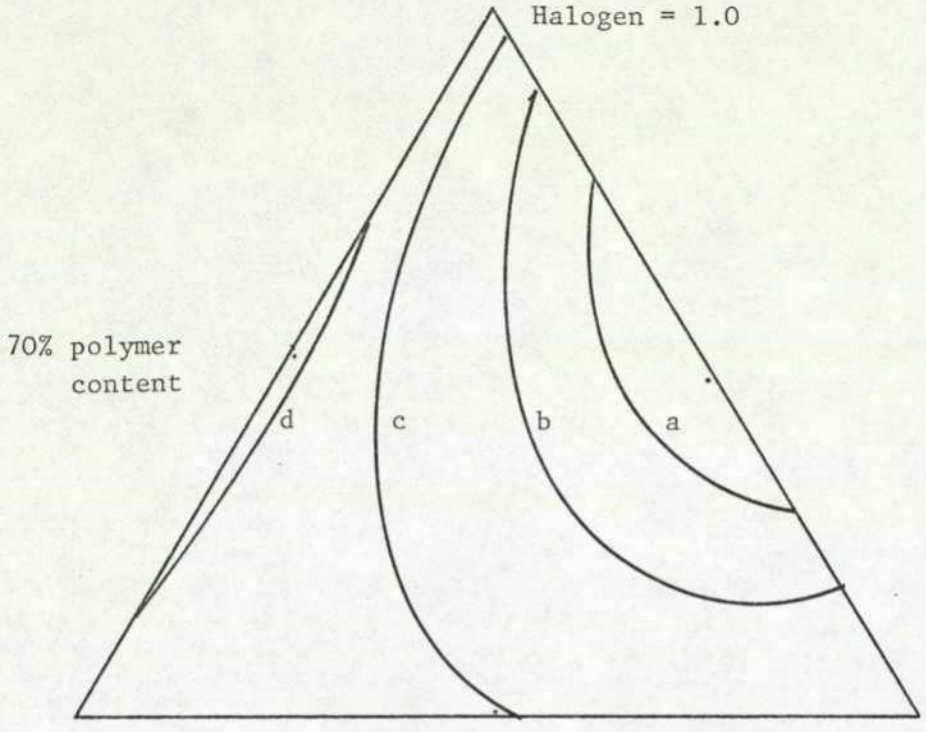
With ABS and 70% of polymer present, this combination of additives appears to have an effect equivalent to that of $Sb_2O_3$ alone at the same concentrations. This may be attributed to the rapid and excessive formation of carbonaceous residue, which physically hinders combustion. The quadratic regression contours illustrate the trends and again suggest that compositions around point 5 will produce a maximum response (Figure 75).

3.2.5.10 SnO/ZnO/halogen compound

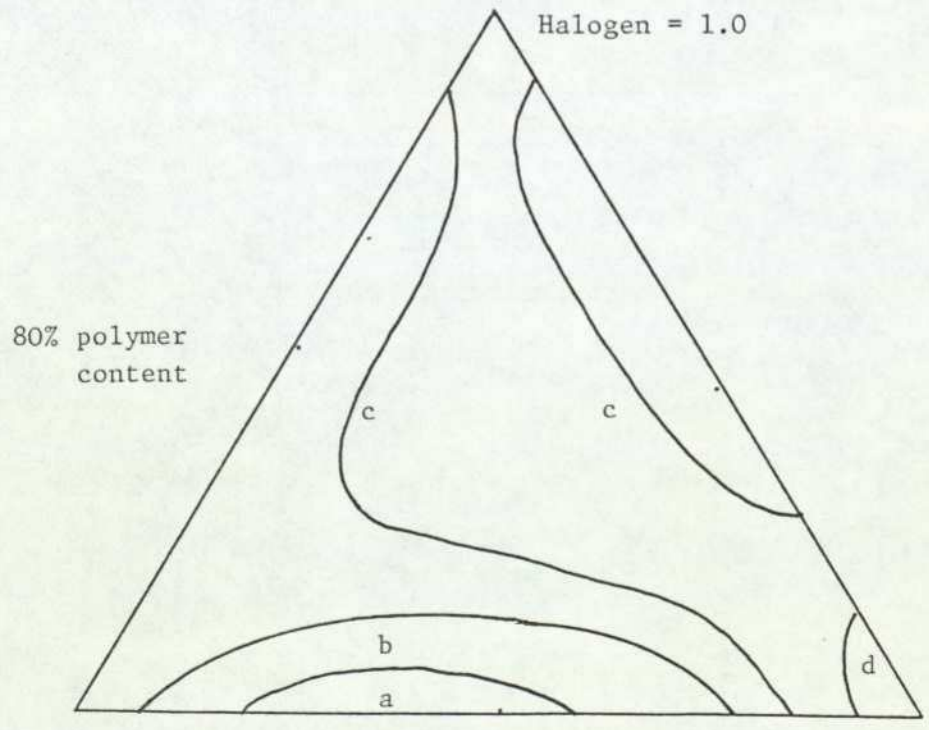
The oxygen index results for systems containing 70% HDPE show an area of maximum flame-retardance at the centre of the triangle (Tables 59 and 60). For systems containing 80% polymer, however, the maximum oxygen index lies between points 2 and 6 (Figure 76), and this shows that SnO is controlling the flame-retardant action with little contribution from ZnO. The inconsistency is reflected in the statistical analysis of the results. Thus the F-test values obtained are smaller than the variance ratio test values at the 90th percentile. It should be noted that, for systems containing 80% HDPE, there is only a small variation of oxygen index throughout the triangle. Longer ignition times were required close to the oxygen index conditions. The flame burned down

FIGURE 74

Oxygen index of three-component systems in HDPE: $SnO_2/Fe_2O_3$/S70



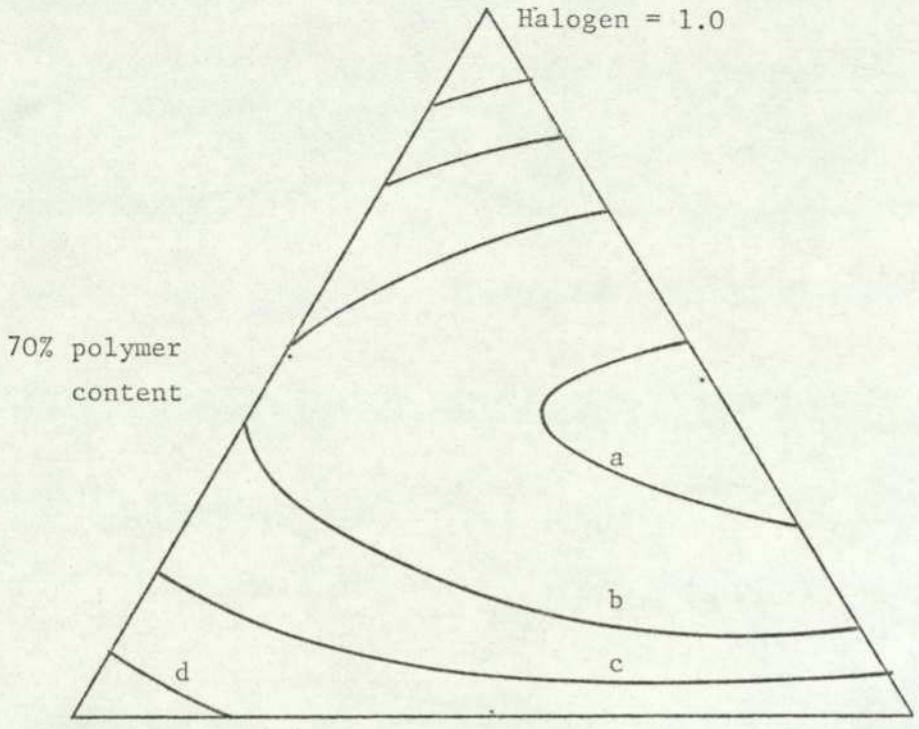

a = 25.0 b = 24.1 c = 23.2 d = 22.3



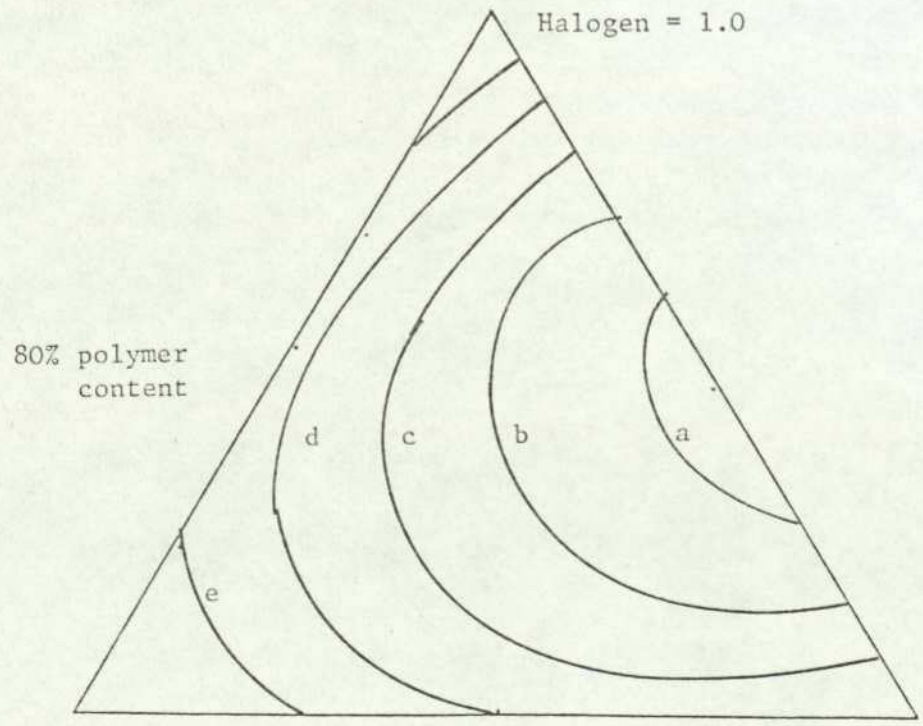

a = 21.8 b = 21.5 c = 21.2, d = 20.9 e = 20.6

FIGURE 75

Oxygen index of three-component systems in ABS: $SnO_2/Fe_2O_3$/Adine



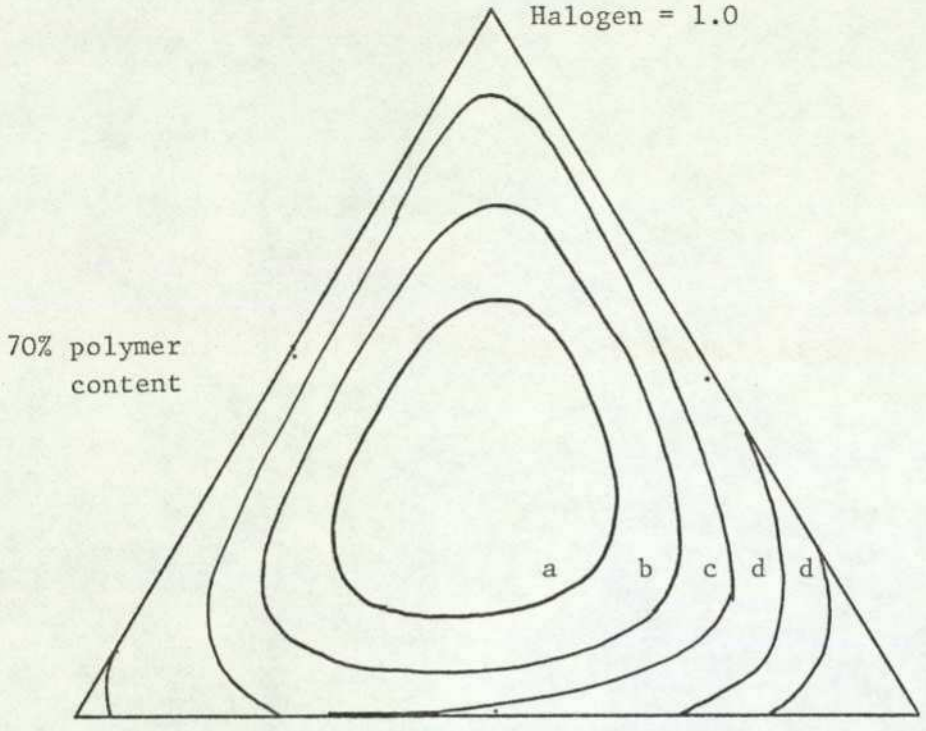

a =30.7, b = 29.4 c = 28.2 d =26.9, e = - .



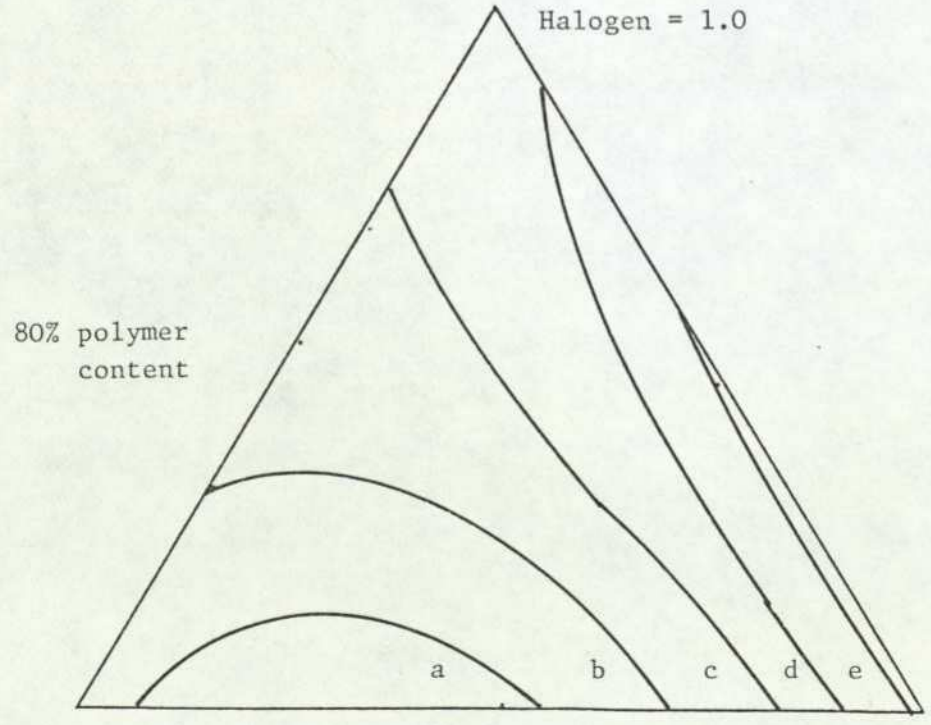

a =28.1 b =27.3 , c =26.5 , d =25.7, e =24.8 .

FIGURE 76

Oxygen index of three-component systems in HDPE: SnO/ZnO/S70




a =23.5, b =22.9, c =22.3, d =21.8 e =21.2.




a = 22.0 b = 21.5 c = 21.0 d = 20.5 e = 20.0

the sides of the candle leaving a thin layer of char on the polymer. The burning was vigorous and the flame died at extinction without flickering. Re-ignition was difficult in areas where char had formed unless sufficient ignition time was allowed for the polymer to melt and decompose and for the fuel to 'filter' through the pores of the carbon to the ignition source.

The ABS copolymer results are shown in Tables 61 and 62 for 70% and 80% polymer respectively. The polymers burned with a sooty flame from beneath a light crust of char. The quadratic plot for compositions containing 70% ABS and the cubic plot (Figure 77) for samples containing 80% ABS indicate a maximisation of the response around point 4 and the residuals lie within the limits of error.

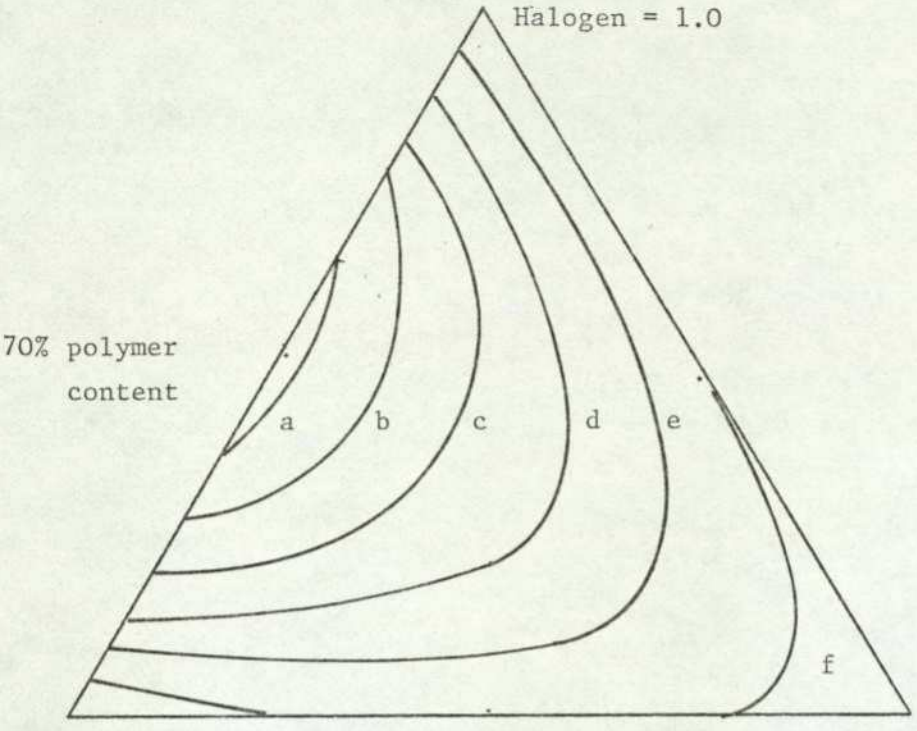
3.2.5.11 SnO/AlOOH/halogen compound

For samples containing 70% HDPE, the cubic regression surfaces highlight a maximum response of ca. 24.7 at the centre of the simplex design. This corresponds to the observed responses for points 7, 8, 9 and 10 (Figure 78) and the contours are statistically significant. A similar cubic response profile is observed for samples containing 80% HDPE and the residuals of $\pm$1.0 are within the expected experimental error. The candles were easy to ignite, but burned down the sides leaving a white, soft and flowery residue on the char.

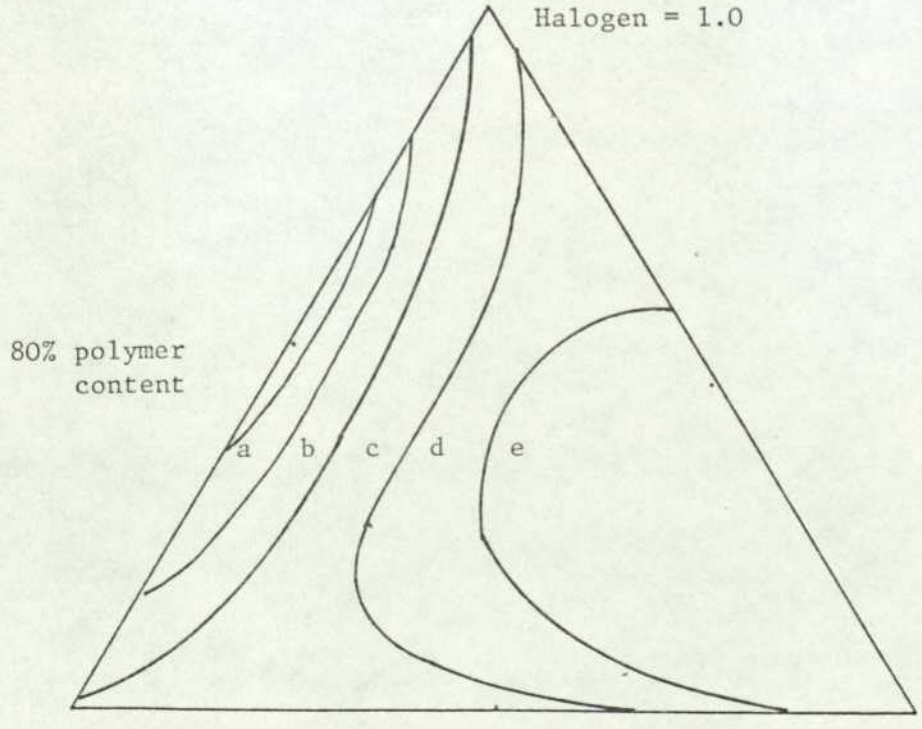
For compositions containing 70% ABS, the reduced cubic

FIGURE 77

Oxygen index of three-component systems in ABS: SnO/ZnO/Adine



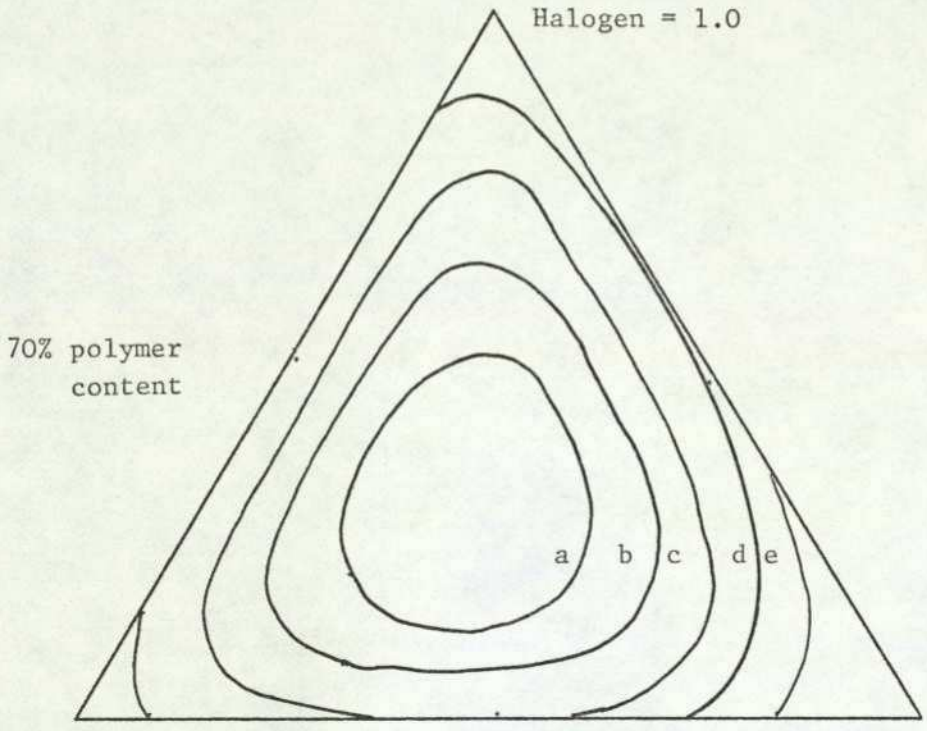

a = 27.8, b = 27.2, c = 26.6, d = 26.0, e = 25.4. f= 24.8



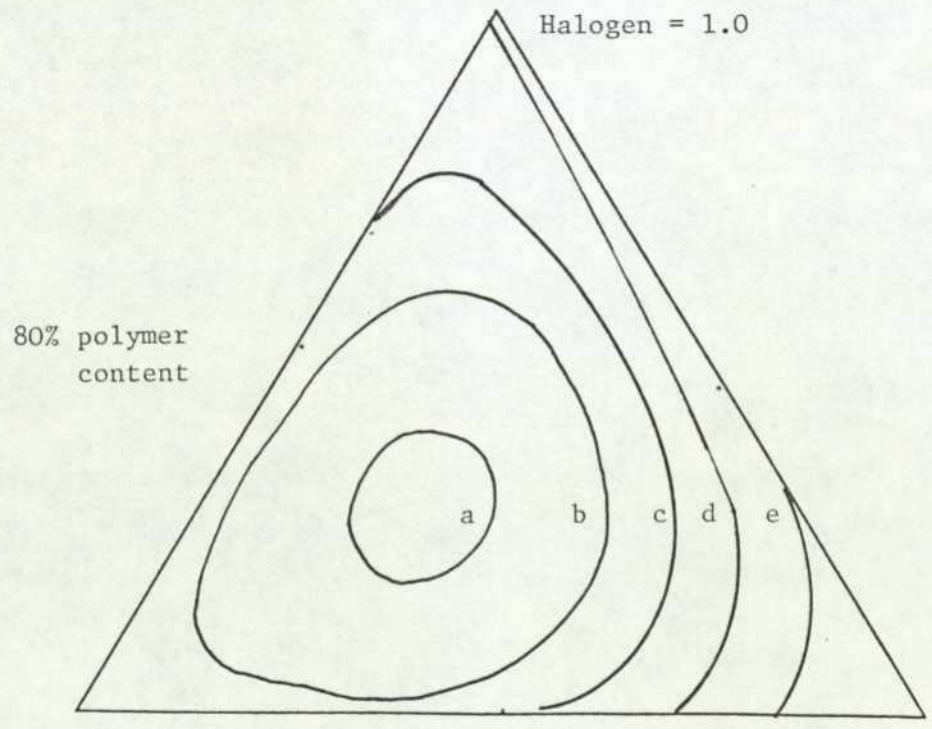

a =24.5 b = 24.0, c = 23.5, d =23.0, e = 22.5.

FIGURE 78

Oxygen index of three-component systems in HDPE: SnO/A1OOH/S7O




a =24.7, b =23.9, c =23.0, d =22.3 e = 21.4

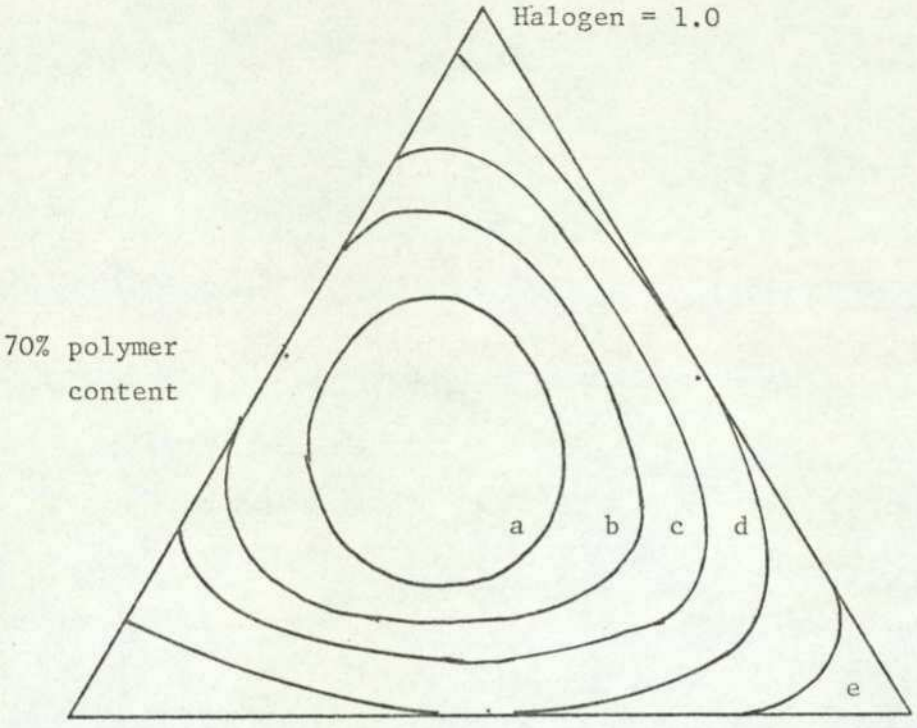



a = 23.1, b = 22.4, c = 21.7, d =21.1 , e = 20.4.

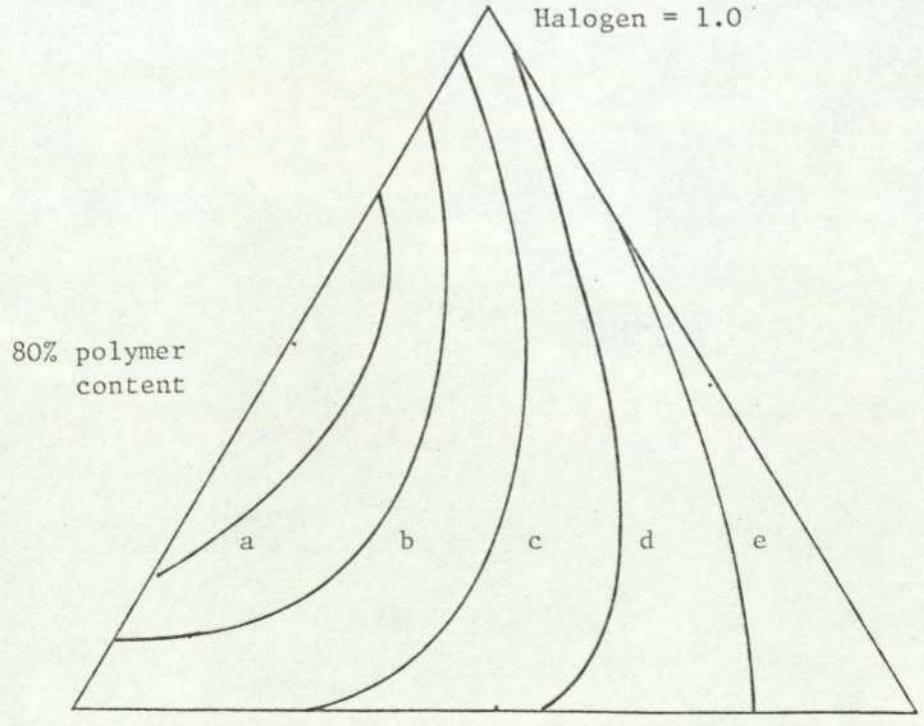
response surface highlights a plateau in the centre of the triangle where the response is a maximum (Figure 79). The quadratic regression is significant for samples containing 80% ABS. A maximum oxygen index of 25.0 is observed at point 4 and this is adequately represented in the plot. The candles burn with a cool flame, producing little soot or char.

FIGURE 79

Oxygen index of three-component systems in ABS: SnO/AlOOH/Adine




a = 28.8, b = 27.8, c = 26.8, d = 25.8, e = 24.8.




a = 24.6 b = 24.2, c = 23.8 , d = 23.4, e = 23.0.

### 3.2.6 Polymer/Inert Fillers

Aluminium oxide trihydrate is known to impart flame retardance to a polymer by increasing both the heat capacity and thermal conductivity of the polymeric "fuel". It also undergoes dehydration so that the water vapour reduces the flammability of the volatiles driven off when the material is subjected to heat. This, however, is not evident for samples of ABS and HDPE containing $Al_2O_3.3H_2O$ up to 75 phr (Tables 63 and 64).

The incorporation of anhydrous alumina and of aluminium oxide monohydrate also caused no variation in the oxygen index of both the polymers. The polymers burned with clean stable flames and ash accumulated at the burning surface. At high filler content, the ash remained standing above the test candle, glowed red in the flame, and appeared to stabilize the flame. At lower filler content, the inert material formed a crust which was periodically shed allowing the flame to flare up.

TABLE 63

The Oxygen Index of samples of HDPE polymer containing $Al_2O_3$, AlOOH and $Al_2O_3.3H_2O$.

| Metal Oxide Content p.h.r. | Oxygen Index | | |
|---|---|---|---|
| | $Al_2O_3$ | AlOOH | $Al_2O_3.3H_2O$ |
| 0 | 18.5 | 18.5 | 18.5 |
| 5 | 18.5 | 18.5 | 18.5 |
| 10 | 18.5 | 18.6 | 18.6 |
| 15 | 18.5 | 18.6 | 18.7 |
| 20 | 18.6 | 18.6 | 18.7 |
| 25 | 18.6 | 18.6 | 18.9 |
| 30 | 18.3 | 18.6 | 19.1 |
| 35 | 18.6 | 18.6 | 19.2 |
| 40 | 18.7 | 18.7 | 19.2 |
| 45 | 18.7 | 18.6 | 19.2 |
| 50 | 18.8 | 18.9 | 19.5 |

TABLE 64

The Oxygen Index of samples of ABS copolymer containing $Al_2O_3$, AlOOH and $Al_2O_3.3H_2O$.

| Metal Oxide Content p.h.r. | Oxygen Index | | |
|---|---|---|---|
| | $Al_2O_3$ | AlOOH | $Al_2O_3.3H_2O$ |
| 0 | 18.6 | 18.6 | 18.6 |
| 5 | 18.8 | 18.8 | 18.8 |
| 10 | 19.2 | 18.9 | 18.8 |
| 15 | 19.2 | 19.1 | 18.8 |
| 20 | 19.4 | 19.3 | 18.8 |
| 25 | 19.5 | 19.4 | 19.0 |
| 30 | 19.5 | 19.4 | 19.2 |
| 35 | 19.5 | 19.6 | 19.6 |
| 40 | 19.4 | 19.7 | 20.0 |
| 45 | 19.5 | 19.7 | 20.0 |
| 50 | 19.5 | 19.7 | 20.2 |
| 55 | 19.5 | 19.8 | 20.2 |
| 60 | 19.5 | 19.5 | 20.4 |
| 65 | 19.7 | 19.8 | 20.7 |
| 70 | 20.1 | 20.2 | 21.0 |
| 75 | 20.8 | 21.0 | 22.4 |

# 4 DISCUSSION

## 4.1 Synergism and Pseudo-synergism

The terms "synergism", and "synergistic effect" and "synergist" have all been used inconsistently throughout the literature on flame retardancy, especially where both ingredients of a mixture under consideration are active flame retardants. Often, the mathematical model by which the additive effect is calculated in order to test for synergism is ill defined. Where an explicit method for calculating the additive response is available, it is frequently based on the stated or implicit assumption that the flame-retardant response is linearly related to flame-retardant concentration. Throughout this work, it has been shown that the concentration-response relationship is usually non-linear and sometimes not even continuous. The definition of synergism is usually that it is an effect which is greater than the sum of the separate effects of two components. However, a consistent mathematical model must be defined before any such effect is confirmed.

The very extensive critical review by Weil[302] on synergism has prompted the following conclusion. The term "synergism" should be used only when a mathematical model supports the deduction of such an effect. If a "synergistic effect" is assumed without mathematical corroboration, then it may be termed "pseudo-synergistic" or "additive".

## 4.2 The Antimony-Halogen System

Antimony trioxide has been found to be of low flame-retardant activity in the absence of halogenated additives. The flame-retardant effect increases as halogen is added to the system, up to an atomic ratio of three halogen atoms per antimony atom. This has been clearly illustrated by keeping the percentage of antimony oxide in a polymer constant and increasing the halogen content. Thermogravimetric studies of antimony-halogen mixtures confirm this ratio[303]. A study of three-component systems shows that the centres of the approximately parabolic curves also correspond to a halogen-to-antimony ratio between 1.6:1 and 3:1 for maximum response.

The combined effect of antimony trioxide and halogen compounds is universally accepted as synergistic. The mathematical model proposed by Cleaver[304] is used to test this finding and serves as a basis for further investigations of the synergism between two flame-retardants. It is assumed that the flame retardant activity of any compound must be dependent upon its concentration and its specific fire-retardant efficiency. This can be expressed in the form of the equation:

$$C \times E = P \qquad \ldots . \quad (22)$$

where C = concentration of compound
E = specific efficiency as a flame regardant
P = overall performance, measured as oxygen index.

For Panel A in Table 65, equation 22 becomes:

$$25E_{Br} = 23.6 \text{ so that } E_{Br} = 0.944$$

where $E_{Br}$ = specific efficiency of bromine as a flame-retardant. For Panel B in Table 65, equation22 becomes:

$$25E_{Sb} = 20.0 \text{ so that } E_{Sb} = 0.800$$

where $E_{Sb}$ = efficiency of antimony as a flame-retardant. If synergism exists between the bromine and antimony, the efficiency of the halogen and antimony would increase when in combination, as in Panel C, so that

$$25E_{Br/Sb} > 12.5\left(E_{Br} + E_{Sb}\right) = P$$

where $E_{Br/Sb}$ is the efficiency of the combined flame-retardant.

Now $12.5\left(E_{Br} + E_{Sb}\right) = 12.5\ (0944 + 0.800)$ and

$$P = 21.8$$
$$P < 26.9$$

thus showing that a synergistic effect does exist. A similar conclusion is reached for the interaction of antimony oxide and S70 Electrofine (chlorine compound).

No attempt has been made to postulate or define the mode of interaction between antimony oxide and the halogen compounds. However, it was noticed that all the antimony-halogen interactions were exothermic, and led to volatilisation of the trihalide. Antimony trihalide species were also identified in this work using mass spectrometry.

TABLE 65

The Oxygen Index values for ABS copolymer containing Adine 0102 and $Sb_2O_3$, for use in synergism calculations.

| | Fire-retardant content | M.O./Halogen species content p.h.r. | Oxygen Index |
|---|---|---|---|
| (A) | Adine 0102 (30 p.h.r.) | 25 | 23.6 |
| (B) | $Sb_2O_3$ (30 p.h.r.) | 25 | 20.0 |
| (C) | Adine 0102 (15 p.h.r.) | 12.5 | 26.9 |
| | $Sb_2O_3$ (15 p.h.r.) | 12.5 | |

## 4.3 The screening of other metal oxides as possible synergists

### 4.3.1 Metal oxides

Benbow and Cullis[305] suggest that "it is possible to determine which metal oxides may be useful, as replacements for antimony oxide, by heating them in 1:3 mixtures with a chlorinated wax. The extent of volatilisation of the metal oxide will depend both on its ability to absorb and react with the liberated hydrogen chloride and also on the boiling point of the metal chloride formed".

The above technique will, of course, only indicate which metal oxides are capable of the same mode of synergistic action as antimony oxide. Involatility in these experiments does not mean that the metal oxide is not capable of exerting any flame-retardant action; rather it stresses that the mechanism of such action is not similar to that of antimony oxide. The initial screening of various metal oxides and hydrated metal oxides showed at least four different types of reproducible behaviour.

(i) Reactive oxides: Certain metal oxides, notably those of antimony, copper(II), and zinc, are volatilised completely as the corresponding halides when heated with chlorinated wax. However, of these, only zinc oxide is worthy of further study as a possible replacement for antimony oxide; the oxide of copper(II) forms a halide which is volatile only above 600°C, so that it may tend to accumulate at the surface of a burning polymer rather than enter the flame.

Mixtures of zinc oxide with oxides of antimony, tin(II) and tin(IV) respectively, do indicate some useful interaction of the metal oxides and chlorinated wax leading to "pseudo-synergistic" volatilisation as their corresponding halides.

(ii) Inert Oxides: The three aluminium oxychlorides and three aluminium oxides, namely $Al_2O_3$, AlOOH and $Al_2O_3.3H_2O$, were not volatilised when heated with chlorinated wax, the decomposition of which is not affected except as a result of the increase in surface area. There is no analytical evidence for the formation of aluminium trichloride in any of these experiments. In the case of oxychlorides, the halogen compound is volatilised at temperatures and rates similar to those at which it normally decomposes on its own.

The decomposition of aluminium oxide trihydrate is extremely endothermic, particularly the two initial reactions during which the material loses 4% and 24% respectively of its initial weight. This is of particular interest as, in the burning process, volatile polymer fragments are produced through an endothermic cracking reaction in the pyrolysis zone as a result of part of the heat of combustion being transferred back to the polymer. These volatile products travel to the combustion zone, where they react exothermically with oxygen. By acting as a heat-sink and sacrificially absorbing a portion of the heat of combustion transmitted

back to the condensed phase, aluminium oxide trihydrate could retard pyrolysis and hence reduce the burning rate. Dilution of combustion gases by water vapour and participation by water in condensed phase reactions is also of importance at least in certain cases.

The monohydrate also decomposes and loses water of hydration endothermically, but the exothermicity of the reactions of the chlorinated wax is not greatly reduced. There is no evidence from thermogravimetric results of "synergism" between aluminium oxide monohydrate and chlorinated wax and the mode of decomposition is very different from that of $Sb_2O_3$ and halogenated wax.

When the monohydrate was mixed with other metal oxides such as $Sb_2O_3$, SnO and $SnO_2$, it appears to interfere with the decomposition of these metal oxides and thus to prevent volatilisation as the corresponding metal halides. This is attributed to the relative lowering of the available heat released during such reactions.

(iii) Catalytic oxides: The oxide of iron(III) did not form the corresponding metal halide when heated with chlorinated wax. However, the compound appears to catalyse the breakdown of the halogen compound, even when used in minute quantities. Other volatile metal oxide/chlorinated wax systems are also affected by small amounts of $Fe_2O_3$.

(iv) Partially volatilised oxides: The anhydrous oxides of tin(II)

and tin(1V) are partially volatilised when heated with chlorinated wax and their usefulness as flame retardant synergists is doubtful. However, β-stannic acid or tin(1V)oxide hydrate showed enhanced reactivity, at much lower temperatures, when heated with chlorinated wax. The exotherm was observed over a narrower temperature range than that when antimony oxide was heated with chlorinated wax. The weight loss was much greater than would be expected if there were no interaction between the components of the mixture. As with antimony oxide, this exothermic weight loss is indicative of a reaction between stannic oxide hydrate (or one of its decomposition products) and the chlorine compound. Hence, it appears that, as Touval[306] suggested, "the water of hydration is, therefore, necessary to activate tin so that it behaves in a manner similar to antimony oxide". In the present investigation, however, such interaction occurs to a much smaller extent. Various mixtures of tin(11)oxide and tin(1V) oxide with other metal oxides undergo partial volatilisation as their metal chlorides. Only in mixtures of the tin oxides with $Fe_2O_3$ and ZnO is any interaction observed which is advantageous from the flame-retardant viewpoint.

4.3.2 Metal "oxy-salts"

When ammonium molybdate was heated alone, it decomposed by a multi-stage endothermic process. When mixed with the chlorinated wax, there seemed to be little

or no interaction between the molybdenum and the halogen. The molybdenum oxide formed as a decomposition product from the ammonium molybdate is volatilised quantitatively. The endothermicity of the reactions of the molybdate did not seem to affect the largely exothermic decomposition of Electrofine S70 in any way.

Ammonium tetraborate, which decomposes in eight small endothermic stages, did not appear to affect the decomposition of Electrofine S70, even though both compounds were volatilised above 400°C.

The thermal decomposition of the various oxychlorides of aluminium, showed little promise as possible flame retardant systems. None of these "oxy-salts", when mixed with S70, showed any flame retardant potential and were not investigated further. However, the effectiveness of Firebrake and mixtures of $Sb_2O_3$ with various molbydenum compounds led to further investigations of the $ZnO/NH_4HB_4O_7.3H_2O$ and $Sb_2O_3/(NH_4)_6Mo_7O_{24}.4H_2O$ systems used in conjunction with S70.

## 4.4 Mixed Metal Oxide/Halogen Systems

The screening of metal oxides in conjunction with chlorinated wax prompted an investigation to test whether two metal oxides when mixed with Electrofine S70, would promote the volatilisation of one another as their corresponding halides. The combinations investigated did not show much promise.

While the interaction between $Sb_2O_3$/ZnO and S70 showed a decrease of ca 10% in the percentage of metal oxide volatilised, that between $Sb_2O_3$/A100H and S70 showed a more positive antagonism than did that between $Sb_2O_3/SnO_2$ and S70. The only encouraging result was the catalytic effect of $Fe_2O_3$ on the volatilisation of $Sb_2O_3$ in conjunction with S70. $Fe_2O_3$ lowers the temperature at which the S70 and $Sb_2O_3$ interact by catalytically decomposing the S70. However, its overall effect is to reduce the magnitude of the interaction. Thus, while the destabilising action of $Fe_2O_3$ may be potentially useful, different (lower) ratios of $Sb_2O_3$ to halogen compound are required to optimise flame retardance with $Sb_2O_3$ when the iron oxide is present. Interaction between $Al_2O_3$ or aluminium oxide trihydrate with $Sb_2O_3$/S70 is not evident, although there is a decrease in the endothermicity of the reaction. This however is of interest as a 50:50 mixture of $Sb_2O_3$: $Al_2O_3.3H_2O$ may be sufficient to act as a heat-sink as

well as to volatilise the $Sb_2O_3$ so that it acts as a flame retardant.

There is no apparent interaction between any of the "screened" metal oxides and the $SnO_2$/S70 or the SnO/S70 systems. However, ZnO does increase the amount of SnO volatilised when mixed with S70.

The majority of the mixtures studied showed little or no interaction and indeed a decrease in the amount of metal oxide volatilised. This, however, does not prove that the systems in question have no potential as flame retardants. The thermogravimetric studies do show, however, that the mode of action of the various mixed metal oxide systems is different from that of the classical $Sb_2O_3$/halogen systems.

## 4.5 Flammability and triangular diagrams

In order to form a basis for discussion, the antimony oxide/halogen flame retardant system was investigated at various ratios and various total flame retardant levels. The two studies of greatest interest are those carried out at 70% polymer levels. The first involved ratios of metal oxide to halogen compound kept at the same overall level as that in any mixture sample in which $Sb_2O_3$ takes the place of both metal oxides. The second involves the same amounts of antimony trioxide and halogen but with increasing percentages of polymer. These studies clearly indicate that, for maximum flame retardant effectiveness, the metal oxide:halogen ratio should be greater than 1:2 w/w in the case of chlorinated wax and greater than 1:3 w/w for decabromobiphenyl. They also show quite definitely that the metal oxide is needed to increase the flame retardance.

The study of the flame-retardant effect of various metal oxide mixtures in halogen-containing polymers was carried out at both 30 and 20% flame retardant loadings. In general, the oxygen index values for 80% polymer, 20% flame retardant were found to be much lower than those for 70% polymer, 30% flame retardant. This is attributed to the fact that, when there is more polymer present, a larger

amount of fuel is produced on heating and the insufficient concentration of flame retardant present cannot significantly hinder the burning process. However, similar trends are observed for both sets of loadings.

When $SnO_2$ was used as a partial substitute for $Sb_2O_3$, it appeared to decrease slightly the flame retardant potential of the antimony oxide/halogen system. This decrease is just above the acceptable limit allowed for experimental error. In ABS, however, a slight synergism is observed between the binary metal oxide/halogen systems. The metal oxides appear to assist one another to volatilise the halogen compound and to act by a mechanism similar to that of the antimony/halogen system. Their effectiveness is increased for a 1:1 w/w mixture. $SnO_2$ seems an adequate, though slightly less effective, partial replacement for $Sb_2O_3$ in ABS. In HDPE, however, a different mechanism appears to operate. There is no apparent synergism between the metal oxides, and the flame retardance seems to be due mainly to the presence of $Sb_2O_3$, but to require lower concentrations of halogen.

The flame retardant effectiveness of $ZnO/Sb_2O_3$ mixtures seems to be smaller than that of antimony trioxide in ABS. Mathematically a slightly less-than-additive effect can be deduced, however, the residuals and mean square deviation suggesting a definite decrease

in flame retardant potential. Both the metal oxides are known to volatilise completely when heated with a halogen source. They do not however appear to help each other when mixed together. In HDPE a similar trend is observed, although when ZnO and $Sb_2O_3$ are present in a 1:4 ratio the oxygen index is found to be the same as that obtained without any zinc oxide. Partial substitution at such a ratio would thus prove slightly economical.

$Fe_2O_3$ produces not only a pronounced catalytic effect but also acts as a filler in the conferment of flame retardance on both ABS and HDPE. Synergism with $Sb_2O_3$ is observed in both polymers. The flame retardant effect is due to greatly increased char formation. This reduces the amount of fuel produced and smothers the flame.

Anhydrous alumina, aluminium oxide monohydrate and aluminium oxide trihydrate appear to have rather similar oxygen index values when mixed with $Sb_2O_3$ and a halogen source according to the experimental design. The deviation of oxygen index values for points within the triangle are less than 2.5 which appears to indicate a similar mode of action. Since the oxygen index values are, in general, greater than those observed for the corresponding antimony content, the oxides of alumina do appear to have some additional flame retardant effect;

although the flame retardance appears to be mainly due to the presence of $Sb_2O_3$.

The incorporation of talc in conjunction with an $Sb_2O_3$/halogen system into ABS copolymer appears to have a greater flame retardant effect than that shown by the hydrated oxides of alumina. This is attributable to the easier and greater release of water by the talc.

It is not possible to demonstrate synergism between ammonium molybdate and antimony oxide. The oxygen index values for mixtures of these compounds are ca. 2.5 lower than those obtained for systems containing the equivalent amount of $Sb_2O_3$ alone. Hence antagonism appears to be indicated. The two compounds are known to confer flame retardance on an organic polymer by two very different mechanisms. These mechanisms, however, interfere with one another and hence do not significantly decrease the flammability of the polymers.

The flammability of both ABS and HDPE is little affected by mixtures of SnO with ZnO and of SnO with AlOOH. It can be seen that there is some synergism between these two metal oxides. Neither is very effective on its own, but when mixed they do show an increased flame retardant effect. Aluminium oxide monohydrate does appear to activate the stannous oxide in some way. However, the flame retardance is not

nearly as marked as with the antimony/halogen system.

Touval[306] suggests that $SnO_2$ is an adequate flame-retardant substitute for $Sb_2O_3$. This is not however evident from the present work. The catalytic effect of $Fe_2O_3$ is also not capable of improving the flame retardance of the $SnO_2$/halogen system. It was however extremely difficult to incorporate $SnO_2$ into either of the polymers. At the temperatures required for incorporation, $SnO_2$ volatilises the halogen to form the hydrogen halide and corresponding metal halides and hence takes the flame retarding species with it. For this reason alone no further work was carried out on any other metal oxide/$SnO_2$ mixtures.

Similarly, ammonium tetraborate was impossible to incorporate into either polymer, even at temperatures $20^{\circ}$ lower than that required for normal incorporation. It was hoped that the use of a ZnO/ammonium tetraborate mixture would help to produce flame retardant effects similar to those observed with Firebrake. Hence, although synergism is sometimes the result of a mathematical calculation, it does not necessarily prove to be advantageous. The substitution of a poor flame retardant by $Sb_2O_3$ may improve its oxygen index; but the converse is not true.

## 4.6 Synergism: The aluminium oxides/halogen systems

If synergism is defined as an effect which is greater than the sum of the separate effects of two components, irrespective of the response relationship, then the addition of a halogen compound to any of the three oxides of aluminium in ABS co-polymer may be said to be synergistic. There appears to be a positive improvement in the oxygen index of alumina (particularly the anhydrous oxide) when increasing quantities of decabromobiphenyl are incorporated, together with it, into ABS and HDPE. Hence alumina appears to activate the decomposition of the halogen compound and to enable it to interfere with the flame reactions. The effect in HDPE containing a chlorinated wax is less significant.

The oxygen index response for samples of ABS copolymer containing aluminium oxide trihydrate and increasing amounts of Adine 0102 shows two distinct curves. This indicates that, above 30 phr Adine, an additional flame retardant mechanism starts to function.

At low loadings of Adine, the bromine present may be converted to aluminium tribromide. Under these conditions, the flame-retardant effect observed can be ascribed partly to the water vapour released and partly to the inhibiting effect of $AlBr_3$ on the condensed-phase

reactions. When the concentration of Adine is increased above 30 phr (so that the Br : Al ratio is greater than 3:1), free hydrogen bromide is formed which acts in the gas phase. The results with HDPE show that the effects, although smaller, are still quite pronounced when decabromobiphenyl is the halogen source. Mass spectrometric analysis of these compounds shows a build-up of the hydrogen halide, but no aluminium/halogen species.

The aluminium oxide monohydrate/halogen system also causes some increase in the oxygen index of the polymers into which it is incorporated. However, the improvement in flame retardance is the least significant found for the three oxides of aluminium. The monohydrated alumina does not act simply as an inert filler; nor does it decompose very endothermically or give off large quantities of water (as $Al_2O_3.3H_2O$ does); no vapour phase aluminium species have been found analagous to the antimony specimes formed from $Sb_2O_3$. However, $Al_2O_3.H_2O$ still appears to have synergistic effect in conjunction with halogen compounds, particularly with high Br : Al ratios.

The interaction of anhydrous alumina with decabromibiphenyl is found to produce a large positive effect on the flame retardance of ABS copolymer. The sharp, roughly linear rise in oxygen index

indicates a definite synergistic interaction which appears to be confirmed by preliminary mass spectrometric studies. Anhydrous alumina evidently reacts with the organic halogen compound at the temperature of the flame and hence considerably increases the flame retardance of the polymer.

The difference between the effect of anhydrous alumina on the one hand and of the hydrated aluminium oxide on the other suggest that water inhibits the condensed-phase action of $AlBr_3$.

The modes of flame-retardant action of the three oxides of aluminium may be somewhat different from one another, although all three compounds show some synergism with bromine compounds. Chlorine-compounds (e.g. Electrofine S70) do not exhibit synergistic effects with the aluminium oxides, at least in HDPE.

# 5 CONCLUSIONS

## 5. Conclusions

(1) Studies have been made of the flame-retardant action of a variety of metal oxides, which have been investigated as possible alternatives for antimony (III) oxide. Attempts have been made to predict those metal oxides which are most likely to be effective flame retardants by means of thermogravimetric studies of their behaviour when they are heated alone, with polymers and with appropriate halogen compounds. The results show, however, that thermogravimetric behaviour is at best only a qualitative indicator of flame retardant activity.

(2) Other metal oxides have been introduced into polymers both as partial substitutes for antimony oxide or in an additive capacity. In general none of the compounds studied is as effective a flame-retardant as $Sb_2O_3$ when used as a substitute for it. However, the substitutes with the greatest flame-retardant effect are $Fe_2O_3$, talc and AlOOH(which has for the first time received attention in this content. Further addition of metal oxides (to polymer-antimony systems) generally improves the flame-retardance. The three aluminium oxides and $Fe_2O_3$ were found to be the most effective.

(3) Thermogravimetric and mass spectrometric investigations indicate that iron (III) oxide acts partly as a filler, but also by promoting char formation and by catalysing the decomposition of the halogen compound. The aluminium oxides all act predominantly as fillers, absorbing heat and diluting flammable gases by the endothermic release of water vapour. Evidence has been obtained (for what is believed to be the first time) for the chemical interaction of anhydrous alumina with the halogen compounds.

# 6 APPENDIX

## 6. Appendix

The City University Cafeteria computer system was used to analyse the oxygen index responses observed .The programme is set to read in an introductory set of statements, followed by the observed values of the oxygen index for one experimental design. The programme then calculates the necessary coefficients (using Scheffe's Simplex Lattice Design) for linear,quadratic and the reduced cubic equations, conducts a statistical analysis on the observed values by comparing them with the values obtained for each response using the lattice model, and then plots each response that satisfies each model.

```
      MASTER FEROZE
      DIMENSION X(10,7),XT(70),XTX(70),Y(70),XTY(70),BETA(49),VARIA(7,
     1,YC(10),EC(10),AP(100,10),TITRE(20),GRAPH(20)
      INTEGER VTL(7),VTM(7)
      DATA X/1.000000,2*0.000000,2*0.500000,0.000000,0.333333,0.666666,
     12*0.166666,0.000000,1.000000,0.000000,0.500000,0.000000,0.500000,
     20.333333,0.166666,0.666666,0.166666,2*0.000000,1.000000,0.000000,
     32*0.500000,0.333333,2*0.166666,0.666666,3*0.000000,0.250000,
     42*0.000000,3*0.111111,0.027778,4*0.000000,0.250000,0.000000,
     52*0.111111,0.027778,0.111111,5*0.000000,0.250000,0.111111,
     60.027778,2*0.111111,6*0.000000,0.037037,3*0.018518/
   41 FORMAT(/30X,'MATRICE X'/30X,9('-')///13X,'X01',9X,'X02',9X,'X03',
     19X,'X04',9X,'X05',9X,'X06'//(10X,6(F8.6,4X)))
   72 FORMAT(//30X,'VECTOR XPRIM Y'/30X,15('-')//10X,3(E12.6,1X)//)
   61 FORMAT(30X,'MATRICE XPRIM X'/30X,15('-')//15X,'X01',10X,'X02',10X
     1'X03',10X,'X04',10X,'X05',10X,'X06'//(10X,6(E12.6,1X)))
   71 FORMAT(//30X,'VECTOR XPRIM Y'/30X,15('-')//10X,6(E12.6,1X)//)
   81 FORMAT(30X,'MATRICE (XPRIM X)-1'/30X,19('-')//15X,'X01',10X,'X02'
     110X,'X03',10X,'X04',10X,'X05',10X,'X06'//(10X,6(E12.6,1X)))
   91 FORMAT(1X,29X,'MODEL POLYNOMIAL OF DEGREE 2'///31X,'MIXTURE OF 3
     1CONSTITUANTS'/31X,'SPECIFICATION OF VARIABLES :'/)
   42 FORMAT(/30X,'MATRICE X'/30X,9('-')///13X,'X01',9X,'X02',9X,'X03',
     1//(10X,3(F8.6,4X)))
   62 FORMAT(30X,'MATRICE XPRIM X'/30X,15('-')//15X,'X01',10X,'X02',10X
     1'X03'//(10X,3(E12.6,1X)))
   82 FORMAT(30X,'MATRICE (XPRIM X)-1'/30X,19('-')//15X,'X01',10X,'X02'
     110X,'X03'//(10X,3(E12.6,1X)))
  991 FORMAT(1X,29X,'MODEL POLYNOMIAL OF DEGREE 1'///31X,'MIXTURE OF 3
     1CONSTITUANTS'/31X,'SPECIFICATION OF VARIABLES :'/)
   10 FORMAT(10F0.0)
   11 FORMAT('1',30X,'LINEAR REGRESSION OF MULTIPLE-MIXTURES'/30X,39('-
     1)//30X,20A4)
```

```
   12 FORMAT(20A4)

   20 FORMAT(8A4)

   21 FORMAT(2F0.0)
   30 FORMAT(35X,8A4)

   40 FORMAT(/30X,'MATRICE X'/30X,9('-')///13X,'X01',9X,'X02',9X,'X03',
     19X,'X04',9X,'X05',9X,'X06',9X,'X07'//(10X,7(F8.6,4X)))

   50 FORMAT('1',/30X,'VECTOR Y' /30X,9('-')//10X,10(F5.2,3X)//)

   60 FORMAT(30X,'MATRICE XPRIM X'/30X,15('-')//15X,'X01',10X,'X02',10X,
     1'X03',10X,'X04',10X,'X05',10X,'X06',10X,'X07'//(10X,7(E12.6,1X)))

   70 FORMAT(//30X,'VECTOR XPRIM Y'/30X,15('-')//10X,7(E12.6,1X)//)

   80 FORMAT(30X,'MATRICE (XPRIM X)-1'/30X,19('-')//15X,'X01',10X,'X02',
     110X,'X03',10X,'X04',10X,'X05',10X,'X06',10X,
     2'X07'//(10X,7(E12.6,1X)))

   90 FORMAT(1X,29X,'REDUCED CUBIC MODEL'///31X,'MIXTURE OF 3 CONSTITUAN
     1TS'/31X,'SPECIFICATION OF VARIABLES :'/)

  994 FORMAT(12X,'X07',8X,E12.6,5X,E12.6)

   94 FORMAT(10X,'COEFFICIENTS'/10X,12('-')/10X,'VARIABLE',6X,'COEFFICIE
     1NT',5X,'SIGMA-SQUARE'/(12X,'X0',I1,8X,E12.6,5X,E12.6))

   96 FORMAT('1',9X,'CALCULATED VALUE'/10X,17('-')/10X,'NUMBER',6X,
     1'Y OBSERVED',6X,'Y CALCULATED',6X,'DIFFERENCE'/(12X,I2,7X,E12.6,
     25X,E12.6,5X,E12.6))

   51 FORMAT(20A4)

   52 FORMAT(5X,18A4)

   53 FORMAT(5X,'LINEAR MODEL',3X,10(F5.2,3X))
   54 FORMAT(5X,'QUADRATIC MODEL',3X,10(F5.2,3X))
   55 FORMAT(5X,'CUBIC MODEL',3X,10(F5.2,3X))
   97 FORMAT('1')

      I=0

  100 I=I+1

      READ(5,20)(VARIA(I,J),J=1,8)

      IF(I-7)100,120,120

  120 READ(5,12,END=1000)(TITRE(J),J=1,20)

      READ(5,51)(GRAPH(J),J=1,20)

      READ(5,10)(Y(I),I=1,10)
```

```
      READ(5,21)YMIN,PAS
      WRITE(6,11)(TITRE(J),J=1,20)
      WRITE(6,991)
      WRITE(6,30)((VARIA(I,J),J=1,8),I=1,3)
  610 WRITE(6,42)((X(I,J),J=1,3),I=1,10)
  615 WRITE(6,50)(Y(I),I=1,10)
      N=10
      M=3
  620 CALL GMTRA(X,XT,N,M)
      N=3
      M=10
      L=3
  630 CALL GMPROD(XT,X,XTX,N,M,L)
  635 WRITE(6,62)(XTX(I),I=1,9)
      NORDRE=3
      CALL MINV(XTX,NORDRE,DETERM,VTL,VTM)
      N=3
      M=10
      L=1
  640 CALL GMPROD(XT,Y,XTY,N,M,L)
  645 WRITE(6,72)(XTY(I),I=1,3)
      WRITE(6,82)(XTX(I),I=1,9)
      N=3
      M=3
      L=1
      CALL GMPROD(XTX,XTY,BETA,N,M,L)
      NCOEF=3
      CALL CALCUL(NCOEF,X,BETA,Y,YC,EC,VR)
      SBETA1=(VR*XTX(1))**0.5
  680 WRITE(6,94)(I,BETA(I),SBETA1,I=1,3)
  690 WRITE(6,96)(I,Y(I),YC(I),EC(I),I=1,10)
      CALL RACINE(BETA,YMIN,PAS,AP)
```

```
      LIGNE=100
      MCOL=10
      LPLOT=0
      NTRI=1
      WRITE(6,97)
      WRITE(6,52)(GRAPH(J),J=1,20)
      WRITE(6,53)(Y(I),I=1,10)
      CALL PLOT(AP,LIGNE,MCOL,LPLOT,NTRI,YMIN,PAS)
      WRITE(6,11)(TITRE(J),J=1,20)
      WRITE(6,91)
      WRITE(6,30)((VARIA(I,J),J=1,8),I=1,6)
  510 WRITE(6,41)((X(I,J),J=1,6),I=1,10)
  515 WRITE(6,50)(Y(I),I=1,10)
      N=10
      M=6
  520 CALL GMTRA(X,XT,N,M)
      N=6
      M=10
      L=6
      CALL GMPROD(XT,X,XTX,N,M,L)
  530 WRITE(6,61)(XTX(I),I=1,36)
      NORDRE=6
  540 CALL MINV(XTX,NORDRE,DETERM,VTL,VTM)
      N=6
      M=10
      L=1
  550 CALL GMPROD(XT,Y,XTY,N,M,L)
  560 WRITE(6,71)(XTY(I),I=1,6)
      WRITE(6,81)(XTX(I),I=1,36)
      N=6
      M=6
      L=1
  570 CALL GMPROD(XTX,XTY,BETA,N,M,L)
```

```
      NCOEF=6
      CALL CALCUL(NCOEF,X,BETA,Y,YC,EC,VR)
      SBETA1=(VR*XTX(1))**0.5
      SBETA2=(VR*XTX(22))**0.5
  580 WRITE(6,94)(I,BETA(I),SBETA1,I=1,3),(I,BETA(I),SBETA2,I=4,6)
  590 WRITE(6,96)(I,Y(I),YC(I),EC(I),I=1,10)
      CALL RACINE(BETA,YMIN,PAS,AP)
      LIGNE=100
      MCOL=10
      LPLOT=0
      NTRI=1
      WRITE(6,97)
      WRITE(6,52)(GRAPH(J),J=1,20)
      WRITE(6,54)(Y(I),I=1,10)
      CALL PLOT(AP,LIGNE,MCOL,LPLOT,NTRI,YMIN,PAS)
      WRITE(6,11)(TITRE(J),J=1,20)
   95 WRITE(6,90)
      WRITE(6,30)((VARIA(I,J),J=1,8),I=1,7)
  110 WRITE(6,40)((X(I,J),J=1,7),I=1,10)
  125 WRITE(6,50)(Y(I),I=1,10)
      N=10
      M=7
  130 CALL GMTRA(X,XT,N,M)
      N=7
      M=10
      L=7
  140 CALL GMPROD(XT,X,XTX,N,M,L)
  145 WRITE(6,60)(XTX(I),I=1,49)
      NORDRE=7
  150 CALL MINV(XTX,NORDRE,DETERM,VTL,VTM)
      N=7
      M=10
```

```
      L=1
  160 CALL GMPROD(XT,Y,XTY,N,M,L)
  165 WRITE(6,70)(XTY(I),I=1,7)
  170 WRITE(6,80)((XTX(I),I=1,49))
      N=7
      M=7
      L=1
  180 CALL GMPROD(XTX,XTY,BETA,N,M,L)
      NCOEF=7
      CALL CALCUL(NCOEF,■,BETA,Y,YC,EC,VR)
  220 SBETA1=(VR*XTX(1))**0.5
      SBETA2=(VR*XTX(25))**0.5
      SBETA3=(VR*XTX(49))**0.5
  230 WRITE(6,94)(I,BETA(I),SBETA1,I=1,3),(I,BETA(I),SBETA2,I=4,6)
      WRITE(6,994)BETA(7),SBETA3
  240 WRITE(6,96)(I,Y(I),YC(I),EC(I),I=1,10)
      CALL RACINE(BETA,YMIN,PAS,AP)
      LIGNE=100
      MCOL=10
      LPLOT=0
      NTRI=1
      WRITE(6,97)
      WRITE(6,52)(GRAPH(J),J=1,20)
      WRITE(6,55)(Y(I),I=1,10)
      CALL PLOT(AP,LIGNE,MCOL,LPLOT,NTRI,YMIN,PAS)
      DO 250 I=1,7
      BETA(I)=0.0
  250 CONTINUE
      GO TO 120
 1000 STOP
      END
      SUBROUTINE RACINE(BETA,YMIN,PAS,AP)
```

```
      DIMENSION BETA(7),AP(100,10),RACIN1(10),RACIN2(10)
      DO 100 I=1,100
      DO 100 J=1,10
      AP(I,J)=0.0
  100 CONTINUE
      L=0
      DO 500 K=1,50
      X1=FLOAT(K-1)/50.0
      YP=YMIN
      DO 350 J=4,10
      A=-X1*BETA(7)-BETA(6)
      B=(-BETA(7)*X1+BETA(4)-BETA(5)-BETA(6)+BETA(7))*X1
      B=B+BETA(2)+BETA(6)-BETA(3)
      C=(-BETA(5)*X1+BETA(1)+BETA(5)-BETA(3))*X1+BETA(3)-YP
      IF(A)320,300,320
  300 RACIN1(J)=-C/B
      RACIN2(J)=0.0
      GO TO 340
  320 DELTA=B*B-4.0*A*C
      RACIN1(J)=-B/2.0/A
      RACIN2(J)=DELTA/4.0/A/A
  340 YP=YP+PAS
  350 CONTINUE
      L=L+1
      XCOTE=X1/2.0
      NX=K-1
      IF(MOD(NX,5))355,355,356
  355 AP(L,3)=XCOTE
      GO TO 357
  356 AP(L,2)=XCOTE
  357 AP(L,1)=0.866*X1
      DO 400 J=4,10
```

```
      IF(RACIN2(J))400,360,360
  360 X2MOIN=RACIN1(J)-(RACIN2(J))**0.5
      IF(X2MOIN)400,370,365
  365 IF(X2MOIN-1.0)370,400,400
  370 X3=1.0-X1-X2MOIN
      IF(X3)400,375,375
  375 AP(L,J)=X3+X1/2.0
  400 CONTINUE
      L=L+1
      XCOTE=1.0-X1/2.0
      IF(MOD(NX,5))455,455,456
  455 AP(L,3)=XCOTE
      GO TO 457
  456 AP(L,2)=XCOTE
  457 AP(L,1)=0.866*X1
      DO 490 J=4,10
      IF(RACIN2(J))490,460,460
  460 X2PLUS=RACIN1(J)+(RACIN2(J))**0.5
      IF(X2PLUS)490,470,465
  465 IF(X2PLUS-1.0)470,490,490
  470 X3=1.0-X1-X2PLUS
      IF(X3)490,475,475
  475 AP(L,J)=X3+X1/2.0
  490 CONTINUE
  500 CONTINUE
      RETURN
      END
      SUBROUTINE GMTRA(A,R,N,M)
      DIMENSION A(70),R(70)
      IR=0
      DO 10 I=1,N
      IJ=I-N
```

```
      DO 10 J=1,M
      IJ= IJ+N
      IR=IR+1
   10 R(IR)=A(IJ)
      RETURN
      END
      SUBROUTINE GMPROD(A,B,R,N,M,L)
      DIMENSION A(70),B(70),R(49)
      IR=0
      IK=-M
      DO 10 K=1,L
      IK=IK+M
      DO 10J=1,N
      IR=IR+1
      JI=J-N
      IB=IK
      R(IR)=0
      DO 10 I=1,M
      JI=JI+N
      IB=IB+1
   10 R(IR)=R(IR)+A(JI)*B(IB)
      RETURN
      END
      SUBROUTINE MINV(A,N,D,L,M)
      DIMENSION A(49),L(7),M(7)
C       SEARCH FOR LARGEST ELEMENT
      D=1.0
      NK=-N
      DO80 K=1,N
      NK=NK+N
      L(K)=K
      M(K)=K
      KK=NK+K
      BIGA=A(KK)
```

```
      DO 20 J=K,N
      IZ=N*(J-1)
      DO 20 I=K,N
      IJ=IZ+I
   10 IF( ABS(BIGA)-ABS(A(IJ))) 15,20,20
   15 BIGA=A(IJ)
      L(K)=I
      M(K)=J
   20 CONTINUE
C
C       INTERCHANGE ROWS
C
      J=L(K)
      IF(J-K)35,35,25
   25 KI=K-N
      DO 30 I=1,N
      KI=KI+N
      HOLD=-A(KI)
      JI=KI-K+J
      A(KI)=A(JI)
   30 A(JI)=HOLD
C       INTERCHANGE COLUMNS
C
C
   35 I=M(K)
      IF(I-K) 45,45,38
   38 JP=N*(I-1)
      DO 40 J=1,N
      JK=NK+J
      JI=JP+J
      HOLD=-A(JK)
      A(JK)=A(JI)
```

```
   40 A(JI)=HOLD
C
C       DIVIDE COLUMN BY MINUS PIVOT (VALUE OF PIVOT ELEMENT
C       IS CONTAINED IN  BIGA)
C
   45 IF(BIGA) 48,46,48
   46 D=0.0
      RETURN
   48 DO 55 I=1,N
      IF(I-K) 50,55,50
   50 IK=NK+I
      A(IK)=A(IK)/(-BIGA)
   55 CONTINUE
C
C       REDUCE MATRIX
C
      DO 65 I=1,N
      IK=NK+I
      HOLD=A(IK)
      IJ=I-N
      DO 65 J=1,N
      IJ=IJ+N
      IF(I-K)60,65,60
   60 IF(J-K)62,65,62
   62 KJ=IJ-I+K
      A(IJ)=HOLD*A(KJ)+A(IJ)
   65 CONTINUE
C
C       DIVIDE  ROW  BY  PIVOT
C
      KJ=K-N
      DO 75 J=1,N
```

```
      KJ=KJ+N
      IF(J-K)70,75,70
   70 A(KJ)=A(KJ)/BIGA
   75 CONTINUE
C
C       PRODUCT OF PIVOTS
C
      D=D*BIGA
C
C       REPLACE PIVOT BY RECIPROCAL
C
      A(KK)=1.0/BIGA
   80 CONTINUE
C
C       FINAL ROW AND COLUMN INTERCHANGE
C
      K=N
  100 K=(K-1)
      IF(K) 150,150,105
  105 I=L(K)
      IF(I-K) 120,120,108
  108 JQ=N*(K-1)
      JR=N*(I-1)
      DO 110 J=1,N
      JK=JQ+J
      HOLD=A(JK)
      JI=JR+J
      A(JK)=-A(JI)
  110 A(JI)=HOLD
  120 J=M(K)
      IF(J-K)100,100,125
  125 KI= K-N
```

```
      DO 130 I=1,N
      KI=KI+N
      HOLD=A(KI)
      JI=KI-K+J
      A(KI)=-A(JI)
  130 A(JI)=HOLD
      GO TO 100
  150 RETURN
      END
      SUBROUTINE CALCUL(N,A,B,C,D,E,VR)
      DIMENSION A(10,7),B(7),C(10),D(10),E(10)
   92 FORMAT('1',9X,'STATISTICS'/10X,11('-')/10X,'RESIDUAL VARIANCE',
     16X,E12.6/10X,'RESIDUAL SIGMA-SQUARE',2X,E12.6/10X,'DEGREES OF FRI
     2DOM',12X,I2/10X,'REGR.CORR.COEFFICIENT',2X,E12.6//)
   93 FORMAT(10X,'ANALYSIS OF VARIANCE'/10X,20('-')/10X,'SOURCE',5X,
     1'DOF      DIFF-OF-SUM       MEAN SQUARE',6X,'F-TEST RATIO'/10X,
     2'ERROR',6X,I2,5X,E12.6,6X,E12.6/10X,'REGRESSION',1X,I2,5X,E12.6,
     36X,E12.6,6X,E12.6/*)
      SOMY=0.0
      SOMY2=0.0
      SOMYO2=0.0
      DO 190 I=1,10
      D(I)=0.0
      DO 192 J=1,N
      D(I)=D(I)+B(J)*A(I,J)
  192 CONTINUE
      E(I)=C(I)-D(I)
      SOMY2=SOMY2+C(I)*C(I)
      SOMY=SOMY+C(I)
      SOMYO2=SOMYO2+D(I)*D(I)
  190 CONTINUE
```

```
      SCE=SOMY2-SOMY02
      SCR=SOMY02-SOMY*SOMY/10.0
      VR=SCE/(FLOAT(10-N))
      SCM=SCR/(FLOAT(N))
         RATIO=SCM/VR
      ECVR=VR**0.5
      NL=10-N
      R2=SCR/(SOMY2-SOMY*SOMY/10.0)
  200 WRITE(6,92)VR,ECVR,NL,R2
  210 WRITE(6,93)NL,SCE,VR,N,SCR,SCM,RATIO
      RETURN
      END
      SUBROUTINE PLOT(A,N,M,NL,NS,YDEBUT,PASY)
      DIMENSION OUT(101),YPR(11),ANG(9),A(1000)
      DATA BLANK,ANG/1H ,1H.,1HX,1H3,1H4,1H5,1H6,1H7,1H8,1H9/
    1 FORMAT(1H ,62X,'X(1)=1.000',4X,'Y MIN =',F6.2,3X,'PAS OF Y =',
     1F6.2/1H ,65X,'X')
    2 FORMAT(1H ,16X,100A1)
    3 FORMAT(1H )
    8 FORMAT(1H0,9X,11F10.2/13X,'X(2)=1.00',90X,'X(3)=1.00')
    5 FORMAT(10A1)
    9 FORMAT(//8X,7('LOI ',I1,'=',F6.2,4X))
   22 FORMAT(1H ,15X,'X',100A1)
      WRITE(6,1)YDEBUT,PASY
      NLL=NL
      IF(NS)16,16,10
        SORT BASE VARIABLE DATA IN ASCENDING ORDER
   10 DO 15 I=1,N
      DO 14 J=1,N
      IF(A(I)-A(J))11,14,14
   11 L=I-N
```

```
      LL=J-N
      DO 12 K=1,M
      L=L+N
      LL=LL+N
      F=A(L)
      A(L)=A(LL)
   12 A(LL)=F
   14 CONTINUE
   15 CONTINUE
   16 IF(NLL) 20,18, 20
   18 NLL=50
   20 CONTINUE
        FIND SCALE FOR BASE VARIABLE
      XSCAL=(A(N)-A(1))/(FLOAT (NLL-1))
        FIND SCALE FOR CROSS VARIABLES
      YMIN=0.0000
      YMAX=1.0000
      YSCAL=(YMAX-YMIN)/100.0

        FIND BASE VARIABLE PRINT POSITION
      XB=A(N)
      L=100
      NDIV=2
      MY=M-1
      I=1
   45 F=I-1
      XPR=XB-F*XSCAL
   50 DO 55 IX=1,101
   55 OUT(IX)=BLANK
   59 DO 60 J=1,MY
      LL=L+J*N
      JP=((A(LL)-YMIN)/YSCAL)+1.5
```

```
      OUT(JP)=ANG(J)
   60 CONTINUE
      L=L-1
      IF(MOD(L,NDIV))59,65,59
   65 WRITE(6,2)(OUT(IZ),IZ=2,101)
      GO TO 80
   70 WRITE(6,3)
   80 I=I+1
      IF(I-NLL)45,84,84
   84 XPR=A(2)
      DO 85 IX=1,101,2
      OUT(IX)=ANG(1)
   85 CONTINUE
      DO 86 IX=2,100,2
      OUT(IX)=BLANK
   86 CONTINUE
      DO 87 IX=11,91,10
      OUT(IX)=ANG(2)
   87 CONTINUE
   88 DO 89 J=1,MY
      LL=L+J*N
      JP=((A(LL)-YMIN)/YSCAL)+1.5
      OUT(JP)=ANG(J)
   89 CONTINUE
      L=L-1
      IF(L)95,95,88
   95 WRITE(6,22)(OUT(IZ),IZ=2,101)
      YPR(1)=YMIN
      DO 90 KN=1,9
   90 YPR(KN+1)=YPR(KN)+YSCAL*10.0
```

```
      YPR(11)=YMAX
      WRITE(6,8)(YPR(IP),IP=1,11)
      YPR(3)=YDEBUT
      DO 100 K=3,8
      YPR(K+1)=YPR(K)+PASY
  100 CONTINUE
      WRITE(6,9)(K,YPR(K),K=3,9)
      RETURN
      END
      FINISH
```

# 7 REFERENCES

## REFERENCES


1 United Kingdom Fire and Loss Statistics. Building Research Establishment, Garston. (Published annually).

2 K. Sumi and Y. Tsuchiya: J. Fire Flammability., 4, 15 (1973).

3 W.D. Woolley:Plast. Polym., 41(156), 280(1973).

4 J.R.Gaskill and C.R. Veith: Fire Technol.,4(3), 185 (1968).

5 I.N. Einhorn, R.W. Michelson, B.Shah and R. Craig: J. Cell. Plast., 4(5), 188(1968).

6 W.C. Kuryla: "Available Flame Retardants" Flame Retardancy of Polymeric Materials, Vol.1, Marcel Dekker, Inc., N.Y. p.1.(1973).

7 M.W. Ranney: "Fire Retardant Polymers", Noyes Data Corp., Park Ridge, N.J., (1970).

8 Anon: Modern Plastic International, 8, (Sept)-.- 1978.

9 C.P. Fenimore and F.J. Martin, Mod. Plast., 44(3),141 (1966).

10 S.L. Madorsky: "Thermal Degradation of Organic Polymers", Interscience Publishers, N.Y. (1964).

11 L.A.Wall (Editor): "The Mechanism of Pyrolysis, Oxidation and Burning of Polymers", 4th Mat.Res.Symp., Oct. 1970, National Bureau of Standards (1972).

12 Encyclopedia of Polymer Science and Technology: Supplement Volume 2. John Wiley and Sons, London, p.270(1977).

13 N. Grassie and R. McGuchan: Eur. Polymer J.,7, 1357(1971).

14 Y. Tsuchiya and K. Sumi: J. Polymer Sci., Part A-1,7, 3151 (1969).

15 N. Grassie: "Chemistry of High Polymer Degradation Processes", p.294, Butterworths, London, (1956).

16 I. Ouchi: J. Polymer Sci., Part A, 3, 2685 (1965).

17 W.C.Geddes: Eur. Polymer J., 3, 733 (1967).

18 A.V. Tobolsky, A.M.Kotlair and T.C.P. Lee: "Thermal Stability of Polymers". Vol.1., ed. R.T. Conley, p.92, Marcel Dekker Inc., N.Y. (1970).

19 W.G. Oakes and R.B. Richards: J. Chem.Soc., p.2929 (1949).

20 L.A. Wall, S.L. Madorsky et. al.: J. Amer. Chem. Soc., 76, 3430 (1954).

21 D. McIntyre, J.H. O'Mara and S. Straus: J.Res. Nat. Bur. Standards., 68A, 153 (1964).

22 T.E. Davis, R.L. Tobias and E.B. Peterli: J. Polymer Sci., 56, 485(1962).

23 L.D. Loan and F.H. Winslow: "Polymer Stabilisation", ed. W.L. Hawkins, p.121, J. Wiley and Sons, Inc., N.Y.(1972).

24 G.J. Minkoff and C.F.H. Tipper: "Chemistry of Combustion Reactions", p.121, Butterworths, London (1962).

25 B. Lewis and G. von Elbe: "Combustion, Flame and Explosion of Gases", 2nd Ed. Academic Press., N.Y.(1961).

26 H.H.G. Jellinek: J. Polymer Sci.,3, 850 (1948).

27 J.R. MacCallum: Makromol. Chem., 83, 129 (1965).

28 L.A. Wall and S. Straus: J. Polymer Sci., 44, 313 (1960).

29 D.R. Witt and J.P. Hogan: J. Polymer Sci., Part A-1, 8, 2689 (1970).

30 K. Tanaka, M. Takakura and Y. Koshino: J. Appl. Polymer Sci., 18, 1131 (1974).

31 H.H.G.Jellinek: J. Polymer Sci., 4, 13 (1949).

32 W.J. Bailey and C.L. Liotta: Amer. Chem. Soc Polym.Prepr., 5(2), 333(1964).

33 W.J. Bailey and L.J. Baccei: Amer. Chem. Soc. Polym. Sci., 12(2), 313 (1971).

34 J. van Schooten and J.K. Evenhuis: Polymer, 6, 343, 561 (1965).

35 Y. Tsuchiya and K. Sumi: J. Polymer Sci., Part A-1, 6, 415 (1968); Part B, 6, 357 (1968).

36 S.L. Madorsky and S. Straus: J. Res. Nat. Bur. Stand., 53, 361 (1954).

37 S.L. Madorsky and S. Straus: J. Polymer Sci., 9, 133 (1952).

38 S.L. Madorsky and S. Straus: J. Res. Nat. Bur. Stand., 62, 219 (1959).

39 W.G. Oakes and R.B. Richards: J. Chem. Soc.(Lond.), 2929 (1949).

40 S.L. Madorsky et al.,: J. Res. Nat. Bur. Stand., 42, 499 (1949).

41 M. Iring, K. Barabas, T. Kelen and F. Tüdös: J. Polymer Sci., Symp 57, 65 (1976).

42 A. Holmström and E.M. Sorvik: J. Polymer Sci., Symp.57, 33 (1976).

43 A. Holmström and E.M. Sorvik: J. Appl. Polymer Sci., 18, 3153 (1974).

44 D.A. Anderson and E.S. Freeman: J. Polymer Sci., 54, 253 (1961).

45 H.W. Thompson and P. Torkington: Proc. Roy. Soc.(Lond.) A.184, 3 (1945).

46 S.L. Madorsky and S. Straus: Soc. Chem. Ind. Monograph No. 13, 60 (1961).

47 S.L. Madorsky: J. Soc. Plast. Eng. 17, 665 (1961).

48 M. Mucha: J. Polymer. Sci., Symp.57, 25 (1976).

49 S.L. Madorsky: "Thermal Degradation of Organic Polymers", Interscience Publishers, N.Y. (1964).

50 C.F. Cullis: Oxidation and Combustion Reviews, 5, 83 (1971).

51 G.G. Cameron: J. Res. Nat. Bur. Stand. 357, 61(1970).

52 G.R. Rideal and J.C. Padget: J. Polymer Sci., Symp.57, 1 (1967).

53 J.M.G. Cowie: "Polymers: Chemistry and Physics of Modern Materials", p.71, International Textbooks, Aylesbury, (1973).

54 M. Nagao and T.Hikita: Kogyo Kagaku Kyokaishi; 22, 234 (1966).

55 S.L. Madorsky, S. Straus, D. Thompson and L. Williamson: J. Polymer Sci., 4, 639 (1949).

56 L.A. Wall: J. Res. Nat. Bur. Stand., 41, 315 (1945).

57 D. Braun and E. Čanji: Angew. Makromol. Chem., 29, 491 (1973).

58 J. Zulaica and G. Guiochon: Bull. Soc. Chim. Fr., p.1351(1966).

59 H.D.R. Schüddemage and D.D. Hummel: Advances in Mass Spectrom., 4, 857 (1968).

60 I.P. Cherenyuk and S.A. Demidova: Khim. Technol. Polim.,p.51 (1972).

61 S. Straus and S.L. Madorsky: J. Res. Nat. Bur. Stand., 61, 77 (1958).

62 H. Staudinger and E. Greiger: Helv. Chim. Acta., 9, 549 (1926).

63 A. Tkáč, V. Kellö and J.Hrivi Ková: Coll.Czech. Chem. Commun., 31, 551 (1966).

64 M.A. Golub and R.J. Gargiulo: J. Polymer Sci., Polymer Letters, 10, 41 (1972).

65 M.A. Golub and M. Sung: J. Polymer Sci., Polymer Letters, 11, 129 (1973).

66 N. Grassie and A. Heaney: J. Polymer Sci., Polymer Letters, 12, 89 (1974).

67 N. Grassie and B. Torrance: J. Polymer Sci., Part A-1, 6, 3303 (1968).

68 N. Grassie and E. Farish: Eur. Polymer. J., 3, 619, 627, 305 (1967).

69 N. Grassie and E. Grant: Eur. Polymer. J., 2, 255 (1966).

70 N. Grassie and D.R. Bain: J. Polymer Sci., Part A-1, 8, 2653, (1970).

71 N. Grassie and D.R. Bain: J. Polymer Sci., Part A-1, 8, 2665 (1970).

72 N. Grassie and D.R. Bain: J. Polymer Sci., Part A-1, 8, 2679, (1970).

73 L.A. Wall: "Analytical Chemistry of Polymers", Part 2, p.220 ed., G.M. Kline, Interscience Publishers, N.Y. (1962).

74 S.L. Madorsky: "Thermal Degradation of Organic Polymers", p.26, Interscience Publishers, N.Y. (1964).

75 G.G. Cameron and G.P. Kerr: Eur. Polymer J., 4, 709 (1968).

76 H.H.G.Jellinek: "Depolymerization", Encyclopedia of Polymer Science and Technology, 4, 740 (1966).

77 S.L. Madorsky and S. Straus: J. Res.Nat. Bur. Stand., 40, 417 (1948).

78 S.L. Madorsky: Soc. Plast. Eng. J., 17, 665 (1961).

79 S.L. Madorsky et al.: J. Res. Nat. Bur. Stand., 66A, 307 (1962).

80 H.H.G. Jellinek: J. Polymer Sci., 3, 850 (1948): 4, 13 (1949).

81 N. Grassie and W.W. Kerr: Trans. Faraday Soc., 55, 1050 (1959).

82 G.G. Cameron and N. Grassie: Makromol. Chem., 51,130 (1962).

83 G.G. Cameron and N. Grassie: Makromol. Chem., 53, 72 (1963).

84 L.A. Wall et al.: J. Phys. Chem., 70, 53 (1966).

85 D.M. Richards and D.A. Salter: Polymer, 8, 153 (1967).

86 L.A. Wall et al.: J. Polymer Sci., 15, 157 (1955).

87 R. Simha and L.A. Wall: J. Polymer Sci., 6, 39 (1951).

88 R. Simha, L.A. Wall and P.J. Blatz: J. Polymer Sci.,5, 615 (1950).

89 G.G. Cameron and J.R. MacCallum: J.Makromol. Sci., Part C, 1, 327 (1965).

90 L.A. Wall, S. Straus and L.J. Fetters: Polymer Preprints, 10(2), 1472 (1969).

91 S.L. Madorsky et al.: J. Res.Nat. Bur. Stand., 66A, 401 (1962).

92 S.L. Madorsky: J. Res. Nat. Bur. Stand., 62, 219 (1959).

93 H.C. Beachell and S.P. Nemphos: J. Polymer Sci., 25, 173 (1957).

94 L.A. Wall and M. Tyron: "Antioxidation and Antioxidants" Volume 2, ed., W.O. Lundburg, p. 919, Interscience Publishers, N.Y. (1962).

95 B.G. Achhammer et al.: J. Polymer Sci., 8, 555(1952).

96 J. Schurz: J. Polymer Sci., 28, 438 (1958).

97 J. Schurz et al.:Z. Phys. Chem.(Leipzig)., 210, 35 (1959)

98 W. Fester: Text. Randsch. 20, 1, (1965).

99 A.A. Berlin et al.:Polymer Sci., (USSR), 6, 2145 (1964).

100 W.J. Burlant and J.L. Parsons: J. Polymer Sci., 22, 249 (1956).

101 N. Grassie et al.: J. Polymer Sci., 31, 205 (1958).

102 E.M. LaCombe: J. Polymer Sci., 24, 152 (1957).

103 L.H. Peebles,Jr., and J. Brandrup: Makromol,Chem.,6, 136 (1969)

104 D. Braun and I.A.A. El-Sayed: Angew. Makromol. Chem.,6, 136 (1969).

105 H.N. Friedlander et al.: Macromolecules, 1, 79 (1968).

106 N. Grassie and R. McGuchan: Eur. Polymer J., 6, 1277 (1970).

107 J.W. Bell and R. Mulchandani: J. Soc. Dyers Colour., 16 (1965).

108 W. Watt and W. Johnson: Proc. 3rd, Carbon Conf.,Soc.Chem. Ind., (London) April(1970).

109 W.G. Vosburgh: Text.Res. J. 30, 882 (1960).

110 W. Makschin and J. Ulbricht: Faserforsch. Textiltech., 20, 321 (1969).

111 W. Watt and J. Green: Proc. Int. Carbon Fibers Conf., Plastics Inst., (London) p.23 (1971).

112 W. Watt and W. Johnson: Polymer Preprints, 9, 1245 (1968).

113 W. Watt: Nature, 222, 265 (1969).

114 N. Grassie and D.R. Bain: J. Polymer Sci., Part A-1,8, 2653 (1970).

115 N. Grassie and J.N. Hay: J. Polymer Sci., 56, 189 (1962).

116 N.P. Setchkin and S.H. Inberg: "Test Criterion for an Incombustible Material", ASTM Proceedings 45: 866-877 (1945).

117 H.W. Emmons: Sci. Amer., 231,(1), 21(1974).

118 R.B. Williamson and F.M. Baron: J. Fire Flammability, 4,99 (1973).

119 C.P. Fenimore and F.J. Martin: Mod. Plast.44(3), 141 (1966).

120 A.J. Hammerl: Soc. Plast. Industry Preprints, 12,4 (1962).

121 U.L. 94 Standard Test: Underwriters' Laboratories, Inc., June (1973).

122 W.F. Moroni: Fire. J., 38, November (1972).

123 D. Gross, et al.: ASTM STP 422, p.166, (1969).

124 D.J. Rasbash and R.P. Phillips: Fire and Mater.,2(3), 102 (1978).

125 R.F. Simmons and H.G. Wolfhard: Combustion and Flame, 1, 55 (1957).

126 J. Eichhorn: J. Appl. Polymer Sci., 8, 2497(1964).

127 C.P.Fenimore and F.J. Martin: Combustion and Flame, 1,155 (1957).

128 C.P.Fenimore and F.J Martin: Combustion and Flame,10, 295 (1966).

129 F.J. Martin: Combustion and Flame,12, 125(1968).

130 C.P. Fenimore and F.J. Martin: Combustion and Flame, 10, 135(1966).

131 J.L. Isaacs: J. Fire Flammability 1, 36(1970).

132 K.B. Goldblum: Soc. Plast. Eng.J., 25, 50(1969).

133 C. Abbott: Europlast. Mon.46, 68(1973).

134 A.E. Williamson: Electrical Research Association Symp., Session 1, Paper 3, London (6 February 1974).

135 J.L. Isaacs: Report No. T1S 69-MAL-13, General Electrical Technical Information Series Louisville, Ky (August 1969).

136 J.L. Isaacs: Mod. Plast. 47, 126(1970).

137 M. Furuya: Sen'i Gakkaishi 29,108(1973).

138 G.L. Nelson and J.L. Webb: Advances in Fire Retd. Text. Vol.5, Progress in Fire Retd. Series, ed.V.M. Bhatnagar, p.271(1974).

139 A.G. Walker: Europlast. Mon. 46, 72(1973).

140 R.M. Murch: Abstracts of the Int. Symp. Fire Safety and Comb. Mat., University of Edinburgh, p.25(1972.

141 BS 2782: Introduction British Standards Institution, London (1975).

142 C.P. Fenimore and F.J. Martin: Mod. Plast. 44, 141 (1966).

143 J. DiPietro and H. Stepniczka: Soc. Plast. Eng. J. 27, 23 (1971).

144 P. Smilek: Plast. Kavc. 13, 264(1976).

145 J.A. Rhys: Electrical Research Association Symp.,Session 1, Paper 4, London (6 February 1974).

146 A.G. Day: Ibid, Paper 3.

147 J.E. Hendrix; G.L. Drake and W.A. Reeves: Text. Res. J. 41, 360 (1971).

148 A.M. Kanury: Abstracts of the Int. Symp. on Fire Safety and Comb. Mat., University of Edinburgh, p.187 (October 1975).

149 C.P. Fenimore and F. J. Martin: "Mechanism of Pyrolysis, Oxidation and Burning", 4th Mat. Res. Symp. N.B.S., Washington, D.C. (1972).

150 C.P. Fenimore and G.W. Jones: J. Appl. Polymer Sci., 13, 285 (1969).

151 C.P. Fenimore and F.J. Martin: "Mechanism of Pyrolysis, Oxidation and Burning"., ed. L.A. Wall, p.159, N.B.S. Spec. Publ., Washington D.C. (1972).

152 J. DiPietro and H. Stepniczka: Soc. Plast. Eng. Conf., p.463 (5 May 1970).

153 J.E. Hendrix et al.: J. Fire Flammability 3, 2(1972).

154 J.DiPietro and H. Stepniczka: J. Fire Flammability 2, 36, (1971).

155 H.K. Reimschuessel, S-W. Shalaby and E.M. Pearce: J. Fire Flammability, 4, 299(1973).

156 G.A. Byrne, D. Gardiner and F.H. Holmes: J. Appl. Chem., London, 16, 81(1966).

157 S.J. Burge and C.F.H. Tipper: Chem. Ind. London 362(1967).

158 D.E. Stuetz, R.P. Barnes, A.H. DiEdwardo and F. Zitomer: Flammability Characteristics of Polymeric Materials Conf. Utah (1970).

159 J.L. Isaacs: J. Fire Flammability, 1, 36 (1970).

160 F.J. Martin: Combustion and Flame, 12, 125 (1968).

161 C.P. Fenimore and G.W. Jones: Combustion and Flame, 10, 295 (1966).

162 S.J. Burge and C.F. H. Tipper: Combustion and Flame, 13, 495 (1969).

163 J.L. Isaacs: Mod. Plast., 47, 124 (1970).

164 F.L. Browne: Report No. 2136, Forest Products Laboratory, Forest Service, U.S. Department of Agriculture, Wisconsin, (1958).

165 G.L. Nelson and J.L. Webb: Advances in Fire Retd. Text., Vol.5, Progress in Fire Retd. Series, ed., V.M. Bhatnager (1974).

166 W.G. Schmidt: Trans. J. Plastics Inst., 33, 247(1965).

167 F. Olstowski et al.: U.S. Patent 3,574,644 (1971).

168 J.L. Bolland: Quart. Rev. (London), 3, 1(1949).

169 R.H. Dahms: Hydrocarbon Processing and Petrol. Refiner, 41, 143 (1952).

170 V.N. Kondrat'ev: "Chemical kinetics of gas reactions", Pergamon Press, London (1964).

171 J.N. Bradley: "Flame and Combustion Phenomena' Methuen, London (1969).

172 E.C. Creitz: National Bureau of Standards Rept. No. 6588 (Nov. 1959).

173 R.W. Little: Textile Res. J., 901 (1951).

174 E.R. Larsen: J. Fire Flammability, Fire Retardant Chemistry, 1, 4(1974).

175 J.W. Lyons: "The Chemistry and Uses of Fire Retardants", Wiley-Interscience, New York, p.14-17 (1970).

176 E.C. Creitz: J.Res. of N.B.S., 74A (4), 521(1970).

177 E.C. Creitz: J.Res. Nat. Bur. Standards , 65A, 389(1961).

178 H.T. Lee: J. Phys. Chem., 67,360 (1963).

179 P. Volans: Trans. J. Plastics Inst. (Conf. Suppl. No.2), 47 (1967).

180 L. Delfosse, C. Baillet and S. Antonik:Fire and Materials 2 (3), 132 (1978).

181 A.W. Benbow: Ph.D. Thesis, The City University (1972).

182 J.W. Lyons: "The Chemistry and Uses of Fire Retardants", Wiley-Interscience, New York, (1970).

183 J.K. Jacques: Trans. J. Plastics Inst.(Conf. Suppl. No.2), 34(1967).

184 J.W. Lyons: J. Fire Flammability, 1, 302(1970).

185 A.J. Papa: Ind. Eng. Chem.Prod.Res.Dev. 16, 2361. (1972).

186 H. Piechota: J. Cell. Plastics., 1, 186(1965).

187 G.S. Learmonth and D.G. Thwaite: Brit.Polymer.J., 2(5), 249(1970).

188 J.K. Backus, W.G. Darr, P.G. Gemeinhardt and J.H. Saunders: J. Cell. Plastics, 1, 178(1965).

189 C.P. Fenimore: "Flammability Characteristics of Polymeric Materials", Polymer Conf. Ser. Wayne State University, June(1966).

190 J.J. Anderson: ibid.

191 I.N. Einhorn and R.W. Mickelson: Amer. Chem. Soc. Div.Org. Coatings Plast. Chem. Prepr. 2(1), 113(1962).

192 A.J. Papa and W.R. Proops: J. Appl.Polymer Sci., 16,2361 (1972).

193 G. Lask and H.Gg. Wagner: Eighth Int. Symp.Combustion, Williams & Wilkins Co., Baltimore, Md., p.432(1962).

194 J.K. Jacques: Plast.Inst.Trans.J., 33(1967).

195 R.R. Hindersinn and G. Witschard: "The Effect of Char and Intumescence on Polymer Fire Retardance", in W.C. Kuryla and A.J. Papa, eds. Flame Retardancy of Polymeric Materials, Vol.3, Marcel Dekker, Inc., New York(1978).

196 C.P. Fenimore and G.W. Jones: Combustion and Flame, 10(3), 295 (1966).

197 E.D. Weil: "Additivity, Synergism and Antagonism in Flame Retardancy", in W.C. Kuryla and A.J. Papa, eds., Flame Retardancy of Polymeric Materials, Vol.4, Marcel Dekker, Inc., New York(1975).

198 C.T. Pumpelly: "Bromide and its compounds", Z.E. Jolles, ed., Ernest Benn, London,(1966).

199 W.G. Schmidt: Trans.J. Plastics Inst., 247(1965).

200 R.W. Little: Flame proofing Textile Fabrics, ACS Monograph, No. 104, Reinhold Publ. Corp., New York (1947).

201 J.A. Rhys and R.F. Cleaver: Plast. Rubber Wkl. 20, Nov. (1970).

202 N.J. Reid and E.G. Heighway-Bury: J.Soc.Dyers Color. 74, 823(1958).

203 I.N. Einhorn: Fire Retardancy of Polymeric Materials, Polymer Conf. Ser., University of Utah, June 14, (1970).

204 J.J. Pitts: "Inorganic Flame Retardants and Their Mode of Action", in W.C. Kuryla and A.J. Papa, eds., Flame Retardancy of Polymeric Materials, Vol. 1, Marcel Dekker, Inc., New York (1973).

205 R.G. Bauer: J. Fire Retd. Chemistry, 5, 200, (1978).

206 Z.E. Jolles and G.I. Jolles: Plastics and Polymer, 40, 319, (1972).

207 G.S. Learmonth and D.G. Thwaite:Brit. Polymer J., 2, 104 (1970).

208 I. Touval and A. Frieman: Paint and Varnish Production, 61, (1972).

209 A.W. Benbow and C.F. Cullis: Int. Symp. "Fire Safety of Combustible Materials". Edinburgh p.218 (1975).

210 J.W. Hastie and C.L. McBee: "Halogenated Fire Suppressants" A.C.S. Symp. Ser. 16, 118(1975).

211 S.K. Brauman et al.: J. Fire Flammability, Fire Retardant Chemistry, 3,66,(1976).

212 S.K. Brauman : J. Fire Flammability, Fire Retardant Chemistry, 3, 117(1976).

213 S.K. Brauman : J. Fire Flammability, Fire Retardant Chemistry, 3, 138(1976).

214 S.K. Brauman et al.: J. Fire Flammability, Fire Retardant Chemistry, 3, 225 (1976)

215 J.A. Abu-Isa: J. Polymer Sci., A.1, 10, 881(1972).

216 L.A. Jordan and L.A. O'Neill: British Pat., 573,472 (1945).

217 F.M.C. Corp.: Belgian Pat. 699,508 (1967).

218 Burns and Russell Co.: British Pat.,1,080,468 (1967).

219 M. Leatherman: U.S. Pat. 2,472,112 (1949).

220 Raychem Corp.: Netherlands Pat. Appl. 6,603,028 (1966).

221 I. Touval: J. Fire Flammability, 3, 130 (1972).

222 T. Takiuchi and H. Date: Japan Pat. 33,338 (1974).

223 H. Date and H. Sakurai: Japan. Pat. 62,842; 62,843 (1973).

224 E.I. Evdokimov: Plast. Massy., 2, 43 (1975).

225 D.A. Church and F.W. Moore:Plast. Eng., 31 (12), 36 (1975).

226 M. Sugahara: Japan Pat. 37,137 (1976).

227 J.F. Coleman and M.L. Dannis: Canadian Pat.1,014,690(1977).

228 T. Okuzono and M. Kifune: Japan Pat. 80,347 (1976).

229 Y. Fujita and T. Ono: Japan Pat. 49,821 (1972).

230 J. Pitts and P.H. Scott: U.S. Pat. 3,697,456 (1972).

231 H. Ida and N. Kato: Japan Pat. 85,252 (1977).

232 S.M. Draganov: German Pat. 2,105,444 (1972).

233 J. Bower et al: J. Fire Flammability , 3, 226 (1972).

234 J. Dulat: Chem. Ind. 7, 312 (1976).

235 D.F. Lawson and E.L. Kay: U.S. Pat. 3,957,723 (1976).

236 I. Touval: U.S. Pat., 3,926,883 (1975).

237 I. Touval: U.S. Pat., 3,876,549 (1975).

238 A. Ohmori et al.: German Pat., 2, 451,391 (1976).

239 Y. Ikegami: Japan Pat. 94,056 (1975).

240 T. Tsuji: Japan Pat., 35,623 (1974).

241 L. Rensmann et al.: German Pat., 2,059,284 (1972).

242 S. Yoshinaga et al.: Plast. Ind. News, 22(7), 99,(1976).

243 K. Ontsuka and T. Takahashi: Japan Pat., 125,453 (1979).

244 W.P. Whelan: U.S. Pat., 3,956,139 (1976).

245 Modern Plastics Encyclopedia: Vol.51, No. 10A, McGraw-Hill Book Co., New York, p.755 (1975).

246 J.J. Pitts: J. Fire Flammability, 3, 51 (1972).

247 A.W. Benbow and C.F. Cullis: Int. Symp. "Fire Safety of Combustible Materials", Edinburgh p.218 (1975).

248 W. Zive: "A Review of the Use of Borates as Fire Retardants in Cellulosic Materials", First Annual Papermakers' Conference, TAPPI, June 5-8 (1972).

249 W.G. Woods: "Boron Compounds as Flame Retardants in Polymers", U.S. Borax Research Corp. Anaheim, Calif. (1967).

250 W.G. Woods and J.G. Bower: Mod. Plast., 47,(6), 140(1970).

251 J. Kestler: Mod. Plast. 47, 96 (1970); 44(1), 102 (1966).

252 Anon: Chemical Week, p.141, June 17 (1970).

253 Diamond Shamrock Chemical Co.: Tech. Bull. TB-38, "Flame Retardant Polyolefins", February 1, (1966).

254 N.J. Alvares: Preprints, ACS Div. of Organic Coatings and Plastics Chem., 36 (2), 480 (1976).

255 A.R. Ingram: U.S. Pat., 3,274,133 (1966).

256 A.R. Ingram: J. Appl. Polymer Sci., 8, 2485 (1964).

256 J. Eichhorn and S.I. Bates: U.S. Pat., 3,058,929 (1962).

258 G.B. Skinner: ASO TR61-408, Monsanto Research Corp., December (1961).

259 J. Eichhorn: U.S. Pat., 3,058,926 (1962).

260 J. Eichhorn: Amer. Chem. Soc., 23, 37 (1963).

261 R.R. Hindersinn: Polymer Conf. Ser., Wayne State University, Detroit, June (1966).

262 C.P. Fenimore et al.: Combustion and Flame, 10, 295(1966), 12, 125(1968); 12, 155(1968).

263 I. Sobolev and E.A. Woycheshin: J. Fire Flammability Fire Retardant Chemistry, 1, 13 (1974).

264 H. Frood and H.P. Alger: British Pat., 183,922 (1921).

265 K.C. Hecker: Rubber World, 159 (3), 59 (1968).

266 Selected Values of Chemical Thermodynamic Properties, NBS Tech. Note 270-3, January (1968).

267 Y.Takahashi, K. Yamada, T. Fukunaga and T.M. Ukaibo: "Heat Capacity of Hydrated and Crystalline Aluminas", Denki Kagaku, 41 (4, (1973).

268 K. Yamada, T. Fukunaga, Y. Takahashi and T. Mukaibo: "Heat of Dehydration of Hydrated Aluminas", Denki Kagaku 41 (4), (1973).

269 F.J. Martin and K.R. Price: "Flammability of Epoxy Resins", J. Appl. Polymer Sci., 12, 143 (1968).

270 D.F. Lawson, E.L. Kay and D.T. Roberts: "Mechanism of Smoke Inhibition by Hydrated Fillers", Rubber Chem. Technol., 48 (1), (1975).

271 D.C. Thompson, J.F. Hagman and N.N. Mueller:"Flame Resistance of Neoprene", Rubber Age (1958).

272 W.J. Connolly and A.M. Thornton: "Aluminium Hydrate Filler in Polyester Systems", Mod. Plast., October (1965).

273 F.J. Ampthor and C.H. Kroekel: "Developments in Low-Profile SMC for Flame Retardant and Electrical Applications, SPI-RP/C Institute Proceedings, February(1972).

274 O.K. Goins and Y.C. Chae: " Tetrachlorophthalic Anhydride Polyesters-Flame Retardancy", ibid.

275 M.A. Rizzi: "Total System Approach to Mixing and Moulding Glass Reinforced Polyester Compounds, ibid.

276 M.W. Ranney et al.: "Silane Coupling Agents in mineral-filled Composites", ibid.

277 T.R. Evans et al.: "Formulated Fire Retardant Polyester Systems for Press Molded Laminates, ibid.

278 T.K. Sprow, W.J. Connolly and E.J. Kerle: Filled Polyester Spray-Up Systems Offering Improved Fire Hazard Classifications, SPI-RP/C Inst. Proc., February (1973).

279 R.H. Tampenau and T.R. Evans: Fire Retardant FRP in Construction, ibid.

280 C.V. Lundberg: "Hydrated Alumira as a Fire Retardant Filler in Styrene-Polyester Casting Compounds, 166th A.C.S. Meeting, Chicago, August 1973.

281 G. James and R.C. James: "Mathematics Dictionary", D. Van Nostrand Co. Inc., Prinston, N.J. (1959).

282 H. Scheffé: "Experiments with Mixture". J. Roy. Stats. Soc., 21B (1), 201 (1958).

283 N.R. Draper and W.E. Lawrence: "Mixture designs for three factors", J. Roy. Stats. Soc., 27B (3), 450 (1965).

284 N.R. Draper and W.E. Lawrence: "Mixture designs for four factors", J. Roy. Stats. Soc., 27 B (3), 473 (1965).

285 J.W. Gorman and J.E. Hinman: "Simplex-lattic designs for multicomponents systems". Technometrics, 4(4), 463 (1962).

286 D.P. Lambrakis: "Experiments with mixtures-an alternative to the simplex-lattic design". J. Roy. Stats. Soc., 31B(2), 234 (1969).

287 J.W. Gorman: "Fitting equations to mixture data with restrains on compositions", J. Quality Control, 592 (1970).

288 I.S. Kurotori: "Experiments with mixtures of components having lower bounds", Ind. Quality Control, 592 (1966).

289 R.A. McLean and V.L. Anderson: "Extreme vertices design of mixture experiments", Technometrics, 8,(3), 447 (1966).

290 W.O. Thompson and R.H. Myers: "Response surface designs for experiments with mixtures", Technometrics, 10(4), 737 (1968).

291 L.H. Krol:"Butadiene and isoprene rubber in giant tyre treads" Rubber Chem. Technol., 39, 452 (1966).

292 O.O. Kenworthy: "Factorial experiments with mixtures using ratios", Ind. Quality Control, 109,(12),24 (1963).

293 W.E. Duckworth: "Statistical Techniques in Technological Research", Methuen & Co. Ltd., London p.37 (1968).

294 W.W. Wendlandt: "Thermal Methods of Analysis", John Wiley and Sons, London (1974).

295 ASTM D-2863-77: Measuring the minimum oxygen concentration to support candle-like combustion of Plastics, 35, 746 (1977).

296 A.W. Benbow and C.F. Cullis: Third Int. Conf. "Non- Flammability of Plastics, Wool and Textiles, Strbske Pleso, Czechoslavakia 1974, p.55, Dom Techniky, Bratislava (1974).

297 E.A. Woycheshin and I. Sobolev: Soc. Plast. Eng., Tech. Pap, 19, 709 (1973).

298 A.G. Day: Plastics and Polymer, 43, 64, 1975.

299 D.W. Van Krevelen: Polymer, 16, 615, 1975.

300 J. DiPietro and H. Stepniczka: J. Fire Flammability 2, 36 (1971).

301 J.J. Pitts: "Inorganic Flame Retardants and Their Mode of Action" in W.C.Kuryla and A.J. Papa, ets., Flame Retardancy of Polymeric Materials, Vol.1 Marcel Dekker Inc., N.Y. (1973).

302 E.D.Weil: "Additivity, Synergism and Antagonism in Flame Retardancy", ibid.

303 A.W. Benbow and C.F. Cullis: Int. Symp. "Fire Safety of Combustible Materials" Edinburgh p.218 (1975).

304 R.F. Cleaver: Plastics and Polymers, 38, 198, (1970).

305 A.W. Benbow and C.F. Cullis: Int. Symp. "Fire Safety of Combustible Materials" Edinburgh p.218 (1975).

306 I. Touval: J. Fire Flammability, 3, 130 (1972).